Electrical synapses: Cellular morphology and identification of connexins in the mouse retina

Von der Fakultät V, Mathematik und Naturwissenschaften
der Carl von Ossietzky Universität Oldenburg
zur Erlangung des Grades und Titels eines Doktors der
Naturwissenschaften (Dr. rer. nat.) angenommene
Dissertation

Von Herrn Luis Pérez de Sevilla Müller,
geboren am 14.07.1979
in Madrid, Spanien

Gutachter: Prof. Dr. Reto Weiler

Zweitgutachter: Prof. Dr. Henrik Mouritsen

Tag der Disputation: 18.09.2008

„ My devotion to the retina is ancient history. The subject always fascinated me because, to my idea, life never succeeded in constructing a machine so subtilely devised and so perfectly adapted to an end as the visual apparatus……

I must not conceal the fact that in the study of this membrane I for the first time felt my faith in Darwinism weakened, being amazed and confounded by the supreme constructive ingenuity revealed not only in the retina and in the dioptric apparatus of the vertebrates but even in the meanest insect eye. There, in fine, I felt more profoundly than in any other subject of study the shuddering sensation of the unfathomable mystery of life. “

(Cajal, 1937)

Contents

Abbreviations

ACs	Amacrine cells
AT	cytoplasmic N-terminal
BPC	Bipolar cell
c-AMP	Adenosin-3',5'-cyclic phosphate
ChAt	Choline acetyltranferase
CNS	Central nervous system
Cx	Connexin
CL	Intracellular loop
CT	Cytoplasmic carboxy-terminal
DHT	5,7-dihydroxytryptamine
EGFP	Enhanced green fluorescent protein
EL	Extracellular loop
ERG	Electroretinogram
FDG	Fluorescein di-beta-D galactopyranoside
GABA	y-aminobutyric acid

GCL	Ganglion cell layer
GCs	Ganglion cells
GluR	Glutamate receptor
HCs	Horizontal cells
INL	Inner nuclear layer
IPL	Inner plexiform layer
kDa	kilodalton
KO	Knock out
Nestin-Cre	Cre-recombinase expression under nestin promoter control
NGS	Normal goat serum
Nm	Nanometer
ONL	Outer nuclear layer
OPL	Outer plexiform layer
PB	Phosphate buffer
PFA	Paraformaldehyde
TM	Transmembrane domains

WFAC	Wide-field amacrine cell
WT	Wild type
μm	Micrometer

Acknowledgments

First of all I have to thank my supervisor Prof. Dr. Reto Weiler who patiently guided my work and helped me to improve my research skills with suggestions and ideas. Despite of being a very busy man, he always could find time to speak about my experiments. Without him, this study would not have been possible.

Big thanks go to Prof. Dr. Ulrike Janssen-Bienhold who gave me the opportunity to work with her in a fascinating project. It was always a pleasure to discuss work with her.

I am thankful to Prof. Dr. Josef Ammermüller who patiently taught me the ERG method and who always found time to discuss with me all my data.

I am thankful to Dr. Jennifer Trümpler who helped me to improve my work and my dissertation.

Dr. Konrad Schultz introduced me to the immunohistochemistry world and showed me the incredible world of the microscopes. I really appreciate all the time he spent helping me with the confocal microscopy and I enjoyed the nice atmosphere he gives in the lab.

Many thanks go to Dr. Karin Dedek and Dr. Timm Schubert who helped me with my experiments.

I express my grateful to all the members of the lab; Josef Meier, Bettina Kewitz, Dr. Petra Dirks, Susanne Wallenstein, Dr. Andreas Feigenspan, Nicole Iben, Tobias Dallenga, Susanne Lorenz, Gerrit Hilgen, Petra Bolte, and Mario Pieper.

Thanks go to Dr. Stephan Maxeiner, Dr. Maria Kreuzberg, and Prof. Dr. Klaus Willecke in Bonn University for providing me the transgenic mice.

Zusammenfassung

Die Retina der Wirbeltiere hat einen stark konservierten Aufbau. Sie besteht aus einer äußeren und einer inneren plexiformen Schicht (synaptische Schichten), die sich zwischen drei zelluläre Schichten einfügen: die äußere, die innere nukleäre und die Ganglienzellschicht. In diesen nukleären Schichten befinden sich die Zellkörper von allen Hauptzelltypen. Die äußere nukleäre Schicht enthält die Zellkörper der Photorezeptoren, während die innere nukleäre Schicht die Zellkörper von Horizontal-, Amakrin- und Bipolarzellen enthält. Die letzte Schicht enthält die Zellkörper der Ganglienzellen.

Von allen Hauptklassen der retinalen Neuronen bilden die Amakrinzellen die verschiedenartigste Zellgruppe in Bezug auf Morphologie, Größe und Netzhautabdeckung. Erstaunlicherweise gibt es bis heute noch keine morphologische Klassifikation der Amakrinzellen in der Mausretina. Obwohl diese Retina aufgrund der gentechnischen Untersuchungsobjekt der Retinaforschung geworden ist.

Das erste Ziel der vorliegenden Dissertation war entsprechend, die Zahl der in der Ganglienzellschicht lokalisierten Amakrinzelltypen zu erforschen. Gefunden wurden zehn verschiedene Typen von deplatzierten Amakrinzellen, sechs davon sind neue Typen, die bisher noch nicht beschrieben wurden.

Amakrinzellen sind durch chemische Synapsen und auch durch Zell-Zell-Kanäle (lat. Nexus, eng. gap junctions)* mit Bipolarzellen, Ganglienzellen und anderen Amakrinzellen verbunden. Eine Gap Junction wird dabei aus zwei Halbkanälen gebildet, wobei jede Zelle einen Halbkanal beisteuert. Die jeweiligen Halbkanäle durchqueren die Zellmembran der Zellen und verbinden sich im Interzellulärraum mit den Halbkanälen der benachbarten Zelle. Die Connexone werden ihrerseits von sechs Proteinen, genannt Connexinen (Cx), gebildet. Die Connexine sind also die

Proteine, die interzelluläre Kanäle bilden, und sind für die Zusammensetzung der Gap Junctions verantwortlich.

Alle wichtigen Zellklassen der Wirbeltierretina enthalten Gap Junctions. In der Retina der Nagetiere ist Cx36 in Zapfen vorhanden. Horizontalzellen sind miteinander durch Cx57 gekoppelt. Bipolarzelltypen enthalten zwei verschiedene Connexine, Cx45 und/oder Cx36. Auch viele Ganglienzelltypen zeigen Tracer-Kopplung mit anderen retinalen Neuronen. Dabei werden von verschiedenen Ganglienzelltypen unterschiedliche Connexine verwendet.

Das zweite Ziel der vorliegenden Arbeit war die Identifikation der Cx45-exprimierenden Amakrinzellen und Cx30.2-exprimierenden Ganglienzellen in transgenen Mäusen. Außerdem wurde ich die Lokalisation von Cx57 in den Horizontalzellen der Mausretina untersucht. Alle diese Connexine (Cx36, Cx45, Cx57 und Cx30.2) haben unterschiedliche und besondere Eigenschaften, die vermutlich in Beziehung zu den verschiedenen Funktionen der verschiedenen Neuronentypen in der Retina stehen.

Die Ergebnisse haben gezeigt, dass Cx45 in bestimmten Typen von Amakrinzellen vorhanden ist, die mit den so genannten S1 und S2 Indoleamin-akkumulierenden Amakrinzellen in der Kaninchenretina und mit den A17 Amakrinzellen in der Katzenretina identisch zu sein scheinen. Diese Zelltypen sind für das Sehvermögen in der Dunkelheit sehr wichtig, da sie eine große Rolle im Stäbchenweg spielen. Diese Zellen proyezieren den Hauptteil ihrer synaptischen Ausgänge zurück auf die Stäbchenbipolarzellen, von denen sie ihren Eingang erhalten. Beide Amakrinzelltypen bilden elektrisch gekoppelte Netzwerke.

Außerdem wurden mindestens sechs verschiedene Typen von Cx30.2-exprimierenden Ganglienzellen gefunden. Eine von ihnen ist ein sehr großer

Ganglionzelltyp, der mit zahlreichen displatzierten Amakrinzellen durch Gap Junctions aus Cx30.2 und einem unbekannten Protein verbunden ist.

Durch die Generierung eines entsprechender Antikörpers, konnte erstmalig die genaue Lokalisation von Cx57 auf den Dendriten und den Axonendigungen von Horizontalzellen erreicht werden. Dies unterstützt vorherige Studien, die zeigten, dass Cx57 in der Mausretina exklusiv in Horizontalzellen exprimiert wird.

In meinem letzten Projekt habe ich die Morphologie von Horizontalzellen in transgenen Tieren im Bezug auf den Verfall der Photorezeptoren analysiert. Verglichen wurden die injizierten Horizontalzellen der transgenen Mäuse mit den Horizontalzellen der wilden Maus. Die Ergebnisse zeigen, dass die Degeneration der Photorezeptoren nicht zur Degeneration der Horizontalzellen führt.

Summary

Vertebrate retinae are all organized in five layers: outer and inner nuclear layers, ganglion cell layer, outer and inner plexiform layers (synaptic layers). The nuclear layers contain the cell bodies of the major classes of retinal neurons. Photoreceptors are located in the outer nuclear layer, horizontal, bipolar, and amacrine cells have their cell bodies in the inner nuclear layer, and ganglion cells are in the ganglion cell layer. Of all the classes of retinal neurons, amacrine cells are the most diverse with respect to morphology, size, and retinal coverage. Surprisingly, a classification of all amacrine cells in the mouse retina has not been created.

The mouse is a widely used animal model for the application of transgenic technology, which offers a new set of tools for studying the functions of the nervous system. The first goal of my thesis project was to classify the amacrine cell types located in the ganglion cell layer of the mouse retina. I found 10 different types of displaced amacrine cells; six of them are novel types which have not been described before.

Retinal neurons communicate using chemical synapses as well as gap junctions, where membranes of the two communicating neurons are linked by a special kind of intercellular contact. Gap junctions are formed by two end-to-end hexameric structures called connexons, formed by six proteins called connexins. Thus connexins are the proteins that form the intercellular channels that compose gap junctions. Gap junctions have been reported to be expressed in all the major classes of the vertebrate retina. In the rodent retina, Cx36 is expressed in cone photoreceptors. Horizontal cells are extensively coupled to other horizontal cells by a specific connexin, Cx57. Bipolar cell types express two different connexins, Cx45 and/or Cx36, and many ganglion cells types exhibit tracer coupling to retinal neurons by expressing different connexins. All

these connexins (Cx36, Cx45, Cx57 and Cx30.2) have different and specific properties which might be correlated to the different functions of these retinal neurons.

The second goal of my work was to identify the Cx45-expressing amacrine cells and Cx30.2-expressing ganglion cells using transgenic mice. My results showed that Cx45 is expressed in a specific amacrine cell type which is identical to the S1 and S2 indoleamine-accumulating amacrine cells in the rabbit and is similar to the A17 amacrine cells in cat retina. These cell types are very important for night vision since they play a role in the rod pathway. The majority of their synaptic output is sent back onto rod bipolar cell axon terminals. Both of these rod amacrine cell types form electrically coupled networks. I found six different types of Cx30.2-expressing ganglion cells. One of these was a giant ganglion cell type coupled to numerous displaced amacrine cells through gap junctions involving Cx30.2 and an unidentified protein.

Lastly, I collaborated on two big projects with horizontal cells. My work in the first project was to demonstrate the expression of Cx57 in horizontal cells of the wild type mouse retina. I showed the presence of Cx57 in dendrites and axon terminals in horizontal cells of the mouse retina, supporting previous studies that reported Cx57 to be specific to horizontal cells. In the second project, I analyzed the morphology of the horizontal cells in transgenic mice where the photoreceptors are degenerated. The injected horizontal cells did not present any morphological anomalies compared to the horizontal cells of the wild-type mouse retina.

1. The retina

The retina or neural portion of the eye is a thin sheet of neuronal tissue and actually part of the central nervous system (CNS). The retina comprises complex neural circuitries that convert the graded electrical activity of photoreceptors into action potentials that travel to the brain via the optic nerve.

Visual signals are processed by five main retinal classes of neurons (Fig.1): Photoreceptors, horizontal cells, bipolar cells, amacrine cells, and ganglion cells. The cell bodies are stacked in the nuclear layers. The somata of the photoreceptors are located in the outer nuclear layer (ONL), whereas the cell bodies of horizontal, bipolar and amacrine cells are in the inner nuclear layer (INL). Horizontal cell somata lie along the outer margin of the INL; bipolar cell bodies are located in the middle of the INL and amacrine cells are arranged along the proximal border of the INL. The ganglion cell bodies make up the last layer, the ganglion cell layer (GCL).

Some exceptions have been found in the retina, when for example ganglion cells are found in the INL, amacrine cells in the GCL, horizontal cells in the GCL and amacrine cells in the outer plexiform layer (OPL) (Silveria et al., 1989; Lima et al., 2005; Abdel-Majid et al., 2005; Lee et al., 2006; Lin and Masland, 2006). Such cells are referred to as displaced cells, although it has been shown conclusively that displaced amacrine cells found in the GCL are a constant feature of many if not all vertebrate retinae.

The processes and synaptic contacts are located in two different layers: the inner plexiform layer (IPL) and the OPL. The terms inner and outer designate relative distances from the center of the eye: inner, near the center of the eye, and outer away from the center.
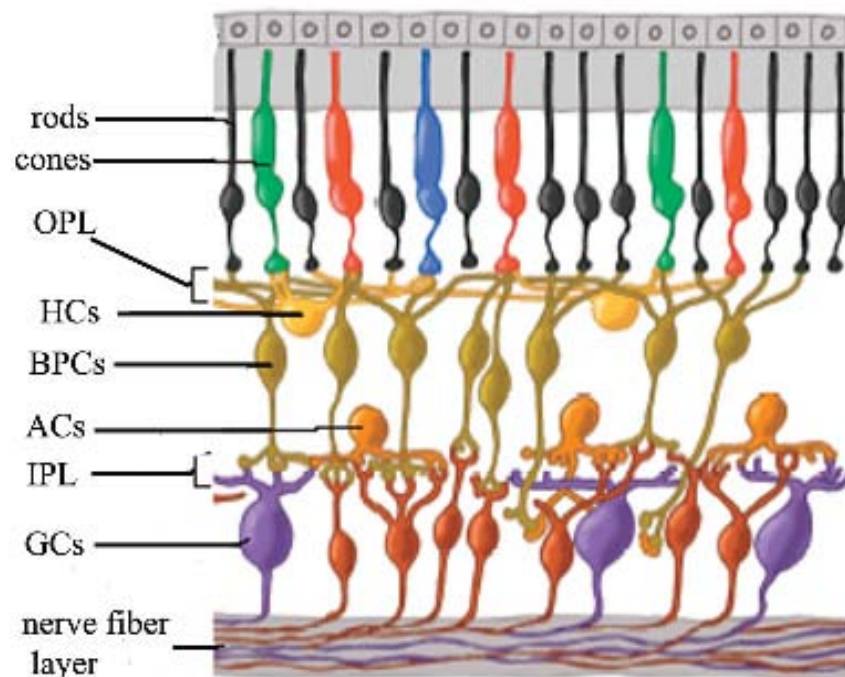
Fig. 1. Diagrammatic scheme of the retina showing the variety of neurons. OPL: outer plexiform layer; HCs: horizontal cells; BPCs: bipolar cells; ACs: amacrine cells; IPL: inner plexiform layer; GCs: ganglion cells. Picture modified from Kolb (2003).

The physiology of the retina comprises two major different functions. First, the retina converts the light into electrical signals by the photoreceptors, which are sensitive to the light. There are two types of photoreceptors, rods and cones. Rod and cone systems are specific for different aspects of vision. Rods are very sensitive to light and are activated at very low levels of light (dim light) and therefore they mediate night vision (scotopic vision). In contrast, the cone system is adapted to detect the brighter conditions of daylight and is the responsible for color and form.

Second function of the retina is the codification of the visual stimuli (form, movement and color).

Photoreceptors make synaptic contacts with the bipolar cells which send the information to the ganglion cells. Photoreceptors respond to a light stimulus with a slow hyperpolarization, and release glutamate at their specialized synaptic terminal, the cone pedicle. The postsynaptic neurons, the bipolar cells, express different sets of glutamate receptors (GluRs) at their contacts with the cone pedicles. OFF cone bipolar cells express ionotropic glutamate receptors, whereas ON cone bipolar cells express the metabotropic glutamate receptor mGluR6. OFF cone bipolar cells transfer their signals onto OFF ganglion cells, whereas ON cone bipolar cells make synapses onto ON ganglion cells.

Ganglion cells relay the information to the central nervous system (CNS) by projecting to the lateral geniculate nucleus, the superior colliculus and to brain stem nuclei (reviewed in Kolb, 2003; Wässle 2004).

2. Electrical synapses

A mode of signal transmission between neurons is constituted through electrical synapses (gap junctions). Electrical synapses have been reported in immature and adult mammalians as well as in invertebrates. In the mammalian retina, gap junction-mediated dye transfer has been found in all the main classes of neurons that form the neuronal retinal network (reviewed in Söhl et al., 2005).

2.1 Gap-junction proteins

2.1.1 The connexins

Gap junction's plaques are clusters of intercellular channels connecting the cytoplasm of two adjoining cells. By providing low-resistance for ions, small molecules (e.g., Ca++, c-AMP, glutathione), nucleotides, amino acids and second messengers, electrical connections allow the direct transmission of electrical signals. Generally, gap junction channels allow the passive diffusion of molecules of up to 1200 Daltons (Simpson et al., 1977; Evans and Martin, 2002). These channels that make up the gap junctions are made of two hemi-channels or connexons. One connexon is located in the membrane of one cell and docks with the connexon of the adjacent cell forming an aqueous pore. Each connexon is made of six proteins coined connexins which are abbreviated as "Cx" (Fig. 2A; for review, see Söhl et al., 2005). Homotypic gap junctions comprise two identical connexons, heterotypic gap junctions are built from two different connexons on the two sides of the junction (reviewed in Söhl et al., 2005).

Connexins are commonly named by their predicted molecular mass in kDa, with a prefix for species where necessary (e.g. Cx45 with 45 kDa, Cx30.2 with 30.2 kDa, mCx36 with mouse 36 kDa connexin, hCx25 with 25 kDa human connexin, and so on). So far, 20 connexin genes have been found in the mouse and 21 in the human genome (Söhl and Willecke, 2003).

In vertebrates (during development, morphogenesis, pattern formation and in the adult organism) most cells communicate via gap junction (Bruzzone et al., 1996; Goodenough et al., 1996; Bennet et al., 2001), but they are absent in adult skeletal muscle, erythrocytes, thrombocytes and spermatocytes.

2.1.2 Gap junction structure

In transmission electron micrographs of ultrathin tissue sections, gap junctions appear as regions where the plasma membranes of two adjacent neurons are separated by a small gap of 2-3 nm (Robertson, 1963; Benedetti and Emelot, 1965; Revel and Karnovsky, 1967). Electron micrographs of freeze-fracture replicas of vertebrate junctions have shown that the connexons (hemichannels) are ordered in a hexagonal pattern.
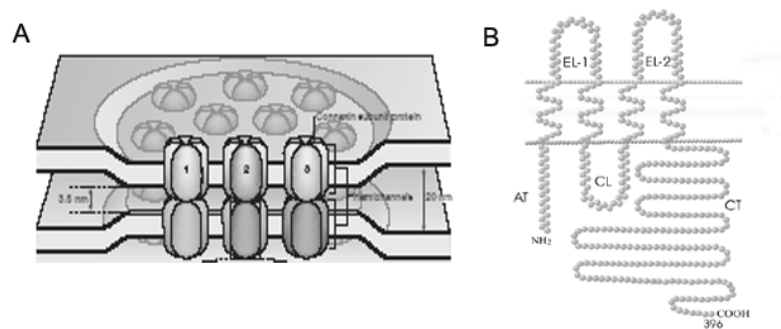
Fig. 2. Gap junction channel and connexin structure. A) Gap junction channels assemble in plaques containing few to several hundred single channels. Each cell contributes one hemichannel called connexon that consists of six connexin proteins. B) Example of a connexin, typically thread through the membrane four times, with the AT, CT and CL exposed to the cytoplasm. Connexin arrangement in the membrane. Yields two extracellular loops designated EL-1 and EL-2. (modified from Söhl et al., 2005; Laird, 2006)

Each connexin protein is an integral membrane protein with four alpha-helical trans-membrane domains (TM) connected by two extracellular loops (EL-1 and EL-2), an intracellular loop (CL) and cytoplasmic N- (AT) and C-terminal (CT) ends which are intracellular (see Fig. 2B). The two EC loops each have three cysteines that are

spaced in a specific manner. This topology was confirmed for Cx43, Cx32 and Cx26 (Hertzberg et al., 1988; Milks et al., 1988; Yancey et al., 1989; Laird and Revel, 1991; Zhang and Nicholson, 1994; Goodenough et al., 1998) and it seems that this topology is a common feature for all connexins. The two extracellular loops can be involved in the interaction between hemichannels of neighboring neurons, and the cysteine set are thought to keep this structure rigid.

2.2 Gap junctions in the mammalian retina

The mammalian retina expresses multiple connexins that mediate the coupling of different cell types. Tracer injections has been a powerful tool in identifying the sites of gap junctions in neurons (Güldenagel et al., 2001; Veruki and Harveit, 2002; Deans et al., 2002; Schubert et al., 2005a,b). In the mammalian retina, four different connexins have so far been reported to build electrical synapses, and it is very likely that this list is not complete. Cx36 has been described in AII amacrine cells (Feigenspan et al., 2001; Mills et al., 2001; Feigenspan et al., 2004), photoreceptors (Deans et al., 2002; Lee et al., 2003; Feigenspan et al., 2004), bipolar cells (Feigenspan et al., 2004; Lin et al., 2005; Han and Massey, 2005) and alpha ganglion cells (Schubert et al., 2005a; Völgyi et al., 2005). AII amacrine cells form homotypic gap junctions made of Cx36 with one type of ON cone bipolar cell (Lin et al., 2005; Han and Massey, 2005) and heterotypic gap junctions involving Cx45 with bipolar cells (Maxeiner et al., 2005; Dedek et al., 2006). Cx45 is expressed in bipolar cells (Maxeiner et al., 2005), bistratified ganglion cells (Schubert et al., 2005b) and in amacrine cells (Maxeiner et al., 2005).

Most mammalian retinae have two types of horizontal cells, the A-type and the B-type (Masland, 2001). Gap junctions in A-type horizontal cells are composed of Cx50 in

the rabbit (O'Brien et al., 2006). In the mouse retina, only one type of horizontal cell has been described (B-type), which expresses Cx57. These cells lose their electrical coupling in Cx57-deficient mice (Hombach et al., 2004).

Despite these known gap junction proteins, it is likely that still other connexin genes are expressed in the mammalian retina. For example, Xin & Bloomfield (1997) showed that many ganglion cell types exhibit tracer coupling. Besides the direction-selective and alpha ganglion cells, the connexin involved in the electrical coupling of the remaining ganglion cell types is unknown. I will focus on the electrical synapses of horizontal, amacrine, and ganglion cells here.

2.2.1 Horizontal cells

Horizontal cells are second-order neurons located in the INL of the retina. They modulate the synaptic transmission between photoreceptors and bipolar cells. It is believed that they are anatomically and functionally rather similar throughout mammals (reviewed in Masland, 2001). One of the most comprehensive, comparative anatomical descriptions of mammalian horizontal cells is that by Ramón y Cajal (1893). He concluded that the basic components of all mammalian retinae are virtually identical and, in particular, that there are two types of horizontal cells: the A-type, an axonless horizontal cell, and the B-type, with a single axon ending in the rod terminals (Peichl and González-Soriano, 1993).

The mouse retina contains only one type of horizontal cell, the axon-bearing type (Suzuki and Pinto, 1986; He et al., 2000). The axonless cell has never been observed in mice. The B-type horizontal cell has an axon that extends 100 µm or more across the retina and at the end, branches to form a telodendritic arbor. Their

dendrites and axonal arborizations form a dense network in the OPL. When the low weight tracer Neurobiotin is intracellularly injected into a horizontal cell, it passes through the gap junctions revealing an extensive coupled network (Fig. 3). The connexin that mediates these coupling patterns has been identified as Cx57 in the mouse retina by Hombach et al., in their 2004 study. They created a mouse line in which the Cx57 is eliminated and replaced by a lacZ reporter gene.

In this mouse line, the expression of beta galactosidase was specifically located in the horizontal cells, tracer coupling was impaired, and the horizontal cell receptive field size was significantly reduced (Hombach et al., 2004; Shelley et al., 2006). However, the exact localization of this connexin on horizontal cells had never been reported since no specific antibodies had been developed. In our lab, a specific antibody was developed and I tested it in injected horizontal cells.
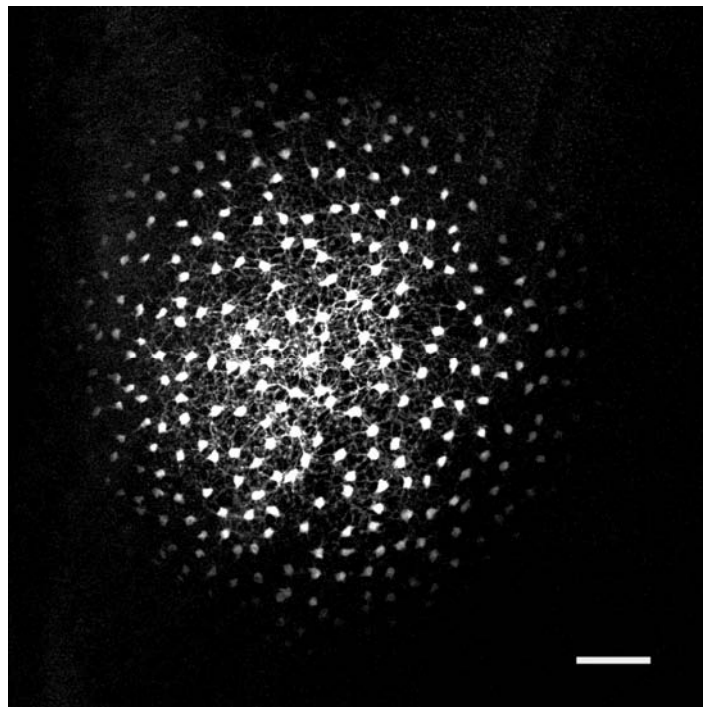
Fig. 3. A Neurobiotin injected horizontal cell shows an extensive coupled network in C57BL/6 mouse retina. Scale bar = 80 µm.

The electrical coupling between the horizontal cells in the mammalian retina has been reported to be modulated by ambient light through neuronal messengers such as dopamine, and retinoic acid (reviewed in Weiler et al., 2000). Under light-adapted conditions, there is a sustained reduction of horizontal cell coupling and this uncoupling is mediated through activation of D_1 receptors. Retinoic acid reduces the coupling between horizontal cells and with the time, the coupling is completely abolished (reviewed in Weiler et al., 2000).

Mammalian horizontal cells receive inputs from both types of photoreceptors (reviewed in Wässle and Boycott, 1991) but the contributions of their inputs to the light responses of the mouse retina have not been investigated. In a work performed by Dr. Jennifer Trümpler (2008, in press), she investigated these contributions. The goal of this project was to analyze the role of the axon by using different mouse lines, in which the contributions of photoreceptors are isolated. She analyzed the light responses of the horizontal cells using the following mouse lines (Cx36, CNGA3, and rhodopsin knock-out mouse lines and CNGA3-Cx36 double knock-out). In the Cx36 knock-out mice (Güldenagel et al., 2001), the coupling between rods and cones is impaired (Deans et al., 2002). In the CNGA3 knock-out mice, the cone inputs to the horizontal cells are eliminated (Biel et al., 1999), and in the rhodopsin knock-out mouse line, the horizontal cells do not receive inputs from rod photoreceptors (Humphries et al., 1997). Since photoreceptors are degenerating in two of these mouse lines, it could produce degeneration in the morphology of horizontal cells. My part of the work was to analyze the morphology of the horizontal cells in the CNGA3-Cx36 knock-out mouse line.

2.2.2 Amacrine cells form electrical networks

The name amacrine cell was given by Cajal to cells that have no axon. Amacrine cells are second-order of inhibitory neurons in the retina that modulate the information flow from bipolar cells to ganglion cells in the IPL. Amacrine cells constitute the most diverse group of cell types within the retina. They have been classified into morphological groups based on two main parameters:

1. - Diameter of the dendritic field

2. - Ramification patterns in the IPL

By the size of the dendritic trees, they are classified into narrow-, small-, medium- and wide-field amacrine cells. According to the ramification patterns they could be mono-, bi-, multistratified or diffuse. Classifications of amacrine cells have been surprisingly few in the mouse retina but despite the fact that the number of amacrine cell types is uncertain, there may be between 30 and 40 types, based on differences in dendritic architecture, retinal distribution, and neurotransmitter used (for review see Wässle and Boycott, 1991).

Amacrine cell bodies are either placed in the INL or situated in the GCL. In the inner part of the INL they form a layer of about two cell bodies thickness, and they comprise 41% of all cells in that layer (Strettoi and Masland, 1995; Jeon et al., 1998). This layer is also called the amacrine cell layer. Despite their diverse morphology, the neurochemical properties look relatively simple. Most of them contain glycine or GABA as primary neurotransmitter and many of them contain a second neuroactive substance (Vaney, 1990).

Glycinergic amacrine cells are generally small-field amacrine cells with diffusely branching dendrites, vertically orientated and often bistratified dendritic trees. They

include at least ten different morphologic types, among which are the AII amacrine cells (Pourcho and Goebel, 1985; Vaney, 1990; Menger et al., 1998; MacNeil and Masland, 1998; Shen and Jiang, 2007). AII amacrine cells are crucial interneurons in the rod pathway that receive input from rod bipolar cells, providing output onto ON-cone bipolar cells through gap junctions and onto OFF-cone bipolar cells through chemical synapses (Kolb and Famiglietti, 1974). Glycinergic amacrine cells inhibit light responses in ganglion cells, suppress glutamate release in bipolar cells, and suppress synapses from other amacrine cell types (Pourcho and Owczarzak, 1991; Maple and Wu, 1998) and they comprise 40-50% of the population of amacrine cells (Pourcho, 1986; Marc, 1989; Pow and Hendrickson, 1999).

GABAergic amacrine cells are usually wide-field amacrine cells and include at least 17 different morphological types (Vaney, 1990; MacNeil and Masland, 1998; Badea and Nathans, 2004; Lin and Masland, 2006). Contrary to the glycinergic amacrine cells, many GABAergic neurons contain or accumulate a second neurosubstance. Examples include the cholinergic starburst amacrine cells (Vaney et al., 1981), the indoleamine accumulating cells (Vaney, 1986), dopaminergic amacrine cells (for review, Witkovsky, 2004), and substance P-immunoreactive amacrine cells (Pourcho and Goebel, 1988, Vaney et al., 1989). GABAergic amacrine cells comprise two different subgroups, axonless and polyaxonal cells. Both subgroups exist in mammalian retinae (Badea and Nathans, 2004; Lin and Masland, 2006). Examples of the axonless wide-field amacrine cells are the "bow-tie" cells and A17 cells, polyaxonal (axon-bearing) amacrine cells seem to be the predominant subgroup of the wide-field amacrine cells in the mouse retina. They present the same characteristics between all of them: they have short dendrites (presumed to be the

input zones) and long axon-like dendrites (output zones) emitted from the soma or dendritic branches.

Amacrine cells are connected with bipolar cells, ganglion cells and other amacrine cells not only by chemical synapses but also by gap junctions (see chapter 2.1). Amacrine cells are coupled to amacrine cells, bipolar cells, ganglion cells or are uncoupled by heterotypic or homotypic gap junctions.

For my thesis, I will focus on the rod amacrine cells, especially the A17 cells.

2.2.2.1 Rod amacrine cells

Three amacrine cell types are essential in the rod pathway in all mammalian retinae. The narrow-field AII amacrine cell, which is a narrow-field amacrine cell with a dendritic tree diameter typically 30-70 µm and has bistratified morphology. This cell type of amacrine cell links the rod and cone pathways so that the rod signals can also use the cone bipolar pathways to make synapses onto ganglion cells. This amacrine cell is primarily postsynaptic to rod bipolar axon terminals in lower sublamina b of the IPL (Strettoi et al., 1992).

The AII passes rod-driven information to cone bipolar cells that make contact with ganglion cells of sublamina b. It does so through large gap junctions with these cone bipolar axons before they make in turn their ribbon synapses to those ganglion cells. Injecting AII amacrine cells with Neurobiotin-filled electrodes have demonstrated that AII amacrine cells contain two different types of electrical synapses. These are homologous coupled to other AII amacrine cells and heterologous coupled to ON-cone bipolar cells. There is strong evidence that AII amacrine cells express Cx36 (Feigenspan et al., 2001; Mills et al., 2001). The heterologous couplings with ON-

cone bipolar cells are heterotypic because they do not express the neuron specific-Cx36 (Feigenspan et al., 2001; Mills et al., 2001).

The ON-cone bipolar cells express a different Cx than Cx36 or Cx57. This Cx has been identified as Cx45 in all ON-cone bipolar cells (Maxeiner et al., 2005) with the exception of the type 7 (according to the classification of Ghosh et al., 2004) which seems to express Cx36 (Lin et al., 2005; Han et al., 2005).

The second rod amacrine cell is the so called A17 type or reciprocal amacrine (see below).

There is another amacrine cell type involved in the rod pathway which influences both AII and the reciprocal amacrine cell. This cell is the dopaminergic cell (interplexiform cell).

2.2.2.1.1 A17 amacrine cells

Using fluorescence histochemical methods in the rabbit retina, Ehinger and Floren (1976) observed that some retinal neurons accumulate serotonin. The endogenous concentration of serotonin is very low in the rabbit retina and therefore these cells were named "indoleamine-accumulating". This group of indoleamine-accumulating cells comprises five subpopulations, two of them located in the GCL and three in the INL (Sandell and Masland, 1986). In the INL, one of these cells could be an interplexiform cell based on its morphology. The other two types are known as S1 and S2 amacrine cells in the rabbit retina (Vaney, 1986). S1 and S2 cells are radial wide-field amacrine cells presenting a large number of thin dendrites, decorated at regular intervals with prominent varicosities. These neuron types were found in the INL and GCL of the rabbit retina but their dendritic trees are flatter than the S1 and

S2 located in the INL (Sandell and Masland, 1986). Dendrites of these cells located in the INL go through the IPL and terminate in strata 5 in a diffuse way, forming a dense plexus (cat: S4 and S5, Nelson and Kolb, 1985; rat: S5, Menger and Wässle, 2000). These cells make reciprocal synapses with rod bipolar cells (Sandell et al., 1989).

Despite being very similar, the S1 and S2 exhibit some differences. The S1 is larger and presents large varicosities while the S2 is much smaller and has more but smaller varicosities (Vaney, 1986; Sandell and Masland, 1986; Zhang et al., 2002). The dendrites of the S2 cell are more tangled, radiating dendrites. Tracer coupling of these cells has been described previously (Vaney, 1994; Xin and Bloomfield, 1997). When Neurobiotin is injected into these cells, the S1 cells show extensive homologous coupling to other S1 cells, whereas S2 cells present less coupling. Crossover coupling between the two cell types has rarely been detected (Li et al., 2002).

These cells are GABAergic, and comprise 20% of all GABAergic amacrine cells (Massey et al., 1992). Confocal analysis done by Zhang et al. (2002) showed that the varicosities of these cells are synaptic sites and are located closed to rod bipolar cell terminals. In addition, Fletcher and Wässle (1999) found the postsynaptic localization of $GABA_A$ and $GABA_C$ receptors on rod bipolar cells.

The morphological differences between S1 and S2 cells could indicate different functions. Zhang et al. (2002) proposed that the lateral inhibitory input close to the rod bipolar cells must be dominated by the S2 cells, because of the distribution of the S2 varicosities, and provide a more local feedback, since these cells are not strongly coupled. S1, having a larger dendritic field and strong coupling (Vaney, 1994; Li et

al., 2002) could provide a more distant signal contributing to the antagonist surround of the rod pathway (Völgyi et al., 2002).

 The A17 rod amacrine cell of the cat is morphologically identical to the S1 indoleamine-accumulating cell of the rabbit (Nelson and Kolb, 1985; Wässle et al., 1987; Vaney, 1994). As in the rabbit retina, A17 cells have been described in the mouse retina (Badea and Nathans, 2004) but the coupling patterns and the connexin involved are unknown.

2.2.2.2 Displaced amacrine cells

In the GCL there are two types of neurons: ganglion cells and amacrine cells which are termed displaced amacrine cells. The difference between these neurons is that the amacrine cells lack an axon whereas the ganglion cells have centrally-projecting axons that send their messages to the brain. Evidence of displaced amacrine cells is now available in almost all mammalian GCL. Equal numbers of each type of neuron were found in the rat retina (Perry and Walker, 1980) while in the rabbit retina about one-third of the neurons in the GCL are displaced amacrine cells (Hughes and Vaney, 1980; Vaney, 1980), and up to 75-80% in the peripheral areas of the cat retina (Hughes and Wieniawa-Narkiewicz, 1980; Wong and Hughes, 1987). In the hamster and ground squirrel retina, approximately one half of the neurons in the GCL are displaced amacrine cells, the other half are ganglion cells (Linden and Esbérard, 1987; Abreu et al, 1993). In humans, displaced amacrine cells represent 3% of the total cells in central retina and nearly 80% in the far periphery (Curcio and Allen, 1990), and in the adult tammar wallaby which has half as many ganglion cells and three times as many displaced amacrines as rabbit and cat (Wong et al., 1986). The squirrel retina has ten types of displaced amacrine cells (Linberg et al., 1996) and in

the rat retina, at least six different types of displaced amacrine cells in the GCL which comprise medium-field cells to wide-field amacrine cells (Perry and Walker, 1980) are known and in the cat four types of displaced amacrine cells where found (Waessle et al., 1987).

In the GCL of the mouse retina the fraction of ganglion cells is 43-44% making the displaced amacrine cells a fraction of 56-57% (Jeon et al., 1998).

The majority of experiments with displaced amacrine cells were done with immunohistochemical experiments and most of these neurons are known only from occasional Golgi impregnations. Studies were also done with Nissl staining and neurons were classified as ganglion cells or displaced amacrine cells according to the disposition of Nissl substance. Experiments with antibodies do not reveal any information of the morphology of the displaced amacrine cells. With the exception of a few displaced amacrine cell types (Badea and Nathans, 2004; Lin and Masland, 2006), the identity of displaced amacrine cells is largely unknown. For my thesis, I have created a classification of displaced amacrine cells in the mouse retina.

2.2.3 Ganglion cells exhibit tracer coupling

Ganglion cells are neurons located in the GCL. Ganglion cells are the output units of the eye sending a message to the brain. As a general rule, the activity of bipolar cells tends to increase the firing rate of the ganglion cell, and the activity of amacrine cells tends to decrease it.

Neuroanatomists have classified the neurons according to the same features. The criteria commonly used have been the soma, dendritic field size, pattern and level of stratification. The morphology of the cells serves as a neuronal signature, allowing one type to be distinguished from another.

In the mouse retina there are at least 10-15 different morphological types of ganglion cells (Masland, 2001; Sun et al., 2002a; Kong et al., 2005; Coombs et al., 2006). Microinjections with Neurobiotin into ganglion cells have demonstrated that coupling is a common feature of many ganglion cell types. Ganglion cells can couple to GABAergic amacrine cells, to glycinergic amacrine cells, to other ganglion cells or to both ganglion and amacrine cells. Interestingly, these coupling patterns are conserved through various animal species as well as the dendritic morphology of several types, for example, "giant" or α-ganglion cells. Since David Vaney (1991) observed tracer coupling in the alpha ganglion cells, the molecular identity of the connexins in retinal neurons has been extensively studied.

Sun et al., in his 2002a study, classified the ganglion cells into four groups based on their soma size, dendritic field size, and pattern and level of stratification. Monostratified ganglion cells were included in three different groups: RGA (see below), RGB and RGC. RGB cells comprised ganglion cells with small to medium-sized dendritic field and RGC neurons have medium to large-sized dendritic field.

Bistratified ganglion cells are included onto the last group (RGD). Briefly, I will summarize the A group of ganglion cells (Sun et al., 2002a) focusing on the gap junctions and the cxs involved.

2.2.3.1 Group RG$_A$

Sun et al., (2002a) classified the ganglion cell types in four different groups. The first group, named RG$_A$, comprises three ganglion cell subtypes, two of them correspond to the well-known alpha ganglion cells and the remaining one corresponds to the "giant" ganglion cells or RG$_{A1}$. All the cell types included in this group exhibit tracer coupling when injected with Neurobiotin (Vaney, 1991; Huxlin and Goodchild, 1997).

2.2.3.1.1 RG$_{A1}$

In the mouse retina, RG$_{A1}$ cells express large, polygonal somata of 18.23 ± 1.2 µm. From the soma, three to five stout primary dendrites branch in a radial pattern, resulting in a large dendritic field size of 281.47 ± 19.38 µm. The dendrites branch distantly from the soma, resulting in few dendrites proximal to the soma. A confocal picture of a typical RG$_{A1}$ is shown in figure 4A. These cells are equivalent to Perry's (1979) type 1 cells, Dreher et al., (1985) and Martin's (1986) class I cells, and the ON alpha cells of Peichl (1989) and Tauchi et al. (1992).

Coupling patterns: In the mouse retina RG$_{A1}$ are heterologously coupled to numerous displaced amacrine cells, whereas in rat retinae, these cells are coupled to ganglion cells and amacrine cells (Huxlin and Goodchild, 1997).

Which connexin is responsible for this tracer coupling? In a work performed by Schubert et al. (2005a), injections in Cx36 knockout of RG$_{A1}$ cells with Neurobiotin demonstrated that Cx36 is not responsible for forming these gap junctions. The identity of the connexin in RG$_{A1}$ ganglion cells will be determined in my thesis work.
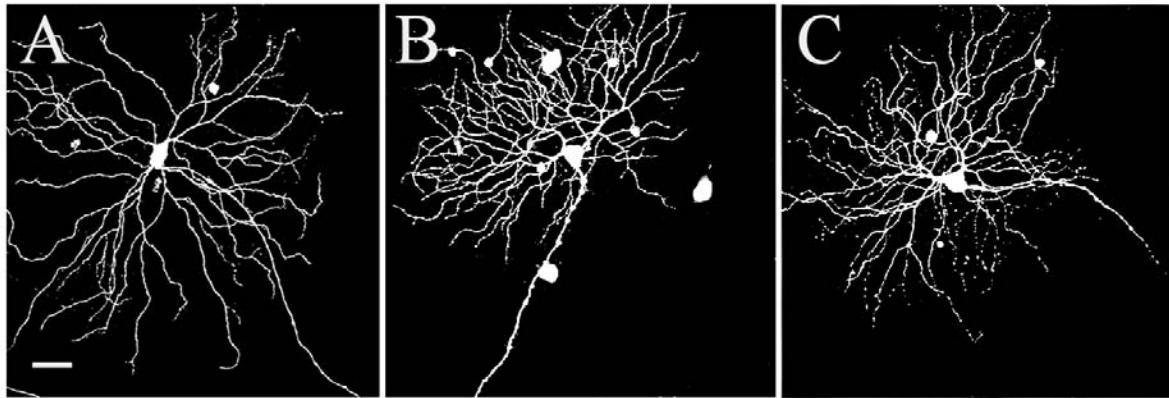
Fig. 4. A comparison between RG$_{A1}$ and RG$_{A2}$. A) shows a RG$_{A1}$ coupled to displaced amacrine cells. B) illustrates a RG$_{A2}$ outer (an OFF alpha cell) coupled to big cells corresponding to other RG$_{A2}$ outer cells and small cells located in the INL corresponding to amacrine cells. C) a RG$_{A2}$ inner (ON alpha cells) showing their typical coupling patterns. Scale bar = 40 µm.

2.2.3.1.2 RG$_{A2}$ or α- ganglion cells

Alpha cells are a type of ganglion cells described first in the cat retina (Boycott and Wässle, 1974) and they comprise 2-4% of the ganglion cell population (Peichl and Waessle, 1981). Two types of α- ganglion cells have been reported in the mouse retina, differentiated on the basis of their stratification patterns. Outer alpha cells (or OFF alpha cells) with a dendritic tree close to the INL border and inner alpha cells (ON alpha cells) close to the GCL border. Alpha cells have a round cell body of approximately 23 ± 4 µm. The shape dendritic trees can be shaped from circular to quite often elliptical (Size = 318 ± 74 µm), and these cells have three to seven primary dendrites that branched proximal to the soma (Sun et al., 2002a ; Schubert et al., 2005a) and very rarely the dendrites overlap (see Fig. 4B, C).

Coupling patterns: Alpha cells conserved their morphology in many, if not all, vertebrate retinae (rat: Perry, 1979; Tauchi et al., 1992; Huxlin and Goodchild 1997;

cat: Peichl and Waessle 1981; rabbit: Peichl et al., 1987; Xin and Bloomfield, 1997). Despite of the conserved morphology, variations in the coupling pattern of these cells have been reported.

In the mouse retina, α- ganglion cells express two distinct tracer coupling pattern: OFF-α ganglion cells are coupled homologously to neighboring OFF-α ganglion cells and heterologously to GABAergic wide-field amacrine cells.

ON-α ganglion cells are coupled to amacrine cells having their somas in the ganglion cell layer or to amacrine cells with somas located in the INL but never show homologous coupling to other alpha cells, as shown by Schubert et al. (2005a) and Völgyi et al. (2005). Interestingly, ON-α ganglion cells in the rabbit retina are not coupled (Hu and Bloomfield, 2003). Mastronarde (1983a–c) speculated that α-cell electrical coupling serves to synchronize the spike activity of neighboring cells. This idea was recently verified by Hu and Bloomfield (2003), who showed that OFF-α cells maintain correlated activity whereas ON-α cells do not, indicating that coupling is essential for synchronization of the discharges between neighboring α cells.

In Cx36 deficient mice, the heterologous coupling of both ON- and OFF- α ganglion cells was lost indicating that the gap junctions between α ganglion cells and amacrine cells depends on Cx36. Whether Cx36 is responsible for the coupling between α cells remains unclear (Völgyi et al., 2005; Schubert et al., 2005a).

3. Aims and objectives

Networks of neurons in several regions of the central nervous system are extensively interconnected by electrical synapses (for review see Galarreta and Hestrin, 2001). The retina provides examples of populations of neurons that make both homologous and heterologous gap junctions. So far, three different connexins have been reported in the mouse retina: Cx36, Cx45, and Cx57 (reviewed in Söhl et al., 2005). But the morphology of many neurons expressing Cx36 and Cx45 is unclear and, it seems very likely that this list of Cxs is not complete. Many different classes of amacrine and ganglion cells have been reported to be coupled (Vaney, 1991; Xin & Bloomfield, 1997) and in many cases, the connexins involved are still unknown. In my thesis I focused on electrical synapses of horizontal, amacrine, and ganglion cells and at the same time on the morphological classification.

3.1 Aim I: Classification of displaced amacrine cells

Amacrine cells are inhibitory interneurons that modulate the information passed from bipolar cells to ganglion cells.

Amacrine cell bodies can be located in the INL or in the GCL (called displaced amacrine cells). The morphology and branching patterns of displaced amacrine cell types have been examined in several mammalian species (e.g. Perry and Walker, 1980; Waessle et al., 1987) but little is known about the displaced amacrine cells in the mouse retina (Badea and Nathans, 2004; Lin and Masland, 2006). The purpose of this work was to classify the displaced amacrine cells in the mouse retina.

3.2 Aim II: Characterization of amacrine cells expressing Cx45

Over the past few years, several studies have revealed an unexpected high density of gap junctions in the retina, composed of different connexins. In this study I classified the Cx45-expressing amacrine cells according to their horizontal and vertical stratification patterns, general morphology, dendritic field size, soma size, coupling patterns, and neurotransmitter content.

3.3 Aim III: Identification of retinal ganglion cells expressing Cx30.2

This connexin, and its putative human orthologue Cx31.9, have been described in the brain, vascular smooth muscles, testis, heart and CNS (Nielsen et al., 2002; Nielsen and Kumar, 2003; Kreuzberg et al., 2005; Kreuzberg et al., 2008). Using a transgenic mouse line in which the Cx30.2 coding region was replaced by the LacZ gene (Kreuzberg et al., 2006), I studied the morphology of the ganglion cell types expressing this protein.

3.4 Aim IV: Morphology of horizontal cells and localization of Cx57

Horizontal cells are extensively coupled by Cx57 (Hombach et al., 2004). My part of the first project was to analyze the localization of the connexin using microinjections and a specific antibody against Cx57. My work in a second project was to study the morphology of these cells in CNGA3-Cx36 double knock-out mice.

4. Material and Methods

4.1 Mouse strains and tissue preparation

All the mice that I used were killed by cervical dislocation in accordance with institutional guidance for animal welfare. Whole-mount retinae were prepared in mouse Ringer medium which contained (in mM) 137 NaCl, 5.4 KCl, 1.8 CaCl $_{2*}$ 2H$_2$O, 1 MgCl$_{2*}$ 6 H$_2$0, 5 HEPES, 10 Glucose, pH adjusted to 7.4 with 0.1 N NaOH at room temperature or in carboxygenated Ames Ringer solution (pH 7.4).

Retinae were individually floated with photoreceptor side down onto black filter paper (Millipore Corporation, Bedford, MA) and mounted in a recording chamber.

For my thesis, I used the following mouse strains: Cx45 fl/fl: Nestin-Cre, Cx45fl/+: Nestin-Cre (Maxeiner et al., 2005), Cx30.2$^{lacZ/lacZ}$, Cx30.2$^{lacZ/+}$ (Kreuzberg et al., 2006), Cx36$^{-/-}$ (Güldenagel et al., 2001), CNGA3$^{-/-}$ /Cx36$^{-/-}$ and wild-type mice (C57BL/6).

4.2 Intracellular injections

The methods for intracellular injections have been described previously (Schubert et al., 2005a,b). Intracellular injections were carried out with borosilicate glass electrodes (170-200 MΩ) that were pulled with a Sutter puller (Sutter P-97, Brown and Flaming Micropipette Puller, Novato, CA) and filled with a solution containing 0.5% Lucifer Yellow (Sigma, St. Louis, MO) or 1% Alexa Fluor 488, 594 or 488 (Molecular Probes, Eugene, OR) and 4% N-(2-aminoethyl-)-biotinamide hydrochloride (Neurobiotin; Vector Laboratories, Burlingame, CA), dissolved in Tris buffer (pH 7.4-7.5).

To visualize ganglion cell bodies in the WT retinae, a few drops of Acridine orange (1 µM, Sigma) were added to the recording chamber containing the mouse retina. For targeted injection in Cx45-EGFP retinae, the EGFP signal was used to target amacrine cells in the GCL (for more details see chapter 7.1; Pérez de Sevilla et al., 2007) and in the INL. Lucifer Yellow (Sigma, St. Louis, MO)/Alexa dyes (Molecular Probes, Eugene, OR) were iontophoresed with negative current of -1 nA (750 ms at 1 Hz). When the dendritic morphology of the cell could be seen, the direction of the current was reversed to inject positively charged Neurobiotin molecules (Vector Laboratories, Burlingame, CA). Cells were injected for 3-4 minutes depending of their size. After the last injection, the retina remained for at least 30 min in the recording chamber, allowing diffusion of Neurobiotin.

To label living LacZ positive cells, retinae from Cx30.2 lacZ were incubated with fluorescein di-beta-D galactopyranoside (FDG). FDG was purchased from Sigma (1:120 in carboxygenated Ames Ringer solution, pH 7.4). After 1 minute incubation, retinae were washed out in dark for 15 minutes in Ames Medium. Cells were injected as described above.

Then the retinae were fixed in 4% paraformaldehyde for 10-15 minutes.

For injecting horizontal cells, eyes were enucleated and transferred to a Petri dish with carboxygenated Ames ringer solution (pH 7.4) at room temperature. The retina was cut in four pieces and incubated in Ames Medium with DAPI (10 µM, Sigma) for 60 minutes in darkness at room temperature. After incubation, the four pieces were washed in Ames Medium for 20 minutes. Retinae were individually floated with photoreceptor side down onto black filter paper (Millipore Corporation, Bedford, MA).

Horizontal cells were recognized by their large nuclei and localization in the INL.

Horizontal cells were targeted with electrodes filled with Lucifer Yellow and Neurobiotin or with electrodes containing Alexa 488 dye. When the morphology of the neurons could be seen, cells were injected for three minutes with positive current (in the case of Neurobiotin) or negative current (in the case of Alexa 488). Two horizontal cells were injected in each piece of retina.

After the injection, all retina pieces were fixed in 2% PFA for ten minutes and then washed several times in PB (pH = 7.4).

Horizontal cells injected with Neurobiotin, were incubated overnight with Streptavidin-Cy3 at 4°C.

4.3 Immunohistochemistry and confocal microscopy

Fixed retinae were washed for at least 30 minutes in 0.1 M phosphate buffer, pH 7.4 (PB). Neurobiotin was visualized by reacting injected retinae overnight with streptavidin-indocarbocyanine (Cy3, Jackson Immunoresearch, West Grove, PA; dilution 1:500), in 0.1 M PB containing 0.3% Triton X 100 (Sigma).

Some retinae from Cx30.2 lacZ mice were processed by using the beta-galactosidase essay as described by Feigenspan et al. (2004). Briefly, whole-mount retinae were washed in lacZ washing solution and incubated with the beta-galactosidase substrate X-gal during three-four days at 37°C. Neurons with beta-galactosidase reactivity were identified by the reaction product, which consisted of one nuclear black/blue dot.

Retinae were mounted in Vectashield Mountin Medium (Vector Laboratories, Burlingame, CA). The perimeter of the slides was sealed with nail polish for prolonged storage. The mounted slides were stored at 4°C protected from light.

Immunocytochemistry with antibodies against specific proteins completed all the experiments.

Images were taken by a Leica TCS SL confocal microscope.

Intensity and contrast of the final images were adjusted by using photoshop adobe (version 7.0)

4.4 ERG measurements

ERG experiments were carried out as described in Maxeiner et al. (2005). Mice (3 months old) were dark adapted over night before the experiment and then anesthetized by intraperitoneal injection of xylazine (50 mg/kg) and ketamine (20 mg/kg) under dim red light. When the mouse was completely anesthetized, a drop of 1% atropine sulfate was used to dilate the pupils. All procedures involving animals were approved by the local institutional animal care and use committees and were in accordance with the Institute for Laboratory Animal Research Guide for Care and Use of Laboratory Animals. Responses were recorded from the corneal surface of the left eye. The ERG was measured using a stainless steel electrode that made contact with the corneal surface. Needle electrodes placed in the cheek and the tail served as reference and ground leads, respectively. At least 10 responses were averaged at each light intensity. Data analysis was done with Chart v.5.1 and Delta Graph v. 4.0 for statistical analysis.

For more details of the methods, see chapters 7.1, 7.3, and 7.4.

5. Results

5.1 Displaced amacrine cells of the mouse retina (Pérez de Sevilla et al., 2007)

There is evidence of 11 types of displaced amacrine cell in the mouse retina (Gustincich et al., 1997; Badea and Nathans, 2004; Lin and Masland, 2006). Since displaced amacrine cells make up about 56-57% of the somata within the mouse GCL (Jeon et al., 1998), it is probably that many amacrine cell types of the GCL have not been described.

5.1.1 Classification of displaced amacrine cells

More than 400 displaced amacrine cells were labeled in this study. Of these, only the cells which were completely labeled were chosen for creating the classification. The majority of amacrine cells in the GCL of the mouse retina exhibited circular or ovoid dendritic fields, and some wide-field amacrine cells had asymmetric dendritic fields. The soma of the displaced amacrine cells ranged in size from 7-10 μm, with some exceptions.

I adopted the Cajal's terminology to describe the amacrine cells presented in this study. Displaced amacrine cells were classified based on their stratification patterns and dendritic field size. Stratification was determined based on the five strata of the inner plexiform layer (IPL), common for all vertebrate retinae (Cajal, 1973). Displaced amacrine cells were divided into two groups according to their dendritic field size: medium-field cells, with dendritic fields ranging from 200-500 μm; and wide-field cells, with dendritic fields over 500 μm. By injecting Neurobiotin into randomly selected somata in a whole-mount retinal preparation, I identified 10 different morphological types of displaced amacrine cells. Four of the medium-field cell types

were monostratified, including the starburst amacrine cell and one type was bistratified. The wide-field group comprised six types of monostratified and one type of multistratified cell (see Fig. 5).

Cells were named according to the IPL stratum in which their dendrites branched.

The displaced amacrine cells identified in this study share many similarities with amacrine cells described in the rat (Perry and Walker, 1980), turtle (Kolb, 1982), cat (Waessle et al, 1987a) and rabbit (McNeil et al, 1998).

5.1.2 Neurotransmitter expression

Amacrine cells are inhibitory neurons in the mammalian retina, and they can express either GABA or glycine. I used antibodies against these neurotransmitters to analyze which neurotransmitter is expressed in the displaced amacrine cells of the mouse retina. GABA antibodies produced a uniform distribution of labeled cell bodies in the GCL (n = 2 retinae) whereas glycine antibodies labeled few cells in the GCL (n = 3). In addition, GABAergic cell bodies had a small mean diameter size (6.2 ± 1.4 µm, n = 20 cells). This mean size is the same as the displaced amacrine cells described in this study; glycinergic cells in the GCL had bigger mean soma size (11.7 ± 3.6 µm, n = 17). This suggests that the majority of displaced amacrine cells are GABAergic neurons. For more information of the displaced amacrine cells see chapter 7.1 (Pérez de Sevilla et al., 2007).
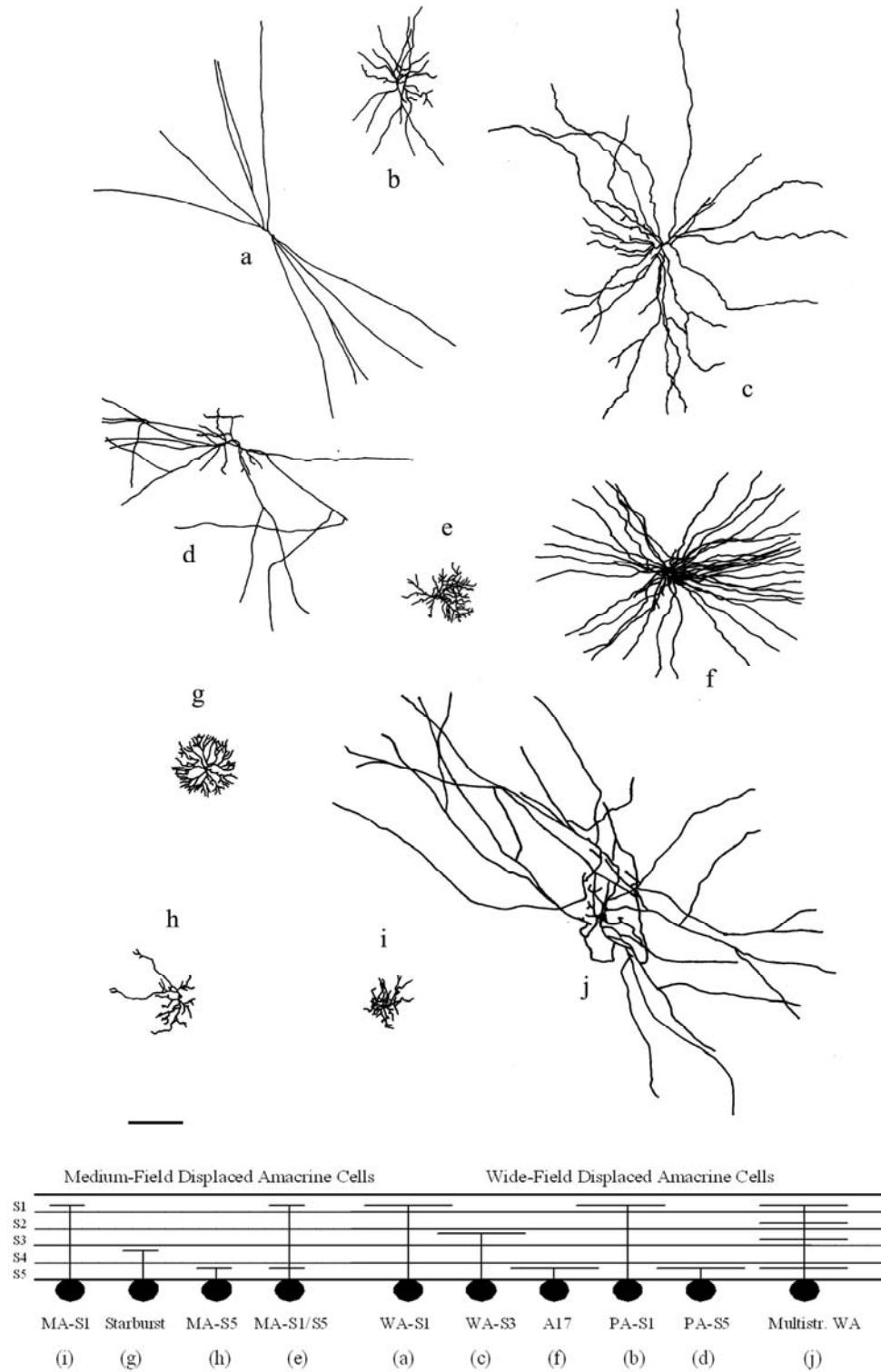
Figure 5 . Illustrations of the ten displaced amacrine cell types identified in this study. The top panel shows the morphology of each cell type; the bottom panel illustrates the stratification depth of each cell type. Scale bar: 200 µm (Pérez de Sevilla et al., 2007).

5.2. Morphological, neurochemical and functional characterization of amacrine cell types expressing connexin45 in the mouse retina

In this study I have characterized these amacrine cells by injecting amacrine cells expressing Cx45 in a transgenic mouse mutant (Cx45fl/fl:Nes-Cre, (Maxeiner et al., 2005)). Briefly, the gene for the cytosolic EGFP was inserted downstream of Cx45 exon 3 in this mouse line. The exon 3 of the Cx45 gene was flanked by loxP sites allowing conditional deletion by Cre-recombinase under the control of the Nestin promoter. These mice express enhanced green fluorescent protein (EGFP) instead of Cx45 gene. Cx45 ablation after removal of exon 3 of the Cx45 gene resulted in a Cx45-deficient retinae.

The expression of EGFP under the control of the Cx45 promoter in Cx45fl/fl: Nes-Cre mice showed neurons in the INL and in the GCL, as well as some blood vessels. EGFP-positive cells in the INL correspond to bipolar cells and amacrine cells (Maxeiner et al., 2005) whereas in the GCL, Schubert et al. (2005b) revealed two types of bistratified ganglion cells expressing Cx45 in the mouse retina.

5.2.1 Classification of Cx45-expressing amacrine cells

Classification of amacrine cells was done based on their horizontal and vertical stratification patterns, general morphology, dendritic field size and soma size. A total of 172 well-filled EGFP-positive amacrine cells were studied in detail for this classification. At least two well-characterized EGFP-positive amacrine cell types were found in the mouse retina.

Type One was a medium-field neuron, with a dendritic field diameter of 366.62 ± 82 µm (mean ± SD; n = 127). This neuron type had a small, round soma of 10.56 ± 1.53

μm and represented approximately 74% of the injected EGFP-positive amacrine cells. These cells had varying morphologies with an oval dendritic field tree and they presented numerous varicosities (Fig. 6). This cell type was always found in the INL but never in the GCL.
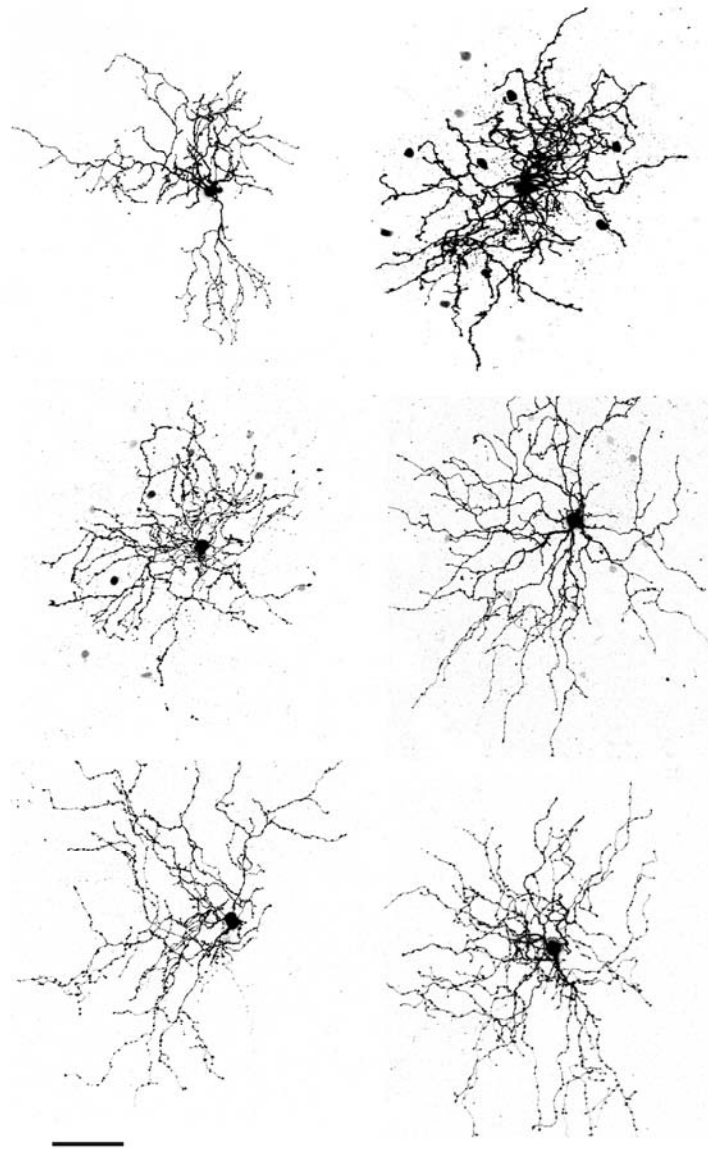
Fig. 6. Confocal pictures of Type One Cx45-expressing medium-field amacrine cells showing the variety of morphologies. These cells were located in the inner nuclear layer. Scale bar = 80 μm.

Type Two was found in the INL and in the GCL. The round soma had a mean diameter of 11.16 ± 1.45 µm (n = 45) and the dendritic field measured 650.17 ± 315 µm. The dendrites branch in a radiate pattern and they are covered by many varicosities. No differences in morphology were found between the cells found in the INL and the GCL (see figure below). These cells were morphologically identical to the S1 cells described in rabbit retina (Vaney, 1986) and the A17 in cat retina (Kolb et al., 1981), respectively.
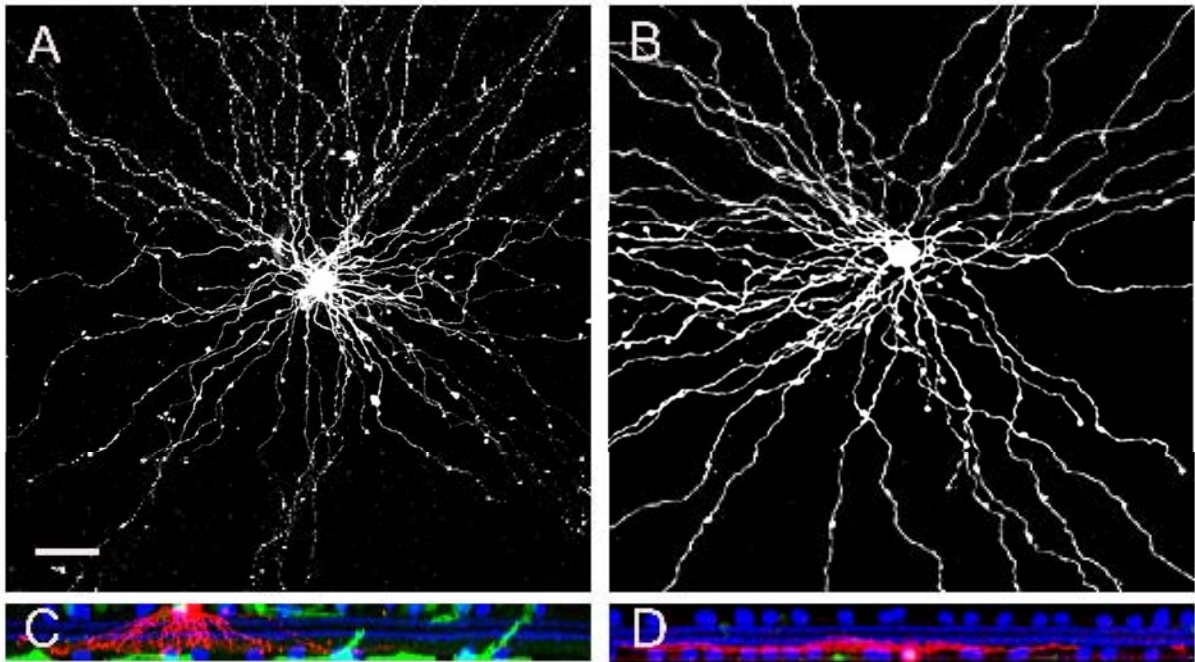
Fig. 7. The radiate amacrine cell morphology in flat-mount and transverse view in A) INL and B) GCL. They do not present any differences in morphology or dendritic field size. C) and D) illustrate the stratification patterns of the neurons in A) and B) (in red). Acetylcholinergic cells are shown in blue, EGFP signal in green. Scale bar = 40 µm.

In order to get an estimation of the vertical distribution of processes within the inner plexiform layer, the two plexi of cholinergic starburst amacrine cells, which characterize the ON and OFF sublaminae, were labeled immunohistochemically with

antibodies against ChAT and used as landmarks. The processes of the acetylcholinergic cells form two bands, corresponding to S2 and S4 in the inner plexiform layer (IPL), dividing the IPL into five strata of equal thickness. The dendrites of the two types of Cx45-expressing amacrine cells stratified in the same way. They gradually descend from the cell body in a diffuse way ending in S5 of the IPL (A17 cells, as shown in Fig. 7C) or in S4/S5 (type one, see Fig. 8C, F). In the case of the displaced A17 amacrine cells, the dendritic tree stratified in S5 but in a monostratified way (Fig. 7D).
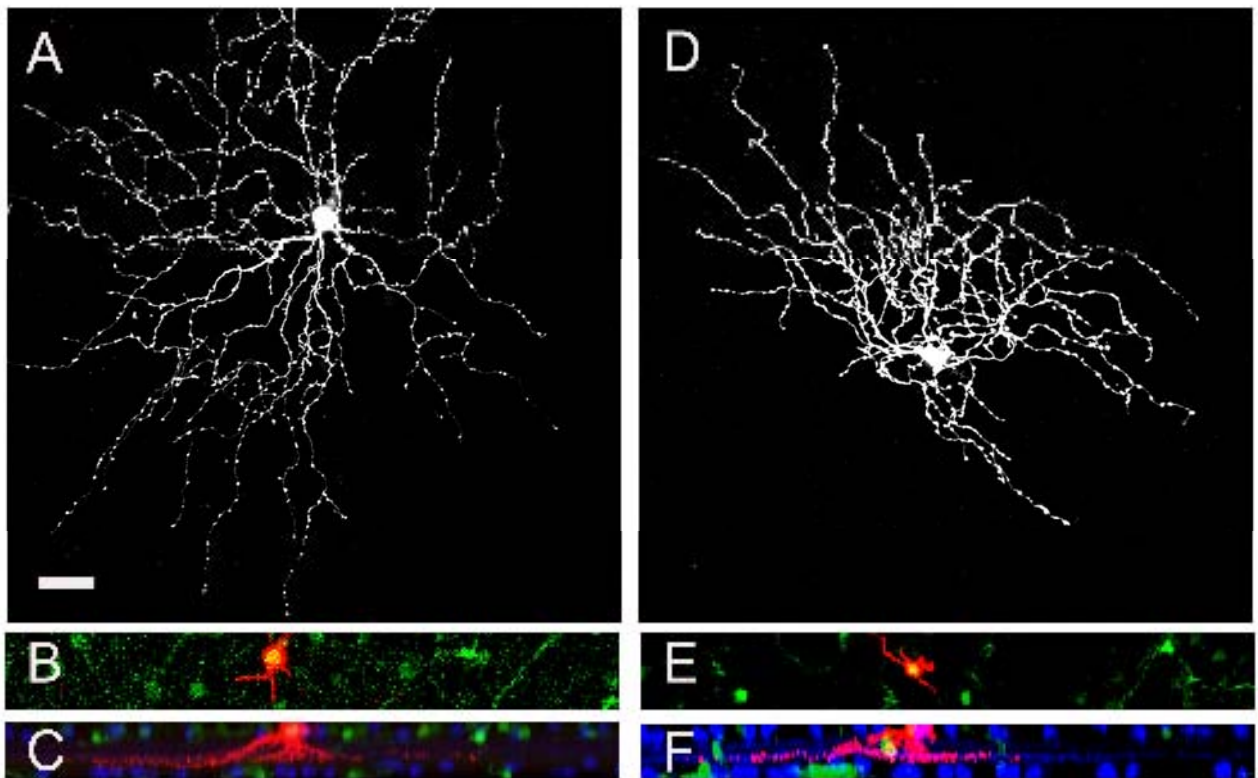
Fig. 8. Morphology and stratification patterns of the Cx45-expressing amacrine cell Type One. A) illustrates the general morphology of a cell in a flat-mounted retina. B) indicates co-localization with the EGFP signal. C) The dendritic arbor ramifies close to the GCL. D) shows another example of a Cx45-expressing type one amacrine cell. E) shows the co-localization with the EFGP signal. E) The type one neuron stratifies in S5 of the IPL. Scale bar = 40 µm.

5.2.2 Coupling patterns of Type One cells

Tracer injection experiments with the Cx45-expressing Type One cells in Cx45 heterozygous mice showed that Neurobiotin can pass directly into adjacent cells. This neuron type was always coupled to numerous amacrine cells located in the INL. I never observed coupled cells located in the GCL. Examples of three cells are shown in figure 9 A, C, and E. The colocalization of the EGFP signal with the injected cells is shown in figure 9 B, D and F. This cell type exhibited homologous (between cells of the same type) and heterologous (between different cell types) coupling. Neurobiotin in coupled cells was observed both in neurons expressing the EGFP signal and in neurons without the EGFP signal (see Fig. 9D). These data indicate that the Type One cell is coupled to other Cx45-expressing amacrine cells, most likely by homotypic gap junctions, and to other amacrine cell type(s) expressing a different connexin, by heterotypic gap junctions.

To evaluate the identity of the coupled partner of this neuron type, EGFP-positive cells (n = 3) were injected with Neurobiotin for ten minutes (see Fig. 9G). The primary dendrites of the EGFP-positive coupled cells did not have the radial morphology of the A17 cells. This suggests that the Cx45-expressing Type One amacrine cell is coupled to other Type One cells. The primary dendrites of the coupled cells that did not contain the EGFP signal (and thus did not express Cx45) could also be visualized (Fig. 9G). They seemed to be medium- or wide-field amacrine cells.
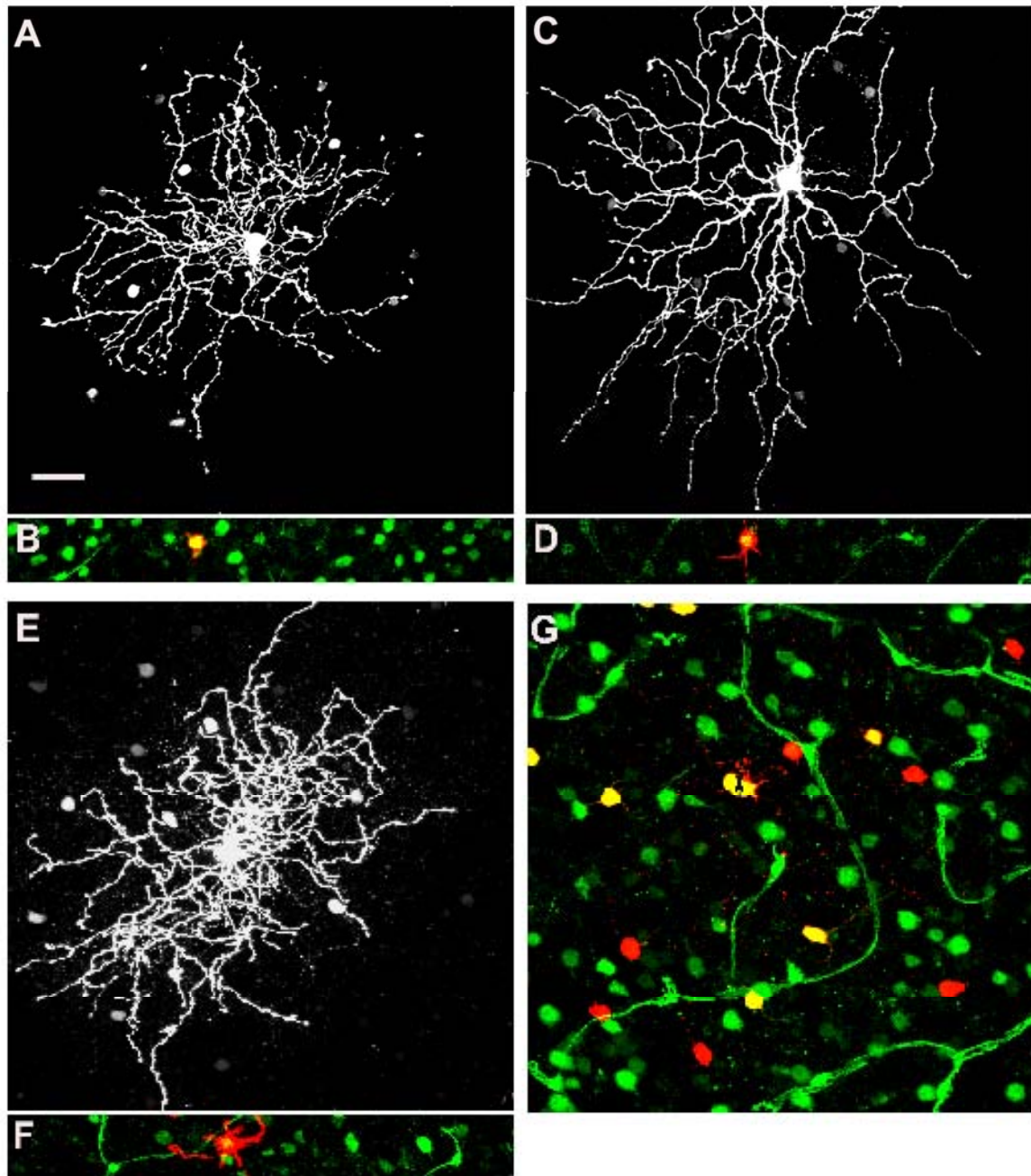
Fig. 9. Coupling patterns of the Cx45-expressing Type One amacrine cells. A), C) and E) show three EGFP-positive cells coupled to numerous amacrine cells. Below the injected cells, the colocalization with the EGFP signal is shown (B, D, F). G) A Type One was injected (*) for 10 min. Type One cells exhibit homologous and heterologous tracer coupling. Homologously coupled cells do not present the radial morphology of the A17 cell, indicating that they are also Type One cells.

Scale bar = 40 µm.

5.2.3 Coupling patterns of A17 cells

In the wild type mouse, A17 cells are strongly coupled to other amacrine cells which have cell bodies in the INL (see Fig. 10A). Unfortunately, only one cell was injected in the WT mouse since these cells are very difficult to find since they are not labeled with EGFP. In Cx45 heterozygous mice (n = 8), electrical coupling of A17 cells is strongly reduced. Only one injected cell exhibited tracer coupling to a few cells. These coupled cells expressed the EGFP signal, indicating that A17 cells are coupled to other amacrine cells by Cx45 (data not shown).
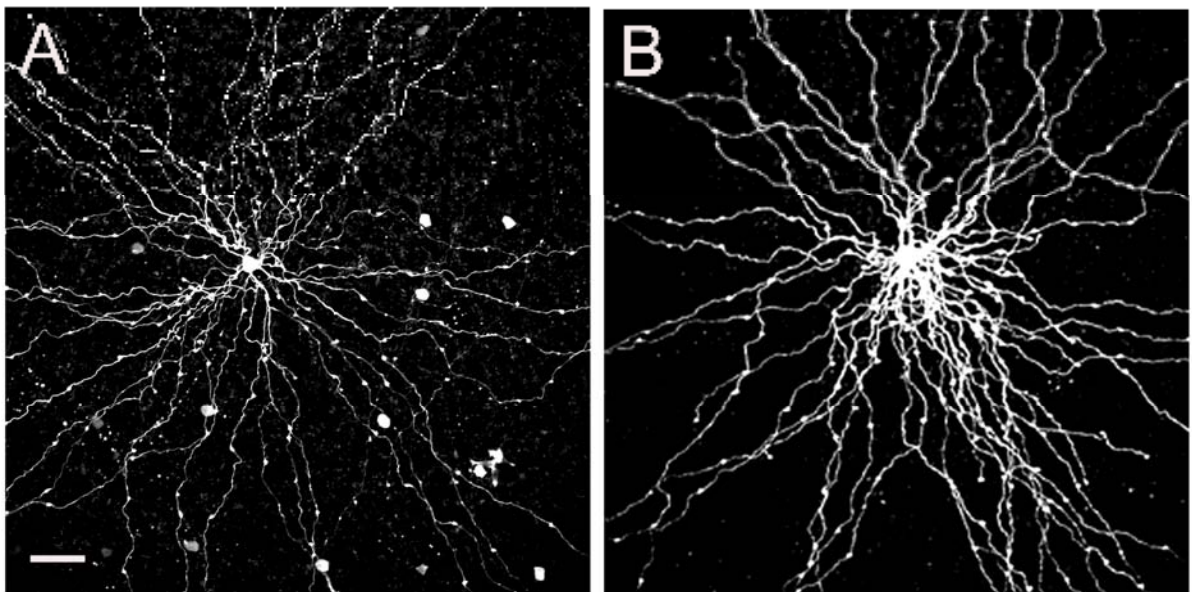
Fig. 10. Right picture illustrates an A17 cell coupled to other amacrine cells of the INL in the WT mouse retina. Left picture is an A17 cell injected in a Cx45 heterozygous mouse. They normally did not show tracer coupling. Scale bar = 40 µm.

5.2.4 Coupling of EGFP amacrine cells in Cx45-deficient mice

Injections with Neurobiotin in the EGFP-expressing amacrine cells were performed in homozygous Cx45-deficient mice. The Type One cells (n = 16) and the A17 amacrine cells (n = 11) showed no tracer coupling as shown in figure 11.
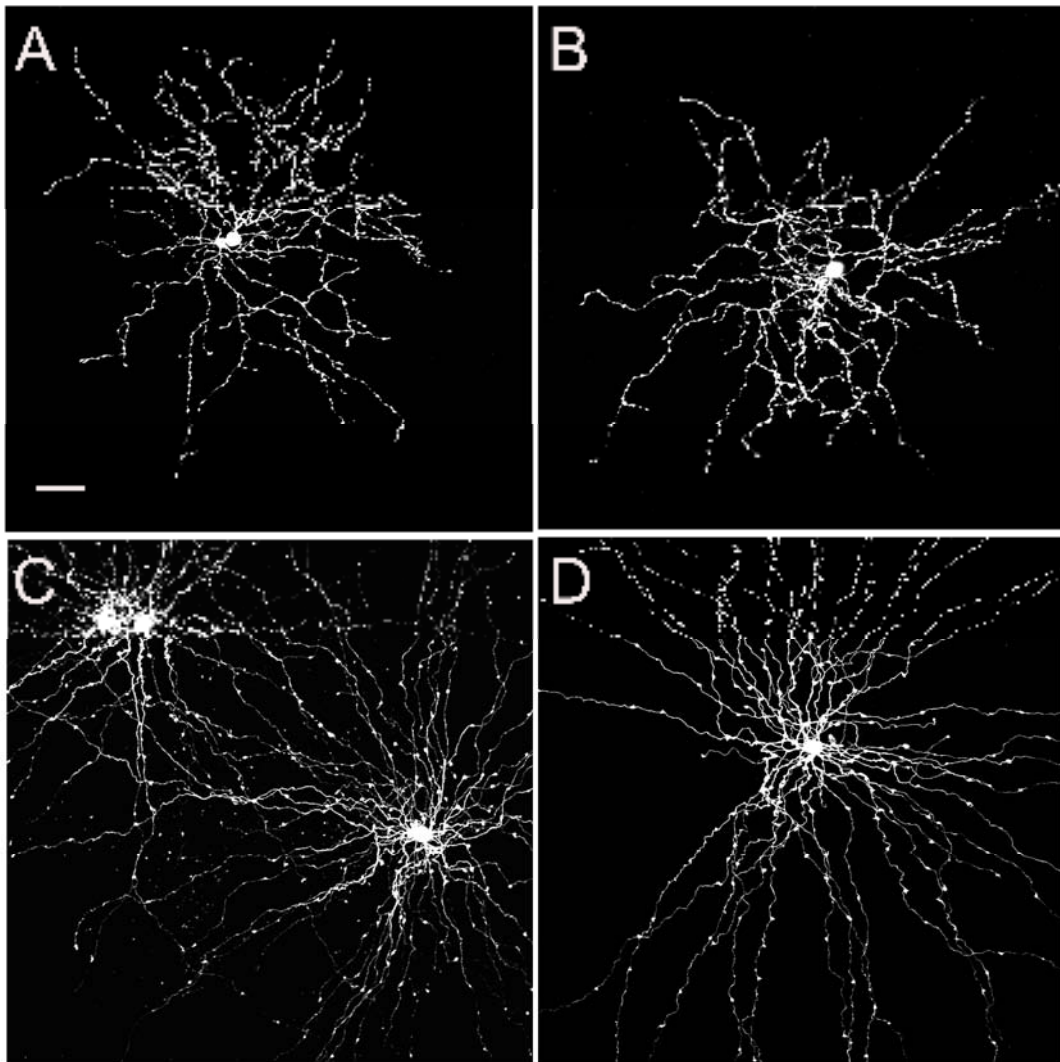
Fig. 11. EGFP-expressing amacrine cells injected in Cx45-deficient mice. A), B) illustrate the Type One with no tracer coupling. C), D) show that A17 cells are not coupled to other cells in Cx45 KO mice. Scale bar = 40 µm.

5.2.5 Neurotransmitter of Cx45-expressing amacrine cells

Amacrine cells can be classified into two groups (GABAergic or glycinergic) depending on the neurotransmitter they contain (Pourcho, 1996). To study the neurotransmitter expression of the Cx45-expressing amacrine cells, whole-mounted retinae of Cx45 fl/fl Nestin-Cre mice were incubated with antibodies against glycine (generously donated by D. Pow; Pow et al., 1995) and GABA (1:500; SIGMA).
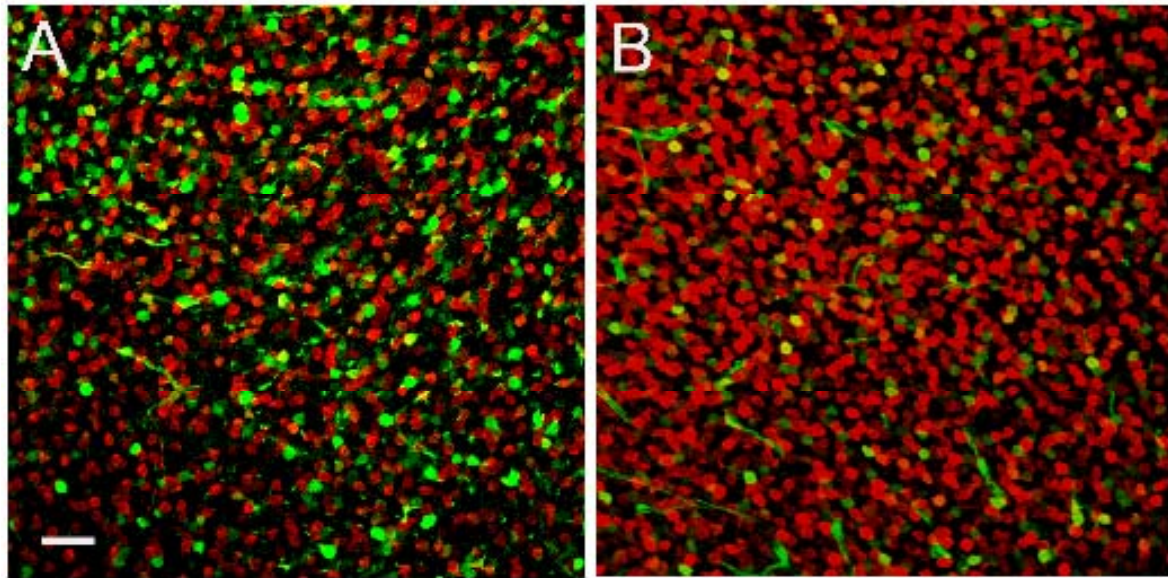
Fig. 12. A) A picture of the amacrine cells expressing EGFP (green) with glycine immunostaining (red). B) GABA immunoreactivity (red) and the EGFP-expressing amacrine cells (green). Scale bar = 40 µm.

Antibodies against glycine and GABA produced an uniform distribution of numerous labeled somata in the INL. A few EGFP-positive cells showed a weaker but still significant glycine labeling (n = 2, Fig. 12A); these cells probably correspond to the Cx45-expressing cone bipolar cells (Maxeiner et al, 2005). They may contain glycine

as a result of their gap junctional coupling to AII amacrine cells in the INL (Vaney et al., 1998).

Incubation of Cx45 fl/fl Nestin-Cre retinae with antibodies against GABA (n = 2; Fig. 12B) showed a strong colocalization with the EGFP-positive amacrine cells. These data indicate that Cx45-expressing amacrine cells contain GABA as a neurotransmitter and not glycine.

In conclusion, two GABAergic amacrine cell types expressing Cx45 were described. Both types showed electrical coupling: A17 cells are homologously coupled with other A17 cells, most likely by homotypic gap junctions whereas type one cells are homologously coupled to other type one cells and heterologously coupled to an unknown amacrine cell type.

5.3 Morphological and functional characterization of ganglion cell types expressing connexin30.2 in the mouse retina (Pérez de Sevilla et al., submitted)

This connexin, and its putative human orthologue Cx31.9, have been described in the brain, vascular smooth muscles, testis and heart (Nielsen et al., 2002; Nielsen and Kumar, 2003; Kreuzberg et al., 2005; Kreuzberg et al., 2008). To study whether Cx30.2 is expressed in the retina, I used a Cx30.2$^{lacZ/lacZ}$ mouse line where the coding region of the Cx30.2 gene was replaced by a lacZ reporter gene expressed under the control of Cx30.2 gene regulatory elements (Kreuzberg et al., 2006). The LacZ signal was expressed in the nuclei of the cells and could be observed in neurons located in the GCL and in the INL.

I have concentrated the study on the GCL using immunocytochemistry and tracer experiments to characterize the morphology of the cells expressing Cx30.2. I found six different ganglion cell types expressing Cx30.2. One of the ganglion cell types expressing Cx30.2 corresponds to the RG_{A1} neurons according to the classification made by Sun et al. (2002a), or giant cells. RG_{A1} neurons have polygonal somata and 3 to 5 primary dendrites leave the soma in a radiate pattern of branching. The dendrites radiate primarily in stratum 5 of the IPL, making it likely that these ganglion cells are ON-ganglion cells. They are coupled to numerous amacrine cells having their somas in the GCL. These displaced amacrine cells do not express Cx30.2 and I conclude that the connecting gap junctions are composed of heterotypic channels involving Cx30.2 and a yet unidentified connexin.

In this study I showed that giant ganglion cells express a new retinal connexin, Cx30.2, and are coupled to displaced amacrine cells by heterotypic gap junctions. For more details, see chapter 7.3.

5.4 Localization of Cx57 in horizontal cells of the mouse retina (Janssen-Bienhold et al., submitted)

Horizontal cells are extensively coupled by gap junctions. Hombach et al. (2004) demonstrated that Cx57 is the connexin responsible for the coupling of the horizontal cell network in the mouse retina, but the exact localization of this connexin in these cells is unknown. To determine the location of Cx57 on the dendrites and/or axons of horizontal cells, whole-mounts of wild type mouse retinae were used.

After injection of horizontal cells (see chapter 4.2), retinae were blocked with 10% NGS and incubated with a specific antibody against Cx57. This polyclonal antibody

(raised in rabbit) recognized a 15 amino acid peptide sequence of the C-terminal end of mouse Cx57. The specificity of the antibodies was tested by Western blots and immunohistochemistry in a Cx57 deficient mouse (Schultz et al., 2007). The cells were analyzed by confocal microscopy and regions of the dendritic field were selected for more detailed analysis.

Strong immunostaining was detected in the OPL and distal INL in the wild-type mouse retina. The co-localization of Cx57 puncta with dendrites and axons of horizontal cells was determined by examining individual sections. The connexin immunolabeling decorated the dendrites and axon terminals, but I always found more labeling in the axon terminals than in the dendrites.

I conclude that Cx57 is expressed in to a lesser degree in dendrites than axon terminals. The localization of the Cx57 in horizontal cells supports previous studies which have shown that Cx57 mediates the coupling pattern of the horizontal cells in the mouse retina (Hombach et al., 2004). More information of the project in chapter 7.4.

5.5 Contribution of photoreceptor inputs to the light responses of the mouse retina (Trümpler et al., in press)

Measuring the light responses in horizontal cells of three different transgenic mouse lines, and comparing them to the light responses of horizontal cells in the wild type mouse retina, Dr. Trümpler showed that probably the cone signals are transmitted from the soma to the axon terminal but not vice versa. The separation of cone and rod input to horizontal cells was achieved using transgenic mouse strains in which one type of photoreceptor was degenerated. Since it is known that neurons depleted

of their synaptic input show a tendency to degenerate (Strettoi et al., 2002; Dick et al., 2003), it was important to control the integrity of the horizontal cells. To control that the horizontal cells do not show anomalies, I injected horizontal cells in CNGA3$^{-/-}$/Cx36$^{-/-}$ mice. The morphology of the cells compared to those in WT had no differences. More information of this article in chapter 7.2.

6. Discussion

Since Feigenspan et al. (2001) described the Cx36 in the mouse retina, the identification of retinal connexins has progressed at an incredible velocity. Three different connexins are known to be expressed in the mouse retina. Connexin57 is exclusively expressed in horizontal cells (Hombach et al., 2004; Shelley et al., 2006), Cx36 in photoreceptors, OFF cone bipolar cells, one type of ON cone bipolar cell, AII amacrine cells and alpha ganglion cells (Feigenspan et al., 2004; Deans et al., 2002, Feigenspan et al., 2001; Mills et al., 2001; Han & Massey, 2005, Lin et al., 2005; Schubert et al., 2005a). The last connexin identified in the mouse retina was Cx45, found in bistratified ganglion cells, OFF and ON cone bipolar cells and amacrine cells (Schubert et al., 2005b; Maxeiner et al., 2005; Pérez de Sevilla et al., 2007).

6.1 Displaced amacrine cells

The term "displaced" as applied to amacrine cells gives the idea that these cells are in the wrong layer, but amacrine cells have been described in the GCL of all classes of vertebrates (rat, Perry and Walker, 1980; rabbit, Hughes and Vaney, 1980; Vaney, 1980; cat, Hughes and Wieniawa-Nakiewicz, 1980; Wong et al., 1986; ground squirrel, Abreu et al., 1993; hamster, Linden and Esbérard, 1987; human, Curcio and Allen, 1990; adult tammar, Wong et al., 1986; chick, Ehrlich and Morgan, 1980). Thus there is strong evidence that amacrine cells have an important role in the GCL. To avoid confusion, however, I used the term "displaced" in this study to conform with the standard of other works.

In this work I showed evidence for 10 different types of displaced amacrine cells in the mouse retina. They comprise four medium- and six wide-field amacrine cell types.

In order to get an estimate of the vertical distribution of processes within the inner plexiform layer, the two plexi of cholinergic amacrine cells which characterize the ON- and OFF-sublaminae were used as landmarks and the IPL was divided into five strata or plexuses. Soma and dendritic field sizes were also used as primary parameters in categorizing the cells. There is not a big difference in soma size of all amacrine cells and they are generally of small size. The small size possibly resulted in some erroneous measurements.

In general, most of the displaced amacrine cells are monostratified, just one type of bistratified amacrine cell was found and only one type of wide-field amacrine cell was classified as multistratified amacrine cell.

This classification is not complete, since other authors have reported other types of displaced amacrine cells that I did not find (Lin and Masland, 2006; Badea and Nathans, 2004).

Some wide-field and polyaxonal amacrine cells showed tracer coupling to other amacrine cells, and many ganglion cells are coupled to displaced amacrine cells in the mouse retina (Völgyi, personal communication). Why do we not we see tracer spread in the displaced amacrine cells to ganglion cells in light-adapted retinae? There are four possible reasons:

1. Neurobiotin must pass through the gap junctions to label the neighboring cells and in the case of the wide-field cells, because of the big dendritic field, probably the Neurobiotin molecules do not reach the coupled cells.

2. The movement of Neurobiotin is regulated by properties of the connexins.

3. Fluorescent histology is not enough to observe all coupled cells and better methods should be used for the analysis.

4. The impalement of the cell and/or application of iontophoretic current can produce cellular damage, closing the gap junctions.

In this study I have shown that the displaced amacrine cells of the mouse retina are most likely GABAergic. GABA is one of the major inhibitory neurotransmitters in the mammalian retina and mediates a diversity of inhibitory signals in the retina. It seems to be a general rule that glycinergic amacrine cells are small amacrine cells (Vaney, 1990; Menger et al., 1998) whereas medium- and wide-field amacrine cells are GABAergic. For more details of displaced amacrine cells in the mouse retina see chapter 7.1.

6. 2 Expression of Cx45 in the mouse retina

In the mouse retina, Cx45 has been shown to be expressed in bipolar cells (Maxeiner et al., 2005) and in ganglion cells (Schubert et al., 2005b). In my thesis, I have classified the Cx45-expressing amacrine cells.

In this study, intracellular microinjections of Neurobiotin were carried out in Cx45 fl/fl: Nestin-Cre and Cx45 fl/+: Nestin-Cre mice (Maxeiner et al., 2005). They revealed that the expression of this connexin is present in at least two different types of GABAergic amacrine cells. One of them is located exclusively in the INL whereas the second type was found in the INL and in the GCL. These types revealed coupling and stratified in the S5 layer of the IPL. Tracer injections in Cx45-deficient mice showed an absence of tracer coupling.

Type One Cx45-expressing amacrine cells resemble the waterfall 1 amacrine cell described in the mouse retina by Badea and Nathans (2004), or the S2 cell described in rabbit retina (Li et al., 2002). However, the method that Badea and Nathans used

did not allow an analysis of the coupling patterns. Type two cells resemble the A17 cell in rat or the S1 cell in rabbit (Kolb et al., 1981; Vaney, 1986).

Type One could be S2 amacrine cells, since they share many similarities. These two cell types have similar morphology and dendritic field size, both cell types have many varicosities and they stratify in the same way. However, they express many differences. In the rabbit retina, S2 amacrine cells are homologously coupled, but not as extensive as S1 amacrine cells (Li et al., 2002). In the mouse retina, the Cx45 Type One cell was homologously coupled to other Type One amacrine cells, and heterologously coupled to another amacrine cell type(s) by heterotypic gap junctions. Another difference between A17 and Type One cells in the mouse retina is the number of coupled cells. A17 cells are more weakly coupled than Type One cells. This weak coupling could be due to fewer gap junctional contacts in the A17 amacrine cell network. Measuring light responses of these cells could help to resolve this issue. For example, if this cell type corresponds to the S2 amacrine cell in rabbit retina, stimulating the Type One with different light intensities, should result in a strong depolarization under scotopic conditions and a weak response in phototopic conditions in case that. In addition, incubating the retina with DHT (5,7-dihydroxytryptamine) could produce an ablation of the A17 and Type One cells, as reported in rabbit retina (Dong and Hare, 2003).

6.3 Localization of Cx57 in horizontal cells of the mouse retina

Cx57 is a specific Cx expressed only in horizontal cells of the mouse retina (Hombach 2004). For the first time, we have demonstrated the presence of Cx57 gap junctions in neurons of the mouse retina. In this study, the most important thing is the specificity of the antibody used to locate Cx57 (see chapter 7.4).

6.4 Cx30.2 is expressed in the mouse retina

I showed that the novel retinal Cx, Cx30.2, is expressed abundantly in ganglion cells. This protein was observed to be present in cells of the INL and GCL. The cells located in the INL correspond presumably to amacrine cells, based on nucleus size, and location of the β-galactoside staining. I performed scotopic electroretinogram (ERG) recordings to study a possible effect on the rod pathway. The a-wave did not differ significantly between wild-type and Cx30.2 deficient mice. However the b-wave threshold was lower in Cx30.2-deficient than in wild-type mice, there differences were not significant (not shown). This analysis indicated that Cx30.2 is not involved in the pathways generating the b-wave. Since the b-wave is principally caused by the depolarization of bipolar cells (Steinberg et al., 1991; Masu et al., 1995), I excluded that Cx30.2 plays a role in the rod pathway.

Since fluorescent assays have been developed for β-galactoside, I labeled the β – gal-positive neurons in Cx30.2$^{lacZ/+}$ and Cx30.2$^{lacZ/lacZ}$ mice using the fluorogenic substrate fluorescein digalactoside (FDG). This method labeled a big subset of neurons and this subset included cells of different types. These types did not vary between retinae. In the GCL, I characterized six different types of ganglion cells expressing Cx30.2. Tracer experiments showed coupling in two types of ganglion

cells in Cx30.2$^{lacZ/+}$ mice and a complete absence of coupling in Cx30.2-deficient mice. The remaining ganglion cell types did not show evidence of tracer spread. This could be because these cells were injected in heterozygous mice where there is less Cx30.2 than in the wild type. Interestingly, the bistratified ganglion cell type described in this work resembles the type two ganglion cells of Schubert et al. (2005b) which is coupled to other bistratified ganglion cells by Cx45. Our data suggest that these cells could form heteromeric gap junctions composed by Cx45 and Cx30.2. Schubert et al. (2005b) observed some residual coupling in Cx45 knockout mice. One possibility could be that Cx30.2 compensates the lack of Cx45 in bistratified ganglion cells but not vice versa since in Cx30.2 deficient mice, these ganglion cells did not show any evidence of tracer spread.

6.4.1 Cx30.2 is expressed in RG$_{A1}$ cells

Sun et al. (2002a) classified four groups of ganglion cells in the mouse into 14 subtypes. The group of the RG$_A$ comprises three different types of neurons, RG$_{A1}$, RG$_{A2}$ inner (ON ganglion cells) and RG$_{A2}$ outer (OFF ganglion cells). Despite being classified into two types, ON alpha cells and RG$_{A1}$ cells share many morphological similarities. They have the largest somas of all ganglion cell types, their dendritic tree branch radially, they stratify in the same stratum, and show tracer coupling to displaced amacrine cells. The main morphological difference is that RG$_{A1}$ cell dendrites are more sparsely branched than those of ON alpha cells. Like alpha ganglion cells, RG$_{A1}$ morphology is apparently conserved across species, but their coupling patterns differ across species. ON alpha cells are uncoupled in the rabbit retina (Hu and Bloomfield, 2003) and RG$_{A1}$ cells are coupled to amacrine cells and

ganglion cells in rat retinae (Huxlin and Goodchild, 1997). In the mouse retina, both cell types are coupled to displaced amacrine cells.

Some authors grouped RG$_{A1}$ and ON alpha cells as one group, ON alpha cells (Peichl, 1989; Pang et al., 2003; Majumdar et al., 2007). Contrary to these authors, our findings suggest that there are important differences between these two types of neurons. ON alpha cell coupling to amacrine cells is mediated by Cx36 (Völgyi et al., 2005; Schubert et al., 2005a) whereas RG$_{A1}$ are coupled to displaced amacrine cells by Cx30.2 (this study) and not by Cx36, which is consistent with the findings of Schubert et al. (2005a). I conclude that RG$_{A1}$ cells express Cx30.2, since the FDG method labeled RG$_{A1}$ neurons in all Cx30.2-lacZ mice. Furthermore, these cells were coupled to numerous amacrine cells with somas in the GCL, and such tracer coupling is absent in Cx30.2 deficient mice indicating that Cx30.2 mediates this cell-to-cell communication. Which cell type is the coupling partner of the RG$_{A1}$ cells? So far, 17 types of displaced amacrine cells have been reported in the mouse retina (Badea and Nathans, 2004; Lin and Masland, 2006, Pérez de Sevilla et al., 2007). Since RG$_{A1}$ neurons stratified in S5 of the IPL, the dendrites of the possible partner should be in the same layer. So far, 6 types have been identified as possible partner: A1, bifid, MA-S5, MA-S1/S5, PA-S5 and a multistratified cell type (Badea and Nathans, 2004; Pérez de Sevilla et al., 2007).

6.4.2 Gap junction protein of the displaced amacrine cells

My data strongly suggest that the RG$_{A1}$ cells are coupled to displaced amacrine cells by heterotypic gap junctions involving Cx30.2 and a yet unidentified connexin. The displaced amacrine cells did not express Cx30.2, since the FDG signal was not observed in the coupled cells. Furthermore, no FDG-labeled displaced amacrine cells

were observed during the FDG incubation, excluding the possibility that the FDG signal leaked out of the cells. I never observed labeled displaced amacrine cells in the Cx30.2 transgenic mice. Since the FDG assay has been shown to label displaced amacrine cells in other mouse lines (Nirenberg and Meister, 1997), I excluded that Cx30.2 is expressed by these amacrine cells. Injections with Neurobiotin in Cx36 - and Cx45-deficient mice showed tracer coupling in the RG$_{A1}$ neurons confirming that the displaced amacrine cells do not express Cx36 or Cx45.

Gap junctions are not the only mechanism for communication between neurons in the retina. Recently, a new family of proteins, pannexins has been described. These proteins share many characteristics with connexins and are abundant in the mouse retina (Panchin, 2005; Ray et al., 2005; Dvoriantchikova et al., 2006). First, we though that pannexins, as a new class of proteins that may form gap junctions, could be the protein of the displaced amacrine cells but, contrary to this idea, new studies demonstrated that pannexins contains a glycosylation site at the extracellular loop, making them unlikely to form gap junctions (Boassa et al., 2007; Penuela et al., 2007). It seems that pannexins may play a role as hemichannels.

Another hypothesis is that an unknown family of proteins exists which forms gap junctions in vertebrate retinae (Shestopalov and Panchin, 2008).

7. Publications

7.1. Luis Pérez de Sevilla Müller, Jennifer Shelley, and Reto Weiler (2007).

Displaced amacrine cells of the mouse retina. J Comp Neurol 505:177-189.

Displaced Amacrine Cells of the Mouse Retina

LUIS PÉREZ DE SEVILLA MÜLLER, JENNIFER SHELLEY, AND RETO WEILER*
Department of Neurobiology, University of Oldenburg, D-26111 Oldenburg, Germany

ABSTRACT

The aim of this study was to characterize and classify the displaced amacrine cells in the mouse retina. Amacrine cells in the ganglion cell layer were injected with fluorescent dyes in flat-mounted retinas. Dye-filled displaced amacrine cells were classified according to dendritic field size, horizontal and vertical stratification patterns, and general morphology. We identified 10 different morphological types of displaced amacrine cell. Six of the cell types identified here are novel cell types that have not been described previously in the mouse retina, to the best of our knowledge. The displaced amacrine cells included four types of medium-field cells, with dendritic field diameters of 200–500 µm, and six types of wide-field cells, with dendritic fields extending over 500 µm. Narrow-field displaced amacrine cells, with dendritic field diameters smaller than 200 µm, were not encountered. The most frequently labeled displaced amacrine cell type was the starburst amacrine cell. At least three cell types identified here have nondisplaced counterparts in the inner nuclear layer as well. Displaced amacrine cells display a rich variety of stratification and branching patterns, which surely reflect the wide range of their functional roles in the processing of visual signals in the inner retina. J. Comp. Neurol. 505:177–189, 2007. © 2007 Wiley-Liss, Inc.

Indexing terms: retina; displaced amacrine cell; mouse; morphology; dye injection

Amacrine cells play an important role in processing of visual information in the inner retina. These neurons make inhibitory synapses onto bipolar and ganglion cells in the inner plexiform layer (IPL), modulating the spatial and temporal properties of the visual signals passed from bipolar cells to ganglion cells. Amacrine cells vary widely in morphology and function (Massey and Redburn, 1987; Vaney, 1990; Strettoi and Masland, 1996; Masland, 2001) and can have complex neurochemical signatures, expressing either GABA or glycine, along with acetylcholine or other neuropeptides (Marc et al., 1995). The main division into GABAergic and glycinergic cells is often correlated with dendritic field size (Vaney, 1990; Wässle and Boycott, 1991).

The cell bodies of amacrine cells can be located in the inner nuclear layer (INL) or in the ganglion cell layer (GCL): amacrine cells located in the GCL are termed *displaced amacrine cells*. Displaced amacrine cells can easily be distinguished from ganglion cells by their small soma and their lack of an axon that projects to the brain. The first evidence that the small cells in the GCL are neurons and not glia cells was presented by Hughes and Wieniawa-Narkiewicz (1980) for the cat retina. Since then, the morphology and branching patterns of displaced amacrine cell types have begun to be examined: six types of displaced amacrine cell have been identified in the rat retina (Perry

and Walker, 1980), 11 types in the guinea pig (Kao and Sterling, 2006), and four types in the cat retina (Wässle et al., 1987a).

So far, 11 types of displaced amacrine cell have been identified in the mouse retina (Gustincich et al., 1997; Badea and Nathans, 2004; Lin and Masland, 2006). However, most of these cell types were identified by using transgenic approaches, which may not reveal every cell type that is present in wild-type mice. Displaced amacrine cells make up about 59% of the somata within the mouse GCL (Jeon et al., 1998); because 20–40 different types of amacrine cell are thought to exist in the vertebrate retina (Massey and Redburn, 1987; Vaney, 1990; Strettoi and Masland, 1996; Masland, 2001), it is likely that many displaced amacrine cell types have been overlooked. With the growing prominence of transgenic mice in retinal re-

search, a better understanding of mouse retinal architecture is essential.

The aim of this study was to characterize and classify the displaced amacrine cells in the mouse retina. A wide range of techniques is available for visualizing retinal neurons. To identify as many cells as possible, we combined two approaches: 1) random dye injection of amacrine cells in the GCL of wild-type retinas and 2) targeted dye injection of amacrine cells in the GCL of transgenic mice in which distinct populations of cells are labeled with green fluorescent protein (EGFP). Displaced amacrine cells were then classified according to their dendritic field size, horizontal and vertical branching patterns, and general morphology. The stratification depth of the amacrine cell processes within the IPL was determined by immunohistochemical labeling of the two plexi of cholinergic starburst amacrine cells, which visually define the five layers of the IPL.

We identified 10 different types of displaced amacrine cell. Four of these cell types were characterized as medium-field, since their dendritic fields had diameters of 200–500 μm. Among the four medium-field amacrine cell types, three types were monostratified, including the starburst amacrine cell, and one type was bistratified. The remaining six displaced amacrine cell types were defined as wide-field, with dendritic fields extending over 500 μm. Wide-field amacrine cells included five types of monostratified and one type of multistratified cell. Four displaced amacrine cell types identified in this study closely resemble amacrine cells described previously in other mammalian retinas (Perry and Walker, 1980; Vaney et al., 1981; Kolb et al., 1981; Wässle et al., 1987a,b; Famiglietti 1992b), indicating common functional roles. Six of the cell types identified here are novel cell types that have not been described previously in the mouse retina. In addition to these six cell types, 11 displaced amacrine cell types have been described previously in studies using transgenic mouse models (Gustincich et al., 1997; Badea and Nathans, 2004; Lin and Masland, 2006). Thus, different methods appear to reveal different cell types selectively, and the present catalog of 17 displaced amacrine cells types might not yet be complete. Nevertheless, this study provides a basic anatomical reference for future functional studies of displaced amacrine cells in the mouse retina.

MATERIALS AND METHODS
Preparation

Animals were handled in accordance with institutional guidelines for animal welfare. Adult C57/Bl6 and Cx45-EGFP (Maxeiner et al., 2005) mice were killed by cervical dislocation. Retinas were removed and mounted photoreceptor side down on black filter paper (Millipore Corporation, Bedford, MA). Retinas were then incubated at room temperature in mouse Ringer, which contained (in mM): 137 NaCl, 5.4 KCl, 1.8 CaCl$_2$ · 2 H$_2$O, 1 MgCl$_2$ · 6 H$_2$O, 5 HEPES, and 10 glucose, adjusted to pH 7.4 with 0.1 N NaOH.

Intracellular injections

The methods for intracellular injections have been described previously (Schubert et al., 2005). Briefly, borosilicate glass electrodes (Hilgenberg GmbH, Malsfeld, Germany) were filled with 4% N-(2-aminoethyl-)-biotinamide hydrochloride (Neurobiotin; Vector Laboratories, Burlingame, CA) and either 0.5% Lucifer yellow (Sigma, St. Louis, MO) or Alexa Fluor 594 (Molecular Probes, Eugene, OR) dissolved in Tris buffer (pH 7.4–7.5), with typical resistances between 170 and 300 MΩ. For random injection of displaced amacrine cells in wild-type retinas, cell bodies in the GCL were visualized with acridine orange (1 μM; Sigma, St. Louis, MO) under a ×40 water-immersion objective. For targeted injection in Cx45-EGFP retinas, the EGFP signal was used to target amacrine cells in the GCL. Lucifer yellow or Alexa Fluor 594 was iontophoresed with negative current of 1 nA (750 msec at 1 Hz); as soon as the dendritic morphology of the cell became visible, the direction of the current was reversed to inject positively charged Neurobiotin molecules. After the final injection, which lasted for 2–3 minutes, the retina remained for at least 30 minutes in the recording chamber, allowing diffusion of Neurobiotin. Retinas were then fixed in 4% paraformaldehyde for 10 minutes and washed for at least 30 minutes in 0.1 M phosphate buffer (PB), pH 7.4. Neurobiotin was visualized by incubating injected retinas overnight with streptavidin-indocarbocyanine (Cy3; Jackson Immunoresearch, West Grove, PA; dilution 1:500), in 0.1 M PB containing 0.3% Triton X-100 (Sigma). Retinas were mounted in Vectashield (Vector Laboratories, Burlingame, CA) and stored in the dark at 4°C.

Immunohistochemistry and confocal microscopy

After cell injection and fixation, retinas were labeled with polyclonal goat antibodies raised against human placental choline acetyltransferase (ChAT; 1:100; No. AB144P; Chemicon International, Temecula, CA). The antiserum stains a single band of 68–70 kD molecular weight in Western blot (manufacturer's technical information). Anti-ChAT antibodies label the dendritic processes of starburst amacrine cells in layers S2 and S4 of the IPL (Haverkamp and Wässle, 2000; Schubert et al., 2005), allowing visualization of the ON and OFF sublaminae of the IPL. In addition, rabbit anti-γaminobutyric acid (GABA; 1:100; raised in rabbit against GABA coupled to porcine thyroglobin; kindly donated by D. Pow, University of Newcastle, Australia; Pow et al., 1995) and rat antiglycine antibodies (1:1,000; raised in rat against glycine coupled to porcine thyroglobin; kindly donated by D. Pow; Pow et al., 1995) were used to determine the neurotransmitter expression of amacrine cells in the GCL. Specificity of the GABA and glycine antibodies was tested previously and has been explained in detail by Pow et al. (1995). Briefly, specificity was tested by using immunoblotting against the same amino acid-paraformaldehyde-thyroglobulin conjugates used to immunize the animals: both antibodies labeled blots containing conjugates of the appropriate amino acid (Pow et al., 1995). All antibodies employed in this study have been used previously on paraformaldehyde-fixed tissue; our results are identical to those previously reported (Haverkamp and Wässle, 2000; Schubert et al., 2005).

Retinas were blocked with donkey serum diluted 1:15 in PB with 0.3% Triton X-100 and incubated overnight at 4°C. Retinas were then incubated for 1 week in primary antibodies (diluted as noted in PB with 0.1% NaN$_3$), washed several times in PB, and incubated overnight at 4°C in the corresponding secondary antibodies: donkey anti-goat Cy3 (1:500; Jackson Immunoresearch; catalog

TABLE 1. Overview of the Classification of the Displaced Amacrine Cells

	Medium-field				Wide-field					
Cell type	MA-S1	Starburst	MA-S5	MA-S1/S5	WA-S1	WA-S3	A17	PA-S1	PA-S5	Multi-stratified
Soma diameter	7.5 ± 1.2	8.3 ± 1.8	7.7 ± 0.8	7.1	7.8 ± 0.5	8.0 ± 0.8	11.8 ± 0.7	12.0 ± 0.2	9.5 ± 0.5	10.0 ± 1.7
Dendritic field diameter	219 ± 21	279 ± 39	350 ± 2	283	1250 ± 560	1510 ± 850	878 ± 285	737 ± 122	1072 ± 220	2210 ± 240
Cells injected	4	87	6	1	12	4	4	2	8	3

No. 705-095-003), goat anti-rat Cy3 (1:500; Dianova, Karlsruhe, Germany; catalog No. 81-9515), or donkey anti-rabbit Cy3 (1:500; Jackson Immunoresearch; catalog No. 711-165-152). Retinas were then washed in PB and mounted in Vectashield. Images were taken with a Leica TCS SL confocal microscope with a ×40 oil-immersion objective. Intensity and contrast of the final images were adjusted in Adobe Photoshop 7.0.

RESULTS
Morphological classification of displaced amacrine cell types

To characterize and classify mouse displaced amacrine cells, we injected amacrine cells in the GCL with Lucifer yellow and Neurobiotin. Dendritic stratification was determined by labeling with anti-ChAT antibodies, which visually define the five strata of the IPL. Over 400 displaced amacrine cells were filled in the course of this study. Among these, 131 met the criterion of complete labeling, established by the appearance of terminal dendritic tips, and were used for analysis. We created a morphological catalog of the injected displaced amacrine cells by using three primary parameters: 1) dendritic field size, 2) depth of stratification in the IPL, and 3) branching pattern of the dendrites. With these criteria, we identified 10 types of displaced amacrine cell in the mouse retina. Nine of these cell types were found in the wild-type retina, whereas one type, the A17 cell, was so rare that it was encountered only with targeted injection of EGFP-labeled neurons in a transgenic mouse line. In general, the size and depth of stratification of the dendritic arbor were sufficient to separate cells into distinct types.

Table 1 gives an overview of the classification of the displaced amacrine cells identified in this study. Displaced amacrine cells were divided into two groups according to their dendritic field size: medium-field cells, with dendritic field diameters ranging from 200 to 500 μm, and wide-field cells, with dendritic fields larger than 500 μm. Most amacrine cells injected in the GCL had round or oblong dendritic fields, although some wide-field amacrine cells with asymmetric dendritic fields were observed. With the exception of the A17 cell and one type of polyaxonal amacrine cell, the somata of the displaced amacrine cells were small, ranging in diameter from 7 to 10 μm. Novel cell types were named according to the IPL strata in which their dendrites branched.

Medium-field displaced amacrine cells

Cells with dendritic field diameters of 200–500 μm were defined as medium-field amacrine cells (MA). These cells were divided into four types based on stratification depth within the IPL (Fig. 1). Three of these cell types, including the starburst amacrine cell, were monostratified, and one type was bistratified.

MA-S1 cells made up 3% of the displaced amacrine cells encountered in this study. A typical cell of this type can be seen in Figure 1b. The dendritic arborization of this cell is approximately 220 μm across and has an asymmetric, though dense and space-filling branching pattern. The dendrites of this cell type stratify in layer S1 of the IPL (Fig. 1a,c) and do not have dendritic spines. The round cell body is small, averaging 7.5 ± 1.2 μm in diameter (n = 4). The distinctive morphology of these neurons was consistent from cell to cell.

Starburst amacrine cells are found in every vertebrate class and are easily recognized by their distinctive morphology (for review see Masland and Tauchi, 1986). These highly symmetrical cells have six or more primary dendrites that project radially from the soma, branching progressively with distance from the soma (Fig. 1e). Starburst cells have round or ovoid dendritic arbors of 279 ± 39 μm diameter (n = 87), which stratify in layer S4 of the IPL (Fig. 1d,f). The cell body has a mean diameter of 8.3 ± 1.8 μm. We found starburst amacrine cells to be the predominant amacrine cell type in the GCL; 66% of the cells injected in this study were starburst amacrine cells. Displaced starburst cells are ON cells, and their OFF counterparts have cell bodies located in the INL and stratify in layer S2.

Monostratified MA-S5 cells made up approximately 5% of the cells injected in this study. An example of this cell type is illustrated in Figure 1h. The MA-S5 cell has a disorganized, asymmetric dendritic field of 350 ± 2 μm diameter (n = 6), which ramifies in layer S5 of the IPL (Fig. 1g,i). Most of the dendrites occupy the same semicircle of space and arise from two to three primary dendrites. These primary dendrites protrude from opposite sides of the cell body and are quite long, although their branches are short and sparse. The dendrites of these cells are covered in prominent varicosities. MA-S5 cell somata have diameters of 7.7 ± 0.8 μm.

The MA-S1/S5 cell was the only type of bistratified amacrine cell that we found in the GCL. This cell type appears to be exceptionally rare: we encountered only one MA-S1/S5 cell in the course of this study. The morphology of this cell type can be seen in Figures 1k and 2. This cell has two narrowly stratified, asymmetric dendritic arbors located in layers S1 and S5 of the IPL (Fig. 1j,l, 2). The dendritic field of this cell extends approximately 283 μm and has a dense and chaotic branching pattern. The dendritic branches in the ON and OFF layers are shown separately in Figure 2.

Wide-field displaced amacrine cells

Wide-field amacrine cells (WA) have dendritic fields larger than 500 μm (Kolb, 1982; Masland, 1988). We identified six types of displaced WA, classified according to their stratification patterns in the IPL. Five of these cell types were monostratified, including two types of polyax-
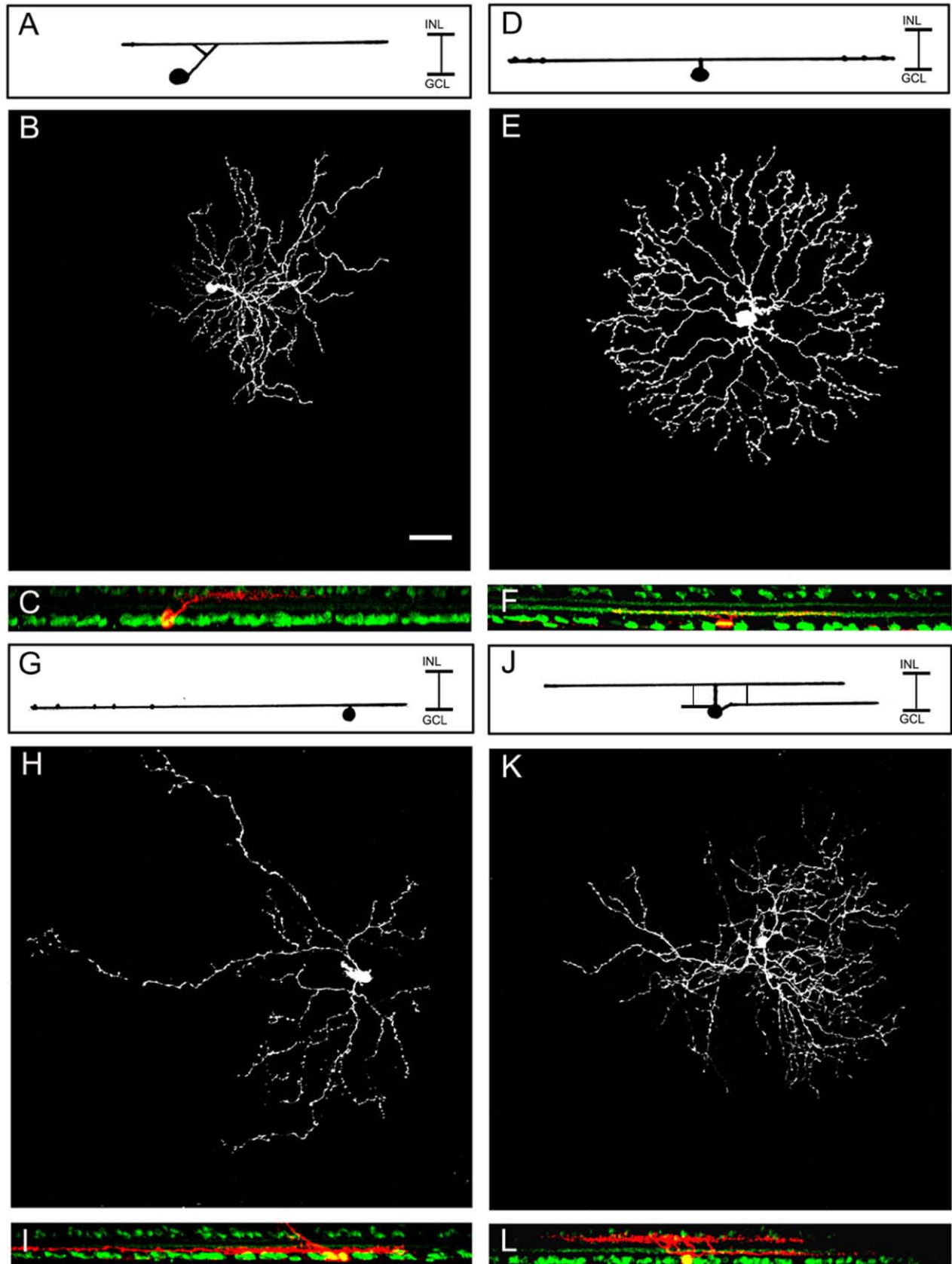
The Journal of Comparative Neurology. DOI 10.1002/cne

180   L. PÉREZ DE SEVILLA MÜLLER ET AL.

Figure 1

The Journal of Comparative Neurology. DOI 10.1002/cne

DISPLACED AMACRINE CELLS OF THE MOUSE RETINA   181

onal amacrine cell, and one type was multistratified (Fig. 3).

The WA-S1 has a distinctive bow tie shape, with three to five unbranched dendrites projecting from either side of its round soma (Fig. 3b). The dendrites are long and straight, covering a distance of up to 1 mm, and stratify in layer S1 of the IPL (Fig. 3a,c). These cells have a soma diameter of 7.8 ± 0.5 μm (n = 12). The WA-S1 cell has been described previously from other species (Gallego, 1971; Perry and Walker, 1980; Wässle et al., 1987b). As with starburst amacrine cells, WA-S1 cells also have non-displaced counterparts in the INL (Perry and Walker, 1980; Wässle et al., 1987b; MacNeil and Masland, 1998).

The WA-S3 was the second type of monostratified wide-field amacrine cell identified in this study. An example of this cell type can be seen in Figure 3e. This cell has a round dendritic field, which stratifies in layer S3 of the IPL (Fig. 3d,f). The dendrites of this amacrine cell are largely unbranched and project radially from the cell body, extending for 1.51 ± 0.85 mm. Prominent varicosities are present on the entire length of the dendrites.

In the Cx45-EGFP mouse retina, distinct populations of cells are labeled with EGFP (Maxeiner et al., 2005). We injected somata in the GCL of these retinas and found that the EGFP-positive amacrine cells were displaced A17 cells. One such cell can be seen in Figure 3h. This cell has a dense dendritic field, which stratifies in layer S5 of the IPL (Fig. 3g,i). The dendrites of this cell extend radially from the cell body and are covered in prominent varicosities. Because of their low density, these highly conserved cells were not encountered in the wild-type retina (see Discussion).

We found only one type of multistratified WA in the GCL. A prominent characteristic of this cell is its kinky dendrites, which make several sharp turns before ending approximately 2 mm from the soma (Fig. 3k). The dendrites of this cell do not fill out the region of arborization; branching is infrequent but dramatic, often at angles larger than 90°. This cell has some long dendrites that stratify in layer S5 of the IPL, whereas shorter dendrites

Fig. 1. Examples of the branching and stratification patterns of the medium-field displaced amacrine cells in the mouse retina. **A:** Illustration of the stratification of the MA-S1 cell. These rare monostratified medium-field displaced amacrine cells stratify in layer S1 of the inner plexiform layer and have asymmetric, densely branched dendrites. **B:** Confocal image of an MA-S1 cell injected with Neurobiotin, showing the dendritic branching pattern in tangential view. **C:** Confocal image of an MA-S1 cell injected with Neurobiotin (red) and counterstained with ChAT antibodies (green) to indicate stratification depth; this image shows the stratification pattern of the MA-S1 cell in radial view. **D:** Illustration of the stratification of the starburst amacrine cell. These widely conserved medium-field cells are highly symmetrical, with six or more primary dendrites projecting radially from the soma and stratifying in layer S4 of the inner plexiform layer. **E,F:** Confocal image of a starburst amacrine cell in tangential (E) and radial (F) views. **G:** Illustration of the stratification of the MA-S5 cell. These cells have asymmetric dendritic fields, which stratify in layer S5 of the inner plexiform layer. Most of the dendrites carve out an approximate semicircle and branch off from two or three primary dendrites. **H,I:** Confocal image of a MA-S5 cell in tangential (H) and radial (I) views. **J:** Illustration of the stratification of the MA-S1/S5 cell. These bistratified cells have densely branching dendrites that stratify in layers S1 and S5 of the inner plexiform layer. **K,L:** Confocal image of a MA-S1/S5 cell in tangential (K) and radial (L) views. Scale bar = 40 μm.

extend into layers S1, S2, and S3 (Fig. 3j,l). The soma of this cell is small and round, with a diameter of 10 ± 1.7 μm (n = 3).

Polyaxonal (PA) amacrine cells have between one and six branching, axon-like processes that project from the cell body or from the dendrites near the cell body. These fine processes maintain a uniform thickness and branch dramatically at right angles (Famiglietti, 1992a,b). Six physiologically distinct PA amacrine cells have been identified in the rabbit retina (Völgyi et al., 2001), and several morphological types exist in the mouse retina as well (Lin and Masland, 2006).

PA-S1 cells have the largest somata of all displaced amacrine cells identified in this study, with a diameter of 12.0 ± 0.2 μm (n = 2). This cell type has an asymmetric dendritic field with a diameter of approximately 740 μm. The dendrites leave the cell body in layer S5, where the dendrites branch off from the axon-like processes. Both dendrites and axon-like processes terminate in layer S1 (Fig. 4a,c). The thin dendrites of this amacrine cell are sparse and somewhat wavy and display the right-angled branch points described previously (Fig. 4b,d; Famiglietti, 1992a,b).

PA-S5 cells have a few large dendrites, which extend approximately 1 mm and stratify in layer S5 of the IPL (Fig. 4e,g). This amacrine cell has thick and comparatively straight axon-like processes that are decorated with prominent varicosities (Fig. 4f). The dendrites of this cell are sparsely branched and asymmetrical (Fig. 4h). This cell type has a round soma with a diameter of 9.5 ± 0.5 μm (n = 8). The PA-S5 cell is similar to the displaced PA2 cell reported for the rabbit retina (Famiglietti 1981, 1992b).
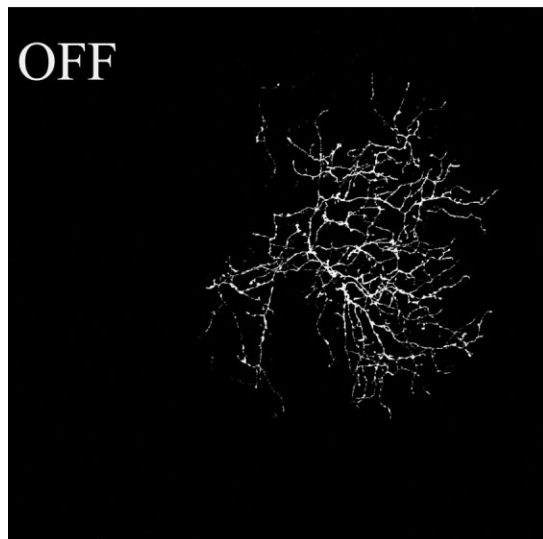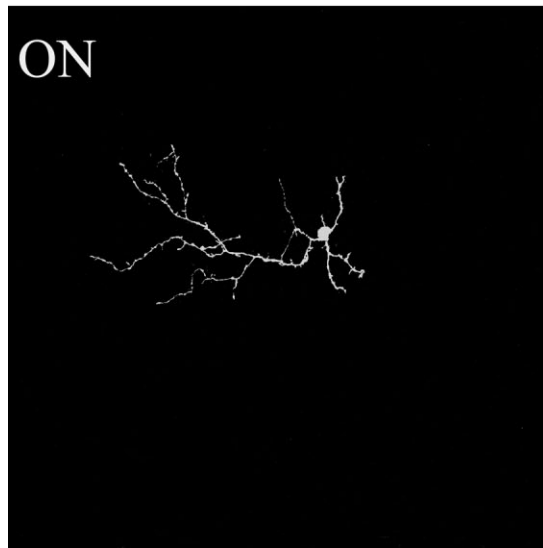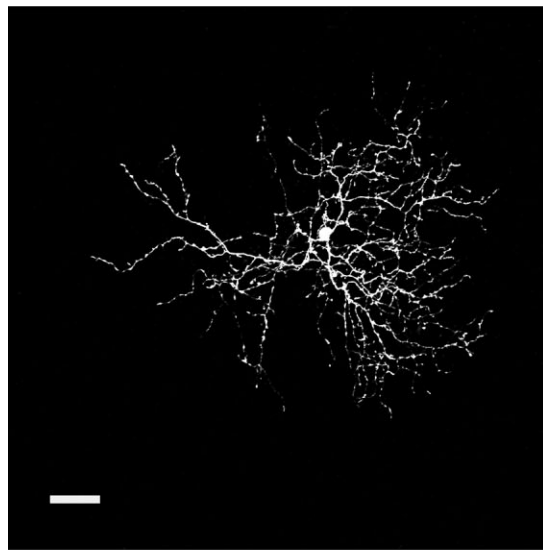
Neurotransmitter expression

Amacrine cells are the major inhibitory neurons in the mammalian retina, and they can use either GABA or glycine for neurotransmission (for review see Vaney, 1990; Wässle and Boycott, 1991). We used antibodies against GABA and glycine to determine which neurotransmitter is expressed in amacrine cells in the GCL. Antibodies against GABA produced a uniform distribution of labeled somata in the GCL (n = 2; Fig. 5a). Because ganglion cells typically do not express GABA (see, e.g., Watt et al., 1994; Zhang et al., 2004), these GABA-positive cells were probably displaced amacrine cells. Very few cells in the GCL were labeled with antibodies against glycine (n = 3; Fig. 5b). The small number of glycine-immunoreactive cell bodies in the GCL was not a result of technical errors, because numerous cell bodies in the INL were strongly labeled (not shown). This finding suggests that most, if not all, displaced amacrine cells use GABA as their neurotransmitter. Similar findings have been reported in other species (Wässle et al., 1987a; Kao and Sterling, 2006).

DISCUSSION

Displaced amacrine cells make up one-third to two-thirds of all neurons in the GCL (Perry and Walker, 1980; Hughes and Vaney, 1980; Hughes and Wieniawa-Narkiewicz, 1980; Linden and Esbérard, 1987; Abreu et al., 1993; Jeon et al., 1998) and comprise several different cell types (Perry and Walker, 1980; Wässle et al., 1987a; Völgyi et al., 2001; Badea and Nathans, 2004; Kao and Sterling, 2006). Although morphological and electrophysiological studies in some species have made progress to-

ward understanding the roles of displaced amacrine cells (e.g., Menger and Wässle, 2000; Völgyi et al., 2001; Aboelela and Robinson, 2004), similar efforts in mouse have just begun (Badea and Nathans, 2004; Lin and Masland, 2006). In this study, we identify 10 morphologically distinct types of displaced amacrine cell in the mouse retina, which include medium- and wide-field cells (Fig. 6); six of these cell types have not been described previously for the mouse.

Methodological considerations

Several different cell labeling techniques have been used to examine displaced amacrine cells. Early classification studies applied Golgi staining (turtle: Kolb, 1982; cat: Wässle et al., 1987a; rabbit: Famiglietti 1992a,b); this method labels a small number of neurons in their entirety but provides no quantitative information. More recently, photofilling (MacNeil et al., 1999) and tracer injection (Völgyi et al., 2001) techniques, as well as immunolabeling combined with tracer injection (Kao and Sterling, 2003), have been used to examine displaced amacrine cells. In contrast to the Golgi method, these techniques allow estimation of population size (see MacNeil et al., 1999). In the present study, we combined two approaches to classify displaced amacrine cells in the mouse retina: we randomly injected amacrine cells in the GCL of wild-type retinas, and we methodically injected EGFP-labeled amacrine cells in transgenic mice (connexin45-expressing cells; see Maxeiner et al., 2005). Targeted injection in the EGFP mouse line revealed only one cell type that was not found by random injection in the wild-type retina: the highly conserved A17 cell. Whereas nondisplaced A17 cells form a highly packed mosaic, displaced A17 cells are much less numerous (approximately 3 cells/mm^2: this study, data not shown; Sandell and Masland, 1986); our failure to encounter this cell type in the wild-type retina is probably a reflection of this low cell density.

Fig. 2. Confocal images of a bistratified MA-S1/S5 cell. The upper panel is a stack showing all dendrites in tangential view. The lower two panels show the dendritic arborizations in the ON and OFF layers separately. Scale bar = 40 μm.

Fig. 3. Examples of the branching and stratification patterns of four types of wide-field displaced amacrine cell. **A:** Illustration of the stratification of the WA-S1 cell. These distinctive wide-field cells have long, straight dendrites extending from either side of the cell body and stratifying in layer S1 of the inner plexiform layer. **B:** Confocal image of an WA-S1 cell injected with Neurobiotin, showing the dendritic branching pattern in tangential view. **C:** Confocal image of an WA-S1 cell injected with Neurobiotin (red) and counterstained with ChAT antibodies (green) to indicate stratification depth; this image shows the stratification pattern of the WA-S1 cell in radial view. **D:** Illustration of the stratification of the WA-S3 cell. These wide-field cells have sparsely branched asymmetrical dendrites that ramify in layer S3 of the inner plexiform layer. **E,F:** Confocal image of a WA-S3 cell in tangential (E) and radial (F) views. **G:** Illustration of the stratification of the A17 cell. These cells were found in retinas of Cx45-EGFP mice, in which some neuron populations are labeled with EGFP (Maxeiner et al., 2005). This highly conserved cell stratifies in layer S5 of the inner plexiform layer. **H,I:** Confocal image of a A17 cell in tangential (H) and radial (I) views. **J:** Illustration of the stratification of the multistratified WA cell. These wide-field cells have several long, dramatically branching dendrites, which stratify in layer S5 of the inner plexiform layer, and shorter dendrites, which extend into layers S1, S2, and S3. **K,L:** Confocal image of a multistratified WA cell in tangential (K) and radial (L) views. Scale bar = 40 μm.

Figure 3

The Journal of Comparative Neurology. DOI 10.1002/cne

184   **L. PÉREZ DE SEVILLA MÜLLER ET AL.**
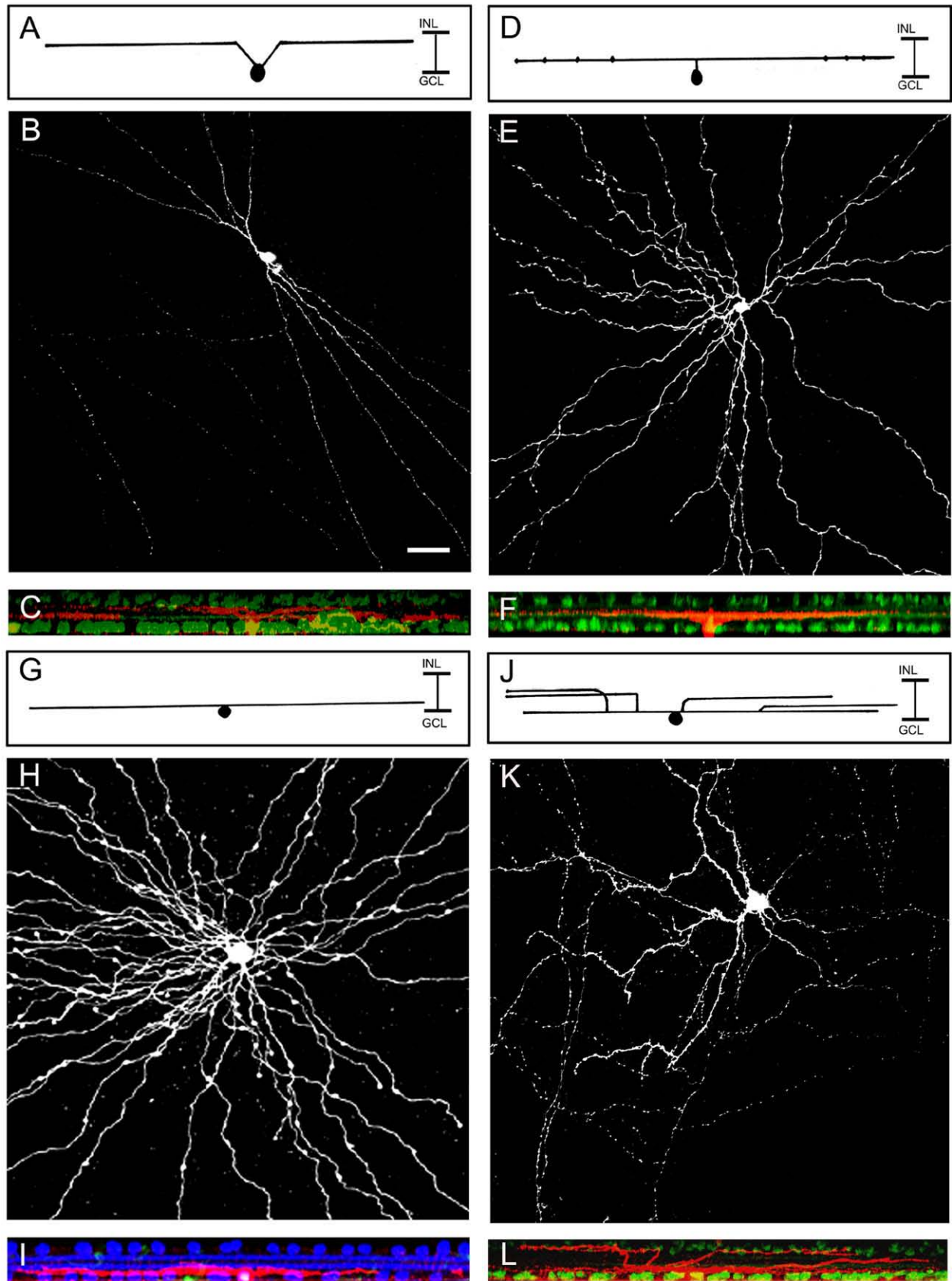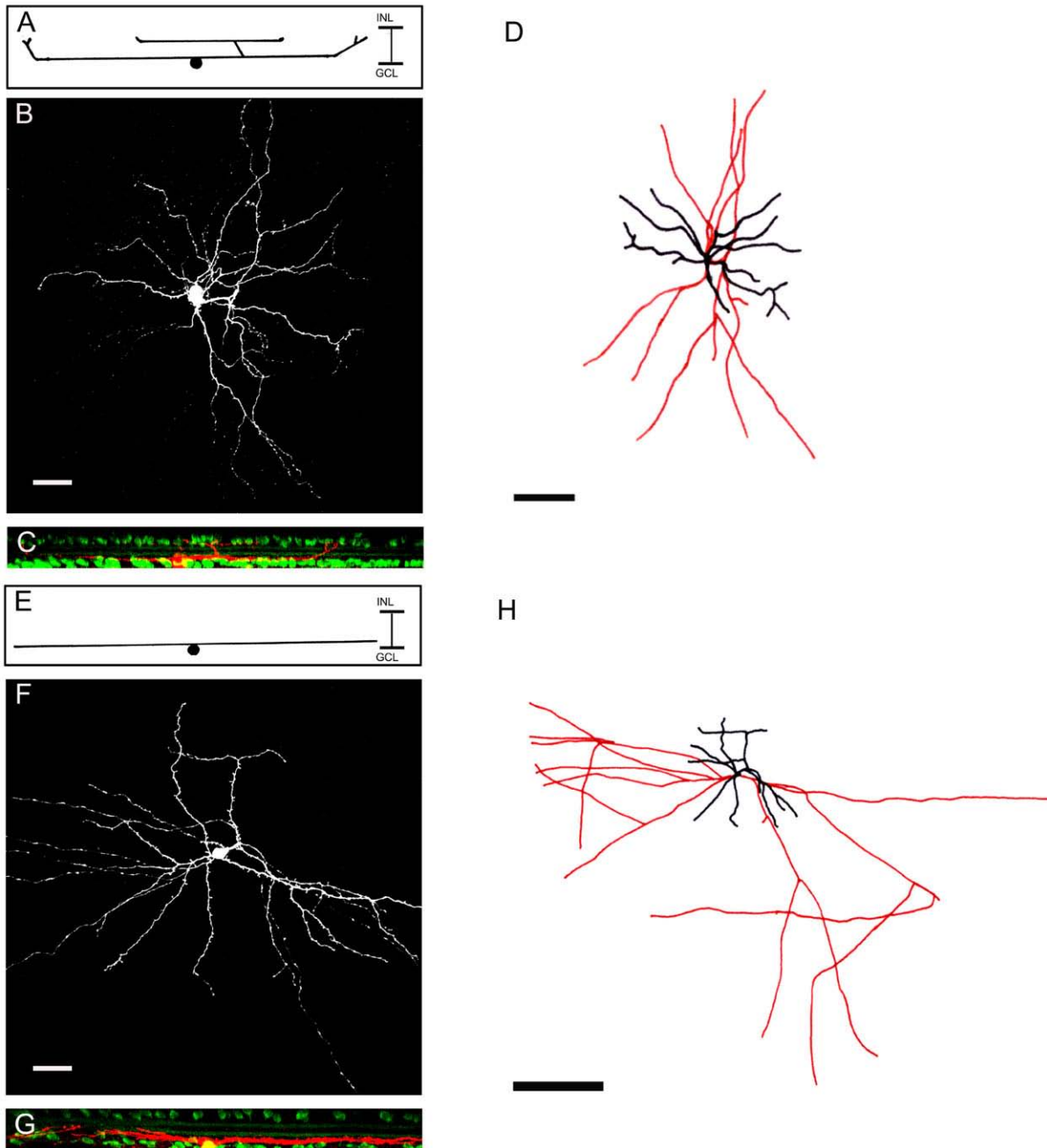
Fig. 4. Examples of the branching and stratification patterns of polyaxonal displaced amacrine cells. **A:** Illustration of the stratification of the PA-S1 cell. These polyaxonal cells have asymmetric dendrites, which leave the cell body in layer S5, where they extend before turning upward and ending in S1 of the inner plexiform layer. **B,C:** Confocal image of a PA-S1 cell in tangential (B) and radial (C) views. **D:** Illustration of the dendritic (black) and axon-like processes (red) of the PA-S1 cell. **E:** Illustration of the stratification of the PA-S5 cell. These polyaxonal cells have sparsely branched, asymmetric dendrites, which stratify in layer S5 of the inner plexiform layer. **F,G:** Confocal image of a PA-S5 cell in tangential (F) and radial (G) views. **H:** Illustration of the dendritic (black) and axon-like processes (red) of the PA-S5 cell. Scale bars = 40 μm in B (applies to B,C); 40 μm in F (applies to F,G); 100 μm in D; 200 μm in H.

How do our results compare with previous studies of displaced amacrine cells in the mouse? Six of the cells identified here have not been described previously in the mouse: MA-S1, MA-S1/S5, WA-S3, PA-S1, displaced A17, and multistratified WA. Starburst amacrine cells have been described extensively in several species, including mouse (see, e.g., Masland and Tauchi, 1986; Menger and Wässle, 2000; Petit-Jacques et al., 2005). The MA-S5 cell may correspond to the displaced cluster 3 cells described by Badea and Nathans (2004). The WA-S1 cell was reported recently by Lin and Masland (2006). Our PA-S5 cell may correspond to the WA4-1 cell of Lin and Masland

The Journal of Comparative Neurology. DOI 10.1002/cne

DISPLACED AMACRINE CELLS OF THE MOUSE RETINA

185

Fig. 5. Neurotransmitter expression in the ganglion cell layer of the mouse retina. **A:** Large numbers of cells are immunoreactive for GABA in the ganglion cell layer; these cells are presumably displaced amacrine cells, because ganglion cells do not show GABA immunoreactivity. In comparison, glycine immunoreactivity is rare in cell bodies in the ganglion cell layer (**B**). Scale bar = 40 μm.

(2006); the morphology is quite similar, although we disagree regarding the cell's stratification. This disagreement could arise from differences in interpretation: Lin and Ma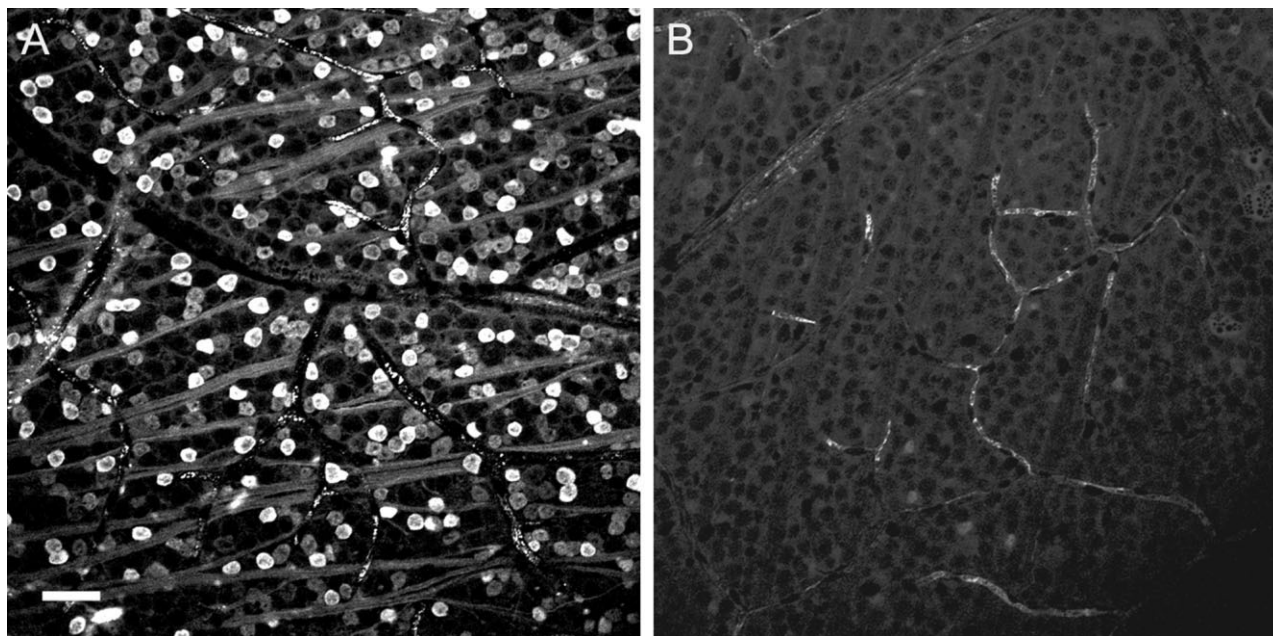sland (2006) did not use any marker to label the strata of the IPL and thus could make stratification assignments only "with some confidence"; in addition, we define stratification as the level at which the dendrites terminate, whereas Lin and Masland (2006) might have looked at the average depth over the length of the dendrites, as was done by Badea and Nathans (2004). However, it is also possible that Lin and Masland's (2006) WA4-1 and our PA-S5 cell are two different cell types with similar morphologies.

Six displaced amacrine cell types identified in transgenic mouse strains by Badea and Nathans (2004) were not found in the present study: A1-1, A1-2, cluster 1, cluster 4, bifid, and giant amacrine cells. In addition, Gustincich et al. (1997) reported a displaced catecholaminergic cell in the mouse retina that stratifies in S3. These discrepancies highlight the importance of comparing the results of several methodological approaches when classifying retinal cell types. Neither our dye injection technique nor the transgenic approaches used by Badea and Nathans (2004) and Lin and Masland (2006) can be certain of finding every cell type. When injecting cells, the experimenter may be biased against some cell types. For example, to avoid filling ganglion cells, we injected cells with small cell bodies; therefore, it is possible that we overlooked displaced amacrine cells with large cell bodies. In addition, cells present in low numbers may be missed with this technique. On the other hand, studies using transgenic mouse lines cannot be certain that every type of cell is labeled by the genetic marker, because this labeling is neither targeted nor specific (Feng et al., 2000;

Badea et al., 2003). The mouse line used by Lin and Masland (2006) showed highly variable reporter expression between transgenic lines that were generated using the same construct (Feng et al., 2000). Therefore, the most complete catalog of cell types must include data from several studies using multiple techniques. At present, 17 types of displaced amacrine cells have been identified in the mouse retina (Table 2; Gustincich et al., 1997; Badea and Nathans, 2004; Lin and Masland, 2006; present study).

Displaced amacrine cells in the mouse compared with other species

Although displaced amacrine cells have been found in almost all vertebrate retinas, the proportions of GCL neurons that are amacrine cells differs from species to species. Displaced amacrine cells make up approximately one-third of the somata in the GCL in rabbit retina (Hughes and Vaney, 1980; Vaney, 1980) and salamander retina (Zhang et al., 2004); 40% in hamster retina (Linden and Esbérard, 1987); 50% in rat retina (Perry and Walker, 1980), guinea pig retina (Kao and Sterling, 2006), and ground squirrel retina (Abreu et al., 1993); and 75–80% in peripheral cat retina (Hughes and Wieniawa-Narkiewicz, 1980; Wässle et al., 1987a) and human retina (Curcio and Allen, 1990). In the mouse retina, displaced amacrine cells make up 59% of the neurons in the GCL (Jeon et al., 1998).

Four cell types identified in this study have been described in other species. The WA-S1 was described by Gallego (1971) and coincides with the type b wide-field unistratified amacrine cell in the rat retina (Perry and Walker, 1980) and the A20 cell in the cat retina (Kolb et al., 1981; Wässle et al., 1987a,b); WA-S1 may be a subtype of the turtle A16 cell (Kolb, 1982). This cell type has a

The Journal of Comparative Neurology. DOI 10.1002/cne

186   L. PÉREZ DE SEVILLA MÜLLER ET AL.
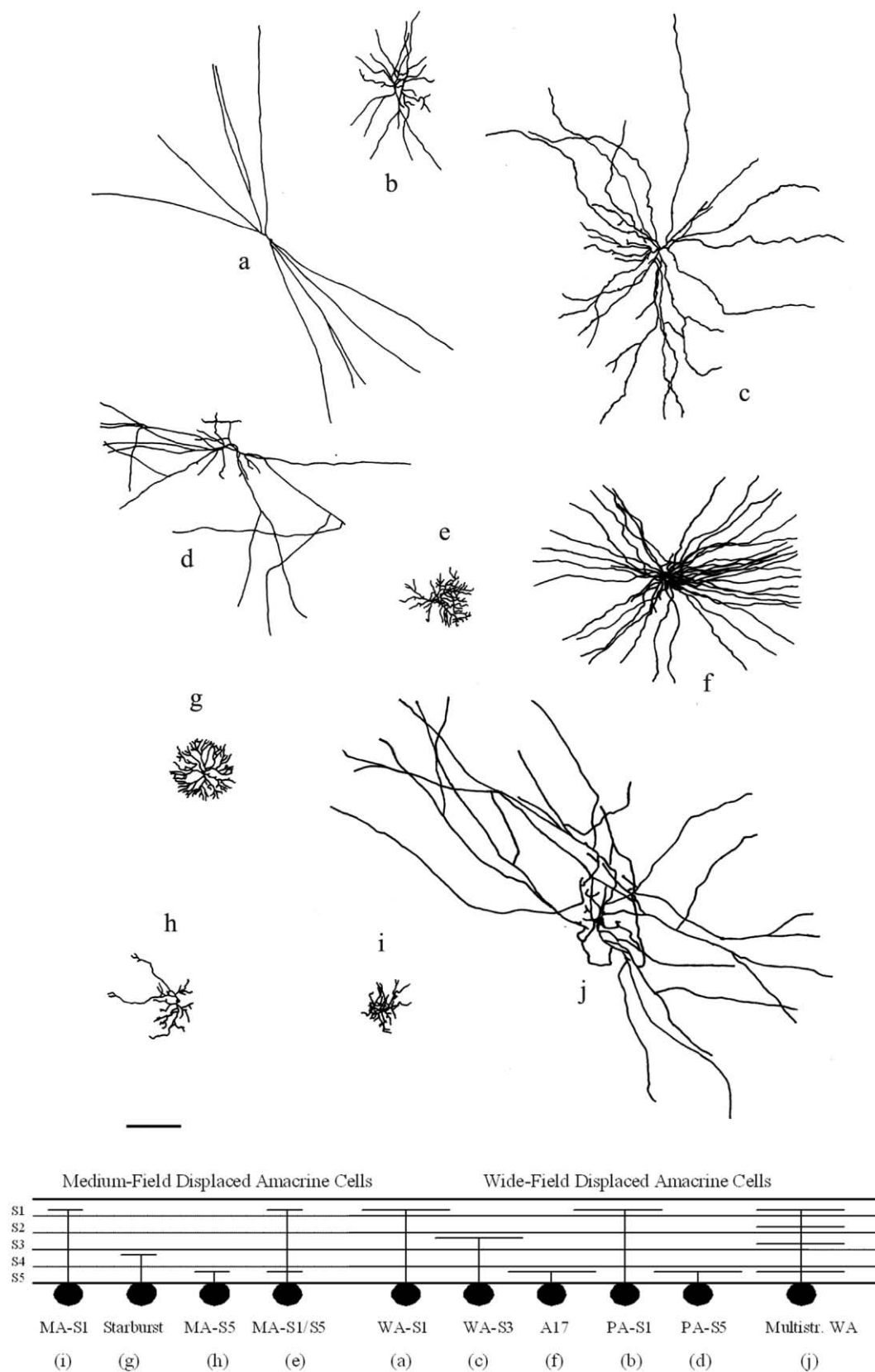

Fig. 6.   Illustrations of the 10 displaced amacrine cell types identified in this study. The top panel shows the morphology of each cell type; the bottom panel illustrates the stratification depth of each cell type. Scale bar = 200 μm.

TABLE 2. Overview of the 17 Displaced Amacrine Cell Types Identified to Date in the Mouse Retinas

This study	Badea and Nathans (2004)	Lin and Masland (2006)	Gustincich et al. (1997)
MA-S1			
STARBURST	STARBURST		
MA-S5	CLUSTER 3		
MA-S1/S5			
WA-S1		WA-1	
WA-S3			
A17			
PA-S1			
PA-S5		WA4-1	
MULT. WA			
	A1		
	A1-2		
	CLUSTER 1		
	CLUSTER 4		
	BIFID		
	GIANT AMACRINE		
			TYPE 2 CATECHOLAMINERGIC CELL

counterpart of similar morphology in the INL (rat: Perry and Walker, 1980; rabbit: MacNeil et al., 1999). The WA-S1 stratifies in layer S1 of the IPL (this study; Lin and Masland, 2006), but cells of similar morphology stratify in other layers: a rat homolog stratifies in the inner part of the IPL (Perry and Walker, 1980); the bifid cell stratifies in layer S5 (Badea and Nathans, 2004); and cluster 1 cells stratify in S3 (Badea and Nathans, 2004); we also encountered one such cell stratifying in S3 (not shown). Whether this diversity in stratification reflects functionally distinct cell types is unclear.

The best-characterized displaced amacrine cell is the starburst amacrine cell (for review see Masland and Tauchi, 1986), which makes up 19.5% of the displaced amacrine cells in the mouse retina (Jeon et al., 1998), 55% in the guinea pig retina (Kao and Sterling, 2006), and 85% in the rabbit retina (Vaney et al., 1981). Displaced starburst amacrine cells stratify in layer S4 of the IPL and are mirrored by cells of the same type located in the INL, which ramify in S2. Starburst amacrine cells play an important role in motion detection: they costratify with ON/OFF bistratified ganglion cells (Famiglietti, 1992c; Vaney and Pow, 2000; Zhang et al., 2005) and provide these ganglion cells with direction-selective inhibition (for review see Taylor and Vaney, 2003). This direction selectivity originates in the individual dendritic branches of the starburst cell: each dendrite is selective for stimuli that move along the dendrite away from the soma (Euler et al., 2002). To achieve this direction selectivity, the dendrites of starburst amacrine cells are functionally compartmentalized, whereby differential expression of chloride cotransporters along the length of the dendrite results in corresponding differential effects of GABA on membrane potential (Gavrikov et al., 2006).

The A17 cell was first described in the cat retina by Kolb et al. (1981). This cell type also has a counterpart of identical morphology in the INL (Wässle et al., 1987a). The displaced A17 cell is described here for the first time in the mouse retina. Both displaced and nondisplaced A17 cells stratify in the innermost layer of the IPL (cat: S4 and S5, Nelson and Kolb, 1985; rat: S5, Menger and Wässle, 2000). This GABAergic cell is an important component of the rod pathway: feedback inhibition at the reciprocal rod bipolar/A17 cell synapse shapes light responses in the inner retina (Dong and Hare, 2003), helping to adjust sensitivity levels over a large area of rod photoreceptors (Nelson and Kolb, 1985) and improve the temporal fidelity of light signals in the inner retina (Singer and Diamond, 2003; Dong and Hare, 2003). A17 cells use a unique form of feedback, whereby GABA release is triggered by calcium influx through AMPA receptors, activated by glutamate released from rod bipolar cells (Chavez et al., 2006).

Polyaxonal amacrine cells have also been described previously; this cell class is made up of several physiologically distinct cell types (Völgyi et al., 2001). The PA-S5 cell identified in this study is similar to the PA2 or type III cell found in the rabbit retina (Famiglietti, 1992b; Völgyi et al., 2001). One subtype of polyaxonal amacrine cell is electrically coupled to ON direction-selective ganglion cells; this coupling synchronizes the activity of neighboring ON direction-selective cells and thus plays a role in encoding stimulus movement (Ackert et al., 2006). Polyaxonal amacrine cells may also be involved in inhibition of ganglion cell spiking during rapid global shifts in scenes, such as during eye movements; this inhibition promotes detection of objects moving in a stationary scene (Roska and Werblin, 2003; Ölveczky et al., 2003).

Functional considerations

The presence of displaced amacrine cells in such ancient species as the Australian lungfish (Bailes et al., 2006) suggests a fundamental role for this class of cells. Truly *misplaced* AII amacrine cells have been reported in the outermost part of the INL; these cells are much less common than displaced amacrine cells and probably result from migration errors (Lee et al., 2006). Nevertheless, it is tempting to speculate on the evolutionary advantage of displacing some amacrine cell somata to the GCL. Is there a space problem in the INL? This is unlikely, in that moving all amacrine cells into the INL would add negligibly to the thickness of this layer. Do displaced amacrine cells require a certain proximity to ganglion cell somata? Changes in extracellular potassium concentration at the ganglion cell axon hillocks could influence the membrane potential of nearby displaced amacrine cells, for example, although this is unlikely, because the axon hillock of each ganglion cell is insulated by a continuous sheath from Müller cells (Stone et al., 1995). Whether there is an additional synaptic layer below the GCL has not been clarified (Koontz et al., 1989; Koontz, 1993). Do displaced amacrine cells synapse with ON bipolar cells, whereas nondisplaced amacrine cells contact OFF cells? This mirror-image arrangement, exemplified by the starburst amacrine cells, offers the advantage that the cell body is closer to the synaptic contacts (Wässle et al., 1987a). However, although this organization may be advantageous for some cell types, others stratify in the same layer of the IPL whether their cell bodies are displaced or not. For example, both displaced and nondisplaced A17 cells ramify in layer S5, where they synapse with rod bipolar cells.

This raises the interesting issue of whether some amacrine cells with cell bodies in the GCL may in fact be misplaced. Wright and Vaney (1999) described an amacrine cell type that has 98% of its somata in the INL and 2% displaced to the GCL; these displaced cells seem to be misplaced from the regular array of somata in the INL (Wright and Vaney, 1999). This may also be the case for

188

The Journal of Comparative Neurology. DOI 10.1002/cne

L. PÉREZ DE SEVILLA MÜLLER ET AL.

A17 cells, which are densely packed in the INL and quite scarce in the GCL. Conversely, some cell types found in the GCL have not been described in the INL (for example, MA-S1 and WA-S3) and therefore seem to be intentionally displaced to the GCL. The OFF starburst amacrine cell is another example of a cell type intentionally displaced to the GCL; this population of cells follows a pattern of development clearly distinct from that of the ON cell population (Knabe et al., 2007).

Several observations suggest that displaced amacrine cells probably have modulatory roles in visual processing. Narrow-field amacrine cells are thought to be involved in the direct pathway of information flow, whereas cells with larger dendritic fields are modulatory, with an indirect influence on information transmission (Masland, 1988); narrow-field amacrine cells are conspicuously absent from the GCL in the mouse (this study), rat (Perry and Walker, 1980), and cat (Wässle et al., 1987a) retinas. Furthermore, the majority of displaced amacrine cells are starburst amacrine cells (this study; Vaney et al., 1981). Thus, although there are many different types of amacrine cell in the GCL, the cells themselves, aside from the starburst cells, are rare, again suggesting a modulatory role in visual processing (see Masland, 1988). Evidence supporting a modulatory role has been provided for polyaxonal amacrine cells, which have been shown to release a number of neurotransmitters, including dopamine (Dacey, 1990) and nitric oxide (Perez et al., 1995).

ACKNOWLEDGMENTS

LITERATURE CITED

Aboelela SW, Robinson DW. 2004. Physiological response properties of displaced amacrine cells of the adult ferret retina. Vis Neurosci 21:135–144.

Abreu M, Kicliter E, Lugo-Garcia N. 1993. Displaced amacrine cells in the ganglion cell layer of the ground squirrel retina. P R Health Sci J 12:137–141.

Ackert JM, Wu SH, Lee JC, Abrams J, Hu EH, Perlman I, Bloomfield SA. 2006. Light-induced changes in spike synchronization between coupled ON direction selective ganglion cells in the mammalian retina. J Neurosci 26:4206–4215.

Badea TC, Nathans J. 2004. Quantitative analysis of neuronal morphologies in the mouse retina visualized by using a genetically directed reporter. J Comp Neurol 480:331–351.

Badea TC, Wang Y, Nathans J. 2003. A noninvasive genetic/pharmacologic strategy for visualizing cell morphology and clonal relationships in the mouse. J Neurosci 23:2314–2322.

Bailes HF, Trezise AEO, Collin SP. 2006. The number, morphology, distribution of retinal ganglion cells and optic axons in the Australian lungfish *Neoceratodus forsteri* (Krefft 1870). Vis Neurosci 23:257–273.

Chavez AE, Singer JH, Diamond JS. 2006. Fast neurotransmitter release triggered by Ca influx through AMPA-type glutamate receptors. Nature 443:705–708.

Curcio CA, Allen KA. 1990. Topography of ganglion cells in human retina. J Comp Neurol 300:5–25.

Dacey DM. 1990. The dopaminergic amacrine cell. J Comp Neurol 301:461–489.

Dong CJ, Hare WA. 2003. Temporal modulation of scotopic visual signals by A17 amacrine cells in mammalian retina in vivo. J Neurophysiol 89:2159–2166.

Euler T, Detwiler PB, Denk W. 2002. Directionally selective calcium signals in dendrites of starburst amacrine cells. Nature 418:845–852.

Famiglietti EV. 1981. Displaced amacrine cells of the retina. Soc Neurosci Abstr 7:620.

Famiglietti EV. 1992a. Polyaxonal amacrine cells of rabbit retina: morphology and stratification of PA1 cells. J Comp Neurol 316:391–405.

Famiglietti EV. 1992b. Polyaxonal amacrine cells of rabbit retina: PA2, PA3, PA4 cells. Light and electron microscopic studies with a functional interpretation. J Comp Neurol 316:422–446.

Famiglietti EV. 1992c. Dendritic co-stratification of ON and ON-OFF directionally selective ganglion cells with starburst amacrine cells in rabbit retina. J Comp Neurol 324:322–335.

Feng G, Mellor RH, Bernstein M, Keller-Peck C, Nguyen QT, Wallace M, Nerbonne JM, Lichtman, JW, Sanes JR. 2000. Imaging neuronal subsets in transgenic mice expressing multiple spectral variants of GFP. Neuron 28:41–51.

Gallego A. 1971. Horizontal and amacrine cells in the mammal's retina. Vis Res Suppl 3:33–50.

Gavrikov KE, Nilson JE, Dmitriev AV, Zucker CL, Mangel SC. 2006. Dendritic compartmentalization of chloride cotransporters underlies directional responses of starburst amacrine cells in retina. Proc Natl Acad Sci U S A 103:18793–18798.

Gustincich S, Feigenspan A, Wu DK, Koopman LJ, Raviola E. 1997. Control of dopamine release in the retina: a transgenic approach to neural networks. Neuron 18:723–736.

Haverkamp S, Wässle H. 2000. Immunocytochemical analysis of the mouse retina. J Comp Neurol 424:1–23.

Hughes A, Vaney DI. 1980. Coronate cells: the displaced amacrine cells of the rabbit retina? J Comp Neurol 189:169–189.

Hughes A, Wieniawa-Narkiewicz E. 1980. A large, newly identified population of presumptive microneurons in the ganglion cell layer of the cat retina. Nature 284:468–470.

Jeon CJ, Strettoi E, Masland RH. 1998. The major cell populations of the mouse retina. J Neurosci 18:8936–8946.

Kao Y-H, Sterling P. 2003. Matching neural morphology to molecular expression: single cell injection following immunostaining. J Neurocytol 32:245–251.

Kao Y-H, Sterling P. 2006. Displaced GAD65 amacrine cells of the guinea pig retina are morphologically diverse. Vis Neurosci 23:931–939.

Knabe W, Washausen S, Happel N, Kuhn H-J. 2007. Development of starburst cholinergic amacrine cells in the retina of *Tupaia belangeri*. J Comp Neurol 502:584–597.

Kolb H. 1982. The morphology of the bipolar cells, amacrine cells and ganglion cells in the retina of the turtle *Pseudemys scripta elegans*. Philos Trans R Soc Lond B Biol Sci 298:355–393.

Kolb H, Nelson R, Mariani A. 1981. Amacrine cells, bipolar cells and ganglion cells of the cat retina: a Golgi study. Vis Res 21:1081–1114.

Koontz MA. 1993. GABA-immunoreactive profiles provide synaptic input to the soma, axon hillock, and axon initial segment of ganglion cells in primate retina. Vis Res 33:2629–2636.

Koontz MA, Hendrickson AE, Ryan MK. 1989. GABA-immunoreactive synaptic plexus in the nerve fiber layer of primate retina. Vis Neurosci 2:19–25.

Lee EJ, Mann LB, Rickman DW, Lim EJ, Chun MH, Grzywacz NM. 2006. AII amacrine cells in the distal inner nuclear layer of the mouse retina. J Comp Neurol 494:651–662.

Lin B, Masland RH. 2006. Populations of wide-field amacrine cells in the mouse retina. J Comp Neurol 499:797–809.

Linden R, Esbérard CE. 1987. Displaced amacrine cells in the ganglion cell layer of the hamster retina. Vis Res 27:1071–1076.

MacNeil MA, Masland RH. 1998. Extreme diversity among amacrine cells: implications for function. Neuron 20:971–982.

MacNeil MA, Heussy JK, Dacheux RF, Raviola E, Masland RH. 1999. The shapes and numbers of amacrine cells: matching of photofilled with Golgi-stained cells in the rabbit retina and comparison with other mammalian species. J Comp Neurol 413:305–326.

Marc RE, Murry RF, Basinger SF. 1995. Pattern recognition of amino acid signatures in retinal neurons. J Neurosci 15:5106–5129.

Masland RH. 1988. Amacrine cells. TINS 11:405–410.

Masland RH. 2001. The fundamental plan of the retina. Nat Neurosci 4:877–886.

Masland RH, Tauchi M. 1986. The cholinergic amacrine cell. TINS 9:218–223.

Massey SC, Redburn DA. 1987. Transmitter circuits in the vertebrate retina. Prog Neurobiol 28:55–96.

The Journal of Comparative Neurology. DOI 10.1002/cne

DISPLACED AMACRINE CELLS OF THE MOUSE RETINA 189

Maxeiner S, Dedek K, Janssen-Bienhold U, Ammermüller J, Brune H, Kirsch T, Pieper M, Degen J, Kruger O, Willecke K, Weiler R. 2005. Deletion of connexin45 in mouse retinal neurons disrupts the rod/cone signaling pathway between AII amacrine and ON cone bipolar cells and leads to impaired visual transmission. J Neurosci 25:566–576.

Menger N, Wässle H. 2000. Morphological and physiological properties of the A17 amacrine cell of the rat retina. Vis Neurosci 17:769–780.

Nelson R, Kolb H. 1985. A17: a broad-field amacrine cell in the rod system of the cat retina. J Neurophysiol 54:592–614.

Ölveczky BP, Baccus SA, Meister M. 2003. Segregation of object and background motion in the retina. Nature 423:401–408.

Perez MT, Larsson B, Alm P, Andersson KE, Ehinger B. 1995. Localisation of neuronal nitric oxide synthase-immunoreactivity in rat and rabbit retinas. Exp Brain Res 104:207–217.

Perry VH, Walker M. 1980. Amacrine cells, displaced amacrine cells and interplexiform cells in the retina of the rat. Proc R Soc Lond B Biol Sci 208:415–431.

Petit-Jacques J, Völgyi B, Rudy B, Bloomfield S. 2005. Spontaneous oscillatory activity of starburst amacrine cells in the mouse retina. J Neurophysiol 94:1770–1780.

Pow DV, Wright LL, Vaney DI. 1995. The immunocytochemical detection of amino-acid neurotransmitters in paraformaldehyde-fixed tissues. J Neurosci Methods 56:115–123.

Roska B, Werblin F. 2003. Rapid global shifts in natural scenes block spiking in specific ganglion cell types. Nat Neurosci 6:600–508.

Sandell JH, Masland RH. 1986. A system of indoleamine-accumulating neurons in the rabbit retina. J Neurosci 6:3331–3347.

Schubert T, Maxeiner S, Krüger O, Willecke K, Weiler R. 2005. Connexin45 mediates gap junctional coupling of bistratified ganglion cells in the mouse retina. J Comp Neurol 490:29–39.

Singer JH, Diamond JS. 2003. Sustained Ca^{2+} entry elicits transient postsynaptic currents at a retinal ribbon synapse. J Neurosci 23: 10923–10933.

Stone J, Makarov F, Hollander H. 1995. The glial ensheathment of the soma and axon hillock of retinal ganglion cells. Vis Neurosci 12:273–279.

Strettoi E, Masland RH. 1996. The number of unidentified amacrine cells in the mammalian retina. Proc Natl Acad Sci U S A 93:14906–14911.

Taylor WR, Vaney DI. 2003. New directions in retinal research. TINS 26:379–385.

Vaney DI. 1980. A quantitative comparison between the ganglion cell populations and axonal outflows of the visual streak and periphery of the rabbit retina. J Comp Neurol 189:215–233.

Vaney DI. 1990. The mosaic of amacrine cells in the mammalian retina. Prog Ret Res 9:49–100.

Vaney DI, Pow DV. 2000. The dendritic architecture of the cholinergic plexus in the rabbit retina: selective labeling by glycine accumulation in the presence of sarcosine. J Comp Neurol 421:1–13.

Vaney DI, Peichl L, Boycott BB. 1981. Matching populations of amacrine cells in the inner nuclear and ganglion cell layers of the rabbit retina. J Comp Neurol 199:373–391.

Völgyi B, Xin D, Amarillo Y, Bloomfield SA. 2001. Morphology and physiology of the polyaxonal amacrine cells in the rabbit retina. J Comp Neurol 440:109–125.

Wässle H, Boycott BB. 1991. Functional architecture of the mammalian retina. Physiol Rev 71:447–480.

Wässle H, Chun MH, Müller F. 1987a. Amacrine cells in the ganglion cell layer of the cat retina. J Comp Neurol 265:391–408.

Wässle H, Voigt T, Patel B. 1987b. Morphological and immunocytochemical identification of indoleamine-accumulating neurons in the cat retina. J Neurosci 7:1574–1585.

Watt CB, Glazebrook PA, Florack VJ. 1994. Localization of substance P and GABA in retinotectal ganglion cells of the larval tiger salamander. Vis Neurosci 11:355–362.

Wright LL, Vaney DI. 1999. The fountain amacrine cells of the rabbit retina. Vis Neurosci 16:1145–1156.

Zhang J, Yang Z, Wu SM. 2004. Immunocytochemical analysis of spatial organization of photoreceptors and amacrine and ganglion cells in the tiger salamander retina. Vis Neurosci 21:157–166.

Zhang J, Li W, Hoshi H, Mills SL, Massey SC. 2005. Stratification of alpha ganglion cells and ON/OFF directionally selective ganglion cells in the rabbit retina. Vis Neurosci 22:535–549.

7.2 Jennifer Trümpler, Karin Dedek, Timm Schubert, Luis Pérez de Sevilla Müller, Mathias Seeliger, and Reto Weiler (2007). Rod and cone contributions to horizontal cell light responses in the mouse retina (in press).

The Journal of Neuroscience

Rod and cone contributions to horizontal cell light responses in the mouse retina

Journal:	*Journal of Neuroscience*
Manuscript ID:	JN-RM-1564-08.R1
Manuscript Type:	Regular Manuscript
Manuscript Section:	Behavioral System Cognitive
Date Submitted by the Author:	07-May-2008
Complete List of Authors:	Trümpler, Jennifer; University of Oldenburg, Department of Neurology Dedek, Karin; University of Oldenburg, Neurobiology Schubert, Timm; University of Oldenburg, Department of Neurobiology Pérez de Sevilla Müller, Luis; University of Oldenburg, Department of Neurobiology Seeliger, Mathias; Eberhard-Karls University, Retinal Diagnostics Research Group, Department of Ophthalmology II Humphries, Peter; Trinity College Dublin, Smurfit Institute of Genetics Biel, Martin; Ludwig Maximilians Universität, Department Pharmazie Weiler, Reto; University of Oldenburg, Neurobiology
Keywords:	CNG, rhodopsin, connexin36, Axon Terminal, Horizontal Cell, Retina
Themes & Topics:	b. Retinal circuitry, interneurons, and ganglion cells < 4. Vision < Theme D: Sensory and Motor Systems, a. Retina: Photoreceptors < 4. Vision < Theme D: Sensory and Motor Systems

Section: Behavioral/Systems/Cognitive

Senior Editor: Dr. David Fitzpatrick

Rod and cone contributions to horizontal cell light responses in the mouse retina

Abbreviated title: Rod/cone inputs to mouse horizontal cells

Jennifer Trümpler[1], Karin Dedek[1], Timm Schubert[1], Luis Pérez de Sevilla Müller[1], Mathias Seeliger[2], Peter Humphries[3], Martin Biel[4] and Reto Weiler[1]

[1]Department of Neurobiology, Carl von Ossietzky University, D-26111 Oldenburg, Germany

[2]Retinal Diagnostics Research Group, Department of Ophthalmology II, Eberhard-Karls University, D-72076 Tübingen, Germany

[3]Smurfit Institute of Genetics, Trinity College, Dublin 2, United Kingdom

[4]Department Pharmazie, Ludwig Maximilians Universität, D-81377 Munich, Germany

Corresponding author:

Dr. Reto Weiler
reto.weiler@uni-oldenburg.de
Department of Neurobiology
University of Oldenburg
telephone: +49-441-798-2581
fax: +49-441-798-3423
P. O. Box 2503
D-26111 Oldenburg
Germany

Number of figures: 7

Number of tables: 1

Number of pages: 24

Number of words in Abstract: 238

Number of words in Introduction: 483

Number of words in Discussion: 1500

Keywords: retina, horizontal cell, axon terminal, CNG, rhodopsin, connexin36

Abstract

Mammalian B-type horizontal cells make contacts with both photoreceptor types: the dendrites contact cone photoreceptors, while the axon terminal processes contact rods. Despite their distinct synaptic contacts, horizontal cell somata and axon terminals receive a mixture of rod and cone inputs. Interaction of the two photoreceptor systems is essential for adaptation of photoreceptor sensitivity to different levels of background illumination, and horizontal cells play a key role in this adaptation. In this study we used transgenic mouse lines to examine the contributions of rod and cone photoreceptor inputs to horizontal cell light responses in the mouse retina: rod signals were isolated by recording intracellularly from horizontal cells in a mouse lacking the cone cyclic nucleotide-gated channel, which lacks cone function, and cone signals were assessed using the rhodopsin knock-out mouse, which is a model for pure cone function. We found that both horizontal cell compartments receive a mixture of inputs from both photoreceptor types. To determine whether these inputs arrive via the long axon connecting the compartments or by way of rod-cone gap junctional coupling, we assessed the rod and cone contributions to horizontal cell somatic and axon terminal light responses in the connexin36-deficient mouse retina, which lacks rod-cone coupling. Our results confirm that rods and cones are coupled by connexin36, and suggest that signal transmission along the axon is unidirectional: signals are passed from horizontal cell soma to axon terminal but not from axon terminal to soma.

Introduction

Interaction between the rod and cone pathways is extensive: rods and cones are electrically coupled (Raviola and Gilula, 1973; Smith et al., 1986; Schneeweis and

Schnapf, 1995; Krizaj et al., 1998; Tsukamoto et al., 2001), and rod signals are funneled into the cone pathways at several stages in visual processing (reviewed by Völgyi et al., 2004). This interaction of the two photoreceptor systems is essential for adaptation of photoreceptor sensitivity to different levels of background illumination. Horizontal cells play a key role in this adaptation.

Mammalian B-type horizontal cells make synaptic contacts with both photoreceptor types: the dendrites contact cone photoreceptors, while the axon terminal processes contact rods (Kolb, 1970, 1974). The horizontal cell soma and axon terminal are connected by a long axon which is thought to electrically isolate the two compartments. Nevertheless, rod inputs have been recorded in horizontal cell somata in the cat retina (Steinberg, 1969a, 1969b, 1969c; Nelson et al., 1975). These rod inputs differed in their sensitivity from rod inputs recorded from axon terminals; it was therefore argued that they could not be arriving at the soma via the horizontal cell axon and axon terminal (Nelson et al., 1975). In addition, Bloomfield and Miller (1982) maintained that if signals spread from axon terminal to soma, then a slit of light displaced across the retina should elicit two peaks of activity at the soma; this was not the case (Bloomfield and Miller, 1982). Thus, rod inputs are thought to reach the horizontal cell soma via rod-cone gap junctions (Nelson et al., 1975). However, while both studies ruled out signal transmission from axon terminal to soma, the possibility of signal transmission from soma to axon terminal has never been examined.

This possibility has been difficult to test due to inadequate experimental procedures: previous studies distinguished rod from cone signals using stimuli of different wavelengths; however, this method provides only partial signal separation. In this study, we recorded pure rod and pure cone signals in horizontal cell somata and axon

terminals using transgenic mice lacking either rod or cone light responses. Rod inputs were isolated by recording from horizontal cells in the CNGA3 knock-out mouse, which lacks cone function as a result of deletion of the cone-specific α subunit of the cyclic nucleotide-gated channel (CNGA3; Biel et al., 1999); and cone signals were assessed in the rhodopsin knock-out mouse, which is a model for pure cone function (Humphries et al., 1997; Jaissle et al., 2001). The contribution of rod-cone gap junctions to the transmission of rod and cone signals to the horizontal cells was examined using connexin36-deficient mice, in which rod-cone coupling is abolished (Deans et al., 2002).

We found that mouse horizontal cell somata and axon terminals respond to a mixture of rod and cone inputs. Recordings from connexin36-deficient mice indicated that signal transduction along the axon is unidirectional: cone signals are passed from horizontal cell soma to axon terminal.

Methods

Wild-type (C57BL/6 and 129/Sv), CNGA3$^{-/-}$ (129/Sv genetic background; Biel et al., 1999), Cx36$^{-/-}$ (75% C57BL/6 genetic background; Güldenagel et al., 2001), and CNGA3$^{-/-}$/Cx36$^{-/-}$ mice (129/Sv genetic background) aged 5 weeks to 3 months, and rhodopsin$^{-/-}$ mice (C57BL/6 genetic background; Humphries et al., 1997) aged 4-7 weeks, were used in these experiments. All experiments were carried out in accordance with the institutional guidelines for animal welfare and the laws on animal experimentation issued by the German government. Careful attention was paid to the age of the mice, since photoreceptor deficiencies can cause degeneration of post-synaptic retinal neurons at later stages in development. For example, rhodopsin-deficient mice were used at 4-7 weeks of age, since at this age, development is

complete but cone degeneration has not begun, thus providing an all-cone retina (Jaissle et al., 2001).

Electrophysiology: intracellular recordings

Preparation Mice were housed under a 12-hour light-dark cycle. Experiments were begun 6-7 hours after the beginning of the light phase; mice were kept in a dark chamber for 18-19 hours before sacrifice. The eye was enucleated in ice-cold Ringer's solution under dim red light. Three or four small incisions were made into the rim of the eyecup to facilitate inversion; the eyecup was then inverted onto a plasticine dome, stabilized with tissue paper, and transferred to the recording chamber. Ringer's solution, warmed to 28°C using a heated cannula (MultiChannel Systems, Reutlingen, Germany), flowed continuously over the preparation from a small needle positioned at the apex of the inverted eyecup. The stabilizing tissue paper also served to drain the Ringer's solution and create a contact to the reference electrode. This configuration facilitated stable recordings lasting up to 1 hour. Ringer's solution contained (in mM): 117 NaCl, 3 KCl, 2 $CaCl_2$, 1 $MgSO_4$, 32 $NaHCO_3$, 0.4 NaH_2PO_4, 15 glucose, 0.1 glutamate, 0.5 ascorbic acid, and was perfused with 95% O_2 / 5% CO_2 to maintain a pH of 7.4-7.5.

Light stimulation Following preparation, retinas were left to recover and dark adapt for 1 hour. Light stimuli were generated by a 100-W tungsten-halogen lamp, and the intensity was controlled by a set of neutral density filters (Zeiss, Oberkochen, Germany) to give a range of 7 log units, with a maximum intensity of 0.32 mW/cm^2. For the experiments, full-field white light flashes of 250 ms duration were presented to the retina with inter-stimulus intervals of at least 10 seconds.

Intracellular recordings The procedure for intracellular recordings has been described (Shelley et al., 2006). Briefly, the membrane potential of the recorded cells was monitored intracellularly with glass microelectrodes (World Precision Instruments Inc., Sarasota, FL) pulled on a custom-made horizontal puller and filled with 3% Neurobiotin (Vector Laboratories, Burlingame, CA) in 3M KCl. The electrodes had resistances of 80-120 MΩ. The amplified signal was recorded with a PowerLab/4SP (AD Instruments) and stored on a computer for offline analysis. Horizontal cells were identified by their large hyperpolarizing responses to light stimuli and by their depth in the retina. To prevent light adaptation, presentation of light flashes during the search for a cell was kept to a minimum; these test flashes had dim intensities (<0.04 $\mu W/cm^2$), evoking responses smaller than 30% of the maximal response amplitude. Intensity-response profiles were derived from photoresponses elicited by full-field white light of increasing intensity; normalized response amplitudes were plotted against relative stimulus intensity. The profile of each cell was fitted with a sigmoidal function, from which the slope and the intensity eliciting half-maximal responses were derived.

Following data collection, cells were injected with Neurobiotin by applying rectangular current pulses of +1 nA amplitude and 750 ms duration at one second intervals. Retinas were then removed from the pigment epithelium, fixed in 4% paraformaldehyde and incubated overnight in streptavidin-indocarbocyanine (Cy3, Jackson Immunoresearch, West Grove, PA) to label the tracer. Only cells successfully injected were accepted for evaluation. For labeling of cone pedicles, retinas containing injected cells were incubated with FITC-conjugated peanut agglutinin (diluted 1:16 in phosphate buffer containing 0.1% bovine serum; Vector Laboratories) overnight at 4°C. Images were

taken using a Leica TCS SL confocal microscope with a 40x or 63x oil-immersion objective, and adjusted using Adobe Photoshop 7.0.

Results

We performed intracellular recordings from horizontal cells in the inverted eyecup preparation to examine the contributions of rod and cone inputs to horizontal cell somatic and axon terminal light responses in the mouse retina. Horizontal cells were identified by their large hyperpolarizing responses to light and their depth in the retina. Although horizontal cells could be reliably distinguished from other cell types by their light responses, somata and axon terminals could not be distinguished from one another in this way. Therefore, all recorded cells were filled with tracer for visual control (fig. 1).

Horizontal cell somata receive mixed rod-cone inputs. Rod and cone contributions to horizontal cell light responses have been studied in detail in the cat retina (Steinberg 1969a, 1969b, 1969c). In general, the rod component of the horizontal cell response is slow, returning to baseline long after stimulus offset. Moderate intensities elicit a long-lasting decay after stimulus offset, referred to as the "rod after-effect" (Steinberg, 1969c; Niemeyer and Gouras, 1973). The cone component is faster and shows a square waveform matching stimulus duration (Steinberg, 1969b).

In order to provide appropriate controls for all of the transgenic mouse lines used in this study, we used two strains of wild-type mice: C57BL/6 and 129/Sv. All of the response characteristics described by Steinberg (1969a, 1969b, 1969c) and Niemeyer and Gouras (1973) could be identified in the light responses of C57BL/6 wild-type mouse horizontal cell somata (fig. 2a), indicating that somata receive a mixture of rod and cone inputs. However, while some C57BL/6 horizontal cell somatic light responses had a

prominent rod component, others had less pronounced rod contributions, or lacked visible rod signals entirely (fig. 2b). Thus, despite careful attention to the adaptational state of the retina (see supplemental fig. 1), C57BL/6 horizontal cell somata showed a wide range of response properties. Horizontal cell somata from the 129/Sv strain showed much more consistent light responses; these cells always responded to light with a strong hyperpolarizing peak at light on, followed by a depolarizing sag and a slow return to baseline (fig. 3a). The return to baseline was much slower in horizontal cells from 129/Sv mice than in cells from C57BL/6 mice.

Mouse rod and cone signals cannot be distinguished based on wavelength because the sensitivity range of the rods (λ_{max} = 500 nm) largely overlaps with that of the middle-wavelength-sensitive cones (λ_{max} = 510 nm; Lyubarsky et al., 1999). Therefore, we used mouse models lacking either rod or cone function to elucidate the contributions of each photoreceptor type to wild-type horizontal cell light responses. In the rhodopsin-deficient retina, the rods cannot respond to light, and thus, all light responses are purely cone-generated. Conversely, in the CNGA3-deficient retina, the cones cannot respond to light, and thus all light responses are generated solely by the rods.

Figure 2c shows traces recorded from a horizontal cell soma in a rhodopsin-deficient retina: as expected for a functionally rodless retina, the slow, rod-driven components were missing from the light responses. This was especially evident at low intensities, where the responses closely followed the stimulus time course. However, the high variability among C57BL/6 wild-type somata made distinction between somatic light responses of wild-type and rhodopsin-deficient retinas difficult. This variability was not seen among horizontal cell somata of rhodopsin-deficient retinas: all light responses had

the fast waveform typical of cone-dominated light responses (n = 12); and most (9 out of 12 cells) showed the depolarizing rollback associated with feedback to the cones.

Conversely, in the CNGA3-deficient retina (fig. 3b), the light responses were much slower, highlighting the slow characteristics of purely rod-driven responses. These response waveforms were rounded and lacked a depolarizing rollback. At moderate intensities, near the threshold for 129/Sv wild-type horizontal cell somata, somata from CNGA3-deficient retinas saturated, and their membrane potentials required several minutes to return to baseline. Higher intensities completely bleached the responses, and the membrane potential did not return to baseline for several tens of minutes (data not shown).

Comparing the intensity-response curves from these two transgenic mouse lines with those of the corresponding wild type gives an indication of the relative contributions of rods and cones to wild-type horizontal cell light responses (fig. 2d, 3c). The intensities which elicit half-maximal responses in horizontal cell somata from rhodopsin-deficient retinas did not differ significantly from those from wild-type retinas (rhodopsin-deficient: $I_{1/2}$ = 2.3 x 10^{-3} ± 1.2 x 10^{-3}, mean ± SE, n = 12; C57BL/6 wild-type: $I_{1/2}$ = 1.4 x 10^{-3} ± 0.5 x 10^{-3}, n = 17; p = 0.14, Student's *t*-test). However, horizontal cell somata from CNGA3-deficient retinas showed a much higher sensitivity than 129/Sv wild-type horizontal cells, responding strongly to intensities that were at threshold level for wild-type horizontal cells. The intensities which elicit half-maximal responses in horizontal cell somata from CNGA-deficient retinas were significantly lower compared to the 129/Sv wild type (CNGA3-deficient: $I_{1/2}$ = 3.5 x 10^{-6} ± 1.4 x 10^{-6}, n = 5; 129/Sv wild type: $I_{1/2}$ = 0.5 x 10^{-3} ± 0.2 x 10^{-3}, n = 8; p < 0.05). This suggests that rod inputs to horizontal cell somata are largely suppressed in the presence of cone inputs in wild-type retinas, as has been

shown previously in amphibian horizontal cells in the mesopic state (Witkovsky et al., 1997).

Further evidence supporting a mixture of rod and cone signals in wild-type horizontal cells can be derived from the slopes of the intensity-response curves. Where two photoreceptor types contribute to the horizontal cell responses, a shallow slope is expected, since the combination of rods and cones leads to responses covering a wider range of intensities. Conversely, where only one photoreceptor type contributes, a steeper slope is expected. The mean intensity-response curve was significantly steeper for rhodopsin- (1.08 ± 0.10) and CNG-deficient horizontal cells (1.01 ± 0.06) than for the corresponding wild types (C57BL/6: 0.84 ± 0.04, $p < 0.01$; 129/Sv: 0.68 ± 0.08, $p < 0.01$). Therefore, we can conclude that wild-type horizontal cell somata receive a mixture of rod and cone inputs.

Horizontal cell axon terminals receive mixed rod-cone inputs. Light responses of axon terminals were very similar to those of somata; axon terminal recordings were confirmed by visual control using tracer injection (fig. 1). Like horizontal cell somata, C57BL/6 axon terminals also showed a mixture of rod and cone inputs and high variability between cells (fig. 4a,b), whereas responses from 129/Sv retinas were more uniform (fig. 5a). Although axon terminal recordings could not be distinguished from somatic recordings, axon terminals did show a higher sensitivity than somata (fig. 6c), as has been reported previously (Suzuki and Pinto, 1986).

Rod and cone contributions to axon terminal light responses were also dissected by recording from axon terminals in CNGA3- and rhodopsin-deficient retinas. The results were similar to those seen in somatic recordings. Figure 4c shows traces recorded from

a horizontal cell axon terminal in a rhodopsin-deficient retina: as was seen in the somatic recordings (fig. 2c), the slow, rod-driven components were missing from the light responses. Conversely, in the CNGA3-deficient retina (fig. 5b), the light responses did not reflect the square time course of the stimulus, as seen in the wild type, particularly at intermediate intensities. However, the strong similarity seen between axon terminals from 129/Sv and CNGA3-deficient retinas suggests a strong rod input to the axon terminal in the wild type.

Again, the intensity-response curves from these two transgenic mouse lines were compared with those of the appropriate wild type to examine the relative contributions of rods and cones to wild-type axon terminal light responses. The intensity-response curves of axon terminals from rhodopsin-deficient retinas were shifted to higher intensities compared to the wild type (fig 4d; rhodopsin-deficient: $I_{1/2} = 1.3 \times 10^{-3} \pm 0.8 \times 10^{-3}$, n = 3; C57BL/6 wild-type: $I_{1/2} = 0.3 \times 10^{-3} \pm 0.08 \times 10^{-3}$, n = 7; p < 0.05). Rod inputs therefore shape the response profile in wild-type axon terminals. As was seen in the somatic recordings, horizontal cell axon terminals from CNGA3-deficient retinas responded to lower intensities than did wild-type axon terminals (fig. 5c; CNGA3-deficient: $I_{1/2} = 1.9 \times 10^{-6} \pm 0.7 \times 10^{-6}$, n = 5; 129/Sv wild-type: $I_{1/2} = 0.25 \times 10^{-6} \pm 0.18 \times 10^{-6}$, n = 5); this difference was not significant.

As described above, further evidence supporting a mixture of rod and cone signals in wild-type horizontal cells can be derived from the slopes of the intensity-response curves. There was no significant difference between the slopes of the intensity-response curves from rhodopsin-deficient (0.92 ± 0.03) and C57BL/6 wild-type horizontal cells (0.92 ± 0.14), but the intensity-response curves were significantly steeper for axon

terminals in CNG-deficient retinas (0.94 $\pm$ 0.09) than for the 129/Sv wild type (0.57 $\pm$ 0.07, p < 0.01). Therefore, we can conclude that wild-type horizontal cell axon terminals receive a mixture of rod and cone inputs; and the cone input strongly influences the sensitivity of the horizontal cell axon terminals.

How do rod inputs reach the soma? We reasoned that there are two possibilities: either rod signals spread to cones through rod-cone gap junctions, or they enter the horizontal cell axon terminal and spread along the axon to the soma. These pathways are not necessarily mutually exclusive. To address this issue, we used a mouse model in which rod-cone coupling is presumably abolished: the Cx36-deficient mouse (Güldenagel et al., 2001; Deans et al., 2002). We hypothesized that if rod signals reach the horizontal cell soma solely by way of rod-cone gap junctions, then somatic responses from Cx36-deficient retinas should resemble the pure-cone responses from rhodopsin-deficient retinas.

Figure 6a shows typical light responses of a horizontal cell soma from a Cx36-deficient mouse. These responses closely resemble the pure-cone responses obtained from rhodopsin-deficient retinas. Their intensity-response profiles did not differ from those of the wild type (fig. 6c; $I_{1/2} = 2.8 \times 10^{-3} \pm 1.2 \times 10^{-3}$, n = 7). However, because the rod component of the somatic responses was so difficult to discern in the wild type, and therefore the somatic responses from rhodopsin- (and Cx36-) deficient retinas closely resemble wild-type responses, a further step was needed to test our hypothesis.

We therefore attempted to record light responses from CNGA3/Cx36 double knock-out mouse retinas; these mice lack both cone responses and rod-cone gap junctions. We reasoned that if light responses could be obtained from horizontal cell somata in these

mice, then these light responses must 1. originate in rods and 2. pass to the horizontal cell soma by way of the horizontal cell axon terminal and axon. We attempted these recordings on 9 mice, and obtained a total of 7 axon terminal recordings; no somatic recordings were obtained (table 1). In our hands, wild-type retinas yield on average 17 somatic recordings for every 7 axon terminals. Therefore, we conclude that the complete absence of somatic recordings in CNGA3/Cx36 double knock-out retinas is significant. It should be noted that the lack of somatic light responses was not a result of photoreceptor degeneration, since light responses were detected in axon terminals in CNGA3/Cx36 double knock-out retinas. These results support the theory of Nelson and colleagues (1975) that signals are not transmitted along the horizontal cell axon from axon terminal to soma. This also confirms the finding of Deans et al. (2002) that Cx36 forms gap junctions coupling the rods and cones in the mouse retina.

How do cone inputs reach the axon terminal? The horizontal cell axon does not transmit signals from axon terminal to soma, but so far the possibility of signal transmission in the opposite direction has not been examined in the mammalian retina. To test whether cone signals reach the axon terminal via rod-cone coupling or by way of the horizontal cell soma and axon, we recorded light responses of horizontal cell axon terminals from Cx36-deficient retinas. We reasoned that if, in the wild type, cone signals reach the axon terminal by way of rod-cone gap junctions, then light responses of axon terminals from Cx36-deficient retinas should resemble those obtained from CNGA3-deficient retinas, in which the cone component of the light responses was missing.

Light responses of an axon terminal from a Cx36-deficient mouse are shown in figure 6b. These light responses closely resemble those obtained from somata from this mouse line, and are also very similar to axon terminal responses obtained from

rhodopsin-deficient retinas (fig. 4c), but quite distinctive from axon terminal responses obtained from CNGA3-deficient retinas (compare fig. 5b). In particular, the responses in Cx36-deficient retinas show clearly the square time course of the stimulus at all intensities. This indicates a strong cone component in these axon terminal light responses, although the cones are no longer coupled to the rods. In addition, their intensity-response profiles did not differ from those of wild-type axon terminals (fig. 6c; $I_{1/2} = 0.3 \times 10^{-3} \pm 0.2 \times 10^{-3}$ Cx36-deficient, n = 3). It should be noted that a shift to lower intensities would be expected if the cone component were absent (compare to fig. 5c). Thus, rod-cone coupling is not necessary for spread of cone signals to horizontal cell axon terminals.

How, then, do cone signals reach the horizontal cell axon terminal? Axon terminals make synaptic contacts with rod photoreceptors in the wild-type retina. However, retinal neurons in transgenic mice with photoreceptor deficiencies have been shown to reorganize their synaptic contacts (for example Strettoi et al., 2002; Dick et al., 2003). To rule out the possibility that axon terminals in Cx36-deficient mice contact cone pedicles, we incubated retinas containing injected axon terminals with peanut agglutinin, which labels the base of the cone pedicles (Hack and Peichl, 1999; Haverkamp et al., 2001). Rotations of single scans revealed no overlap between axon terminal and cone pedicle labeling (fig. 7; n = 3). In addition, axon terminal morphology appeared normal; no evidence of sprouting or reorganization was seen. Thus, our data suggest that axon terminals receive cone inputs from the horizontal cell soma by way of the axon.

Discussion

Mouse horizontal cell somata receive synaptic inputs from cone photoreceptors, while their axon terminals receive synaptic inputs solely from rods. Despite this clear separation of synaptic inputs, both the somata and axon terminals of horizontal cells respond to a mixture of rod and cone inputs. Recordings from Cx36-deficient retinas indicated that rod signals reach horizontal cell somata via Cx36-containing gap junctions, thus confirming the role of Cx36 in rod-cone coupling. However, Cx36 was not required for conductance of cone signals to horizontal cell axon terminals. Our data suggest that transduction along the horizontal cell axon is unidirectional, from soma to axon terminal.

Methodological considerations.

Rod signals in horizontal cells can be determined by the horizontal cell's light response waveform, since the temporal properties of the rod response are not significantly filtered by signal transmission from photoreceptor to horizontal cell (Verweij et al., 1999). Since rod and cone signals cannot be easily dissected in the mouse retina using stimuli of different wavelengths, we took an alternative approach, using transgenic mouse lines: cone signals were assessed using the rhodopsin knock-out mouse, which is a model for pure cone function (Humphries et al., 1997; Jaissle et al., 2001); rod inputs were isolated in the CNGA3 knock-out mouse, which lacks cone function (Biel et al., 1999). This strategy offers the advantage that rod and cone signals can be cleanly isolated, and thus their contributions to wild-type light responses can be accurately assessed.

However, loss of synaptic input commonly causes morphological rearrangement in transgenic mouse retinas (Strettoi et al., 2002; Dick et al., 2003). In particular, deletion

of rhodopsin or CNGA3 has been shown to lead to degeneration and/or synaptic rewiring of retinal interneurons (Jaissle et al., 2001; Haverkamp et al., 2006). Nevertheless, detailed morphological studies have determined the time window in which retinas from these mice are fully matured but have not yet started to reorganize; in the present study, care was taken to use mice within this time frame. As an extra precaution, we carefully examined the morphology of the horizontal cells in age-matched mice, using targeted dye injection and immunohistochemistry. We found no signs of degeneration or reorganization in any of the transgenic mouse retinas used in this study (data not shown).

It is possible that, although we detected no morphological changes in the transgenic retinas, functional changes could have taken place. For example, since rods have been shown to have a tonic suppressive effect on cone pathways (Frumkes and Eysteinsson, 1987), one could speculate that loss of rod responses could result in enhancement of cone responses. However, this point was discounted by Williams et al. (2005), who showed that loss of one type of photoreceptor does not effect visual discrimination of the other photoreceptor type.

In order to provide appropriate controls for both rhodopsin- and CNGA3-deficient mice, we used two different wild-type strains in this study. Interestingly, light responses from C57BL/6 mice differed noticeably in waveform from those of 129/Sv mice (compare figs. 2a,b and 3a); furthermore, axon terminals from 129/Sv mice were more sensitive than those of C57BL/6 mice (figs. 4d and 5c). In electroretinograms, a-waves from C57BL/6 retinas showed a higher sensitivity than those from 129/Sv retinas (Pinto et al., 2007). Thus, the differences seen here probably arise from differences in connectivity between photoreceptors and horizontal cells, rather than from differences in photoreceptor

sensitivity. C57BL/6 horizontal cells have larger dendritic fields than those in 129/Sv retinas (Reese et al., 2005), suggesting that they may contact more cones; this could result in a larger suppression of rod inputs than in 129/Sv retinas.

Rod and cone inputs to horizontal cells

The horizontal cell axon is believed to electrically isolate the soma from the axon terminal in the mammalian retina. This theory is based on an early study which showed that rod inputs to B-type horizontal cell somata and axon terminals differed in sensitivity; thus rod signals could not be reaching the soma via the axon terminal (Nelson et al., 1975). Their conclusion was supported by theoretical evidence which suggested that the physical dimensions of the axon were not suited for passive electrical communication between the two cellular compartments (Nelson et al., 1975). It is important to note that their study addressed rod signals, and did not look at how cone inputs arrive at the axon terminals.

In cone horizontal cells in the carp retina, light responses have been measured in axon terminals despite the lack of direct photoreceptor inputs to these structures. These light responses were similar in amplitude to those recorded in somata (Weiler and Zettler, 1978, Zettler and Weiler, 1981). It has been suggested that the low conductance of the axon terminal may allow signal conduction from the soma by reducing leakage of signals arriving from the axon (Yagi and Kaneko, 1988). It is not clear whether cone signals pass along the axon to the axon terminal by passive spread (Yagi and Kaneko, 1988), or active propagation (Weiler and Zettler, 1978), or by gap junctional coupling between axon terminals and the axon near the cell body (Yagi, 1986).

Our findings support the conclusion of Nelson and colleagues (1975) that rod signals are transmitted to the horizontal cell somata via rod-cone coupling, but suggest that, as seen in fish, cone signals are conducted along the axon from soma to axon terminal. The ion channel composition of the horizontal cell soma differs from that of the axon terminal (A. Feigenspan, unpublished observations). In addition, the channel composition of the axon is not known. Thus it is possible that specific expression of ion channels in the soma and/or axon allows unidirectional passage of signals from soma to axon terminal.

However, it cannot be ruled out that cone signals reach the axon terminal via gap junctions which do not contain Cx36. This latter hypothesis suggests that Cx36-containing rod-cone gap junctions are asymmetrical, allowing signal passage from rods to cones but not vice versa. This is supported by expression of Cx36 in cones but not rods in the mouse retina (Feigenspan et al., 2004); these gap junctions are heterotypic. A separate set of gap junctions that allows passage of cone signals into rods could be modulated by different mechanisms, thus allowing distinct regulation of rod-to-cone and cone-to-rod signal spread.

On the distinctive roles of horizontal cell somata and axon terminals.

Interaction between the rod and cone pathways is extensive: rods and cones are electrically coupled (Raviola and Gilula, 1973; Smith et al., 1986; Schneeweis and Schnapf, 1995; Krizaj et al., 1998; Tsukamoto et al., 2001), and rod signals piggyback onto cone pathways at several stages in visual processing (reviewed by Völgyi et al., 2004). This interaction of the two photoreceptor systems is essential for adaptation of photoreceptor sensitivity to different levels of ambient illumination. Horizontal cell

somata play a key role in this adaptation by averaging light inputs over a large area of retina and feeding this averaged signal back to the cone photoreceptors (Baylor et al., 1971). This feedback adjusts the cone gain to different light levels. It is therefore logical that horizontal cell somata receive inputs from both rod and cone photoreceptors.

It has long been assumed that rod signals reach the horizontal cell somata by way of rod-cone coupling. Raviola and Dacheux (1990) showed that axonless horizontal cells in the rabbit retina receive rod inputs via rod-cone gap junctions. Rod-cone coupling makes up the secondary rod pathway in the mouse retina, and is thought to be mediated by Cx36: mice lacking Cx36 show no intermediate-sensitivity ON and OFF ganglion cell responses (Deans et al., 2002; Völgyi et al., 2004). For these reasons, we hypothesized that horizontal cell somata in Cx36-deficient mice should not receive rod inputs; this was confirmed in CNGA-Cx36 double knock-out mice. Thus our data confirm that rods and cones are coupled by Cx36 in the mouse retina.

While the functional role of the horizontal cell soma is straightforward, the role of the axon terminal is less well understood. Axon terminals have an extraordinarily elaborate morphology (see fig. 7), but no known synaptic output. This structure receives synaptic inputs from the rod photoreceptors, but feedback to the rods has never been demonstrated. While horizontal cell dendrites synapse onto midget bipolar cells in primate cone pedicles (Raviola and Gilula, 1975), axon terminals have not been shown to synapse onto bipolar cells in the mammalian retina. And here we show that axon terminals do not relay signals to the horizontal cell somata.

Horizontal cells have recently been shown to be pre-synaptic to dopaminergic interplexiform cells in the mouse retina, but it is not clear whether the synaptic contacts

are made by the axon terminals or the somata (Viney et al., 2007). Our data suggest that horizontal cell axon terminals receive cone signals from the horizontal cell somata; axon terminals therefore receive a mixture of rod and cone signals. These structures could potentially integrate light signals over the entire visual intensity range and over large areas of the retina; they are therefore ideally suited to play a modulatory role in visual processing.

References

Baylor DA, Fuortes MGF and O'Bryan PM (1971) Receptive fields of cones in the retina of the turtle. J Physiol 214:265-294.

Biel M, Seeliger M, Pfeifer A, Kohler K, Gerstner A, Ludwig A, Jaissle G, Fauser S, Zrenner E, Hofmann F (1999) Selective loss of cone function in mice lacking the cyclic nucleotide-gated channel CNG3. PNAS 96:7553-7557.

Bloomfield SA and Miller RF (1982) A physiological and morphological study of the horizontal cell types of the rabbit retina. J Comp Neurol 208:288-303.

Deans M, Völgyi B, Goodenough DA, Bloomfield SA, and Paul DL (2002) Connexin36 is essential for transmission of rod-mediated visual signals in the mammalian retina. Neuron 36:703-712.

Dick O, tom Dieck S, Altrock WD, Ammermüller J, Weiler R, Garner CC, Gündelfinger ED and Brandstätter JH (2003) The presynaptic active zone protein bassoon is essential for photoreceptor ribbon synapse formation in the retina. Neuron 37:775-786.

Feigenspan A, Janssen-Bienhold U, Hormuzdi S, Monyer H, Degen J, Söhl G, Willecke K, Ammermüller J and Weiler R (2004) Expression of connexin36 in cone pedicles and off-cone bipolar cells of the mouse retina. J Neurosci 24:3325-3334.

Frumkes and Eysteinsson (1987) Suppressive rod-cone interaction in distal vertebrate retina: intracellular records from *Xenopus* and *Necturus*. J Neurophysiol 57:1361-1382.

Güldenagel M, Ammermüller J, Feigenspan A, Teubner B, Degen J, Söhl G, Willecke K and Weiler R (2001) Visual transmission deficits in mice with targeted disruption of the gap junction gene connexin36. J Neurosci 21:6036-6044.

Hack I and Peichl L (1999) Horizontal cells of the rabbit retina are non-selectively connected to the cones. Eur J Neurosci 11:2261-2274.

Haverkamp S, Grünert U, and Wässle H (2001) The synaptic architecture of AMPA receptors at the cone pedicle of the primate retina. J Neurosci 21:2488-2500.

Haverkamp S, Michalakis S, Claes E, Seeliger MW, Humphries P, Biel M and Feigenspan A (2006) Synaptic plasticity in CNGA3(-/-) mice: cone bipolar cells react on the missing cone input and form ectopic synapses with rods. J Neurosci 26:5248-5255.

Humphries M, Rancourt D, Farrar J, Kenna P, Hazel M, Bush R, Sieving P, Shiels D, Creighton P, Erven Al, Boros A, Gulya K, Capecchi M, Humphries P (1997) Nat Genet 15:216-219.

Jaissle G, May A, Reinhard J, Kohler K, Fauser S, Lütjen-Drecoll E, Zrenner E, Seeliger M (2001) Evaluation of the rhodopsin knockout mouse as a model of pure cone function. IOVS 42:506-513.

Kolb H (1970) Organization of the outer plexiform layer of the primate retina: electron microscopy of golgi-impregnated cells. Phil Trans R Soc Lon B Biol Sci 258:58261-58283.

Kolb H (1974) The connections between horizontal cells and photoreceptors in the retina of the cat: electron microscopy of Golgi preparations. J Comp Neurol 155:1-14.

Krizaj D, Gábriel R, Owen WG and Witkovsky P (1998) Dopamine D2 receptor-mediated modulation of rod-cone coupling in the xenopus retina. J Comp Neurol 398:529-538.

Lyubarsky AL, Falsini B, Pennesi ME, Valentini P and Pugh Jr EN (1999) UV- and midwave-sensitive cone-driven retinal responses of the mouse: a possible phenotype for coexpression of cone photopigments. J Neurosci 19:442-455.

Nelson R, Lützow AV, Kolb H, and Gouras P (1975) Horizontal cells in cat retina with independent dendritic systems. Science 189:137-139.

Niemeyer G and Gouras P (1973) Rod and cone signals in S-potentials of the isolated perfused cat eye. Vision Res 13:1603-1612.

Pinto LH, Invergo B, Shimomura K, Takahashi JS and Troy JB (2007) Interpretation of the mouse electroretinogram. Doc Ophthalmol ISSN: 1573-2622

Raviola E, and Dacheux RF (1990) Axonless horizontal cells of the rabbit retina: synaptic connections and origin of the rod aftereffect. J Neurocytol 19:731-736.

Raviola and Gilula (1973) Gap junctions between photoreceptor cells in the vertebrate retina. PNAS 70:1677-1681.

Raviola and Gilula (1975) Intramembrane organization of specialized contacts in the outer plexiform layer of the retina. J Cell Biol 65:192-222.

Reese BE, Raven MA and Stagg SB (2005) Afferents and homotypic neighbors regulate horizontal cell morphology, connectivity, and retinal coverage. J Neurosci 25:2167-2175.

Schneeweis DM and Schnapf JL (1995) Photovoltage of rods and cones in the macaque retina. Science 268:1053-6.

Shelley J, Dedek K, Schubert T, Feigenspan A, Hombach S, Willecke K, and Weiler R (2006) Horizontal cell receptive fields are reduced in connexin57-deficient mice. Eur J Neurosci 23:3176-3186.

Smith RG, Freed MA, and Sterling P (1986) Microcircuitry of the dark-adapted cat retina: functional architecture of the rod-cone network. J Neurosci 6:3505-3517.

Steinberg RH (1969a) Rod and cone contributions to s-potentials from the cat retina. Vision Res 9:1319-1329.

Steinberg RH (1969b) Rod-cone interaction in s-potentials from the cat retina. Vision Res 9:1331-1344.

Steinberg RH (1969c) The rod after-effect in s-potentials from the cat retina. Vision Res 9:1345-1355.

Strettoi E, Porciatti V, Falsini B, Pignatelli V and Rossi C (2002) Morphological and functional abnormalities in the inner retina of the rd/rd mouse. J Neurosci 22:5492-5504.

Suzuki H and Pinto LH (1986) Response properties of horizontal cells in the isolated retina of wild-type and pearl mutant mice. J Neurosci 6:1122-1128.

Tsukamoto Y, Morigiwa K, Ueda M and Sterling P (2001) Microcircuits for night vision in mouse retina. J Neurosci 21:8616-8623.

Verweij J, Dacey DM, Peterson BB and Buck SL (1999) Sensitivity and dynamics of rod signals in H1 horizontal cells of the macaque monkey retina. Vision Res 39:3662-3672.

Viney TJ, Balint K, Hillier D, Siegert S, Boldogkoi Z, Enquist LW, Meister M, Cepko CL and Roska B (2007) Local retinal circuits of melanopsin-containing ganglion cells identified by transsynaptic viral tracing. Curr Biol 17:981-988.

Völgyi B, Deans MR, Paul DL and Bloomfield SA (2004) Convergence and segregation of the multiple rod pathways in mammalian retina. J Neurosci 24:11182-11192.

Weiler R and Zettler F (1978) The axon-bearing horizontal cells in the teleost retina are functional as well as structural units. Vision Res 19:1261-1268.

Williams GA, Daigle KA and Jacobs GH (2005) Rod and cone function in coneless mice. Vis Neurosci 22:807-816.

Yagi T (1986) Interaction between the soma and the axon terminal of retinal horizontal cells in cyprinus carpio. J Physiol 375:121-135.

Yagi T and Kaneko A (1988) The axon terminal of goldfish retinal horizontal cells: a low membrane conductance measured in solitary preparations and its implication to the signal conduction from the soma. J Neurophysiol 59: 482-494.

Zettler F and Weiler R (1981) Propagation of non-spike signals in retinal neurons. Vision Res 21:1589-1590.

Figures

Figure 1. Morphological control: following intracellular recordings, horizontal cells were injected with Neurobiotin. Horizontal cell somata (A) were easily distinguishable from axon terminals (B). Scale bars: 50 µm.

Figure 2. Somatic light responses from C57BL/6 wild-type (A, B) and rhodopsin-deficient retinas (C). Light stimuli consisted of full-field white light flashes of 250 ms duration. Increasing response amplitude reflects increasing stimulus intensity. A,B: C57BL/6 wild-type horizontal cell somata showed a range of response properties. The cell in A showed prominent rod components, including slow responses at low intensities and the rod after effect at intermediate intensities. The cell in B showed primarily cone-dominated response properties. C: Somata from rhodopsin-deficient mice showed exclusively cone-dominated response properties. D: Normalized intensity-response profiles for C57BL/6 wild-type (n = 17) and rhodopsin-deficient horizontal cell somata (n = 12); means ± standard errors. There was no significant difference in the intensity which elicited half-maximal responses in C57BL/6 wild-type and rhodopsin-deficient horizontal cell somata.

Figure 3. Somatic light responses from 129/Sv and CNGA3-deficient retinas. Light stimuli as in Fig. 2. A: 129/Sv wild-type horizontal cell somata showed much more consistent light response properties than somata from C57BL/6 mice. B: Somatic recordings from CNGA3-deficient retinas were easily distinguishable from the wild type. The square time course of the stimulus, visible in wild-type responses, is absent in responses from CNGA3-deficient retinas. C: Normalized intensity-response profiles for 129/Sv wild-type (n = 8) and CNGA3-deficient horizontal cell somata (n = 5); means ±

standard errors. Horizontal cell somata from CNGA3-deficient retinas responded to much lower light intensities than did 129/Sv wild-type horizontal cells ($p < 0.05$). This huge shift in the intensity-response profile reflects the pure rod input to horizontal cells in the CNGA3-deficient retina.

Figure 4. Axon terminal light responses from C57BL/6 wild-type (A, B) and rhodopsin-deficient retinas (C). Light stimuli as in Fig. 2. A,B: C57BL/6 wild-type horizontal cell axon terminals showed a range of response properties. The axon terminal in A showed prominent rod components, including slow responses at low intensities and the rod after effect at intermediate intensities. The axon terminal in B showed primarily cone-dominated response properties. C: Axon terminals from rhodopsin-deficient mice showed exclusively cone-dominated response properties. D: Normalized intensity-response profiles for C57BL/6 wild-type (n = 7) and rhodopsin-deficient horizontal cell axon terminals (n = 3); means ± standard errors. The intensity which elicited half-maximal responses in axon terminals was higher for rhodopsin-deficient retinas than for the wild type ($p < 0.05$).

Figure 5. Axon terminal light responses from 129/Sv wild-type (A) and CNGA3-deficient retinas (B). Light stimuli as in Fig. 2. Axon terminal recordings from CNGA3-deficient retinas were less distinguishable from the wild type, reflecting the strong rod input to these structures in the wild-type retina. C: Normalized intensity-response profiles for 129/Sv wild-type (n = 5) and CNGA3-deficient horizontal cell axon terminals (n = 5); means ± standard errors. The intensity which elicited half-maximal responses in axon terminals was lower for CNGA3-deficient retinas than for 129/Sv wild-type axon terminals; this difference was not significant. The response profiles of axon terminals

from CNGA3-deficient retinas were significantly steeper than those from the wild type, confirming the mixture of inputs into wild-type axon terminals.

Figure 6. Somatic (A) and axon terminal (B) recordings from Cx36-deficient retinas. Light stimuli as in Fig. 2. Both somatic and axon terminal light responses closely resembled responses from wild-type and rhodopsin-deficient retinas, reflecting a strong cone component in both the soma and axon terminal. C: Normalized intensity-response profiles for C57BL/6 wild-type horizontal cell somata (n = 17) and axon terminals (n = 7), and Cx36-deficient somata (n = 7) and axon terminals (n = 3); means ± standard errors. The intensity which elicited half-maximal responses did not differ significantly between wild-type and Cx36-deficient horizontal cell somata or between wild-type and Cx36-deficient horizontal cell axon terminals.

Figure 7. Morphological control. An injected axon terminal (green) from a Cx36-deficient retina labeled with peanut agglutinin (red). No evidence of sprouting of the axon terminal or synaptic contacts with cones was seen. A: image stack; B: single scan; C: high magnification of the boxed area in B. Scale bars: A,B 20 μm; C 10 μm.

Table 1. Rod and cone inputs to somata and axon terminals of the mice used in this study. The photoreceptor contributions to the somatic light responses in the Cx36-deficient retinas could not be determined, since the wild-type light responses were strongly dominated by cone inputs. However, the complete lack of light responses in the somata of CNGA3/Cx36 double knock-out mice indicates that rod signals cannot pass to the horizontal cell somata in the absence of rod-cone coupling.
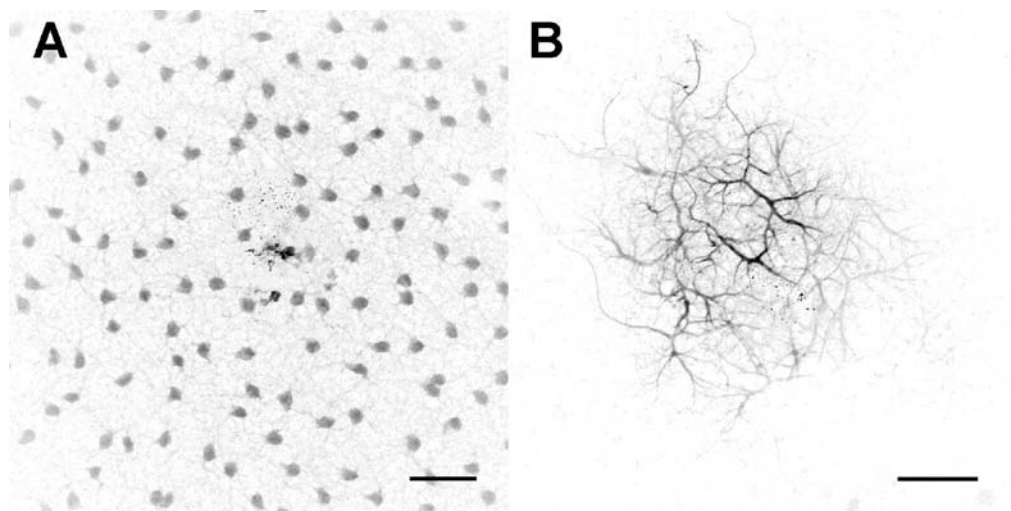
Figure 1. Morphological control: following intracellular recordings, horizontal cells were injected with Neurobiotin. Horizontal cell somata (A) were easily distinguishable from axon terminals (B). Scale bars: 50 µm.
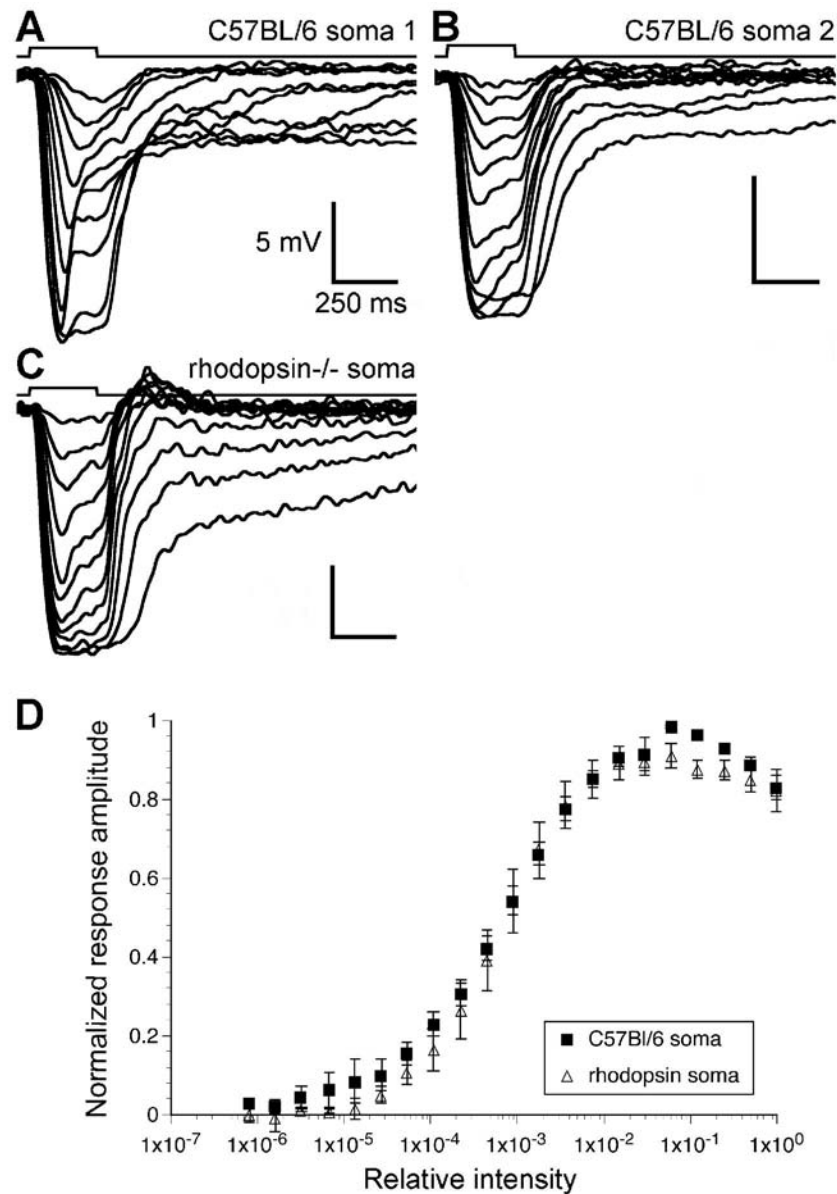115x57mm (600 x 600 DPI)

Figure 2. Somatic light responses from C57BL/6 wild-type (A, B) and rhodopsin-deficient retinas (C). Light stimuli consisted of full-field white light flashes of 250 ms duration. Increasing response amplitude reflects increasing stimulus intensity. A,B: C57BL/6 wild-type horizontal cell somata showed a range of response properties. The cell in A showed prominent rod components, including slow responses at low intensities and the rod after effect at intermediate intensities. The cell in B showed primarily cone-dominated response properties. C: Somata from rhodopsin-deficient mice showed exclusively cone-dominated response properties. D: Normalized intensity-response profiles for C57BL/6 wild-type (n = 17) and rhodopsin-deficient horizontal cell somata (n = 12); means ± standard errors. There was no significant difference in the intensity which elicited half-maximal responses in C57BL/6 wild-type and rhodopsin-deficient horizontal cell somata.
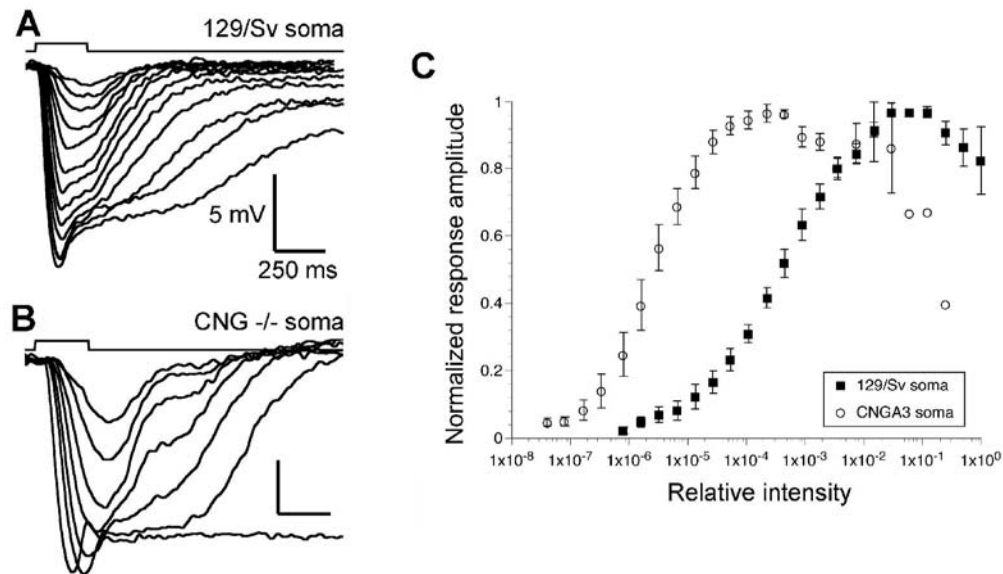85x119mm (600 x 600 DPI)

Figure 3. Somatic light responses from 129/Sv and CNGA3-deficient retinas. Light stimuli as in Fig. 2. A: 129/Sv wild-type horizontal cell somata showed much more consistent light response properties than somata from C57BL/6 mice. B: Somatic recordings from CNGA3-deficient retinas were easily distinguishable from the wild type. The square time course of the stimulus, visible in wild-type responses, is absent in responses from CNGA3-deficient retinas. C: Normalized intensity-response profiles for 129/Sv wild-type (n = 8) and CNGA3-deficient horizontal cell somata (n = 5); means $\pm$ standard errors. Horizontal cell somata from CNGA3-deficient retinas responded to much lower light intensities than did 129/Sv wild-type horizontal cells ($p < 0.05$). This huge shift in the intensity-response profile reflects the pure rod input to horizontal cells in the CNGA3-deficient retina.
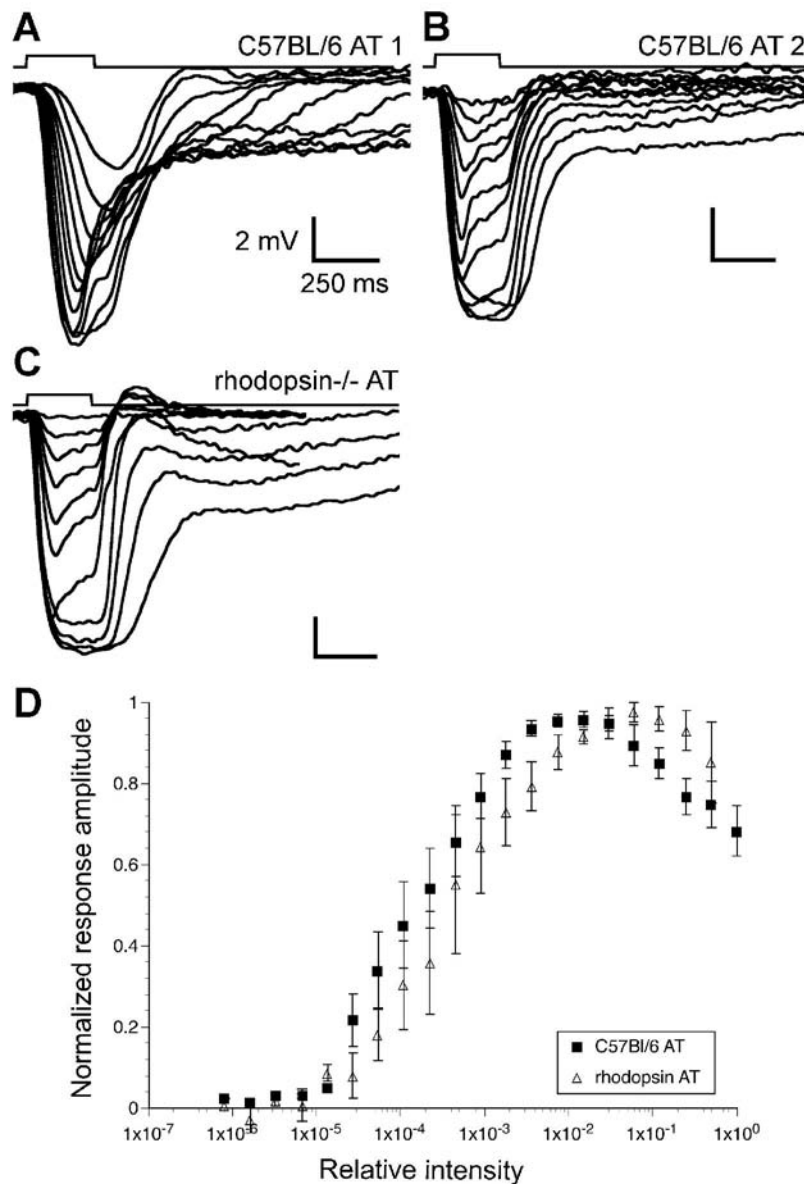115x67mm (600 x 600 DPI)

Figure 4. Axon terminal light responses from C57BL/6 wild-type (A, B) and rhodopsin-deficient retinas (C). Light stimuli as in Fig. 2. A,B: C57BL/6 wild-type horizontal cell axon terminals showed a range of response properties. The axon terminal in A showed prominent rod components, including slow responses at low intensities and the rod after effect at intermediate intensities. The axon terminal in B showed primarily cone-dominated response properties. C: Axon terminals from rhodopsin-deficient mice showed exclusively cone-dominated response properties. D: Normalized intensity-response profiles for C57BL/6 wild-type (n = 7) and rhodopsin-deficient horizontal cell axon terminals (n = 3); means ± standard errors. The intensity which elicited half-maximal responses in axon terminals was higher for rhodopsin-deficient retinas than for the wild type (p < 0.05).
85x125mm (600 x 600 DPI)

Figure 5. Axon terminal light responses from 129/Sv wild-type (A) and CNGA3-deficient retinas (B). Light stimuli as in Fig. 2. Axon terminal recordings from CNGA3-deficient retinas were less distinguishable from the wild type, reflecting the strong rod input to these structures in the wild-type retina. C: Normalized intensity-response profiles for 129/Sv wild-type (n = 5) and CNGA3-deficient horizontal cell axon terminals (n = 5); means ± standard errors. The intensity which elicited half-maximal responses in axon terminals was lower for CNGA3-deficient retinas than for 129/Sv wild-type axon terminals; this difference was not significant. The response profiles of axon terminals from CNGA3-deficient retinas were significantly steeper than those from the wild type, confirming the mixture of inputs into wild-type axon terminals.
115x67mm (600 x 600 DPI)

Figure 6. Somatic (A) and axon terminal (B) recordings from Cx36-deficient retinas. Light stimuli as in Fig. 2. Both somatic and axon terminal light responses closely resembled responses from wild-type and rhodopsin-deficient retinas, reflecting a strong cone component in both the soma and axon terminal. C: Normalized intensity-response profiles for C57BL/6 wild-type horizontal cell somata (n = 17) and axon terminals (n = 7), and Cx36-deficient somata (n = 7) and axon terminals (n = 3); means ± standard errors. The intensity which elicited half-maximal responses did not differ significantly between wild-type and Cx36-deficient horizontal cell somata or between wild-type and Cx36-deficient horizontal cell axon terminals.
115x66mm (600 x 600 DPI)
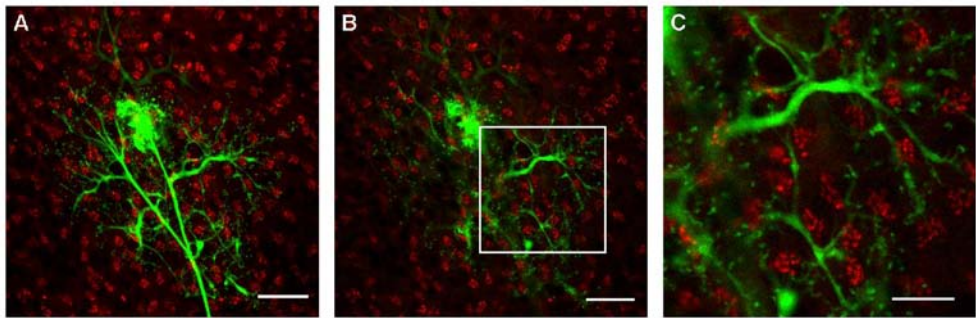
Figure 7. Morphological control. An injected axon terminal (green) from a Cx36-deficient retina labeled with peanut agglutinin (red). No evidence of sprouting of the axon terminal or synaptic contacts with cones was seen. A: image stack; B: single scan; C: high magnification of the boxed area in B. Scale bars: A,B 20 Âµm; C 10 Âµm.
176x60mm (300 x 300 DPI)

	soma	axon terminal
wild-type	rod + cone	rod + cone
rhodopsin -/-	cone	cone
CNG -/-	rod	rod
Cx36 -/-	?	rod + cone
CNG -/- Cx36 -/-	–	rod

Table 1. Rod and cone inputs to somata and axon terminals of the mice used in this study. The photoreceptor contributions to the somatic light responses in the Cx36-deficient retinas could not be determined, since the wild-type light responses were strongly dominated by cone inputs. However, the complete lack of light responses in the somata of CNGA3/Cx36 double knock-out mice indicates that rod signals cannot pass to the horizontal cell somata in the absence of rod-cone coupling.
85x41mm (600 x 600 DPI)
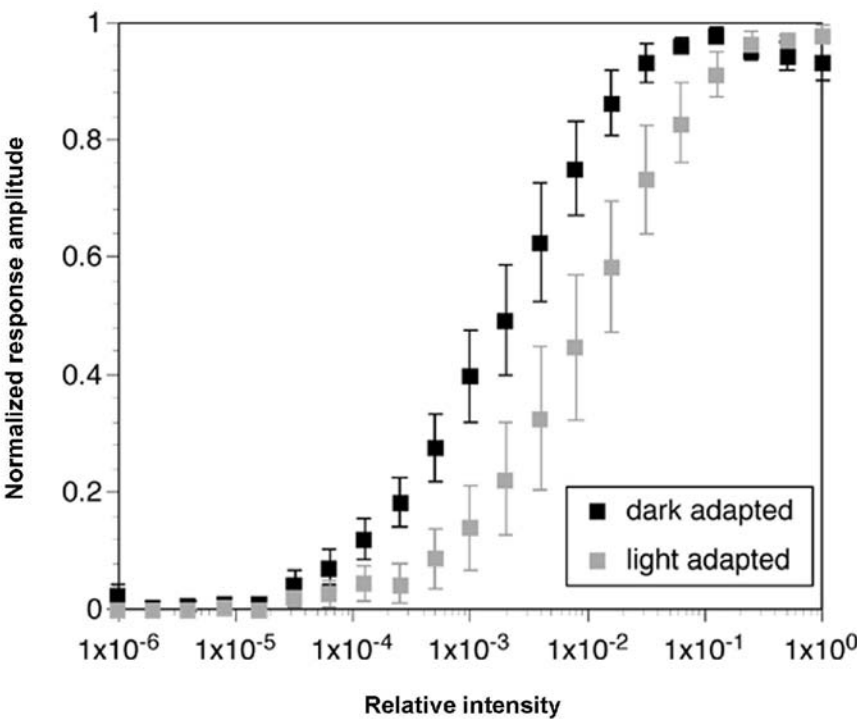
Supplemental figure 1.

Intensity profiles of C57BL/6 wild-type horizontal cell somata before (black squares) and after (grey squares) brief adaptation to moderate white light (15 minutes; I/Io = -2.4). Symbols represent means ± standard errors (n = 5). The high variation in response form of C57BL/6 horizontal cells (fig. 2a, b) suggests an equally high variation in the adaptational states of the retinas. However, as shown in this figure, even a short period of light adaptation causes a strong shift in the intensity profile to higher intensities. The variation in the intensity profiles was quite low amongst the wild-type horizontal cells examined in this study, as reflected in the small error bars in figure 2D. Therefore, it is unlikely that the adaptational states of the retinas varied significantly.

176x203mm (300 x 300 DPI)

7.3 Luis Pérez de Sevilla Müller, Karin Dedek, Ulrike Janssen-Bienhold, Maria M. Kreuzberg, Susanne Lorenz, Klaus Willecke, and Reto Weiler. Expression and modulation of Connexin30.2, a novel gap junction protein in the mammalian retina. (Submitted)

Expression and modulation of connexin30.2, a novel gap junction protein in the mammalian retina

Luis Pérez de Sevilla Müller[1], Karin Dedek[1], Ulrike Janssen-Bienhold[1], Maria M. Kreuzberg[2], Susanne Lorenz[1], Klaus Willecke[2], and Reto Weiler[1]

[1]Department of Neurobiology, University of Oldenburg, D-26111 Oldenburg, Germany
[2]Institute for Genetics, University of Bonn, D-53117 Bonn, Germany

Running title: Expression of connexin30.2 in the mouse retina

Corresponding author:

Professor Reto Weiler
reto.weiler@uni-oldenburg.de
Department of Neurobiology
University of Oldenburg
Telephone: + 49-441-798-2581
Fax: + 49-441-798-3423
P. O. Box 2503
D-26111 Oldenburg
Germany

Total pages: 31

Number of figures: 6

Number of tables: 1

Total number of words: 8722

Number of words in the Abstract: 238

Number of words in the Introduction: 496

Abstract 238 words (250 allowed)

Mammalian retinae express multiple connexins that mediate the metabolic and electrical coupling of various cell types. Here we describe a novel retinal connexin, connexin30.2 (Cx30.2), and its regulation in the mouse retina. To analyze the expression of Cx30.2, we used a transgenic mouse line in which the coding region of Cx30.2 was replaced by a lacZ reporter gene. We detected the lacZ signal in the nuclei of neurons located in the inner nuclear layer and the ganglion cell layer. In this study, we focused on the ganglion cell layer and characterized the morphology of the Cx30.2-expressing cells. Using immunocytochemistry and intracellular dye injections, we found six different types of Cx30.2-expressing ganglion cells: one type of ON-OFF, three types of OFF and two types of ON ganglion cells; among the latter was the RG_{A1} type. We show that RG_{A1} cells were heterologously coupled to numerous displaced amacrine cells, and our results suggest that these gap junctions must be heterotypic and involve Cx30.2 and a connexin yet unidentified in the mouse retina.

Gap junction coupling can be modulated by protein kinases, a process which plays a major role in retinal adaptation. Therefore, we studied the protein kinase-induced modulation of coupling between RG_{A1} and displaced amacrine cells. Our data provide evidence that coupling of RG_{A1} cells to displaced amacrine cells is mediated by the novel retinal connexin Cx30.2 and that the extent of this coupling is modulated by protein kinase C.

Introduction **494 words (500 allowed)**

Gap junctions are clusters of intercellular conduits which connect the cytoplasms of two contacting cells and allow metabolic and electrical coupling. Gap junctions are formed by proteins called connexins. Six of these proteins form a connexon, and the docking of two connexons from two adjacent cells generates a functional gap junction channel. Homotypic gap junctions comprise two identical connexons, heterotypic gap junctions are built from two different connexons. At least 20 connexin genes have been reported in the murine genome (reviewed in Söhl *et al.*, 2005).

In the mammalian retina, connexins are expressed in all neuronal cell classes (Vaney, 1991) where they form coupled networks. These neuronal networks are modulated by light and neuromodulators which can alter the extent of coupling when the visual environment changes (for review see Weiler *et al.,* 2000). These adaptational processes presumably are mediated by protein kinases which can alter the gap junction properties by phosphorylating either the connexins involved or other target proteins which can in turn change connexin characteristics.

Among retinal connexins, Cx36 is predominant. It has been described in photoreceptors (Deans *et al.*, 2002; Lee *et al.*, 2003; Feigenspan *et al.*, 2004), bipolar cells (Feigenspan *et al.*, 2004; Lin *et al.*, 2005; Han & Massey, 2005), AII amacrine cells (Feigenspan *et al.*, 2001; Mills *et al.*, 2001), and alpha ganglion cells (Schubert *et al.*, 2005a; Völgyi *et al.*, 2005). AII amacrine cells form homotypic gap junction composed of Cx36 to one type of ON cone bipolar cell (Lin *et al.*, 2005; Han & Massey, 2005) and heterotypic gap junctions consisting of Cx36 and Cx45 to other ON cone bipolar cell types (Maxeiner *et al.*, 2005; Dedek *et al.*, 2006). Cx45 is also expressed in OFF bipolar cells (Maxeiner *et al.*, 2005), bistratified ganglion cells (Schubert *et al.*, 2005b) and in amacrine cells (Maxeiner *et al.*, 2005; Pérez de Sevilla *et al.*, 2007). Two other retinal connexins, Cx57 and Cx50, mediate the extensive coupling of horizontal cells (Hombach *et al.*, 2004; O'Brien *et al.*, 2006).

Despite this plethora of gap junction proteins, it seems likely that still other connexin genes are expressed in the mammalian retina. For example, Xin & Bloomfield (1997) showed that many ganglion cell types exhibit tracer coupling. However, the corresponding connexins, except for those expressed in alpha (Cx36) and bistratified ganglion cells (Cx45) have not yet been identified. Therefore, we studied the expression pattern of the gap junction protein Cx30.2 in the mouse retina. Cx30.2 was first shown to be expressed in cardiac myocytes (Kreuzberg *et al.*, 2005). Recently, Cx30.2 was also found in neurons, namely in inhibitory interneurons of the hippocampus (Kreuzberg *et al.*, 2008). To study Cx30.2 expression in the mouse retina, we used a transgenic mouse line which expressed a lacZ reporter gene instead of the Cx30.2 coding region (Kreuzberg *et al.*, 2006). We found Cx30.2 in six different types of ganglion cells and studied protein kinase-induced phosphorylation as a potential mechanism to modulate ganglion cell networks coupled by Cx30.2.

Materials and Methods

Mouse strains and tissue preparation

Retinae were obtained from several different mouse lines: $Cx30.2^{lacZ/lacZ}$, $Cx30.2^{+/lacZ}$ (Kreuzberg *et al.*, 2006), Cx45fl/fl:Nestin-Cre (Maxeiner *et al.*, 2005), $Cx36^{-/-}$ (Güldenagel *et al.*, 2001), $Cx40^{-/-}$ (Kirchhoff *et al.*, 1998) and wild-type (WT) mice (C57BL/6). Mice were killed by cervical dislocation in accordance with the institutional guidelines for animal welfare issued by the Federal Republic of Germany. Eyes were enucleated and were kept at room temperature in a Petri dish with carboxygenated Ames' medium (Sigma, pH 7.4). Retinae were mounted photoreceptor side down on black filter paper (Millipore Corporation, Bedford, MA, USA).

Intracellular injections

Intracellular injections were carried out as described (Schubert *et al.*, 2005a; Pérez de Sevilla *et al.*, 2007). Briefly, borosilicate glass electrodes (Hilgenberg, Malsfeld, Germany) were pulled with a Sutter P-97 puller (Sutter, Novato, CA, USA). Electrode tips were filled with 1% Alexa594 or Alexa568 sodium hydrazide (Invitrogen), or Lucifer Yellow (Sigma) and 4% N-(2-aminoethyl-)-biotinamide hydrochloride (Neurobiotin, Vector, Burlingame, CA, USA). Electrodes were backfilled with Tris buffer, pH 7.4, and typically had resistances between 100 and 140 MΩ. To visualize ganglion cell bodies in WT retinae, a few drops of Acridine Orange (1 µM; Sigma) were added to the bath solution. After a few minutes, retinae were washed and ganglion cells were injected. Alexa dye/Lucifer Yellow was iontophoresed with a current of -1 nA (750 ms at 1 Hz). When the dendritic morphology of the cell could be discerned, the direction of the current was reversed to +1 nA to inject Neurobiotin.

Labeling lacZ-expressing cells

To label lacZ-expressing cells *in vivo,* retinae from Cx30.2$^{lacZ/lacZ}$ and Cx30.2$^{+/lacZ}$ mice were incubated with fluorescein-di-beta-D-galactopyranoside (FDG; Sigma). FDG is a fluorogenic substrate for beta-galactosidase and can be used to visualize lacZ-expressing cells (Nirenberg & Cepko, 1993). It was applied in Ames' medium at a concentration of 1.5 mg/ml in 1.25% dimethyl sulfoxide (Sigma). After 1-2 minutes incubation, retinae were washed in the dark for 15 minutes in carboxygenated Ames' medium. LacZ-positive ganglion cells, now labeled with fluorescein, were injected as described above.

Pharmacological experiments

In another set of experiments, we aimed to identify the protein kinase involved in the modulation of tracer coupling between Cx30.2-expressing RG$_{A1}$ cells and displaced amacrine cells. For that purpose, retinae of WT mice were incubated with cAMP (1 mM, Sigma), 3-isobutyl-1-methylxanthine (IBMX, 100 µM, Sigma, cat nr 7018), forskolin (500 µM, Merck/Calbiochem), staurosporine (10 µM, Sigma), or 4-beta-phorbol-12,13-dibutyrate (PDBu, 10 µM, Sigma) prior to injection. Retinae were washed in Ames' medium before injecting RG$_{A1}$ cells for 3 minutes. After the last injection, the retinae remained for 20-30 minutes in the recording chamber, allowing diffusion of Neurobiotin.

Immunostaining in whole-mount retinae

After intracellular dye injection, retinae were fixed in 4% paraformaldehyde for 15 minutes. Fixed retinae were washed for at least 30 minutes in 0.1 M phosphate buffer (PB), pH 7.4. Neurobiotin was visualized by incubating injected retinae overnight with streptavidin-indocarbocyanine (Cy3, 1:500, Jackson Immunoresearch, West Grove, PA, USA), in 0.1 M PB containing 0.3% TritonX-100 (Sigma).

Some retinae from Cx30.2$^{lacZ/lacZ}$ and Cx30.2$^{+/lacZ}$ mice were processed using the beta-galactosidase essay as described by Feigenspan *et al.* (2004). Briefly, whole-mount retinae were washed in lacZ washing solution and incubated with the beta-galactosidase substrate X-gal for three to four days at 37 °C. Neurons with beta-galactosidase reactivity were identified by the reaction product which consisted of one blue dot in the cell's nucleus.

In order to reveal the stratification level of ganglion cell processes within the inner plexiform layer, the two plexuses of cholinergic starburst amacrine cells which mark the ON- and OFF-sublaminae were immunocytochemically labeled and used as landmarks. Polyclonal anti-goat choline acetyltransferase (ChAT) antibodies (1:500, Chemicon International, Chandlers Ford, UK) were used as a specific marker for cholinergic amacrine cells.

Other injected retinae were incubated with antibodies against parvalbumin (1:500, Swant, Bellinzona, CH), calbindin (1:1000, Swant) or calretinin (1:500, Chemicon) for a week, washed several times in PB, and incubated overnight at 4°C in the corresponding secondary antibodies (goat anti-rabbit Cy5, 1:500, Jackson ImmunoResearch; goat anti-mouse Cy5, 1:500, Jackson ImmunoResearch; donkey anti-goat Cy5, 1:500, Jackson ImmunoResearch). After final washes with PB, retinae were mounted in Vectashield Mounting Medium (Vector Laboratories). Coverslips were sealed with nail polish for prolonged storage. Slides were stored at 4 °C protected from light.

Immunostaining in retinal cryosections

Mouse eyecups were fixed in 2% paraformaldehyde for 20 minutes. Vertical cryosections (12-14 μm) from Cx30.2$^{+/lacZ}$ and Cx30.2$^{lacZ/lacZ}$ mice were stained for beta-galactosidase activity as described previously (Feigenspan *et al.*, 2004). Briefly, slices were washed in lacZ washing solution and incubated with the beta-galactosidase substrate X-gal for one to two days at 37 °C. For single and double staining, we used polyclonal antibodies against calretinin (1:500 and 1:5000, respectively, Chemicon), parvalbumin (1:500, Swant), and calbindin (1:1000,

Swant). Cryosections were blocked with 5-10% normal goat serum or mouse serum in 0.1 M

PB + 0.3% Triton-X100 at room temperature for 1 h. Sections were incubated with the first

antibody at 4 °C overnight. After three washes, the corresponding secondary antibodies (see

above) were applied at room temperature for 2 h. Finally, sections were washed and mounted

in Vectashield. Omitting the primary antibody in the immunostaining procedures was done as

a control; no labeling was ever found.

Image analysis and statistics

Images were taken with a Leica TCS SL confocal microscope with a 40x oil-immersion

objective. Intensity and contrast of the final images were adjusted in Adobe Photoshop 7.0

(Adobe). All values are given as mean ± SD and were compared for statistical differences

using the unpaired t-test in SigmaPlot (Systat Software Inc., San Jose, CA, USA).

Results

Localization of Cx30.2 in the mouse retina

In recent years, four different connexins (Cx36, Cx45, Cx50 and Cx57) have been reported to be involved in electrical synapses between neurons in mouse and rabbit retinae. Nevertheless, it seems very likely that this list is not complete. Many different classes of amacrine and ganglion cells have been described to be coupled (Vaney, 1991; Xin & Bloomfield, 1997) and in many cases the connexins involved in this coupling are still unknown. Very recently, a novel connexin, Cx30.2, has been described to be expressed in the central nervous system of the mouse (Kreuzberg *et al.*, 2008). To study whether Cx30.2 is expressed in the retina, we used a transgenic mouse line in which the coding region of the Cx30.2 gene was replaced by a lacZ reporter gene expressed under the control of Cx30.2 gene regulatory elements (Kreuzberg *et al.*, 2006).

In retinal cryosections, staining for beta-galactosidase activity in Cx30.2$^{lacZ/lacZ}$ mice revealed lacZ-positive cells in the ganglion cell layer (GCL) (Fig. 1A) and in the inner nuclear layer (INL) (arrows). Based on the localization of the lacZ signal and the size of the labeled cells in the INL, we hypothesized that all lacZ-positive neurons corresponded to amacrine cells and that these cells comprised at least two different types of neurons. One subtype had its nucleus close to the border between the INL and the inner plexiform layer (IPL) whereas the second type had its nucleus further away from that border. Rarely, we found some nuclei in the INL that were as big as the ones in the GCL. These cells might correspond to displaced ganglion cells or large amacrine cells.

We studied the lacZ-positive cells in the GCL by staining whole mount retinae from Cx30.2$^{lacZ/lacZ}$ mice. There, lacZ-positive cells were distributed over the entire retina (Fig. 1B). At higher magnification (Fig.1C), big (arrows) and small lacZ-positive nuclei (arrowheads) could be differentiated, suggesting that there were at least two subpopulations of Cx30.2-expressing neurons in the GCL. Big lacZ-positive nuclei most likely represent ganglion cells,

9

and small lacZ-positive nuclei might represent small ganglion cells or displaced amacrine cells, which are very frequent in the mouse retina (Jeon *et al.*, 1998; Badea & Nathans, 2004; Lin & Masland, 2006; Pérez de Sevilla *et al.*, 2007).

In the GCL, the spatial distribution of Cx30.2-expressing neurons was evaluated for three retinae. LacZ-stained retinae were divided into four sections (ventral, dorsal, nasal and temporal) and lacZ-positive cells were counted (Fig. 1B). The density of Cx30.2-expressing cells showed an even distribution from the central area of the retina to the peripheral retina in all sectors with no statistical difference between the four sectors (data not shown).

Electroretinograms of WT and Cx30.2-deficient mice did not show any significant differences in a and b waves (Pérez de Sevilla, unpublished observation). Considering the lacZ expression pattern described above, this was not surprising, since the a and b waves are mainly generated by photoreceptor and ON bipolar cell responses, respectively, and these two cell types never showed any lacZ signal in Cx30.2-deficient mice.

Immunocytological characterization of lacZ-positive cells in Cx30.2-deficient retinae

To examine the morphology of the Cx30.2-expressing cells in detail, we focused on the GCL. We used different immunocytochemical markers to analyze whether the Cx30.2-expressing cells comprised several cell types. Retinae from Cx30.2$^{lacZ/lacZ}$ mice were stained for the calcium-binding proteins calbindin, calretinin, and parvalbumin. Table 1 summarizes the results (for more details see Supplementary Material Fig. 1). Retinal neurons expressing Cx30.2 were differentially immunolabeled by these markers. For example, ganglion cells with big nuclei (>8 µm) often expressed parvalbumin, which was never expressed by ganglion cells with small nuclei (<8 µm). However, some cells with small nuclei were positive for calretinin and some were, in rare cases, also positive for calbindin. Taken together, these stainings suggested that Cx30.2 is expressed in multiple ganglion cell types in the mouse retina.

Classification of Cx30.2-expressing ganglion cells

We injected ganglion cells with sharp electrodes in retinae from Cx30.2$^{lacZ/lacZ}$ and Cx30.2$^{+/lacZ}$ mice and stained them afterwards for lacZ expression. However, we had some difficulties with this method since the injected Lucifer Yellow masked the lacZ signal in the injected cells. This made it almost impossible to identify the Cx30.2-expressing cells.

To circumvent this problem, we identified the lacZ-positive cells before injection. Living cells containing beta-galactosidase can be stained with FDG (Nirenberg & Cepko, 1993; Nirenberg & Meister, 1997); hydrolysis of FDG by beta-galactosidase leads to an accumulation of fluorescein in the cytoplasm of the lacZ-positive cell. This approach enabled us to visualize the lacZ-positive cells, now fluorescent green, and made them easy to target with sharp dye-filled electrodes (see Supplementary Material Fig. 2) to characterize them. However, a disadvantage of the FDG method was that we could only inject 5-8 cells per retina since the marker sometimes leaked out of the cells over time.

In order to characterize and classify the Cx30.2-expressing ganglion cells, we injected ganglion cells prelabeled with FDG (n = 68), with Neurobiotin and Alexa568 or Alexa594 hydrazide. Both the Alexa dyes and Neurobiotin filled the cells completely, demonstrated by the tapering endings of their dendrites. Dendritic stratification was determined by labeling the retina with anti-ChAT antibodies, which visually define the five different strata of the IPL. This classification was made with retinae from Cx30.2$^{+/lacZ}$ and Cx30.2$^{lacZ/lacZ}$ animals. We created a morphological catalog of the injected ganglion cells using the dendritic field and soma sizes, dendritic depth within the IPL, general morphology, and coupling patterns as characteristics.

We divided the Cx30.2-expressing ganglion cells into three different classes: (1) ON-OFF cells, (2) OFF cells and (3) ON cells.

(1) ON-OFF cells

Only one type of ON-OFF cell was found. This *bistratified ganglion cell* type (Fig. 2A) had

dendritic arbors with a diameter of 278.8 ± 56 μm (n = 6). Cell bodies had a mean diameter of

18.7 ± 0.7 μm. The dendrites were recursive and loop-forming (Fig. 2A). The ON dendrites

stratified in stratum S4 and the OFF processes in stratum S2 of the IPL (Fig. 2B) suggesting

that this cell type is identical with the ON-OFF direction selective ganglion cell RG_{D2} (Sun *et

al.* 2002a; Weng *et al.*, 2005). Interestingly, RG_{D2} cells have been shown to be coupled to

other bistratified ganglion cells by Cx45 (Schubert *et al.*, 2005b; see discussion).

(2) OFF cells

Three types of OFF ganglion cells expressed Cx30.2. None of these cell types could be found

in the classification of mouse ganglion cells provided by Sun *et al.* (2002a).

   OFF type 1 cells (Fig. 2C) had big cell bodies of 14.2 ± 1.6 μm in diameter and

large dendritic arbors of 373.8 ± 48.2 μm (n = 16) which stratified close to the INL, in stratum

S1 of the IPL (Fig. 2D). Occasionally, two of 16 cells, the OFF type 1 cells were coupled to

amacrine cells which had their somata located in the INL. The general morphology of this cell

type was similar to OFF alpha ganglion cells described in the mouse retina (Schubert *et al.*,

2005a; Völgyi *et al.*, 2005) but there was a prominent difference: OFF alpha cells are coupled

to amacrine cells and to neighboring alpha cells (Schubert *et al.*, 2005a; Völgyi *et al.*, 2005)

but we never observed coupling of OFF-type 1 cells to other ganglion cells.

   OFF type 2 cells (Fig. 2E) had large and asymmetric dendritic arborizations

which extended 285.5 ± 125 μm in diameter (n = 7). The cell bodies were round (17.9 ± 1.4

μm). Their processes stratified in stratum 1 of the IPL close to the INL (Fig. 2F). We never

observed tracer coupling in these cells.

   OFF type 3 cells had the smallest dendritic fields of the Cx30.2-expressing

ganglion cells identified in this study, with a diameter of 241.7 ± 85.9 μm (n = 12). The

dendritic arbors were round or ovoid (Fig. 2G) and dendrites stratified in stratum S1 of the IPL (Fig. 2H). The mean diameter of the round somata was 19.2 ± 1.4 µm. OFF type 3 cells never showed tracer coupling to other cells.

(3) ON cells

ON type 1 cells (n = 5) were defined by their small somata and medium-to-large dendritic fields. They presented round somata of 13.4 ± 1.3 µm and dendritic fields of 391.8 ± 81.4 µm in diameter (Fig. 3A). Their processes extended to stratum S5 of the IPL (Fig. 3B). The ending tips of the dendrites overlapped sparsely. When injected in heterozygous mice, no coupling was observed. This ganglion cell type had a lot of similarities with the ganglion cell RG_{C1} found in the rat by Huxlin & Goodchild (1997).

$\qquad$ *ON type 2 cells* (n = 16) had big polygonal cell bodies from which 3 to 7 primary dendrites (mean: 4.9 ± 1) left the soma to ramify in a branching radial pattern, resulting in few dendrites close to the soma (Fig. 3C). Dendrites were smooth, often overlapped at the ending tips and frequently formed hook-like terminals. The soma was always placed in the center of the dendritic field. Cell somata had diameters of 18.2 ± 1.2 µm. The dendritic field size averaged 281.5 ± 19.4 µm. ON type 2 cells were always coupled to numerous small cells which had their somata in the GCL (Fig. 3C and E). The image in Figure 3D corresponds to an injected cell whose soma showed the FDG signal (Fig. 3E). ON type 2 cells were monostratified with processes located in stratum 5 of the IPL, just below the cholinergic band produced by the ON starburst cells (Fig. 3F). According to the ganglion cell classification by Sun *et al.* (2002a), the morphology of this ganglion cell type corresponded to RG_{A1} cells.

Tracer coupling between RG$_{A1}$ and displaced amacrine cells

In the following, we focused on the RG$_{A1}$ cells (*ON type 2 ganglion cells*) to analyze the cells' coupling pattern and its modulation. RG$_{A1}$ cells are well described in rodent retinae (Huxlin & Goodchild, 1997; Sun *et al.*, 2002a, b; Badea & Nathans, 2004; Kong *et al.*, 2005) and are identical to the giant cells reported by Bunt (1976) in the albino rat retina.

To study the coupling of RG$_{A1}$ cells, we injected these cells in WT, Cx30.2$^{+/lacZ}$ and Cx30.2$^{lacZ/lacZ}$ retinae. RG$_{A1}$ were easy to recognize in WT retinae by their shape and big somata. Both in WT (n = 15) and Cx30.2$^{+/lacZ}$ mice (n = 9), RG$_{A1}$ cells were heterologously coupled to 2-8 amacrine cells (4.7 ± 2.3 cells; Fig. 3C, 4A). The number of tracer coupled cells was not significantly different between Cx30.2$^{+/lacZ}$ and WT mice (Fig. 3C, 4; p > 0.76). Tracer coupled cells were always located within the dendritic field of the RG$_{A1}$ cell and had their somata in the GCL. They had relatively round, small somata with a mean size of 7.9 ± 2 μm. Though the cells' dendrites could not be visualized, the small soma size suggested that these cells were most likely displaced amacrine cells.

An injected RG$_{A1}$ of a Cx30.2$^{+/lacZ}$ mouse is illustrated in Fig. 4A showing its normal tracer spread. The coupled cells (Fig. 4B) never showed the green fluorescent signal produced by FDG incubation. To exclude the possibility that the FDG signal leaked out of these cells over time, we incubated Cx30.2$^{+/lacZ}$ retinae with FDG and immediately looked for RG$_{A1}$ cells. We never saw displaced amacrine cells positive for fluorescein in the proximity of the green fluorescing RG$_{A1}$ cells. This suggested that Cx30.2 was not expressed by the displaced amacrine cells coupled to RG$_{A1}$ cells. We therefore concluded that RG$_{A1}$ cells most likely form heterotypic channels with displaced amacrine cells involving Cx30.2 and a yet unidentified protein.

In Cx30.2$^{lacZ/lacZ}$ mice, coupling of RG$_{A1}$ cells (Fig. 4C and D; n = 7) was significantly reduced compared to WT (p < 0.005) and Cx30.2$^{+/lacZ}$ mice (p < 0.002). Again, we used the

FDG signal (Fig. 4D) to confirm that the injected cell (Fig. 4C) expressed the lacZ reporter gene.

We also injected the other Cx30.2-expressing ganglion cell types and found that none of the ganglion cells exhibited tracer coupling (n = 12, not shown) in Cx30.2$^{lacZ/lacZ}$ mice. To exclude that coupling was abolished due to reasons other than the lack of Cx30.2, we injected alpha ganglion cells in the same retinae. However, alpha cells exhibited their well-described coupling pattern (data not shown). Thus, our results show that Cx30.2 mediates the coupling of at least two different ganglion cell types including the coupling between RG$_{A1}$ cells and displaced amacrine cells.

Coupled displaced amacrine cells did not express Cx36, Cx45 or Cx40

Since the displaced amacrine cells coupled to RG$_{A1}$ cells did not express Cx30.2, we tested whether the heterotypic gap junctions between these two cell types were made up of Cx30.2 and another known retinal connexin. In the mouse retina, three neuronal connexins (Cx36, Cx45 and Cx57) have been described so far. Cx57 is exclusively expressed in horizontal cells of the mouse retina (Hombach *et al.*, 2004). Therefore, we did not test for Cx57 but for Cx36 and Cx45 (Fig. 5).

Cx36 has only been described in one type of amacrine cell: the AII amacrine cell (Feigenspan *et al.*, 2001; Mills *et al.*, 2001). To test whether Cx36 is the connexin involved in the heterologous coupling between RG$_{A1}$ and displaced amacrine cells, we injected RG$_{A1}$ cells (n = 4) in Cx36$^{-/-}$ mice (Güldenagel *et al.*, 2001). However, RG$_{A1}$ cells were still coupled to displaced amacrine cells (Fig. 5A and D). There was no significant difference between the coupling in WT (n = 15) and Cx36-deficient mice (n = 4, p > 0.85) with 4.7 ± 2.3 and 4.5 ± 1.5 coupled cells in WT and Cx36-deficient mice, respectively. These results are consistent with previous findings (Schubert *et al.*, 2005a) and exclude Cx36 as the connexin participating at the junction between RG$_{A1}$ and displaced amacrine cells.

We also tested for Cx45, which is expressed by bipolar cells (Maxeiner *et al.*, 2005; Dedek *et al.*, 2006), bistratified ganglion cells (Schubert *et al.*, 2005b), and several types of amacrine cells including one type of displaced amacrine cell (Pérez de Sevilla *et al.*, 2007). To examine whether Cx45 forms heterotypic channels with Cx30.2, RG_{A1} cells were tracer injected in Cx45-deficient mice (Maxeiner *et al.*, 2005). We found that RG_{A1} cells were still coupled to displaced amacrine cells in Cx45-deficient mice (n = 3, Fig. 5B and D). Coupling in WT and Cx45-deficient mice was not significantly different (p > 0.66) indicating that these heterotypic gap junctions do not involve Cx45.

Another possible candidate connexin is Cx40, since it has been found in bovine and rat retinae (Matesic *et al.*, 2003) and recently also in the mouse retina (Kihara *et al.*, 2006), though it is not yet clear in which retinal cells Cx40 is expressed. However, Cx40 is strongly expressed in mouse heart where it may form heterotypic gap junctions with Cx30.2 (Kreuzberg *et al.*, 2005). To test whether this is also the case for the coupling between displaced amacrine cells and RG_{A1} cells, we analyzed this coupling in Cx40-deficient mice (Kirchhoff *et al.*, 1998). We found that RG_{A1} cells were still coupled to displaced amacrine cells in Cx40-deficient mice (n = 3, Fig. 5C and D). The extent of coupling was similar in WT and Cx40-deficient retinae (p > 0.24), indicating that Cx40 is not involved in the gap junction between displaced amacrine and RG_{A1} cells. Instead, our data suggest that an unknown gap junction protein participates in the coupling between these two cell types.

Modulation of the tracer coupling between RG_{A1} and displaced amacrine cells

Gap junction coupling of retinal neurons is influenced by different ambient light levels and by neuromodulators (for review see Weiler *et al.,* 2000) which alter the conductance of gap junction channels most likely by inducing protein kinase-mediated phosphorylation (Xia & Mills, 2004; Urschel *et al.*, 2006). To analyze whether the coupling between RG_{A1} cells and

displaced amacrine cells is modulated by protein kinases, we tested inhibitors and activators for both PKA and PKC (Fig. 6).

Again, RG_{A1} cells were injected with Neurobiotin in WT retinae. The average number of coupled displaced amacrine cells was 4.8 ± 2.2 (n = 13, Fig. 6A and B). To test for PKA-mediated phosphorylation, we incubated retinae prior to injection with the membrane-permeable cAMP analog dibutyryl-cAMP (1 mM), which activates PKA. However, the number of coupled cells was not significantly different from control conditions (Fig. 6A, control, n = 13, dibutyryl-cAMP, n = 4, p > 0.19). Next, we incubated retinae prior to injection with forskolin and IBMX, which increase the intracellular cAMP concentration and thereby activate PKA. However, this treatment also had no impact on tracer spread from RG_{A1} cells to displaced amacrine cells (Fig. 6A, forskolin + IBMX, n = 5, p > 0.31). Thus, we concluded that the Cx30.2-mediated coupling between these cells was not modulated by PKA.

Alpha ganglion cells were used as a control for this study. These cells are coupled to other cells by Cx36 which is regulated by PKA (Xia & Mills, 2004; Urschel *et al.*, 2006). In retinae incubated with forskolin and IBMX, tracer spread in alpha ganglion cells was significantly decreased. However, dibutyryl-cAMP had no effect on these cells (for more details, see Supplementary Material Fig. 3).

To test for involvement of PKC, we incubated retinae from WT mice prior to injection with staurosporine, a cell-permeable inhibitor of PKC. We found no difference in the coupling patterns of RG_{A1} cells (Fig. 6B, control, n = 13, staurosporine, n = 6, p > 0.77). In contrast, incubation with the potent PKC activator PDBu led to a significant reduction in the number of coupled cells (Fig. 6B, PDBu, n = 6, $p < 9x10^{-5}$). Thus, our results indicate that the heterotypic coupling between RG_{A1} and displaced amacrine cells is mediated by Cx30.2 and an unknown connexin, and may be modulated by PKC, but not by PKA.

Discussion

In this study, we identified Cx30.2 as a novel connexin in the mouse retina. Using Cx30.2-lacZ reporter mice, we found that Cx30.2 is expressed in six different types of ganglion cells. Among these types were the RG_{A1} cells (Sun *et al.*, 2002a) which were coupled to displaced amacrine cells. Coupling between these two cell types was abolished in Cx30.2$^{lacZ/lacZ}$ mice, was regulated by PKC, and was heterotypic, involving Cx30.2 and an unknown connexin.

Cx30.2 as a novel retinal connexin

Since Söhl *et al.* (1998) first described the expression of Cx36 in the mouse retina, several new connexins have been identified in this tissue. Cx36 and Cx45 were assigned to multiple retinal cell types, whereas Cx57 was found exclusively in horizontal cells (reviewed in Söhl *et al.*, 2005). In this work, we show for the first time that Cx30.2 is expressed in mouse retinal neurons, namely in several different types of amacrine and ganglion cells. This confirms Cx30.2 as a new neuronal connexin in the central nervous system (Kreuzberg *et al.*, 2008). Cx30.2 is expressed in both inhibitory interneurons (hippocampus, retina) and in projecting neurons (retina).

Cx30.2 expression in the mouse retina

Cx30.2 expression was observed in cells in the INL and GCL of the mouse retina. Cells located in the INL corresponded presumably to amacrine cells, based on nucleus size and location of the lacZ staining with respect to the borders of the INL. Thus, Cx30.2 is a likely candidate protein for mediating the coupling of different amacrine cell classes (Xin & Bloomfield, 1997; Wright & Vaney, 2000; Wright & Vaney, 2004).

However, in this work, we focused on the GCL. To identify the Cx30.2-expressing cells in this layer, we labeled the lacZ-positive neurons in Cx30.2$^{+/lacZ}$ and Cx30.2$^{lacZ/lacZ}$ mice using a fluorogenic substrate (FDG). Nirenberg & Meister (1997) showed that 95% of all

lacZ-positive cells could be labeled in this way. With this method, we labeled big subsets of neurons in each Cx30.2-deficient retina. These subsets did not vary between retinae, and comprised six different types of Cx30.2-expressing ganglion cells: one type of ON-OFF, three types of OFF and two types of ON ganglion cells. Interestingly, the bistratified ON-OFF ganglion cell described in this work resembled the direction-selective RG_{D2} cell (Sun *et al.*, 2002a; Weng *et al.*, 2005), which is coupled to other bistratified ganglion cells by Cx45 (Schubert *et al.*, 2005b). This suggests that Cx30.2 and Cx45 might form heteromeric or heterotypic channels as was shown previously in transfected HeLa cells (Kreuzberg *et al.*, 2005). Consistent with this idea, Schubert *et al.* (2005b) reported some residual tracer coupling in RG_{D2} cells of Cx45-deficient mice. However, the bistratified ganglion cells injected in Cx30.2$^{+/lacZ}$ mice never showed tracer coupling.

Cx30.2-mediated tracer coupling in the mouse retina

Only two of the six Cx30.2-expressing ganglion cell types were tracer coupled in Cx30.2$^{+/lacZ}$ mice: OFF type 1 cells and ON type 2 cells, which correspond to RG_{A1} cells described by Sun *et al.* (2002a). In both cell types, coupling was completely absent in Cx30.2$^{lacZ/lacZ}$ mice indicating that coupling was mediated by Cx30.2. Surprisingly, the other four ganglion cell types, including the bistratified RG_{D2} cell mentioned above, showed no tracer coupling. One reason for that may be that the amount of Cx30.2 protein was not sufficient to allow for dye coupling, since cells were injected in mice lacking one Cx30.2 allele (Cx30.2$^{+/lacZ}$). Another reason may be that Neurobiotin passes poorly through Cx30.2 gap junctions. This is supported by the fact that Cx30.2 has the lowest unitary conductance of all connexins studied to date (Kreuzberg *et al.*, 2005). Passage of Neurobiotin through Cx30.2 channels expressed in HeLa cells was significantly lower than through Cx43 channels (Kreuzberg *et al.*, 2005). Thus, lack of coupling in four of the six types of Cx30.2-expressing ganglion cells may be due to the biophysical properties of Cx30.2 or the lack of one allele for Cx30.2. However, this

work provides clear evidence that coupling of the OFF type 1 and RG_{A1} cells was mediated by Cx30.2.

Gap junction protein of the displaced amacrine cells coupled to RG_{A1} cells

We focused our study on the coupling of RG_{A1} cells. Our data strongly suggest that the RG_{A1} cells are coupled to displaced amacrine cells by heterotypic gap junctions involving Cx30.2 and another connexin that has not yet been unidentified. This conclusion was based on the following findings: 1) Coupled displaced amacrine cells did not express the lacZ reporter gene as shown by *in vitro* staining with FDG. Thus, we excluded that coupled displaced amacrine cells expressed Cx30.2. 2) Injections with Neurobiotin in Cx36^{-/-} mice (Güldenagel *et al.*, 2001), Cx45-deficient mice (Maxeiner *et al.*, 2005) and Cx40^{-/-} mice (Kirchhoff *et al.*, 1998) showed unimpaired tracer coupling between RG_{A1} and displaced amacrine cells, thereby confirming that the displaced amacrine cells did not express Cx36, Cx45 or Cx40. Since the only other known neuronal connexin in the mouse retina, Cx57, is exclusively expressed in horizontal cells (Hombach *et al.*, 2004), we concluded that the displaced amacrine cells coupled to RG_{A1} cells must express a yet unidentified connexin.

Tracer coupling of RG_{A1} cells is modulated by PKC

During retinal adaptation, the networks of coupled neurons are modulated by light and by neuromodulators such as dopamine (Hampson *et al.*, 1992; He *et al.*, 2000). These act by activating protein kinases which can directly or indirectly alter gap junction properties (for review see Moreno & Lau, 2007). Here we show that the serine/threonine kinase PKC is involved in the regulation of the Cx30.2-mediated coupling between RG_{A1} and displaced amacrine cells. Activation of PKC by PDBu led to a significant decrease in gap junction coupling. This decrease in coupling might have been caused by direct phosphorylation of Cx30.2, which harbors several consensus sites for PKC-mediated phosphorylation (web-based

analysis with NetPhosK 1.0 server). Reduction in connexon permeability by direct PKC-mediated phosphorylation has been shown, for example, for Cx43 (Bao *et al*., 2004). However, PKC activation might not only have influenced the connexon on the RG_{A1} cell side but also the unknown connexin in the coupled displaced amacrine cells. Also, PKC activation might have had indirect effects which could lead to the observed decrease in coupling.

We also showed that activators of the serine/threonine kinase PKA (dibutyryl-cAMP, forskolin and IBMX) did not impair the coupling between RG_{A1} and displaced amacrine cells. However, PKA has been shown to mediate the phosphorylation of Cx36, and to reduce the extent of coupling in AII amacrine cells (Xia & Mills, 2004; Urschel *et al.*, 2006) as well as in alpha ganglion cells (this study, see Supplementary Material Fig. 3).

Thus, our results suggest that different retinal networks are modulated by different protein kinases. This may reflect the need for a precise control of coupled neuronal networks to ensure that retinal resolution and sensitivity are adapted optimally to the visual environment with its changing light conditions.

Abbreviations

ChAT, choline acetyltransferase; Cx, connexin; FDG, fluorescein-di-beta-D-galactopyranoside; GCL, ganglion cell layer; 3-isobutyl-1-methylxanthine, IBMX; INL, inner nuclear layer; IPL, inner plexiform layer; PB, phosphate buffer; PDBu, 4-beta-phorbol-12,13-dibutyrate; WT, wild-type.

Literature

Badea, T. D. & Nathans, J. (2004) Quantitative analysis of neuronal morphologies in the mouse retina visualized by using a genetically directed reporter. *J. Comp. Neurol.*, **480**, 331-351.

Bao, X., Altenberg, G. A. & Reuss, L. (2004) Mechanism of regulation of the gap junction protein connexin 43 by protein kinase C-mediated phosphorylation. *Am. J. Physiol. Cell. Physiol.,* **286**, C647-54.

Bunt, A. H. (1976) Ramification patterns of ganglion cells dendrites in the retina of the albino rat. *Brain Res.*, **103**, 1-8.

Deans, M. R., Volgyi, B., Goodenough, D. A., Bloomfield, S. A. & Paul, D. L. (2002) Connexin36 is essential for transmission of rod-mediated visual signals in the mammalian retina. *Neuron*, **36**, 703-712.

Dedek, K., Schultz, K., Pieper, M., Dirks, P., Maxeiner, S., Willecke, K., Weiler, R. & Janssen-Bienhold, U. (2006) Localization of heterotypic gap junctions composed of connexin45 and connexin36 in the rod pathway of the mouse retina. *Eur. J. Neurosci.*, **24**, 1675-1686.

Feigenspan, A., Teubner, B., Willecke, K. & Weiler, R. (2001) Expression of neuronal connexin36 in AII amacrine cells of the mammalian retina. *J. Neurosci.*, **21**, 230-239.

Feigenspan, A., Janssen-Bienhold, U., Hormuzdi, S., Monyer, H., Degen, J., Söhl, G., Willecke, K., Ammermüller, J. & Weiler, R. (2004) Expression of connexin36 in cone pedicles and OFF-cone bipolar cells of the mouse retina. *J. Neurosci.*, **24**, 3325-3334.

Güldenagel, M., Ammermüller, J., Feigenspan, A., Teubner, B., Degen, J., Söhl, G., Willecke, K. & Weiler, R. (2001) Visual transmission deficits in mice with targeted disruption of the gap junction gene connexin36. *J. Neurosci.,* **21**, 6036-6044.

Hampson, E. C., Vaney, D. I. & Weiler, R. (1992) Dopaminergic modulation of gap junction permeability between amacrine cells in mammalian retina. *J. Neurosci.,* **12**, 4911-4922.

Han, Y. & Massey, S. C. (2005) Electrical synapses in retinal ON cone bipolar cells: Subtype-specific expression of connexins. *Proc. Natl. Acad. Sci. U. S. A.,* **102**, 13313-13318.

He, S., Weiler, R. & Vaney, D. I. (2000) Endogenous dopaminergic regulation of horizontal cell coupling in the mammalian retina. *J. Comp. Neurol.*, **418**, 33-40.

Hombach, S., Janssen-Bienhold, U., Söhl, G., Schubert, T., Büssow, H., Ott, T., Weiler, R. & Willecke K. (2004) Functional expression of connexin57 in horizontal cells of the mouse retina. *Eur. J. Neurosci.,* **19**, 2633-2640.

Huxlin, K. R. & Goodchild, A. K. (1997) Retinal ganglion cells in the albino rat: revised morphological classification. *J. Comp. Neurol.,* **385**, 309-323.

Jeon, C. J., Strettoi, E. & Masland, R. H. (1998) The major cell populations of the mouse retina. *J. Neurosci.*, **18**, 8936-8946.

Kihara, A.H., de Castro, L.M., Moriscot, A.S. & Hamassaki, D.E. (2006) Prolonged dark adaptation changes connexin expression in the mouse retina. *J. Neurosci. Res.*, **83,** 1331-1341.

Kirchhoff, S., Nelles, E., Hagendorff, A., Krüger, O., Traub, O. & Willecke, K. (1998) Reduced cardiac conduction velocity and predisposition to arrhythmias in connexin40-deficient mice. *Curr. Biol.*, **8**, 299-302.

Kong, J. H., Fish, D. R., Rockhill, R. L. & Masland R. H. (2005) Diversity of ganglion cells in the mouse retina: unsupervised morphological classification and its limits. *J. Comp. Neurol.,* **489**, 293–310.

Kreuzberg, M. M., Söhl, G., Kim, J. S., Verselis, V. K., Willecke, K. & Bukauskas, F. F. (2005) Functional properties of mouse connexin30.2 expressed in the conduction system of the heart. *Circ. Res.*, **96**, 1169-1177.

Kreuzberg, M. M., Schrickel, J. W., Ghanem, A., Kim, J. S., Degen, J., Janssen-Bienhold, U., Lewalter, T., Tiemann, K. & Willecke, K. (2006) Connexin30.2 containing gap junction channels decelerate impulse propagation through the atrioventricular node. *Proc. Natl. Acad. Sci. U S A.,* **103**, 5959-5964.

Kreuzberg, M. M., Deuchars, J., Weiss, E., Schober, A., Sonntag, S., Wellershaus, K., Draguhn, A. & Willecke, K. (2008) Expression of connexin30.2 in interneurons of the central nervous system in the mouse. *Mol. Cell. Neurosci.,* **37**, 119-134.

Lee, E. J., Han, J. W., Kim, H. J., Kim, I. B., Lee, M. Y., Oh, S. J., Chung, J. W. & Chun, M. H. (2003) The immunocytochemical localization of connexin 36 at rod and cone gap junctions in the guinea pig retina. *Eur. J. Neurosci.*, **18**, 2925-2934.

Lin, B., Jakobs, T. C. & Masland, R. H. (2005) Different functional types of bipolar cells use different gap-junctional proteins. *J. Neurosci.*, **25**, 6696-6701.

Lin, B. & Masland, R. H. (2006) Populations of wide-field amacrine cells in the mouse retina. *J. Comp. Neurol.*, **499,** 797-809.

Matesic, D., Tillen, T. & Sitaramayya, A. (2003) Cx40 expression in bovine and rat retinae. *Cell. Biol. Int.*, **27**, 89-99.

Maxeiner, S., Dedek, K., Janssen-Bienhold, U., Ammermüller, J., Brune, H., Kirsch, T., Pieper, M., Degen, J., Krüger, O., Willecke, K. & Weiler, R. (2005) Deletion of connexin45 in mouse retinal neurons disrupts the rod/cone signaling pathway between AII amacrine and ON cone bipolar cells and leads to impaired visual transmission. *J. Neurosci.*, **25**, 566-576.

Mills, S. L., O'Brien, J. J., Li, W., O'Brien, J. & Massey, S. C. (2001) Rod pathways in the mammalian retina use connexin 36. *J. Comp. Neurol.*, **436**, 336-350.

Moreno, A. P. & Lau, A. F. (2007) Gap junction channel gating modulated through protein phosphorylation. *Prog. Biophys. Mol. Biol.*, **94**, 107-119

Nirenberg, S. & Cepko, C. (1993) Targeted ablation of diverse cell classes in the nervous system in vivo. *J. Neurosci.*, **13**, 3238-3251.

Nirenberg, S. & Meister, M. (1997) The light response of retinal ganglion cells is truncated by a displaced amacrine circuit. *Neuron,* **18**, 637-650.

O'Brien, J. J., Li, W., Pan, F., Keung, J., O'Brien, J. & Massey, S. C. (2006) Coupling between A-type horizontal cells is mediated by connexin 50 gap junctions in the rabbit retina. *J. Neurosci.,* **26**, 11624-11636.

Pérez de Sevilla Müller, L., Shelley, J. & Weiler, R. (2007) Displaced amacrine cells of the mouse retina. *J. Comp. Neurol.,* **505**, 177-189.

Schubert, T., Degen, J., Willecke, K., Hormuzdi, S. G., Monyer, H. & Weiler, R. (2005a) Connexin36 mediates gap junctional coupling of alpha-ganglion cells in mouse retina. *J. Comp. Neurol.,* **485**, 191-201.

Schubert, T., Maxeiner, S., Kruger, O., Willecke, K. & Weiler, R. (2005b) Connexin45 mediates gap junctional coupling of bistratified ganglion cells in the mouse retina. *J. Comp. Neurol.,* **490**, 29-39.

Shelley, J., Dedek, K., Schubert, T., Feigenspan, A., Schultz, K., Hombach, S., Willecke, K. & Weiler, R. (2006) Horizontal cell receptive fields are reduced in connexin57-deficient mice. *Eur. J. Neurosci.,* **23**, 3176-3186.

Söhl, G., Degen, J., Teubner, B. & Willecke, K. (1998) The murine gap junction gene connexin36 is highly expressed in mouse retina and regulated during brain development. *FEBS Lett.,* **428**, 27-31.

Söhl, G., Maxeiner, S. & Willecke, K. (2005) Expression and functions of neuronal gap junctions. *Nat. Rev. Neurosci.,* **6**, 191-200.

Sun, W., Li, N. & He, S. (2002a) Large-scale morphological survey of mouse retinal ganglion cells. *J. Comp. Neurol.,* **451**, 115-126.

Sun, W., Li, N. & He, S. (2002b) Large-scale morphological survey of rat retinal ganglion cells. *Vis. Neurosci.,* **19**, 483-493.

Urschel, S., Höher, T., Schubert, T., Alev, C., Söhl, G., Wörsdörfer, P., Asahara, T., Dermietzel, R., Weiler, R. & Willecke, K. (2006) Protein kinase A-mediated phosphorylation of connexin36 in mouse retina results in decreased gap junctional communication between AII amacrine cells. *J. Biol. Chem.,* **281**, 33163-33171.

Vaney, D. I. (1991) Many diverse types of retinal neurons show tracer coupling when injected with biocytin or Neurobiotin. *Neurosci. Lett.,* **125**, 187-190.

Völgyi, B., Abrams, J., Paul, D. L., & Bloomfield, S. A. (2005) Morphology and tracer coupling pattern of alpha ganglion cells in the mouse retina. *J. Comp. Neurol.,* **492**, 66-77.

Weiler, R., Pottek, M., He, Su., & Vaney D. I. (2000) Modulation of coupling between retinal horizontal cells by retinoic acid and endogenous dopamine. *Brain Res. Rev.,* **32**, 121-129.

Weng, S., Sun, W. & He, S. (2005) Identification of ON-OFF direction-selective ganglion cells in the mouse retina. *J. Physiol.,* **562**, 915-923.

Wright, L. L. & Vaney, D. I. (2000) The fountain amacrine cells of the rabbit retina. *Vis. Neurosci.,* **17**, 1145-1156.

Wright, L. L. & Vaney, D. I. (2004) The type 1 polyaxonal amacrine cells of the rabbit retina: a tracer-coupling study. *Vis. Neurosci.,* **21**, 145-155.

Xia, X. B. & Mills, S. L. (2004) Gap junctional regulatory mechanisms in the AII amacrine cell of the rabbit retina. *Vis. Neurosci.*, **21**, 791-805.

Xin, D. & Bloomfield, S. A. (1997) Tracer coupling pattern of amacrine and ganglion cells in the rabbit retina. *J. Comp. Neurol.,* **383**, 512-528.

Tables

Table 1

	big nuclei	small nuclei
calbindin	-	+
parvalbumin	++	-
calretinin	-	+
calbindin + calretinin	-	+/-
parvalbumin + calretinin	-	+/-

Summary of the immunostaining for parvalbumin, calbindin and calretinin in Cx30.2-expressing ganglion cells in the mouse retina. Numbers of stained cells ranged from frequent (++) to zero (-). LacZ-positive ganglion cells were divided into two groups according to their nucleus size: large nuclei, > 8 μm, small nuclei , < 8 μm.

Figure Legends

Figure 1

Expression of Cx30.2/lacZ in retinae from Cx30.2$^{lacZ/lacZ}$ mice. (A) Expression pattern of the lacZ reporter gene visualized by staining for beta-galactosidase activity. LacZ staining was found in amacrine cells in the INL (arrows) and ganglion cells in the GCL. (B) LacZ-positive cells were distributed evenly over the entire GCL, as shown in the whole mount retina. V, D, N and T give the ventral, dorsal, nasal and temporal orientation, respectively. (C) High magnification of the GCL. Big (arrows) and small nuclei (arrowheads) were labeled for beta-galactosidase activity. Scale bars: A, 40 μm; B, 1 mm; C, 100 μm.

Figure 2

Examples of the Cx30.2-expressing ON-OFF and OFF ganglion cell types. Ganglion cells were injected in retinae from Cx30.2$^{+/lacZ}$ mice and their stratification pattern were determined. (A) Confocal image of a *bistratified ganglion cell* injected with Neurobiotin, showing the dendritic branching pattern in tangential view. This cell type was similar to the RG$_{D2}$ cell described by Sun *et al.* (2002a). (B) Stratification of the bistratified ganglion cell. Dendrites stratified in strata S2 and S4 of the IPL. (C) Confocal image of the *OFF type 1 ganglion cell*. Coupled cells are marked with arrowheads. (D) Stratification of OFF type 1 ganglion cells. These cells stratified in stratum S1 of the IPL close to the INL. (E) Confocal image of the asymmetric *OFF type 2 ganglion cell* in tangential view. (F) OFF type 2 ganglion cells stratified in stratum 1 of the IPL. (G) Morphology of the *OFF type 3 ganglion cell*. These cells had the smallest dendritic fields of all Cx30.2-expressing ganglion cells and stratified in stratum 1 of the IPL (H). Scale bar: 40 μm.

Figure 3

Examples of the two types of Cx30.2-expressing ON ganglion cells. Ganglion cells were injected in retinae from Cx30.2$^{+/lacZ}$ mice. (A) Confocal image of the *ON type 1 ganglion cell*. (B) These cells stratified in layer S5 of the IPL. (C) Morphology of *ON type 2 cells*. These cells were always coupled to displaced amacrine cells. ON type 2 cells corresponded to the RG$_{A1}$ cells described by Sun *et al.*, (2002a). Coupled cells are marked with arrows. (D) Soma of the injected RG$_{A1}$ cell. (E) The injected cell was positive for FDG, indicating lacZ expression. (F) Illustration of the stratification pattern of the RG$_{A1}$ cell. The dendrites of these cells ramified in stratum S5 of the IPL. Scale bar: 40 μm.

Figure 4

Coupling between RG_{A1} and displaced amacrine cells was mediated by Cx30.2. (A) Confocal image of an RG_{A1} cell injected in a retina from a Cx30.2$^{+/lacZ}$ mouse. The cell displayed coupling to three displaced amacrine cells. (B) Same injected RG_{A1} cell as in (A) showing the colocalization with the FDG signal (lacZ reporter gene expression). The coupled amacrine cells did not show the FDG signal and thus did not express Cx30.2. (C) An injected RG_{A1} cell in a Cx30.2$^{lacZ/lacZ}$ mouse. Coupling to displaced amacrine cells was completely abolished. (D) Confocal image showing the same cell as in (C) with colocalization of the FDG signal. (E) Histogram showing the mean number of coupled displaced amacrine cells in WT, Cx30.2$^{+/lacZ}$ and Cx30.2$^{lacZ/lacZ}$ mice. Coupling patterns were not significantly different between WT and Cx30.2$^{+/lacZ}$ mice (WT, n = 15; Cx30.2$^{+/lacZ}$, n = 9, p > 0.76). In mice lacking both Cx30.2 alleles (Cx30.2$^{lacZ/lacZ}$ mice), coupling of RG_{A1} cells was completely abolished (n = 7). Differences to WT (p < 0.005) and Cx30.2$^{+/lacZ}$ mice (p < 0.002) were significant. ** p values, t-test, p $\leq$ 0.01, scale bar: 40 μm.

Figure 5

Coupling of RG_{A1} and displaced amacrine cells was preserved in Cx36-, Cx45- and Cx40-deficient mice. (A) RG_{A1} cell injected in a Cx36-deficient mouse (Güldenagel *et al.*, 2001). Arrows point to coupled amacrine cells. (B) RG_{A1} cell injected in a Cx45-deficient mouse (Maxeiner *et al.*, 2005). (C) Injected RG_{A1} cell from a Cx40-deficient mouse (Kirchhoff *et al.*, 1998). (D) Histogram indicating the mean number of displaced amacrine cells coupled to the injected RG_{A1} cell in WT, Cx36$^{-/-}$, Cx40$^{-/-}$ and Cx45-deficient mice. In Cx-deficient mice, coupling between RG_{A1} and displaced amacrine cells was not significantly different from WT (WT, n = 15; Cx36$^{-/-}$, n = 4; p > 0.85; Cx45fl/fl: Nestin-Cre, n = 3; p > 0.65, Cx40$^{-/-}$, n = 3; p > 0.24). Scale bar: 40 μm.

Figure 6

Tracer coupling between RG_{A1} and displaced amacrine cells was modulated by PKC but not by PKA. (A) Test for PKA-mediated phosphorylation: RG_{A1} cells injected under control conditions (left), in the presence of dibutyryl-cAMP (middle), and forskolin and IBMX (right) exhibited their typical tracer spread (bar graph). Coupled cells are marked with arrows. We found no significant differences in tracer spread under these conditions (control, n = 13, cAMP, n = 4, p > 0.19; forskolin + IBMX, n = 5, p > 0.31). (B) Test for PKC-mediated phosphorylation: RG_{A1} cells injected under control conditions (left), in the presence of staurosporine (middle) and PDBu (right). Coupled cells are marked with arrows. Staurosporine did not significantly reduce the tracer spread (bar graph, control, n = 13, staurosporine, n = 6, p > 0.77). When incubated with PDBu, the number of coupled cells was significantly reduced (bar graph, PDBu, n = 6, $p < 9 \times 10^{-5}$). ** p values, t-test, $p \leq 0.01$, scale bar: 40 μm.

Supplementary Material

Figure 1

Immunostaining in $Cx30.2^{lacZ/lacZ}$ retinae. Vertical cryosections of $Cx30.2^{lacZ/lacZ}$ retinae were

immunostained with antibodies against Calbindin (CB), Calretinin (CR), and Parvalbumin (PV). LacZ expression was tested with an X-gal staining for beta-galactosidase activity. (A) Staining for lacZ and CB. CB antibodies stained horizontal cells, amacrine cells and bipolar cells. Some CB-positive cells showed colocalization with the lacZ signal (arrows). (B) Immunostaining for PV stained ganglion cells and colocalized in big nuclei with the staining for beta-galactosidase (arrows). (C) Immunostaining for CR. CR labeled ganglion cells and amacrine cells, and colocalized occasionally with small nuclei positive for lacZ (arrows). (D) Double immunostaining for CB (green) and CR (red). Only a few ganglion cells showing beta-galactosidase activity were stained for both CB and CR (arrows). (E) Double immunostaining for PV (green) and CR (red). Occasionally, some Cx30.2-expressing ganglion cells showed a colocalization for PV and CR (arrow). Scale bar: 40 µm.

Figure 2

Staining lacZ-expressing retinal cells with FDG from a Cx30.2$^{lacZ/lacZ}$ mouse. The focal plane is on the GCL. (A) Retinal whole mount (*in vivo*). The retina was treated with the fluorogenic beta-galactosidase substrate FDG (3 mg/ml in 2.5% DMSO) to label the lacZ-expressing cells with dye and facilitate ganglion cell injection. (B) Retinal whole-mount (fixed in 4% paraformaldehyde). Occasionally, the primary dendrites of the stained neurons can be seen. Scale bars: A, 20 µm, B, 20 µm.

Figure 3

Tracer coupling of alpha ganglion cells is modulated by PKA in the WT retina. ON alpha cells were coupled to displaced amacrine cells (7.2 ± 2 cells, n = 4) and OFF alpha cells were homologously coupled to other alpha cells (2.8 ± 0.9 cells, n = 5) and heterologously to

amacrine cells located in the INL (7.4 ± 3 cells, n = 5). Alpha ganglion cells injected under control conditions (A), after incubation with cAMP (B), forskolin + IBMX (C), staurosporine (D), or PDBu (E). (F) Histogram indicating the number of ganglion cells (GC) coupled to injected OFF alpha cells. Incubation with forskolin and IBMX led to a significant decrease in tracer coupling (control, n = 5, forskolin + IBMX, n = 4, $p \leq 0.05$). Incubation with staurosporine, however, had no effect on tracer coupling (control, n = 5, staurosporine, n = 2, $p > 0.11$). (G) Histogram indicating the number of amacrine cells (AC) coupled to injected OFF alpha cells. Again, incubation with forskolin and IBMX led to a significant decrease in tracer spread (control, n = 5, forskolin + IBMX, n = 4, $p \leq 0.05$). Staurosporine showed no effect on coupling extent (staurosporine, n = 2, $p > 0.31$). (H) Histogram indicating the number of displaced amacrine cells (DAC) coupled to the injected ON alpha cell in WT retinae. Incubation with forskolin and IBMX decreased the tracer spread (n = 4, $p \leq 0.05$) whereas cAMP (n = 2, $p > 0.46$) and PDBu (n = 2, $p > 0.66$) did not have an effect. Scale bar: 40 µm.
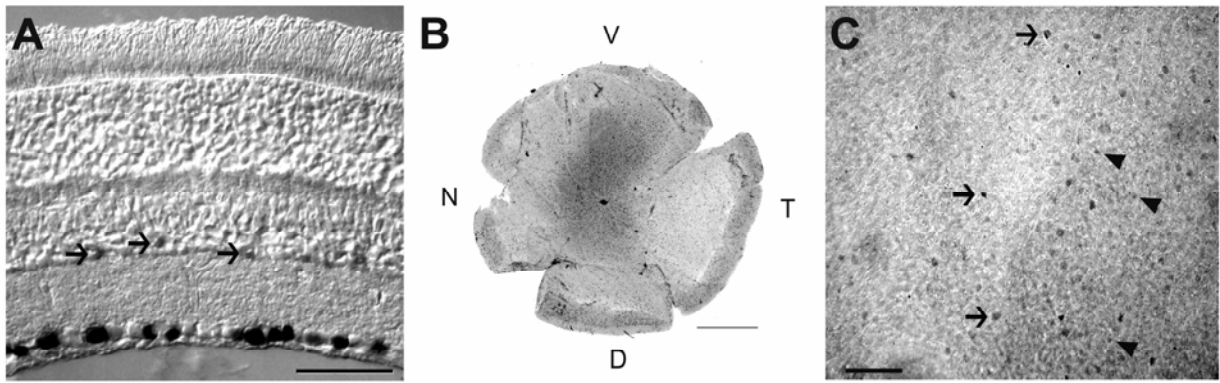
Figure 1

Figure 2

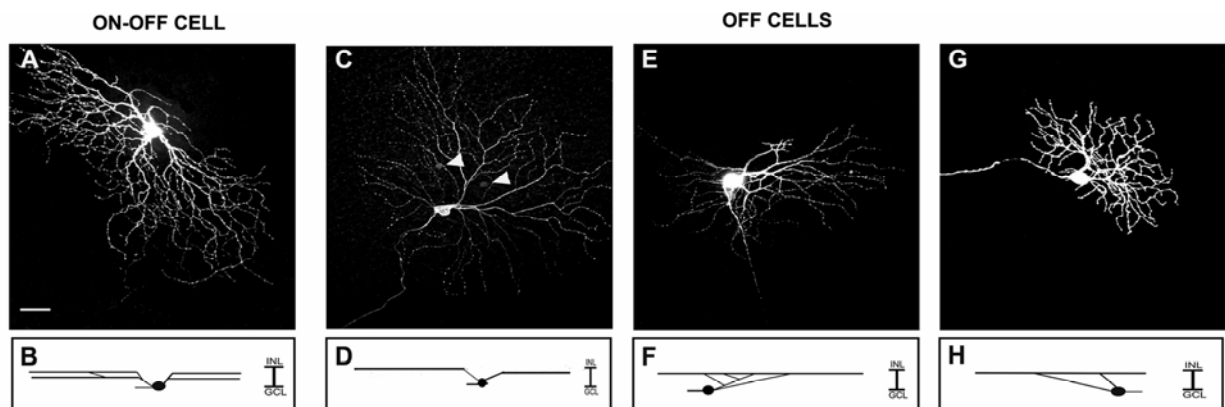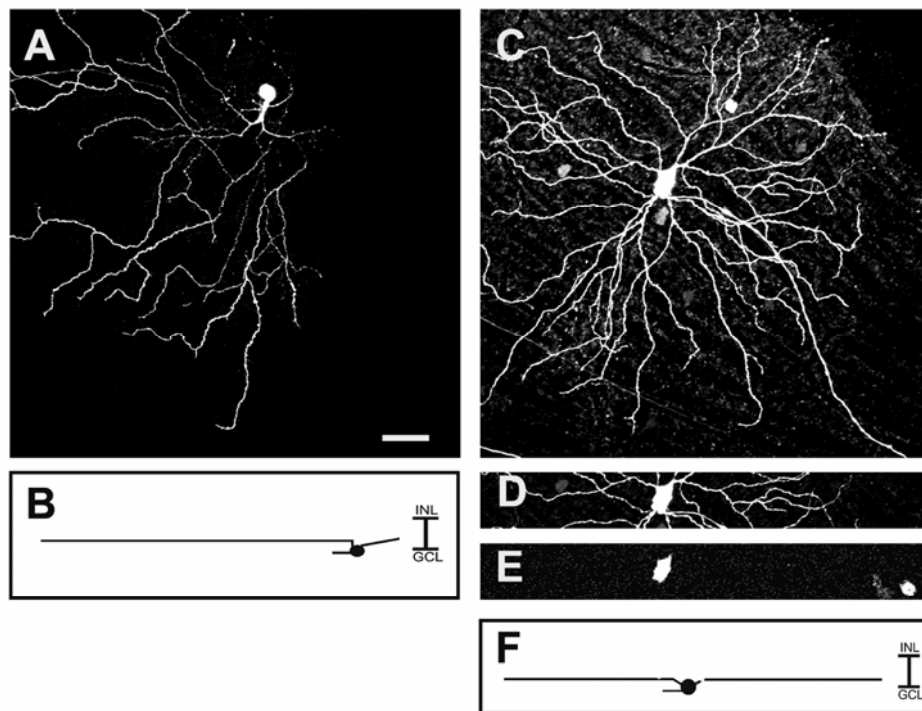**Figure 3**

ON CELLS

Figure 4
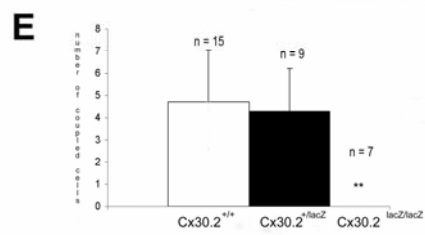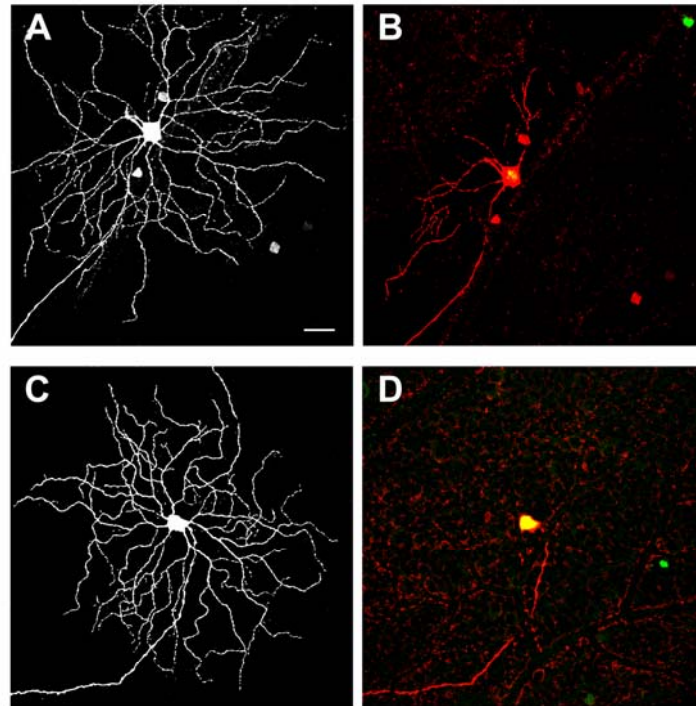
Figure 5
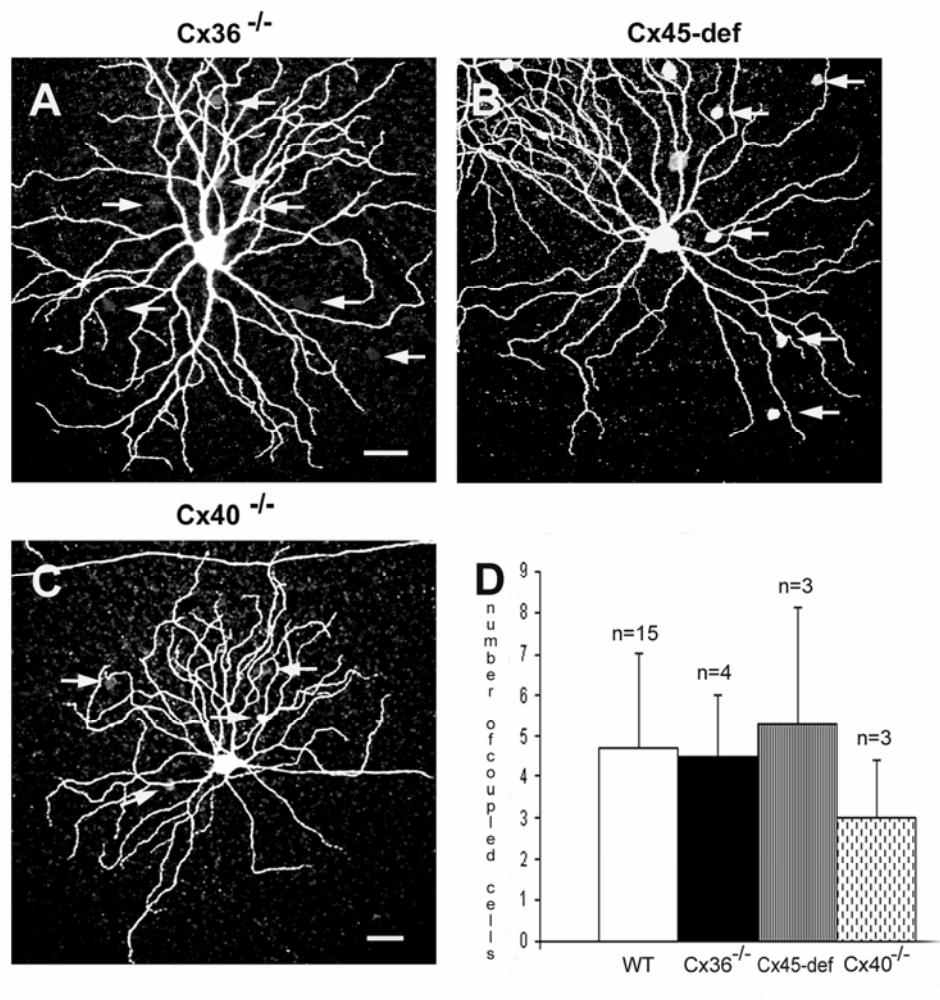
Figure 6
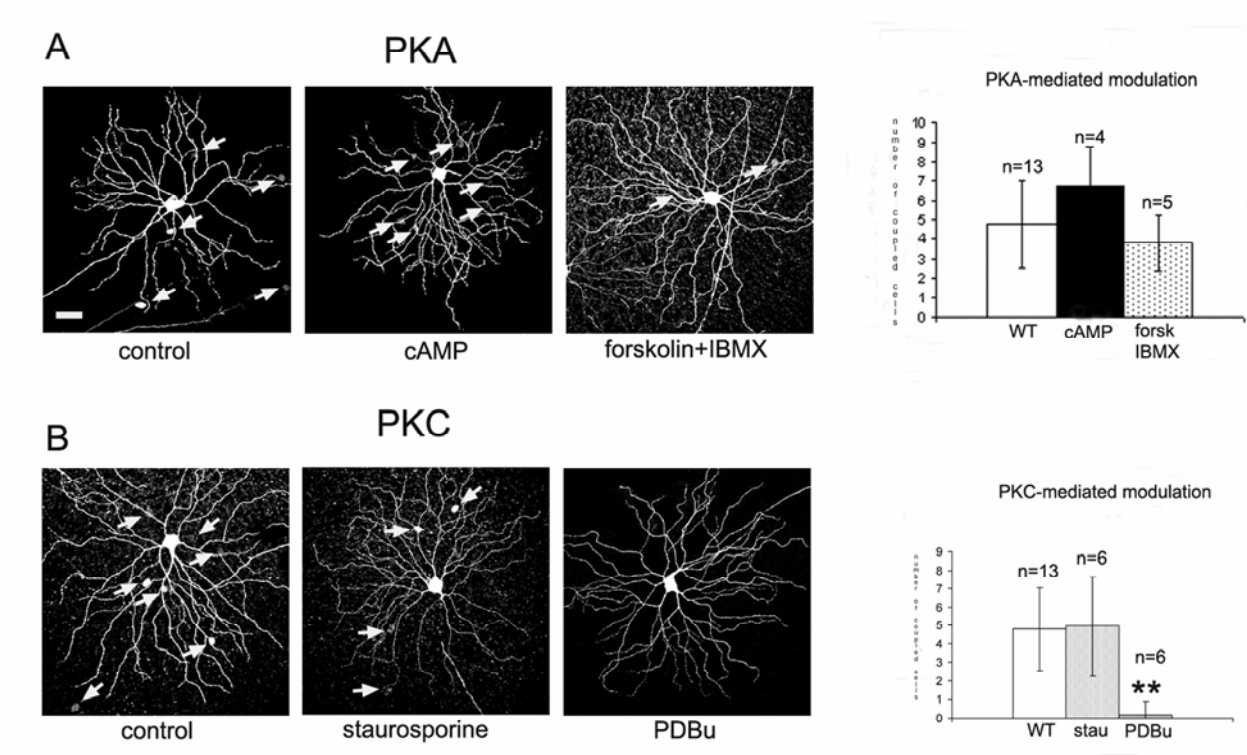
Figure 1 supplement
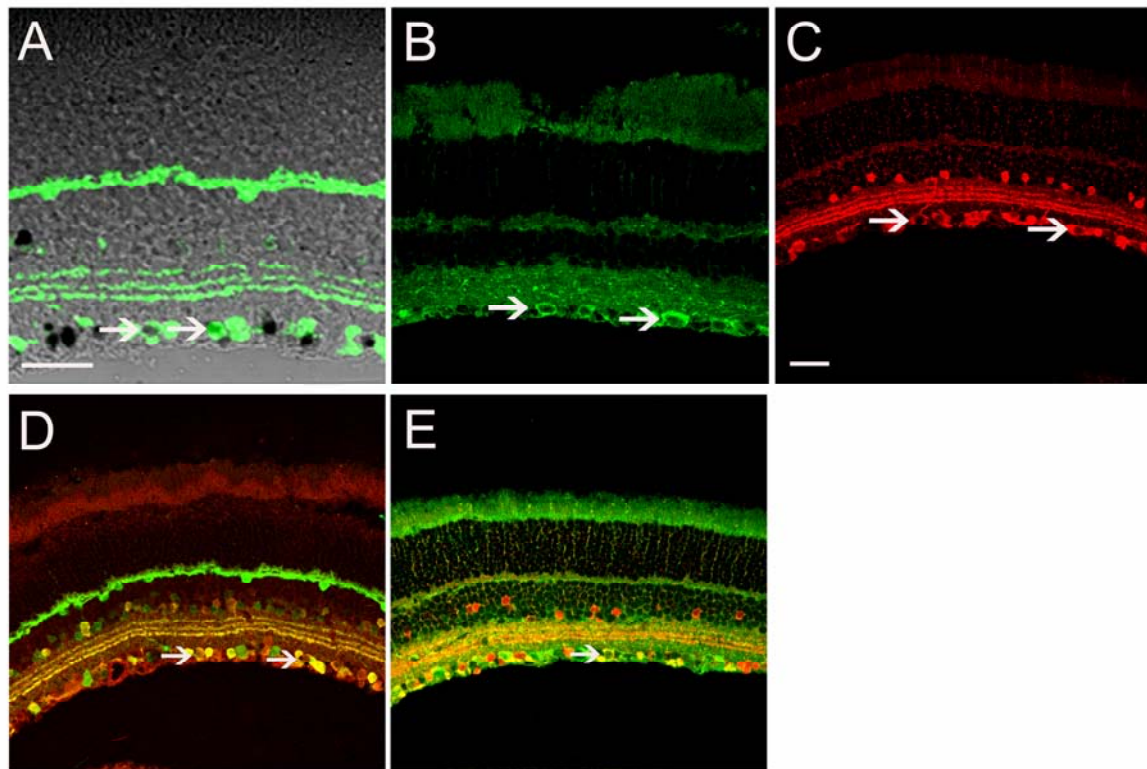
Figure 2 supplement
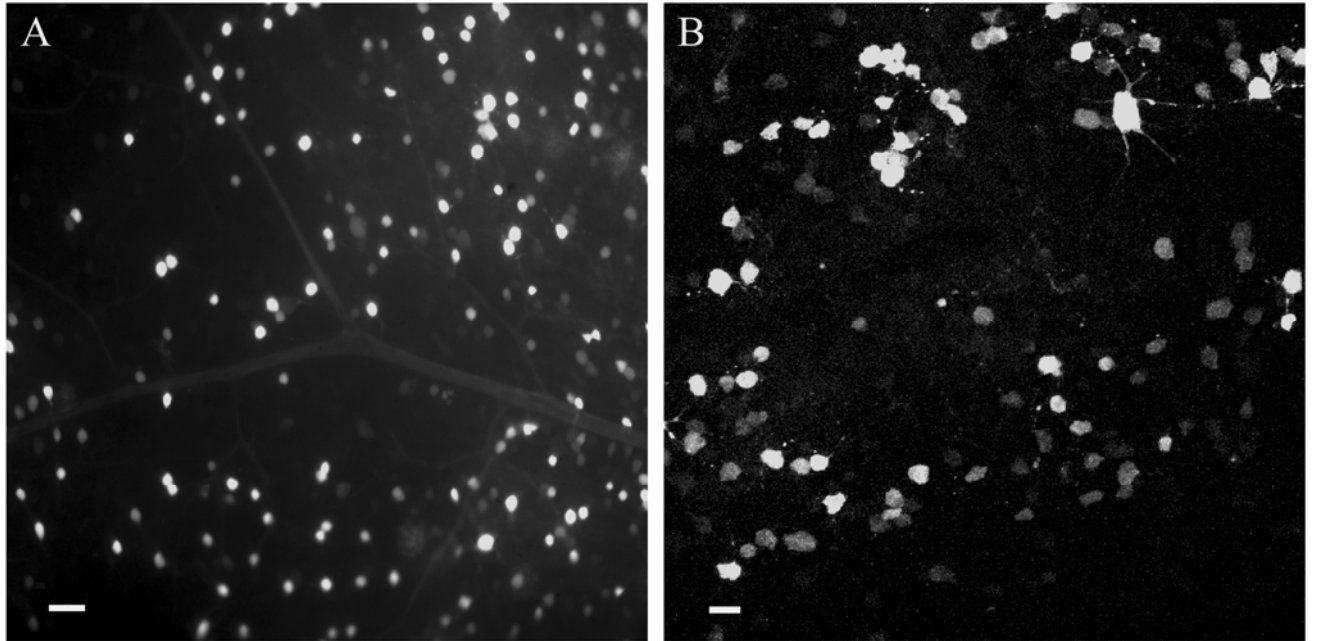
Figure 3 supplement
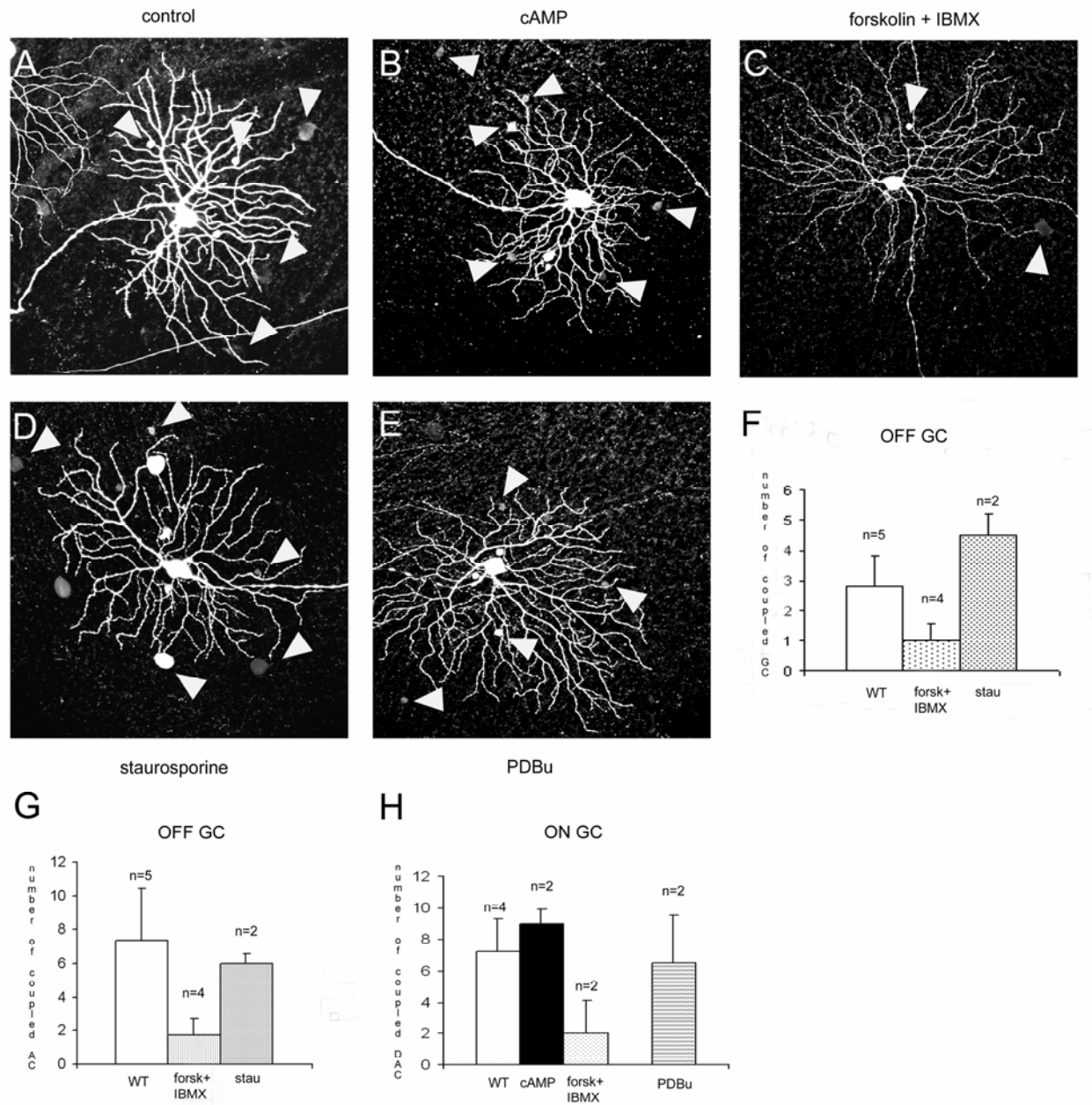
7.4 Ulrike Janssen-Bienhold , Jennifer Trümpler, Gerrit Hilgen, Konrad Schultz, Luis Pérez de Sevilla Müller, Stephan Sonntag, Karin Dedek, Petra Dirks, Klaus Willecke, and Reto Weiler. Connexin57 is expressed in dendro-dendritic and axo-axonal gap junctions of mouse horizontal cells and its distribution is modulated by light (submitted).

Connexin57 is expressed in dendro-dendritic and axo-axonal gap junctions of mouse horizontal cells and its distribution is modulated by light.

1

Connexin57 is expressed in dendro-dendritic and axo-axonal gap junctions of mouse horizontal cells and its distribution is modulated by light

Ulrike Janssen-Bienhold[1][*], Jennifer Trümpler[1][*], Gerrit Hilgen[1], Konrad Schultz[1], Luis Pérez de Sevilla Müller[1], Stephan Sonntag[2], Karin Dedek[1], Petra Dirks[1], Klaus Willecke[2] and Reto Weiler[1]

[1]Department of Neurobiology, University of Oldenburg, D-26111 Oldenburg, Germany

[2]Institute for Genetics, Department of Molecular Genetics, University of Bonn, D-53117 Bonn, Germany

Corresponding author: Dr. Ulrike Janssen-Bienhold, Department of Neurobiology, University of Oldenburg, D-26111 Oldenburg, Germany

Phone: 49 441 798-3419

Fax: 49 441 798-3423

E-mail: ulrike.janssen.bienhold@uni-oldenburg.de

Running title: Subcellular localization of Cx57 in horizontal cells

Number of pages: 28

Number of figures: 6

Total number of words: 7822

Number of words in the Abstract: 191

Number of words in the Introduction: 484

Keywords: Electrical synapse, gap junction, Cx57, horizontal cells, retina, mouse

Abstract

Mouse horizontal cells are coupled by gap junctions composed of connexin57. These gap junctions are regulated by ambient light via multiple neuromodulators including dopamine. We developed antibodies against mouse retinal connexin57 in order to analyze the distribution and structure of horizontal cell gap junctions and examine the effects of light adaptation on gap junction density. Using immunohistochemistry in retinal slices, flat-mounted retinas, and dissociated retinal cells, we showed that connexin57 is expressed in the dendrites and axon terminal processes of mouse horizontal cells. No staining was found in retinas of connexin57-deficient mice. Significantly more connexin57-positive puncta were found in the distal than in the proximal outer plexiform layer, indicating a higher level of expression in axon terminal processes than in the dendrites. Immunoelectron microscopy confirmed that connexin57 does not form hemichannels in the horizontal cell dendritic tips. Light adaptation resulted in a significant increase in the number of connexin57-immunoreactive plaques in the outer plexiform layer, but had no effect on plaque size. This study shows for the first time the detailed location of connexin57 expression within mouse horizontal cells, and provides the first ultrastructural data on mouse horizontal cell gap junctions.

Introduction

Horizontal cells are tightly coupled by gap junctions, allowing them to collect light information over a large area of the retina and adjust the gain of the photoreceptors to different levels of ambient light (reviewed by Kamermans and Spekreijse, 1999; Thoreson et al., 2008). In addition, evidence from fish retina suggests that hemichannels located at the tips of horizontal cell dendrites mediate feedback of horizontal cells onto photoreceptors (Kamermans et al., 2001; Kamermans and Fahrenfort, 2004). Gap junctional coupling of the horizontal cell network is regulated by ambient light (Tornqvist et al., 1988; Baldridge and Ball, 1991; Xin and Bloomfield, 1999), and this regulation is mediated by several neuromodulators via multiple pathways (Mangel and Dowling, 1985; Pottek and Weiler, 2000; Xin and Bloomfield, 2000). Changes in connexin expression levels (Kihara et al., 2006) and phosphorylation (Urschel et al., 2006), as well as gap junction structure (Wolburg and Kurz-Isler, 1985) have been proposed as mechanisms underlying light-dependent modulation of electrical coupling.

The mouse has one type of horizontal cell, of the axon-bearing B-type morphology (Suzuki and Pinto, 1986; Peichl and Gonzalez-Soriano, 1994). Mouse horizontal cells are coupled by connexin57 (Cx57); deletion of the Cx57 coding region almost completely eliminates tracer coupling (Hombach et al., 2004) and strongly reduces receptive field size in horizontal cell somata and axon terminals (Shelley et al., 2006). However, feedback from the horizontal cells to the photoreceptors is intact in Cx57-deficient mice (Shelley et al., 2006; Dedek et al., 2008), suggesting that Cx57 does not form hemichannels at the horizontal cell dendritic tips.

In the retina, functional splicing of the Cx57 coding region results in replacement of the predicted 25 C-terminal amino acids (Manthey et al., 1999) with 12 different

amino acid residues coded further downstream (Hombach et al., 2004). Commercially-available Cx57 antibodies, presumably designed to detect the originally published C terminus, produced similar labeling in wild-type and Cx57-deficient retinas. Antibodies specific for mouse retinal Cx57 are an essential tool for investigating horizontal cell gap junction structure and function. Therefore, we generated polyclonal antibodies against 12 C-terminal amino acid residues of mouse retinal Cx57. These antibodies produced dense, punctate labeling in the outer plexiform layer (OPL) in wild-type mice; this labeling was specific for mouse Cx57, since no labeling was seen in the OPL of retinas from Cx57-deficient mice.

We used our newly-developed antibodies against mouse retinal Cx57 to analyze the distribution of Cx57 hemichannels within mouse horizontal cells. We also examined the structure of the dendritic and axon terminal gap junctions using immunoelectron microscopy. We found high levels of Cx57 expression in dendrites as well as axon terminal processes, indicating that both networks are coupled by Cx57. Furthermore, we investigated the effects of dark adaptation on Cx57 plaque size and density. This study shows for the first time the detailed location of Cx57 expression within mouse horizontal cells, and provides the first ultrastructural data on mouse horizontal cell gap junctions.

Materials and methods

C57BL/6 wild-type, Cx57$^{lacZ/lacZ}$ and Cx57$^{+/lacZ}$ mice (C57BL/6 genetic background; Hombach et al., 2004) aged 2-8 months were used for the experiments. Mice were maintained under a 12-hour light/dark cycle. All experiments were carried out in accordance with the institutional guidelines for animal welfare and the laws on animal experimentation issued by the German government.

Light/dark adaptation

For experiments examining the specificity of our Cx57 antibodies and the distribution of Cx57 within the retina, mice were removed from the housing facility 2 hours after the start of the light phase and killed under normal room lighting.

For experiments examining the effects of ambient light on the Cx57 immunoreactivity pattern, mice were removed from the housing facility 2 hours after the start of the light phase. For immunohistochemistry on retinal slices, mice were dark adapted for 4 hours. Eyecups were prepared under dim red light, and left to equilibrate 30 minutes in Ames solution. One eyecup from each mouse was subjected to bright white light (Schott KL 1500, 150 W) for 1 hour, while the second eye from each mouse was kept in darkness. Eyecups were then fixed under the respective lighting conditions and processed for immunohistochemistry.

Characterization of connexin57 antibodies and Western blot analysis

Polyclonal Cx57 antibodies were raised in rabbits (Pineda Antibody Service, Berlin, Germany). The peptide used for immunization comprised 15 amino acid (aa) residues (C**SM**S**MILELSSIMKK**), corresponding the C-terminal end of the homologous connexin expressed in fish horizontal cells (U. Janssen-Bienhold, unpublished observation); the aa residues marked in bold correspond to twelve aa residues of the C-terminal end of mouse retinal Cx57 (Hombach et al., 2004).

SDS-gel electrophoresis and Western blot analysis were carried out with crude subcellular fractions (nuclei, membrane, and soluble) prepared from mouse retinas and HeLa cell homogenates. HeLa cells were transfected with the eukaryotic expression vector pMJ-Cx57Go (Degen, et al., 2004) containing the coding region for retinal Cx57 fused C-terminally to that of enhanced green fluorescent protein (EGFP; theoretical molecular weight of the fusion protein: 82 kDa). The fusion proteins GST-Cx57CT (CT: C-terminus; aa 241-492) and GST-Cx57CL (CL: cytoplasmic loop; aa

101-150) were used as positive and negative controls, respectively; the fusion proteins were generated using the pGEX-6T vector (Amersham Biosciences, Braunschweig, Germany) and *BL21 E.coli* (Amersham Biosciences). Aliquots (60-150 μg of protein or 5 μg of fusion protein) were resuspended in gel-loading buffer (Laemmli, 1970). Proteins were separated by SDS-PAGE on 8-10% gradient gels and transferred to nitrocellulose (Optitran BA-S 85, Schleicher Schuell, Dassel, Germany).

Enhanced chemiluminescence-mediated immunodetection was carried out following a standard protocol. Incubation with the rabbit anti-mouse Cx57 (1:1000 in TBS-Tween: 20 mM Tris/HCl, 150 mM NaCl, 0.2% Tween-20) and mouse anti-EGFP antibodies (1:15,000; JL-8, BD Biosciences Clontech, Heidelberg, Germany) was carried out overnight, and immunoreactive proteins were visualized with horseradish peroxidase-conjugated goat anti-rabbit IgG or goat anti-mouse IgG secondary antibodies (1:3000 in TBS-Tween with 2% powdered milk; Biorad Laboratories, Munich, Germany) using the Pierce enhanced chemiluminescence detection system (Pierce, Rockford, IL). In some experiments, the same blots were used for detection of non-specific immunoreactive proteins. Bound Cx57 antibodies were removed in two wash steps in a shaking incubator at 37°C for 1 hour each: 1. 10 mM Tris/HCl, pH 8.8, 1% SDS, 10 mM β-mercaptoethanol; 2: 100 mM sodium citrate, pH 3.0, 1% SDS, 10 mM β-mercaptoethanol. After intensive rinsing in TBS-Tween, blots were blocked again and either probed with the preimmune serum (1:8000) or Cx57 antibodies (1:1000) preadsorbed with the immunization peptide (1 μg/μl stock-solution diluted 1:100).

Immunohistochemistry with retinal cryosections and whole mounts

For immunohistochemistry of retinal sections, eyecups were fixed with 2% paraformaldehyde (PFA) for 20 minutes and embedded in Cryoblock (Medite GmbH, Germany) at -20°C. Vertical cryosections (15 µm) were blocked with 10% normal goat serum (NGS, Sigma, Deisenhofen, Germany) in Tris-buffered saline containing 0.3% Triton X-100 (TTBS) and then incubated with rabbit anti-Cx57 (1:750 in TTBS) and monoclonal mouse anti-calbindin (1:8000; Swant, Bellinzona, Switzerland) at 4°C overnight. Secondary antibodies (goat anti-rabbit Alexa568; goat anti-mouse Alexa488, Invitrogen, Karlsruhe, Germany; or goat anti-mouse Cy5, Jackson Immunoresearch, West Grove, PA), diluted 1:600 in TTBS containing 2% NGS, were applied at room temperature for 2 hours. Finally, sections were washed in TBS and mounted in Vectashield (Vector Laboratories, Burlingame, CA).

In some experiments, additional labeling of the cone axon terminal bases with fluorescein-conjugated peanut agglutinin (FITC-PAG; Vector Laboratories) was carried out to divide the OPL into proximal and distal layers. This enabled a detailed analysis of the distribution of Cx57 within the OPL. Immunostained sections were washed in phosphate-buffered saline (PBS), incubated with FITC-PAG (300 µg/ml) in PBS containing 1 mg/ml BSA (Sigma) for 1 hour at room temperature, washed, and mounted in Vectashield.

For whole-mount immunohistochemistry, isolated retinas were fixed in 2% PFA for 20 minutes, washed in TTBS, mounted ganglion cell side up on black filter paper (Millipore Corporation, Bedford, MA) and blocked with 10% NGS overnight at 4°C. Immunostaining was performed with the same antibody concentrations and buffer conditions as for cryosections, but in the presence of 0.02% sodium azide, and the

incubation times with primary and secondary antibodies were extended to five and two days, respectively.

Immunohistochemistry on dissociated retinal neurons

Isolated wild-type mouse retinas were dissociated as described previously (Feigenspan and Weiler, 2004). The resulting cell suspension was plated on concanavalin-A-coated (1 mg/ml) slides and coverslips, and cells were allowed to adhere in 5% CO_2/55% O_2 for 1 hour at 36°C before they were fixed in 2% PFA. Fixed cells were washed in TBS, and labeled with Cx57 and calbindin antibodies as described for cryosections, except that TBS was used for washing instead of TTBS.

Pre-embedding immunoelectron microscopy

For immunoelectron microscopy, eyecups were fixed in 2% PFA in Sörensen's buffer ($0.1M$ KH_2PO_4, $0.1M$ Na_2HPO_4) for 30 minutes; retinas were then dissected from the eyecups and fixed for a further 30 minutes. Following cryoprotection, retinas were subjected to two 15-minute freeze-thaw cycles in 30% sucrose, at -80°C and room temperature, respectively, to improve infiltration of antibodies. Finally, retinas were embedded in 2% Agar 100 Resin (Plano, Wetzlar, Germany) in PBS, and vertical sections (200 µm) were sliced on a vibratome (Leica, Nussloch, Germany). Slices were blocked with 10% NGS and incubated with Cx57 antibodies (1:500 in Sörensen-buffer + 0.02% sodium azide) on a shaking platform for five days at 4°C. After several washes in buffer, slices were incubated with secondary antibodies (biotinylated goat anti-rabbit IgG, Vector Laboratories; 1:250), at 4°C for 2 days, washed, and Cx57 binding sites were detected with the VectaStain *Elite* ABC Kit (Vector Laboratories). Slices were incubated in 0.05% 3,3-diaminobenzidine (Sigma) activated by H_2O_2. Slices were washed and postfixed in 2.5% glutaraldehyde and 1% PFA, subjected to silver intensification, as described elsewhere (Sassoe-Pognetto et al., 1994), and

fixed in 1% OsO_4. Slices were dehydrated in increasing acetone concentrations (30–100%) and embedded in Epon 812. Ultrathin sections were analyzed and photographed on a Zeiss 902 electron microscope.

Fluorescent image acquisition and statistical analysis

Confocal micrographs of fluorescent specimen were taken with a Leica TCS SL confocal microscope. Scanning was performed with a 63x/1.32 Plan-Apochromat objective at a resolution of 1024 x 1024 or 128 x 1024 pixels. Scans of different wavelengths were done sequentially to rule out cross talk between red, green, and blue (far-red) channels. Images are presented either as single scans of 0.2 µm or projections of stacks of 2-10 x 0.2 µm scans. To evaluate colocalization, images were superimposed and adjusted in brightness and contrast using either Photoshop 7.0 (Adobe, San Jose, CA) or ImageJ.

Plaque distribution and size were analyzed with ImageJ. Cryosections triple-labeled for Cx57, calbindin and FITC-PAG were used to analyze the plaque distribution in the OPL. Regions of 70 x 60 pixels were divided horizontally along the FITC-PAG-labeled cone pedicle bases, and plaques were counted in the distal (upper 70 x 30 pixels) and proximal (lower 70 x 30 pixels) halves of the OPL.

The analysis of Cx57 plaques in light- and dark-adapted retinas was performed with retinal cryosections within ~2 mm of the optic disk, and images were taken at a maximum distance of 1 mm from the section center. Cx57 plaques were counted in 12 regions of 150 x 150 pixels (1211 µm^2) per retinal section. Light- and dark-adapted sections were placed on the same slide and incubated under identical conditions.

Results

Cx57 is expressed exclusively in retinal horizontal cells in the mouse nervous system (Hombach et al., 2004). We generated polyclonal antibodies against 12 C-terminal amino acid residues of mouse retinal Cx57 in order to determine the distribution of Cx57 hemichannels within the horizontal cell.

Specificity and characterization of Cx57 antibodies

Specificity of the affinity-purified Cx57 antibodies was tested using immunohistochemistry and Western blot analysis in wild-type and Cx57-deficient mouse retinas. In cryosections of wild-type ($Cx57^{+/+}$) retinas, immunofluorescent puncta were observed in the OPL. This immunoreactivity pattern was reduced in heterozygous ($Cx57^{+/-}$) mice, and completely absent in homozygous Cx57-deficient mice ($Cx57^{-/-}$; Fig. 1A). Sparse immunosignals were observed occasionally in the inner nuclear and ganglion cell layers, but these were considered non-specific, since they were also present in $Cx57^{+/-}$ and $Cx57^{-/-}$ retinas. Staining in the OPL of wild-type retinas was absent when the sections were incubated in the pre-immune serum or Cx57 antibodies preadsorbed with the immunization peptide.

Specificity of Cx57 antibodies was also tested using Western blot analysis. One protein with a molecular weight of approximately 54 kDa was labeled in the membrane fraction of the wild-type retina; this protein was not detected by the antibodies in the two samples derived from Cx57-deficient mice (Fig. 1B, black asterisk). This 54 kDa protein was weakly detected in retinal homogenates and not detected in nuclear and soluble fractions of wild-type mouse retinas (Fig. 1C); this protein was also not detected by the pre-immune serum (Fig. 1D). A Cx57 C-terminus-GST fusion protein (GST-Cx57CT; aa 241-492), with an expected molecular weight of approximately 55 kDa, served as a positive control (Fig. 1B, E; CT). A

Cx57-GST fusion protein of approximately 33 kDa, containing the cytoplasmic loop of Cx57 (GST-Cx57CL; aa 101-150), served as a negative control, and was not detected by the Cx57 antibodies. Cross-reactivity of the Cx57 antibodies with Cx46 and Cx50, which are expressed in the lens (White et al., 1992; Rong et al., 2002) and in A-type horizontal cells of the rabbit (Cx50; O'Brien et al., 2006), was ruled out (Fig. 1B). These data indicate that the labeled protein is mouse retinal Cx57.

In addition to the band at 54 kDa, some additional bands are also seen on the blots. These extra bands may arise from protein dimerization, phosphorylation, or dephosphorylation, which alter the molecular weight of the protein. Potential dimers are indicated with an asterisk in Figure 1C, D. In addition, Cx57 may bind to other proteins, which would also alter the effective molecular weight on the blot. In retinal membrane samples, the antibodies labeled several proteins with molecular weights larger than 55 kDa; this labeling was seen in membrane samples derived from both wild-type and Cx57$^{-/-}$ retinas (Fig. 1B). In addition, some bands differed between wild-type and Cx57-deficient retinas, suggesting that the antibody may bind other proteins in addition to Cx57.

To identify proteins in addition to Cx57 which may interact with our Cx57 antibody, we performed a BLAST search of the UniProt Knowledgebase rodentia database. Mouse retinal Cx57 is not yet in the UniProt database, and differs in its C terminus from the mouse Cx57 found in the database. Therefore, the highest hits generated by BLAST searches were for unrelated proteins. No protein had more than 7 amino acids in common with our 15-amino acid antibody. Most of these potential interaction partners were cytosolic proteins, such as acetyl-CoA synthetase 1 (6 aa of 7; 78.8 kDa) and ADP-ribosylation factor-like protein 9 (6 aa of 7; 150 kDa). The only membrane-associated proteins that were recognized as possible interaction partners,

among the top 30 hits, were retinal short chain dehydrogenase reductase-similar protein (7 aa from 11; 35 kDa) and interleukin-6 receptor subunit beta precursor (6 aa of 7; 102.5 kDa). Another possible interaction partner of potential interest, because of its molecular weight and cellular function, is the cytoskeleton protein catelin-like protein 1 (6 aa of 6; 81.5 kDa), which is involved in adhesion junctions. Therefore, there are several potential interaction partners for our antibody, but none which is recognized with such affinity as Cx57.

To further underscore the specificity of our antibodies, we transfected HeLa cells with a Cx57-EGFP fusion protein. In lysates of Cx57eGFP-transfected HeLa cells, but not in non-transfected controls, the Cx57 antibodies detected a protein of the expected size of approximately 82 kDa (Fig. 1E). This protein was also detected by an EGFP antibody after stripping and reprobing the blot (Fig. 1E).

In conclusion, we have several lines of evidence which indicate that our antibodies are specific for mouse retinal Cx57: 1. Immunohistochemistry in retinal slices produces clear, punctate labeling in the outer plexiform layer, which is absent in the Cx57-deficient mouse (Fig. 1A). 2. The antibody detects a protein of 54 kDa on Western blots of wild-type retina samples, which is not detected in Cx57-deficient retinas. 3. Western blots of HeLa cells transfected with a Cx57-EGFP fusion protein produced a clear band at the correct molecular weight, which was absent in non-transfected cells (Fig. 1E). 4. BLAST searches of the UniProt Knowledgebase rodentia database did not generate any matches with more than 7 identical amino acids.

Immunohistochemical localization of Cx57 in the OPL

We used immunohistochemistry on retinal cryosections, dissociated retinal cells, and whole-mounted retinas to examine in detail the location of Cx57 expression within the

horizontal cell. Antibodies against calbindin were used as a marker for horizontal cells (Haverkamp and Wässle, 2000). In retinal slices, Cx57-immunoreactive plaques were found in the OPL co-localized with or directly neighboring calbindin-positive horizontal cell processes; little Cx57 immunoreactivity was observed on horizontal cell somata (Fig. 2A). Cx57 plaques had a mean area of 0.41 ± 0.02 µm^2 (± SE; n = 4); there was no obvious difference in plaque size between central and peripheral retina.

Next we examined the distribution of Cx57 labeling in dissociated horizontal cell somata and axon terminals. Horizontal cells could be distinguished from other neurons by their morphology (Feigenspan and Weiler, 2004); cell type was confirmed by calbindin labeling. Cx57-immunoreactive puncta were found along the length of horizontal cell axon terminals (Fig. 2B, C) and dendrites (Fig. 2D, E). Along the distal dendrites and axon terminal processes, Cx57 plaques often resembled pearls on a string (Fig. 2C, E). Isolated cone photoreceptors, bipolar and ganglion cells were not labeled by the Cx57 antibodies.

Next, we examined in detail the distribution of Cx57 immunoreactivity in the OPL, to determine whether there are quantitative differences in Cx57 expression levels between the dendro-dendritic and axo-axonal networks. We used FITC-conjugated peanut agglutinin (FITC-PAG), which labels cone pedicle bases (Hack and Peichl, 1999; Haverkamp et al., 2001), to divide the OPL into inner and outer halves; we then counted the Cx57 plaques in each half of the OPL. Image stacks of an FITC-PAG-labeled retinal section co-labeled for Cx57 are shown in Figure 3A-C. There was significantly more Cx57 staining above the midline of the OPL (6 ± 0.03 plaques/100 µm^2; mean ± SE; 63%) than below (3.5 ± 0.03 plaques/100 µm^2; 37%; n

= 3 retinas; p<0.001). These data suggest that Cx57 expression is higher in the horizontal cell axon terminals than in the dendrites.

This finding was confirmed in whole mount preparations labeled for calbindin and Cx57. We examined the distribution of Cx57 at three different sublayers of the OPL, as shown in Figure 3D-F. In the proximal OPL, numerous Cx57 plaques were found concentrated at dendritic intersections. Few Cx57 plaques were seen on horizontal cell somata (Fig. 3D). Fine, distal dendritic processes and major axon terminal branches stratify in the center of the OPL, near the photoreceptor terminals. Cx57 plaques were much more plentiful at this level (Fig. 3E). The ends of the axon terminal branches are located in the most distal part of the OPL. At this level, Cx57 immunoreactivity was evident primarily between terminal processes, and only partially co-localized with calbindin (Fig. 3F).

Ultrastructural distribution of Cx57 in the OPL

Horizontal cell gap junctions have been described at the ultrastructural level in cat, rabbit, and monkey retinas (Kolb, 1974; 1977; Raviola and Gilula, 1975), but these structures have not been described in the mouse retina to date. To fill this gap, and to confirm that Cx57 does not form hemichannels in the horizontal cell dendritic tips, we performed immunoelectron microscopy with our newly-developed antibodies against Cx57.

Gap junctions are recognizable by the close apposition of cell membranes from neighboring cells. Cx57 immunoreactivity was observed in gap junctions between horizontal cell dendrites (Fig. 4A) and axon terminal processes (Fig. 4C). Cx57-positive gap junctions between dendrites were slightly smaller in length (85.4 ± 25.8 nm; mean ± SD; n = 14 gap junctions) than those between axon terminal processes (101.2 ± 23.7 nm; n = 12). Dendritic Cx57-positive gap junctions displayed prominent

submembranous immunoreactivity along the adjoining membranes. Gap junctions were flanked with zonula adherens, as shown previously for dendritic gap junctions in cat (Kolb, 1974, 1977) and turtle (Witkovsky et al., 1983; Kolb and Jones, 1984). Zonula adherens also displayed Cx57 immunoreactivity, suggesting a reservoir of hemichannels in the apposing membranes, presumably in preparation for docking. Several Cx57-positive regions were observed which did not resemble the characteristic septalaminar ultrastructure of gap junctions; these may represent hemichannels in zonula adherens which flank gap junctions located in an adjacent section.

Cx57 immunoreactivity in axon terminals was restricted almost exclusively to the gap junctions (Fig. 4C). There was no prominent staining in the apposing membranes flanking the gap junction, like that observed in dendritic gap junctions. We frequently observed a row of two or more small Cx57-positive gap junctions separated by small gaps. This feature was observed in dendro-dendritic and axo-axonal gap junctions, and was regarded as specific for two reasons: the distribution was similar to that observed on dendrites and axon terminals of dissociated horizontal cells (Fig. 2B, D); and Cx57 immunoreactivity was absent in the OPL of Cx57-deficient retinas (Fig. 4B, D). In Cx57-deficient retinas, membranes of horizontal cell dendrites (Fig. 4B) and axon terminals (Fig. 4D) narrowed at some regions along the processes, but did not exhibit the characteristic septalaminar structure of gap junctions, and were not labeled by Cx57 antibodies.

To find out whether Cx57 forms hemichannels at horizontal cell dendritic tips within the photoreceptor terminals, we examined Cx57 immunoreactivity in tangential sections through the photoreceptor terminals (Fig. 5). Diffuse cytoplasmic staining was detected occasionally within profiles flanking the rod spherules (Fig 5A).

However, this was regarded as non-specific, since it was also observed in control samples not incubated with the primary antibodies (Fig. 5E). Membrane and cytoplasmic labeling of axon terminal processes flanking the synaptic ribbon in rod spherules was also regarded as non-specific, because these staining patterns were detected in both wild-type and Cx57-deficient retinas (Fig. 5A, B). No Cx57 immunolabeling was detected associated with the membranes of horizontal cell terminal dendrites within the cone pedicles (Fig. 5C, wild type: n = 2; Fig. 5D, Cx57-deficient: n = 2), indicating that Cx57 does not form hemichannels within the cone pedicle.

Cx57 expression is modulated by light

Horizontal cell coupling is modulated by ambient light (Tornqvist et al., 1988; Baldridge and Ball, 1991; Xin and Bloomfield, 1999) via modulators such as dopamine (Mangel and Dowling, 1985; Perlman and Ammermüller, 1994; He et al., 2000). To determine whether light-mediated modulation of Cx57-containing gap junctions is reflected in changes in Cx57 expression, we examined the Cx57 immunoreactivity patterns in retinal sections from light- and dark-adapted wild-type mouse retinas (Fig. 6). Light adaptation resulted in a significant increase in the number of Cx57-immunoreactive plaques in the OPL (light-adapted: 3.59 ± 0.19 plaques/100 μm^2; dark-adapted: 1.46 ± 0.08; mean $\pm$ S.E.; n = 4 retinas per condition; $p < 0.001$; Fig. 6C). We also analyzed the effects of light adaptation on Cx57 plaque size. Although the plaques in light-adapted retinas appeared to produce more immunofluorescence than in dark-adapted retinas (compare insets 6A, B), no significant difference in plaque size was found (light-adapted: 0.41 ± 0.02 μm^2; dark-adapted: 0.37 ± 0.01 μm^2; n = 4 retinas per condition; $p > 0.1$; Fig. 6D).

Discussion

The B-type horizontal cell has a large cell body connected by a long, thin axon to a highly-branched axon terminal; these two cellular compartments form separate coupled networks. In this study, we show for the first time the detailed distribution of Cx57 within the two compartments of the mouse horizontal cell, and demonstrate modulation of Cx57 expression by ambient light. Furthermore, we rule out Cx57 as a candidate for hemichannel-mediated feedback to photoreceptors.

Cx57 expression on horizontal cell dendrites and axon terminals

Cx57 is expressed along the length of the horizontal cell dendrites and axon terminal branches, indicating extensive gap junction formation along these processes. The increase in connexin density from central retina to periphery reported in rabbit horizontal cells (O'Brien et al., 2006) was not observed in the mouse. This probably reflects the constant horizontal cell dendritic field size across the retina in the mouse (Raven and Reese, 2002); the increase in connexin density in rabbit is thought to compensate for the decline in cell density from center to periphery (O'Brien et al., 2006). The number of gap junctions per unit area of horizontal cell dendritic field is therefore invariant across the retina in both mouse and rabbit.

Our data showed that Cx57 expression is higher in the horizontal cell axon terminals than in the dendrites. This contradicts tracer coupling data, which shows that coupling is much stronger between mouse horizontal cell somata than between axon terminals (J. Trümpler, unpublished observations). This discrepancy may arise from the extensive branching of the axon terminal system, which results in a larger volume compared to the somatic network. Because of the larger volume, diffusion of tracer within axon terminals should be slower than within somata. Thus a higher level of Cx57 expression may be required to effectively couple the axon terminal system.

The ultrastructural morphology of horizontal cell gap junctions has been examined electron microscopically in rabbit, cat, and monkey (Kolb, 1974, 1977; Raviola and Gilula, 1975). Our immunoelectron microscopic data provide the first description of these structures in the mouse retina. Dendritic gap junctions were smaller than those between axon terminal processes. Cx57 immunoreactivity was observed at sites along the dendritic membrane which were not involved in gap junctions; this non-gap junctional staining was not seen in axon terminals, and may represent hemichannel reservoirs which flank gap junctions in neighboring sections. A recent study using fluorescent immunohistochemistry showed Cx57 immunoreactivity located near bassoon-labeled rod spherules; that study proposed that horizontal cell axon terminals form gap junctions within the rod spherules (Ciolofan et al., 2007). However, on the electron microscopic level, Cx57 staining was not seen inside the rod spherules or cone pedicles.

On the functional role of Cx57 in mouse horizontal cells

The physiological role of the coupling of the horizontal cell network is not completely understood. For several decades, horizontal cell coupling was thought to mediate the surround antagonism of ganglion cell receptive fields (Werblin and Dowling, 1969; Mangel and Dowling, 1985). However, a recent study by Dedek et al. (2008) showed that ganglion cell receptive fields are unaltered in Cx57-deficient mice, suggesting that horizontal cell coupling is not involved in surround formation. The tight coupling of the horizontal cells allows the network to collect light information over a large area of the retina; feedback from horizontal cells to photoreceptors thus likely serves to adjust the gain of the photoreceptors to different levels of ambient light (reviewed by Kamermans and Spekreijse, 1999). In addition to the feedback to cone photoreceptors, horizontal cell feedback to rods was recently demonstrated in

salamander retina (Thoreson et al., 2008). Thus, it is possible that the somatic and axon terminal networks in the mouse retina provide distinct feedback signals to cone and rod photoreceptor cells. This idea is underscored by the strong depolarizing rollback seen in the light responses of axon terminals in the mouse retina (Trümpler et al., 2008).

Horizontal cell coupling is modulated by ambient light in a triphasic manner: at low and high light levels, coupling is reduced, while at intermediate light levels, coupling is maximal (Xin and Bloomfield, 1999). This modulation is mediated by multiple neuromodulators, including dopamine (Mangel and Dowling, 1985; Perlman and Ammermüller, 1994; He et al., 2000), retinoic acid (Weiler et al., 1998; Pottek and Weiler, 2000), and nitric oxide (DeVries and Schwartz, 1989; Pottek et al., 1997; Lu and McMahon, 1997; Xin and Bloomfield, 2000). All of these neuromodulators reduce horizontal cell coupling, suggesting multiple distinct pathways for dark- and light-induced modulation.

These pathways may involve distinct mechanisms. For example, retinoic acid may interact directly with the gap junction proteins, or with nearby proteins in the membrane, thus modulating the gating of the gap junctions (Weiler et al., 2000). Alternatively, coupling can be modulated by altering the expression levels of the gap junction proteins. Dark adaptation has been shown to reduce the expression level of Cx57 in the mouse retina (Kihara et al., 2006). Furthermore, freeze fracture studies in fish horizontal cells have demonstrated a correlation between connexon density and adaptational state: dark adaptation resulted in smaller gap junctions with higher connexon densities than found following light adaptation (Wolburg and Kurz-Isler, 1985). Thus it is likely that the reduction in Cx57 fluorescence that we observed following dark adaptation results from changes in gap junction structure as well as

expression levels. Further work will be needed to show which neuromodulators trigger these changes in gap junction expression and structure.

It is interesting to note that this array of mechanisms for uncoupling horizontal cells is conserved across species. The morphology and subtypes of horizontal cells vary widely across species, but dopamine and retinoic acid modulate their coupling in all species studied to date (reviewed by Weiler et al., 2000). Thus these multiple mechanisms likely reflect distinct pathways driven by common environmental factors. For example, changes in expression levels take place very slowly, and are more suitable as a response to changes in ambient light over the course of the day than to fast changes triggered by, for example, stepping out from a dark cave. Accurate responses to these rapid changes would be better achieved by changes in channel gating, which is much faster. Dopamine causes rapid changes in horizontal cell coupling by indirectly altering gap junction gating; activation of D1 receptors leads to an increase in cyclic AMP, which in turn leads to phosphorylation of gap junctional proteins by protein kinase A (reviewed by Dowling, 1991). Retinoic acid also causes fast changes in horizontal cell coupling, but its role in development suggests that it may also have unknown long-term effects on cell coupling; retinoic acid is known to act via nuclear receptors to alter gene expression (reviewed by Hyatt and Dowling, 1997). Thus it is possible that retinoic mediates the light-induced changes in expression seen in this study.

Increasing evidence suggests that hemichannels located in the horizontal cell terminal dendrites mediate feedback to the photoreceptors (Kamermans et al., 2001). In this ephaptic mechanism, current flow through hemichannels results in a local extracellular voltage drop in the synaptic cleft. ZfCx55.5 has been proposed for this role in the zebrafish retina (Shields et al., 2007). Cx57 is unlikely to play a role in

horizontal cell feedback to the photoreceptors for several reasons: 1. Mouse Cx57 is homologous to zebrafish Cx52.6, which forms gap junctions between horizontal cells in the zebrafish (Shields et al., 2007) as Cx57 does in mouse; ZfCx52.6 is not involved in hemichannel-mediated feedback, making it unlikely that the mouse homolog Cx57 plays this role. The mouse homolog of zfCx55.5, which forms hemichannels in zebrafish (Shields et al., 2007) has not yet been identified. 2. In both wild-type and Cx57-deficient mice, horizontal cell light responses show a distinct roll-back, which is associated with feedback (Shelley et al., 2006); thus it is unlikely that Cx57 plays a role in feedback. 3. Blocking horizontal cell feedback by low-dosage cobalt results in a shift in ganglion cell tuning to lower frequencies in both wild-type and Cx57-deficient mice (Dedek et al., 2008), indicating that the feedback mechanism is still in place in the absence of Cx57. 4. Our immunoelectron microscopy data show that Cx57 is not expressed in the dendritic tips located in the photoreceptor terminals. Similar results were demonstrated in B-type horizontal cells in the rabbit retina: Cx57 is expressed along axon terminal processes, but not at the tips of these processes in the photoreceptor terminals (Cha, J., ARVO Abstract 3047, 2008).

Development of horizontal cells has been shown to be unimpaired in Cx57-deficient mice: dendritic morphology and mosaic distribution were comparable to those in wild-type retinas (Shelley et al., 2006). This indicates that gap junctions are not required for fine tuning of dendritic coverage of the retina. Reese et al. (2005) showed that horizontal cell position and dendritic field size are determined by the proximity to neighboring horizontal cells, suggesting that cell contact is crucial. Our electron microscopic images of the Cx57-deficient retina revealed frequent sites along neighboring horizontal cell processes at which the two membranes draw close together, forming what resemble adherent junctions. Such structures have also been

observed between monkey horizontal cells (Raviola and Gilula, 1975). Cell-cell interaction proteins have been proposed to help developing retinal neurons find each other within the heterogeneous cell pool (Honjo et al., 2000). Differential expression of cadherins by different cell populations in the retina (Nagae et al., 2007), and defective amacrine cell spacing in mice lacking Down syndrome cell adhesion molecule (Fuerst et al., 2008) support this hypothesis. Thus it is likely that formation of the horizontal cell network is modulated primarily by external guiding signals and cell adhesion molecules, and that the role of gap junctional communication in network development is secondary.

Acknowledgements

Abbreviations

aa: amino acid

Cx: connexin

EGFP: enhanced green fluorescent protein

FITC-PAG: fluorescein-conjugated peanut agglutinin

OPL: outer plexiform layer

PBS: phosphate-buffered saline

PFA: paraformaldehyde

TTBS: tris-buffered saline containing 0.3% Triton X-100

References

Baldridge WH and Ball AK (1991) Background illumination reduces horizontal cell receptive-field size in both normal and 6-hydroxydopamine-lesioned goldfish retinas. Vis Neurosci 7:441-450.

Ciolofan C, Lynn BD, Wellershaus K, Willecke K and Nagi JI (2007) Spatial relationships of connexin36, connexin57 and zonula occludens-1 in the outer plexiform layer of mouse retina. Neuroscience 148:473-488.

Dedek K, Pandarinath C, Alam NM, Wellershaus K, Schubert T, Willecke W, Prusky GT, Weiler R and Nirenberg S (2008) Ganglion cell adaptability: does the coupling of horizontal cells play a role? PlosOne 3:e1714

Degen J, Meier C, van der Giessen RS, Söhl G, Petrasch-Parwez E, Urschel S, Dermietzel R, Schilling K, de Zeeuw CI and Willecke K (2004) Expression pattern of lacZ reporter gene representing connexin36 in transgenic mice. J Comp Neurol 473:511-525.

DeVries SH and Schwarz EA (1989) Modulation of an electrical synapse between solitary pairs of catfish horizontal cells by dopamine and second messengers. J Physiol 414:351-375.

Dowling J (1991) Retinal neuromodulation: The role of dopamine. Vis Neurosci 7:87-97.

Feigenspan A and Weiler R (2004) Electrophysiological properties of mouse horizontal cell GABA A receptors. J Neurophysiol 92:2789-2801.

Fuerst PG, Koizumi A, Masland RH and Burgess RW (2008) Neurite arborization and mosaic spacing in the mouse retina require DSCAM. Nature 451:470-474.

Hack I and Peichl L (1999) Horizontal cells of the rabbit retina are non-selectively connected to the cones. Eur J Neurosci 11:2261-2274.

Haverkamp S and Wässle H (2000) Immunocytochemical analysis of the mouse retina. J Comp Neurol 424:1-23.

Haverkamp S, Grünert U and Wässle H (2001) The synaptic architecture of AMPA receptors at the cone pedicle of the primate retina. J Neurosci 21:2488-2500.

He S, Weiler R and Vaney DI (2000) Endogenous dopaminergic regulation of horizontal cell coupling in the mammalian retina. J Comp Neurol 418:33-40.

Hombach S, Janssen-Bienhold U, Söhl G, Schubert T, Büssow H, Ott T, Weiler R and Willecke K (2004) Functional expression of connexin57 in horizontal cells of the mouse retina. Eur J Neurosci 19:2633-2640.

Honjo M, Tanihara H, Suzuki S, Tanaka T, Honda Y and Takeichi M (2000) Differential expression of cadherin adhesion receptors in neural retina of the postnatal mouse. IOVS 41:546-551.

Hyatt GA and Dowling JE (1997) Retinoic acid. A key molecule for eye and photoreceptor development. IOVS 38: 1471-1475.

Kamermans M, and Spekreijse H (1999) The feedback pathway from horizontal cells to cones: A mini review with a look ahead. Vision Res 39:2449-2468.

Kamermans M and Fahrenfort I (2004) Ephaptic interactions within a chemical synapse: hemichannel-mediated ephaptic inhibition in the retina. Curr Opin Neurobiol 14:531-541.

Kamermans M, Fahrenfort I, Schultz K, Janssen-Bienhold U, Sjoersdam T and Weiler R (2001) Hemichannel-mediated inhibition in the outer retina. Science 292:1178-1180.

24

Kihara AH, de Castro LM, Moriscot AS and Hamassaki DE (2006) Prolonged dark adaptation changes connexin expression in the mouse retina. J Neurosci Res 83:1331-1341.

Kolb H (1974) The connections between horizontal cells and photoreceptors in the retina of the cat: electron microscopy of Golgi preparations. J Comp Neurol 155 :1-14.

Kolb H (1977) The organization of the outer plexiform layer in the retina of the cat: electron microscopic observations. J Neurocytol 6:131-153.

Kolb H and Jones J (1984) Synaptic organization of the outer plexiform layer of the turtle retina: an electron microscope study of serial sections. J Neurocytol 13:567-591.

Laemmli UK(1970) Cleavage of structural proteins during assembly of the head of bacteriophage T4. Nature 227:680-685.

Lu C and McMahon DG (1997) Modulation of hybrid bass retinal gap junctional channel gating by nitric oxide. J Physiol 499:689-699.

Mangel SC and Dowling JE (1985) Responsiveness and receptive field size of carp horizontal cells are reduced by prolonged darkness and dopamine. Science 229:1107-1109.

Manthey D, Bukauskas F, Lee CG Kozak CA and Willecke K (1999) Molecular cloning and functional expression of the mouse gap junction gene connexin-57 in human HeLa cells. J Biol Chem 274(21):14716-14723.

Nagae S, Tanoue T and Takeichi M (2007) Temporal and spatial expression profiles of the fat3 protein, a giant cadherin molecule, during mouse development. Dev Dyn 236:534-543.

O'Brien JJ, Li W, Pan F, Keung J, O'Brien J and Massey SC (2006) Coupling between A-type horizontal cells is mediated by connexin 50 in the rabbit retina. J Neurosci 26:1124-11636.

Peichl L and Gonzalez-Soriano J (1994) Morphological types of horizontal cell in rodent retinae: a comparison of rat, mouse, gerbil, and guinea pig. Vis Neurosci 11:501-517.

Perlman I and Ammermüller J (1994) Receptive-field size of L1 horizontal cells in the turtle retina: effects of dopamine and background light. J Neurophysiol 72(6):2786-2795.

Pottek M and Weiler R (2000) Light-adaptive effects of retinoic acid on receptive field properties of retinal horizontal cells. Eur J Neurosci 12:437-445.

Pottek M, Schultz K and Weiler R (1997) Effects of nitric oxide on the horizontal cell network and dopamine release in the carp retina. Vision Res 37:1091-1102.

Raven MA and Reese BE (2002) Horizontal cell density and mosaic regularity in pigmented and albino mouse retina. J Comp Neurol 454:168-176.

Raviola E and Gilula NB (1975) Intramembrane organization of specialized contacts in the outer plexiform layer of the retina. J Cell Biol 65:192-222.

Reese BE, Raven MA and Stagg SS (2005) Afferents and homotypic neighbors regulate horizontal cell morphology, connectivity, and retinal coverage. J Neurosci 25:2167-2175.

Rong P, Wang X, Niesman I, Wu Y, Benedetti LE, Dunia I, Levy E, and Gong X (2002) Disruption of *Gja8* (α8 connexin) in mice leads to microphthalmia associated with retardation of lens growth and lens fibre maturation. Develop 129:167-174.

Sassoé-Pognetto M, Wässle H and Grünert U (1994) Glycinergic synapses in the rod pathway of the rat retina: Cone bipolar cells express the α1 subunit of the glycine receptor. J Neurosci 14:5131-5146.

Shelley J, Dedek K, Schubert T, Feigenspan A, Schultz K, Hombach S, Willecke K and Weiler R (2006) Horizontal cell receptive fields are reduced in connexin57-deficient mice. Eur J Neurosci 23:3176-3186.

Shields CR, Klooster J, Claassen Y, Ul-Hussain M, Zoidl G, Dermietzel R and Kamermans M (2007) Retinal horizontal cell-specific promoter activity and protein expression of zebrafish connexin 52.6 and connexin 55.5. J Comp Neurol 501:765-779.

Suzuki H and Pinto LH (1986) Response properties of horizontal cells in the isolated retina of wild-type and pearl mutant mice. J Neurosci 6:1122-1128.

Thoreson WB, Babai N and Bartoletti TM (2008) Feedback from horizontal cells to rod photoreceptors in vertebrate retina. J Neurosci 28:5691-5695.

Tornqvist K, Yang XL and Dowling JE (1988) Modulation of cone horizontal cell activity in the teleost fish retina. III. Effects of prolonged darkness and dopamine on electrical coupling between horizontal cells. J Neurosci 8:2279-2288.

Trümpler J, Dedek K, Schubert T, de Sevilla Müller LP, Seeliger M, Humphries P, Biel M and Weiler R (2008) Rod and cone contributions to horizontal cell light responses in the mouse retina. J Neurosci 28:6818-6825.

Urschel S, Höher T, Schubert T, Alev C, Söhl G, Wörsdörfer P, Asahara T, Dermietzel R, Weiler R and Willecke K (2006) Protein kinase A-mediated phosphorylation of connexin36 in mouse retina results in decreased gap junctional communication between AII amacrine cells. J Biol Chem 281:33163-33171.

Weiler R, Schultz K, Pottek M, Tieding S and Janssen-Bienhold U (1998) Retinoic acid has light-adaptive effects on horizontal cells in the retina. Proc Natl Acad Sci USA 95:7139-7144.

Weiler R, Pottek M, He S, and Vaney DI (2000) Modulation of coupling between retinal horizontal cells by retinoic acid and endogenous dopamine. Brain Res Brain Res Rev 32:121-129.

Werblin FS and Dowling JE (1969) Organization of the retina of the mudpuppy, Necturus maculosus. II. Intracellular recording. J Neurophysiol 32:339-355.

White TW, Bruzzone R, Goodenough DA and Paul DL (1992) Mouse Cx50, a functional member of the connexin family of gap junction proteins, is the lens fiber protein MP70. Mol Biol Cell 3:711-720.

Witkovsky P, Owen WG and Woodworth M (1983) Gap junctions among the perikarya, dendrites, and axon terminals of the luminosity-type horizontal cell of the turtle retina. J Comp Neurol 216:359-368.

Wolburg H and Kurz-Isler G (1985) Dynamics of gap junctions between horizontal cells in the goldfish retina. Exp Brain Res 60:397-401.

Xin D, and Bloomfield SA (1999) Dark- and light-induced changes in coupling between horizontal cells in mammalian retina. J Comp Neurol 405:75-87.

26

Xin D, and Bloomfield SA (2000) Effects of nitric oxide on horizontal cells in the rabbit retina. Vis Neurosci 17:799-811.

Figures

Figure 1. The Cx57 antibodies are specific for mouse retinal Cx57. A: Specificity in retinal cryosections. The Cx57 antibodies produced dense, punctate labeling in the outer plexiform layer of the wild-type mouse retina (Cx57+/+). This labeling was absent in the Cx57-deficient retina (Cx57-/-). An intermediate expression level was seen in heterozygous retinas (Cx57+/-). Sparse labeling in the inner nuclear layer was unspecific. Scale bar: 40 µm. B: Specificity of Cx57 antibodies in Western blots. A protein of 54 kDa was labeled in membrane samples from wild-type mouse retina (WT; black asterisk); this protein was not detected in samples from Cx57-deficient mice (KO). CT: A Cx57 C-terminus-GST fusion protein, with an expected molecular weight of 55 kDa, served as a positive control (white asterisk). Le: Cross-reactivity of the Cx57 antibodies with connexins expressed in the lens was excluded. C: Cx57 was detected in the membrane fraction from wild-type retinas (M), but not in the nuclear (N) or soluble (S) fractions. Minimal labeling was observed in the total homogenate (TH). Bands representing Cx57 and its potential dimer are labeled with black asterisks. D: Labeling was absent when the blot was incubated with the pre-immune serum. E: In lysates of Cx57eGFP-transfected HeLa cells (lane 2), but not in non-transfected controls (lane 1), the Cx57 antibodies detected a protein of the expected size of approximately 82 kDa (left panel, white star). This protein was also detected by an EGFP antibody after stripping and reprobing the blot (right panel). CT: A Cx57 C-terminus-GST fusion protein, was detected by the Cx57 antibodies (white asterisk), but not by the EGFP antibodies.

Figure 2. Localization of Cx57 (magenta) in a retinal section (A), an isolated horizontal cell axon terminal (B) and soma (D) labeled with calbindin (green). Each image comprises a single optical section of 200 nm thickness. C: High magnification of box in B; E: high magnification of box in D. Scale bars A,B,D: 20 µm; C,E: 10 µm.

Figure 3. Distribution of Cx57 within the outer plexiform layer (OPL). A-C: Quantification of Cx57 puncta in the distal and proximal OPL. Image stack of retinal sections labeled for Cx57 (A, magenta) and FITC-conjugated peanut agglutinin (FITC-PAG; B, green). C: Overlay of A and B. There was significantly more Cx57 staining above the PAG-labeled pedicle bases (arrow) than below (arrowhead). D-F: Distribution of Cx57 in three sublayers of the OPL of a calbindin-labeled whole-mounted retina. D: proximal OPL; E: center of the OPL near the photoreceptor terminals; F: distal OPL. Scale bars: A-C: 20 µm; D-F: 10 µm.

Figure 4. Cx57 immunoreactivity in gap junctions (asterisks) between horizontal cell dendrites (A) and axon terminal processes (C) in the wild-type retina. Dendritic gap junctions were flanked with zonula adherens (arrowheads), which also displayed Cx57 immunoreactivity. Several Cx57-positive regions were observed which did not resemble the characteristic septalaminar ultrastructure of gap junctions (arrows in A). In Cx57-deficient retinas, membranes of horizontal cell dendrites (B) and axon terminals (D) narrowed at some regions along the processes (arrowheads), but did

not exhibit the characteristic structure of gap junctions, and were not labeled by Cx57 antibodies. Scale bars: 100 nm.

Figure 5. No Cx57 immunoreactivity was seen within rod spherules (A, B) or cone pedicles (C, D) of wild-type (A, C) or Cx57-deficient mice (B, D). Diffuse, non-specific cytoplasmic staining was detected occasionally within a few of the profiles flanking the photoreceptor terminals (arrowhead in A, E). E, F: Rod spherule and cone pedicle from a wild-type retina without primary Cx57 antibody. Asterisks indicate invaginating horizontal cell processes. Scale bars: A, B, E: 250 nm; C, D, F: 500 nm.

Figure 6. Cx57 immunoreactivity pattern is modulated by ambient light. Image stacks of light- (A) and dark-adapted (B) retinal sections labeled with Cx57 antibodies. Insets: high magnification of boxed regions in A and B. Scale bar: 5 µm. C: Light adaptation resulted in a significant increase in the number of Cx57-immunoreactive plaques in the OPL (light-adapted: 3.59 ± 0.19 plaques/100 μm^2; dark-adapted: 1.46 ± 0.08 ; mean $\pm$ S.E. ; n = 4 retinas per condition; $p < 0.001$; t-test). D: No significant difference in plaque size was found (light-adapted: 0.41 ± 0.02 μm^2; dark-adapted: 0.37 ± 0.01 μm^2; mean $\pm$ S.E.; n = 4 retinas per condition; $p > 0.1$).
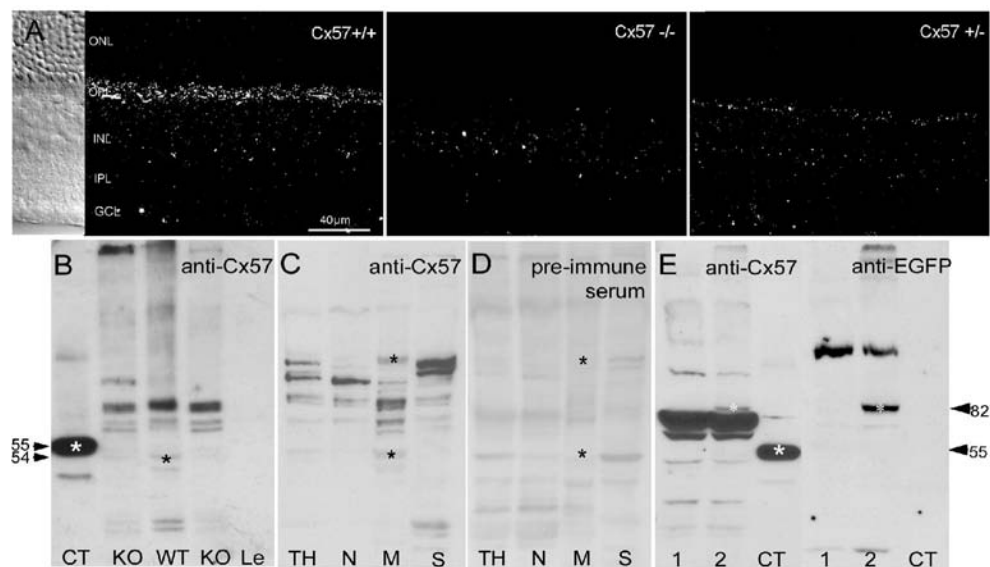
Figure 1. The Cx57 antibodies are specific for mouse retinal Cx57. A: Specificity in retinal cryosections. The Cx57 antibodies produced dense, punctate labeling in the outer plexiform layer of the wild-type mouse retina (Cx57+/+). This labeling was absent in the Cx57-deficient retina (Cx57-/-). An intermediate expression level was seen in heterozygous retinas (Cx57+/-). Sparse labeling in the inner nuclear layer was unspecific. Scale bar: 40 μm. **B: Specificity of Cx57 antibodies in Western blots.** A protein of 54 kDa was labeled in membrane samples from wild-type mouse retina (WT; black asterisk); this protein was not detected in samples from Cx57-deficient mice (KO). CT: A Cx57 C-terminus-GST fusion protein, with an expected molecular weight of 55 kDa, served as a positive control (white asterisk). Le: Cross-reactivity of the Cx57 antibodies with connexins expressed in the lens was excluded. **C:** Cx57 was detected in the membrane fraction from wild-type retinas (M), but not in the nuclear (N) or soluble (S) fractions. Minimal labeling was observed in the total homogenate (TH). Bands representing Cx57 and its potential dimer are labeled with black asterisks. **D:** Labeling was absent when the blot was incubated with the pre-immune serum. **E:** In lysates of Cx57eGFP-transfected HeLa cells (lane 2), but not in non-transfected controls (lane 1), the Cx57 antibodies detected a protein of the expected size of approximately 82 kDa (left panel, white star). This protein was also detected by an EGFP antibody after stripping and reprobing the blot (right panel). CT: A Cx57 C-terminus-GST fusion protein, was detected by the Cx57 antibodies (white asterisk), but not by the EGFP antibodies.
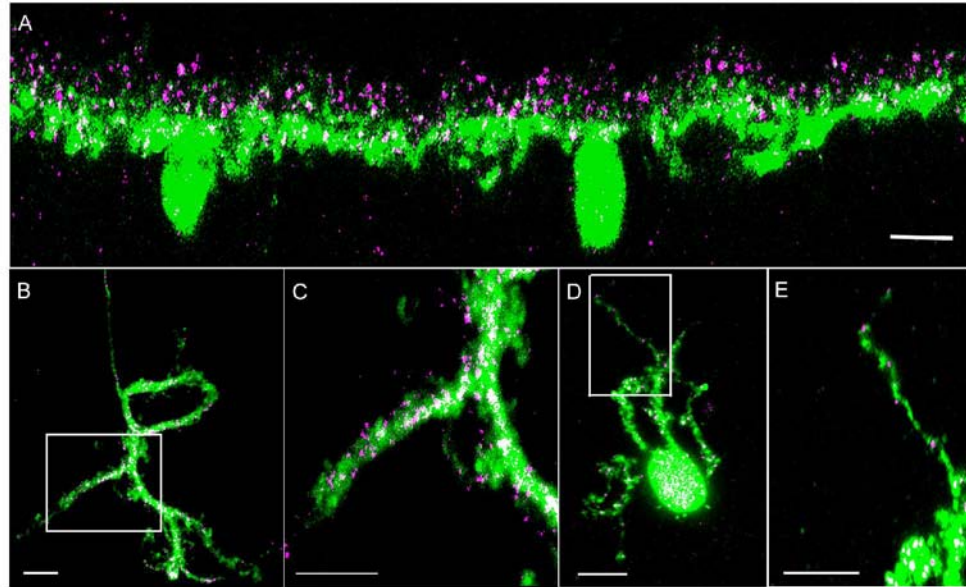
172x105mm (300 x 300 DPI)

Figure 2. Localization of Cx57 (magenta) in a retinal section (A), an isolated horizontal cell axon terminal (B) and soma (D) labeled with calbindin (green). Each image comprises a single optical section of 200 nm thickness. C: High magnification of box in B; E: high magnification of box in D. Scale bars A,B,D: 20 μm; C,E: 10 μm.
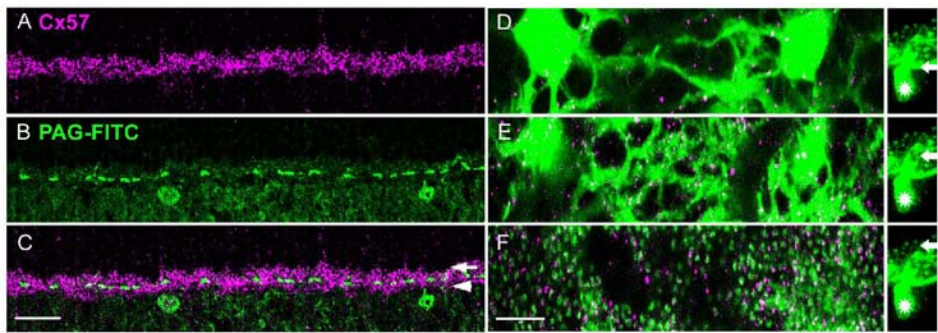172x111mm (300 x 300 DPI)

Figure 3. Distribution of Cx57 within the outer plexiform layer (OPL). A-C: Quantification of Cx57 puncta in the distal and proximal OPL. Image stack of retinal sections labeled for Cx57 (A, magenta) and FITC-conjugated peanut agglutinin (FITC-PAG; B, green). C: Overlay of A and B. There was significantly more Cx57 staining above the PAG-labeled pedicle bases (arrow) than below (arrowhead). D-F: Distribution of Cx57 in three sublayers of the OPL of a calbindin-labeled whole-mounted retina. D: proximal OPL; E: center of the OPL near the photoreceptor terminals; F: distal OPL. Scale bars: A-C: 20 μm; D-F: 10 μm.
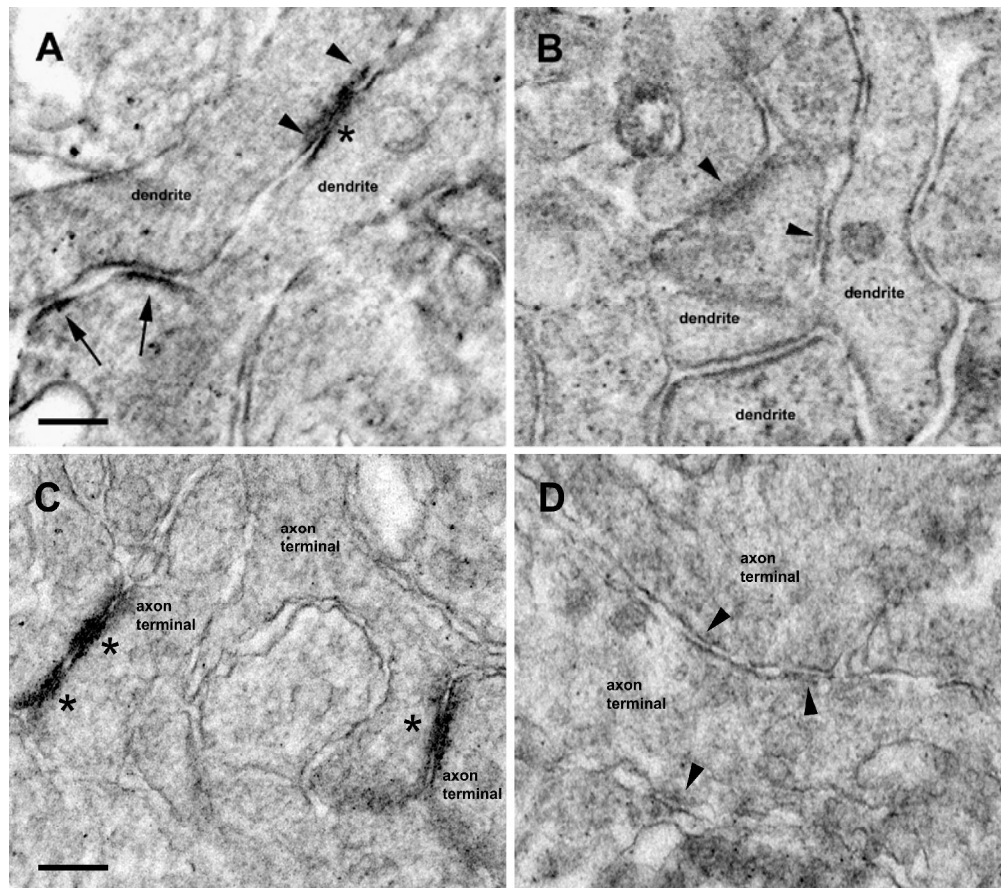172x90mm (300 x 300 DPI)

Figure 4. Cx57 immunoreactivity in gap junctions (asterisks) between horizontal cell dendrites (A) and axon terminal processes (C) in the wild-type retina. Dendritic gap junctions were flanked with zonula adherens (arrowheads), which also displayed Cx57 immunoreactivity. Several Cx57-positive regions were observed which did not resemble the characteristic septalaminar ultrastructure of gap junctions (arrows in A). In Cx57-deficient retinas, membranes of horizontal cell dendrites (B) and axon terminals (D) narrowed at some regions along the processes (arrowheads), but did not exhibit the characteristic structure of gap junctions, and were not labeled by Cx57 antibodies. Scale bars: 100 nm.
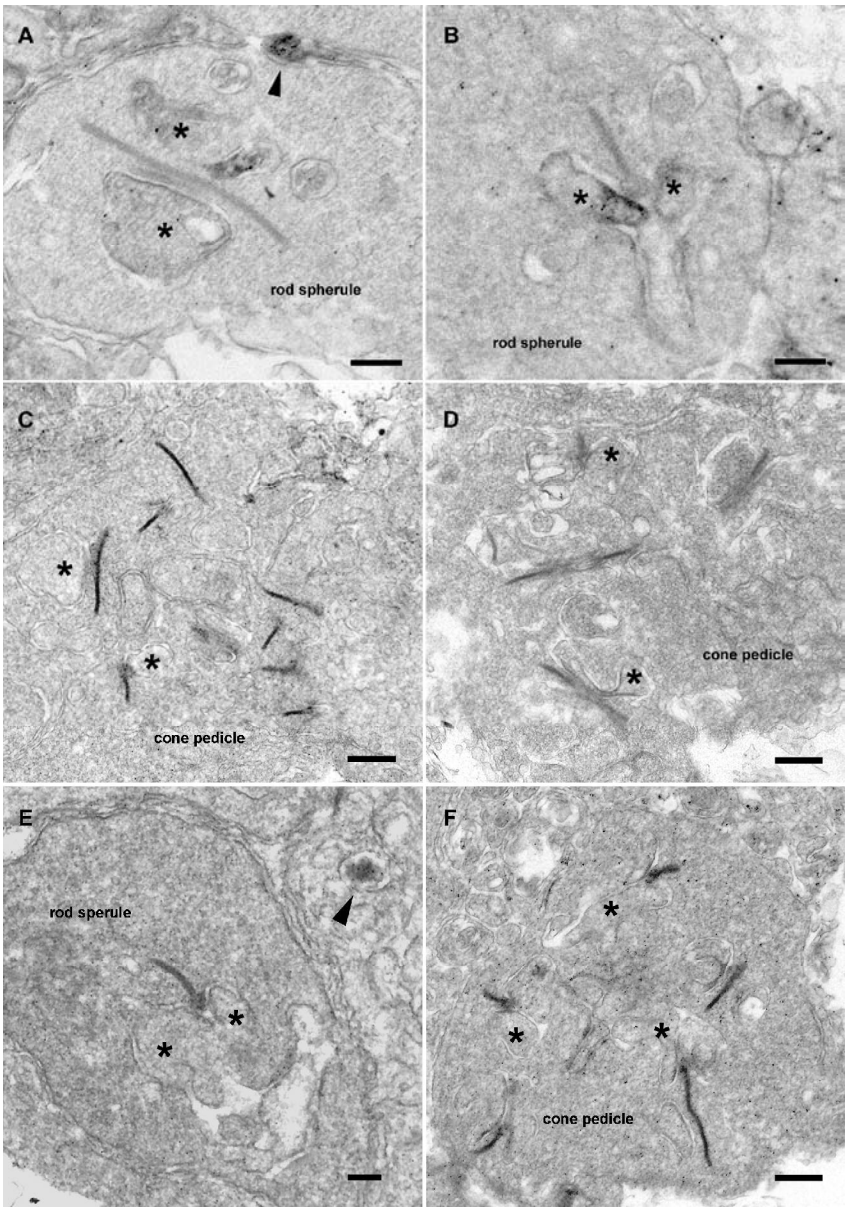154x137mm (600 x 600 DPI)

Figure 5. No Cx57 immunoreactivity was seen within rod spherules (A, B) or cone pedicles (C, D) of wild-type (A, C) or Cx57-deficient mice (B, D). Diffuse, non-specific cytoplasmic staining was detected occasionally within a few of the profiles flanking the photoreceptor terminals (arrowhead in A, E). E, F: Rod spherule and cone pedicle from a wild-type retina without primary Cx57 antibody. Asterisks indicate invaginating horizontal cell processes. Scale bars: A, B, E: 250 nm; C, D, F: 500 nm.
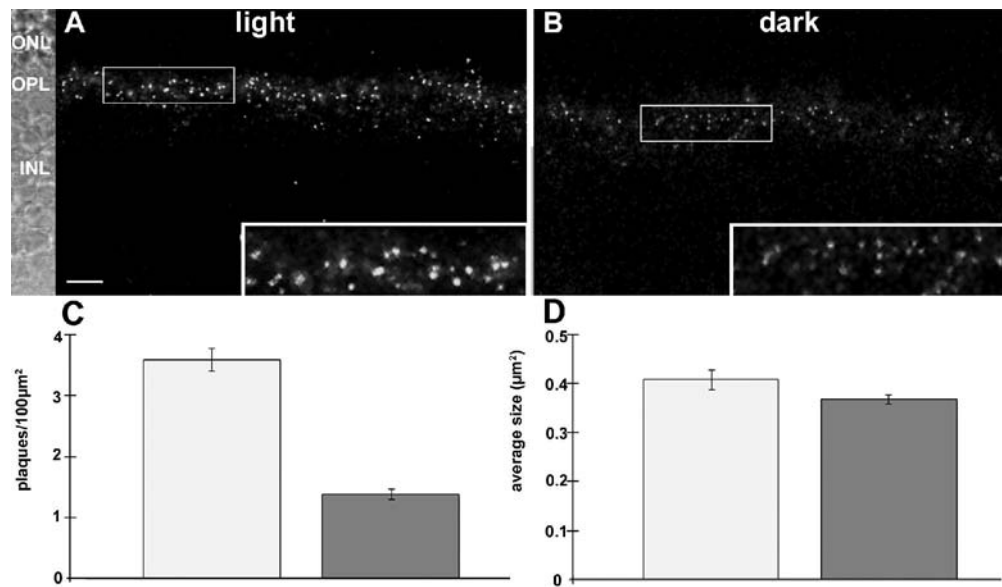160x228mm (300 x 300 DPI)

Figure 6. Cx57 immunoreactivity pattern is modulated by ambient light. Image stacks of light- (A) and dark-adapted (B) retinal sections labeled with Cx57 antibodies. Insets: high magnification of boxed regions in A and B. Scale bar: 5 μm. C: Light adaptation resulted in a significant increase in the number of Cx57-immunoreactive plaques in the OPL (light-adapted: 3.59 ± 0.19 plaques/100 μm2; dark-adapted: 1.46 ± 0.08 ; mean ± S.E. ; n = 4 retinas per condition; p < 0.001; t-test). D: No significant difference in plaque size was found (light-adapted: 0.41± 0.02 μm2; dark-adapted: 0.37 ± 0.01 μm2; mean ± S.E.; n = 4 retinas per condition; p > 0.1).
172x102mm (300 x 300 DPI)

8. Literature

- Abdel-Majid RM, Archibald ML, Tremblay F, and Baldridge WH. 2005. Tracer coupling of neurons in the rat retina inner nuclear layer labeled by Fluorogold. Brain Res. 1063:114-120.

- Aboelela SW, and Robinson DW. 2004. Physiological response properties of displaced amacrine cells of the adult ferret retina. Vis. Neurosci. 21:135-144.

- Abreu M, Kicliter E, and Lugo-Garcia N. 1993. Displaced amacrine cells in the ganglion cell layer of the ground squirrel retina. P. R. Health Sci J 12:137-41.

- Ackert JM, Wu SH, Lee JC, Abrams J, Hu EH, Perlman I, and Bloomfield SA. 2006. Light-induced changes in spike synchronization between coupled ON direction selective ganglion cells in the mammalian retina. J. Neurosci. 26:4206-4215.

- Badea TC, Wang Y, and Nathans J. 2003. A noninvasive genetic/pharmacologic strategy for visualizing cell morphology and clonal relationships in the mouse. J. Neurosci. 23:2314-22.

- Badea TC, and Nathans J. 2004. Quantitative analysis of neuronal morphologies in the mouse retina visualized by using a genetically directed reporter. J. Comp. Neurol. 480:331-51.

- Bailes HF, Trezise AEO, and Collin SP. 2006. The number, morphology, and distribution of retinal ganglion cells and optic axons in the Australian lungfish Neoceratodus forsteri (Krefft 1870). Vis. Neurosci. 23:257-273.

- Baldridge WH, and Ball AK. 1991. Background illumination reduces horizontal cell receptive-field size in both normal and 6-hydroxydopamine-lesioned goldfish retinas. Vis. Neurosci. 7:441-450.

- Baylor DA, Fuortes MGF and O'Bryan PM (1971) Receptive fields of cones in the retina of the turtle. J. Physiol. 214:265-294.

- Benedetti EL and Emmelot P. 1965. Electron microscopic observations on negatively stained plasma membranes isolated from rat liver. J. Cell. Biol. 26: 299–305.

- Bennett MV, Barrio LC, Bargiello TA, Spray DC, Hertzberg E, and Sáez JC. 1991. Gap junctions: new tools, new answers, new questions. Neuron 6: 305–320.

- Biel M, Seeliger M, Pfeifer A, Kohler K, Gerstner A, Ludwig A, Jaissle G, Fauser S,

- Zrenner E, Hofmann F. 1999. Selective loss of cone function in mice lacking the cyclic nucleotide-gated channel CNG3. PNAS 96:7553-7557.

- Bloomfield SA and Miller RF. 1982. A physiological and morphological study of the horizontal cell types of the rabbit retina. J. Comp. Neurol. 208:288-303.

- Bloomfield SA. 1994. Orientation-sensitive amacrine and ganglion cells in the rabbit retina. J. Neurophysiol. 71:1672-91.

- Bloomfield SA, and Dacheux RF. 2001. Rod vision: pathways and processing in the mammalian retina. Prog. Retin. Eye Res. 20:351-84.

- Boassa D, Ambrosi C, Qiu F, Dahl G, Gaietta G, and Sosinsky G. 2007. Pannexin1 channels contain a glycosylation site that targets the hexamer to the plasma membrane. J. Biol. Chem. 282:31733-43.

- Boycott BB, Wässle H. 1974. The morphological types of ganglion cells of the domestic cat's retina. J. Physiol. 240:397-419.

- Bruzzone R, White TW, and Paul DL. 1996. Connections with connexins: the molecular basis of direct intercellular signaling. Eur. J. Biochem. 238:1-27.

- Bunt, A.H. (1976) Ramification patterns of ganglion cells dendrites in the retina of the albino rat. Brain Res., 103, 1-8.

- Cajal, SR. 1893. Lá rétine des vertebras. La Cellule 9:17-257

- Chavez AE, Singer JH, and Diamond JS. 2006. Fast neurotransmitter release triggered by Ca influx through AMPA-type glutamate receptors. Nature 443:705-8.

- Ciolofan C, Lynn BD, Wellershaus K, Willecke K, and Nagi JI. 2007. Spatial relationships of connexin36, connexin57 and zonula occludens-1 in the outer plexiform layer of mouse retina. Neuroscience 148:473-488.

- Coombs J, van der List D, Wang GY, and Chalupa LM. 2006. Morphological properties of mouse retinal ganglion cells. Neuroscience 140:123-36.

- Curcio CA, and Allen KA. 1990. Topography of ganglion cells in human retina. J. Comp. Neurol. 300:5-25.

- Dacey DM. 1990. The dopaminergic amacrine cell. J. Comp. Neurol. 301:461-89.

- Deans, M.R., Volgyi, B., Goodenough, D.A., Bloomfield, S.A., and Paul, D.L. 2002. Connexin36 is essential for transmission of rod-mediated visual signals in the mammalian retina. Neuron, 36, 703-12.

- Dedek, K., Schultz, K., Pieper, M., Dirks, P., Maxeiner, S., Willecke, K., Weiler, R. & Janssen-Bienhold, U. (2006) Localization of heterotypic gap junctions composed of connexin45 and connexin36 in the rod pathway of the mouse retina. Eur. J. Neurosci., 24, 1675-86.

- Degen J, Meier C, van der Giessen RS, Söhl G, Petrasch-Parwez E, Urschel S, Dermietzel R, Schilling K, de Zeeuw CI, and Willecke K. 2004 Expression pattern of lacZ reporter gene representing connexin36 in transgenic mice. J. Comp. Neurol. 473:511-525.

- DeVries SH, Schwarz EA. 1989. Modulation of an electrical synapse between solitary pairs of catfish horizontal cells by dopamine and second messengers. J. Physiol. 414:351-375.

- Dick O, tom Dieck S, Altrock WD, Ammermüller J, Weiler R, Garner CC, Gündelfinger ED and Brandstätter JH. 2003. The presynaptic active zone protein bassoon is essential for photoreceptor ribbon synapse formation in the retina. Neuron 37:775-786.

- Dong CJ, and Hare WA. 2003. Temporal modulation of scotopic visual signals by A17 amacrine cells in mammalian retina in vivo. J. Neurophysiol. 89:2159-66.

- Dreher B, Sefton AJ, Ni SY and Nisbett G. 1985. The morphology, number, distribution, and central projections of Class I retinal ganglion cells in albino and hooded rats. Brain behavior and Evolution 26:10-48

- Dvoriantchikova G, Ivanov D, Panchin Y, and Shestopalov VI. 2006. Expression of pannexin family of proteins in the retina. FEBS Lett. 580:2178-82.

- Ehinger B, and Florén I. 1976. Indoleamine-accumulating neurons in the retina of rabbit, cat and goldfish. Cell Tissue Res. 175:37-48.

- Ehrlich D, and Morgan IG. 1980. Kainic acid destroys displaced amacrine cells in post-hatch chicken retina. Neurosci. Lett. 17:43-8.

- Euler T, Detwiler PB, and Denk W. 2002. Directionally selective calcium signals in dendrites of starburst amacrine cells. Nature 418:845-52.

- Evans WH and Martin PE. 2002. Gap junctions: structure and function. Mol. Membr. Biol. 19: 121–136.

- Famiglietti EV. 1981. Displaced amacrine cells of the retina. Soc. Neurosci. Abstr. 7:620.

- Famiglietti EV. 1992a. Polyaxonal amacrine cells of rabbit retina: morphology and stratification of PA1 cells. J. Comp. Neurol. 316:391-405.

- Famiglietti EV. 1992b. Polyaxonal amacrine cells of rabbit retina: PA2, PA3, and PA4 cells. Light and electron microscopic studies with a functional interpretation. J. Comp. Neurol. 316:422-46.

- Famiglietti EV. 1992c. Dendritic co-stratification of ON and ON-OFF directionally selective ganglion cells with starburst amacrine cells in rabbit retina. J. Comp. Neurol. 324:322-35.

- Feigenspan, A., Teubner, B., Willecke, K., and Weiler, R. 2001. Expression of neuronal connexin36 in AII amacrine cells of the mammalian retina. J. Neurosci., 21, 230-9.

- Feigenspan, A., Janssen-Bienhold, U., Hormuzdi, S., Monyer, H., Degen, J., Sohl, G., Willecke, K., Ammermüller, J., and Weiler, R. 2004. Expression of connexin36 in cone pedicles and OFF-cone bipolar cells of the mouse retina. J. Neurosci., 24, 3325-34.

- Feng G, Mellor RH, Bernstein M, Keller-Peck C, Nguyen QT, Wallace M, Nerbonne JM, Lichtman, JW, and Sanes JR. 2000. Imaging neuronal subsets in transgenic mice expressing multiple spectral variants of GFP. Neuron 28:41-51.

- Fletcher EL, and Wässle H. 1999. Indoleamine-accumulating amacrine cells are presynaptic to rod bipolar cells through GABA(C) receptors. J. Comp. Neurol. 413:155–167.

- Freed MA, Smith RG, and Sterling P. 1987. Rod bipolar array in the cat retina: pattern of input from rods and GABA-accumulating amacrine cells. J. Comp. Neurol. 266:445-55.

- Frumkes and Eysteinsson.1987. Suppressive rod-cone interaction in distal vertebrate retina: intracellular records from Xenopus and Necturus. J. Neurophysiol. 57:1361-1382.

- Gallego A. 1971. Horizontal and amacrine cells in the mammal's retina. Vis. Res. Suppl. 3:33-50.

- Gavrikov KE, Nilson JE, Dmitriev AV, Zucker CL, and Mangel SC. 2006. Dendritic compartmentalization of chloride cotransporters underlies directional responses of starburst amacrine cells in retina. PNAS 103:18793-8.

- Goodenough DA, Goliger JA, and Paul DL. 1996. Connexins, connexons, and intercellular communication. Annu. Rev. Biochem. 65:475-502.

- Goodenough, D. A., Paul D. L., and Jesaitis, L. 1998. Topological distribution of two connexin32 antigenic sites in intact and split rodent hepatocyte gap junctions. J. Cell Biol. 107: 1817-1824

- Ghosh KK, Bujan S, Haverkamp S, Feigenspan A, and Wässle H. 2004. Types of bipolar cells in the mouse retina. J. Comp. Neurol. 469:70-82.

- Grünert U, and Martin PR. 1991. Rod bipolar cells in the macaque monkey retina: immunoreactivity and connectivity. J. Neurosci. 11:2742-58.

- Güldenagel, M., Ammermüller, J., Feigenspan, A., Teubner, B., Degen, J., Söhl, G., Willecke, K., & Weiler, R. 2001. Visual transmission deficits in mice with targeted disruption of the gap junction gene connexin36. J. Neurosci., 21, 6036-44.

- Gustincich S, Feigenspan A, Wu DK, Koopman LJ, and Raviola E. 1997. Control of dopamine release in the retina: a transgenic approach to neural networks. Neuron 18:723-36.

- Hack I, and Peichl L. 1999. Horizontal cells of the rabbit retina are non-selectively connected to the cones. Eur. J. Neurosci. 11:2261-2274.

- Hampson, E.C., Vaney, D.I., & Weiler, R. 1992. Dopaminergic modulation of gap junction permeability between amacrine cells in mammalian retina. J. Neurosci., 12, 4911-22.

- Han, Y., and Massey, S.C. 2005. Electrical synapses in retinal ON cone bipolar cells: Subtype-specific expression of connexins. PNAS, 102, 13313-18.

- Haverkamp S. Wässle H. 2000. Immunocytochemical analysis of the mouse retina. J. Comp. Neurol. 424:1-23.

- Haverkamp S, Grünert U, Wässle H. 2001. The synaptic architecture of AMPA receptors at the cone pedicle of the primate retina. J. Neurosci. 21:2488-2500.

- Haverkamp S, Michalakis S, Claes E, Seeliger MW, Humphries P, Biel M and Feigenspan A. 2006. Synaptic plasticity in CNGA3(-/-) mice: cone bipolar cells react on the missing cone input and form ectopic synapses with rods. J Neurosci 26:5248-5255.

- He, S., Weiler, R., and Vaney, D.I. 2000. Endogenous dopaminergic regulation of horizontal cell coupling in the mammalian retina. J. Comp. Neurol., 418, 33-40.

- Herzberg, E. L., Disher, R. M., Tiller, A. A., Zhou, Y. and Cook, R. G. 1988. Topology of the Mr 27,000 liver gap junction protein. Cytoplasmic localization of amino- and carboxyl termini and a hydrophilic domain which is protease-hypersensitive. J. Biol. Chem. 263:19105-19111

- Hombach, S., Janssen-Bienhold, U., Söhl, G., Schubert, T., Büssow, H., Ott, T., Weiler, R., and Willecke K. 2004. Functional expression of connexin57 in horizontal cells of the mouse retina. Eur. J. Neurosci., 19, 2633-40.

- Hu EH, and Bloomfield SA. 2003. Gap junctional coupling underlies the short-latency spike synchrony of retinal alpha ganglion cells. J. Neurosci. 23:6768-77.

- Hughes A, and Vaney DI. 1980. Coronate cells: the displaced amacrine cells of the rabbit retina? J. Comp. Neurol. 189:169-89.

- Hughes A, and Wieniawa-Narkiewicz E. 1980. A large, newly identified population of presumptive microneurons in the ganglion cell layer of the cat retina. Nature 284:468-70.

- Huxlin, K.R., and Goodchild, A.K. 1997. Retinal ganglion cells in the albino rat: revised morphological classification. J. Comp. Neurol., 385, 309-23.

- Jaissle G, May A, Reinhard J, Kohler K, Fauser S, Lütjen-Drecoll E, Zrenner E, and Seeliger M. 2001. Evaluation of the rhodopsin knockout mouse as a model of pure cone function. IOVS 42:506-513.

- Janssen-Bienhold U, Schultz K, Gellhaus A, Schmidt P, Ammermüller J, and Weiler R. 2001. Identification and localization of connexin26 within the photoreceptor-horizontal cell synaptic complex. Vis. Neurosci. 18:169-178.

- Jeon CJ, Strettoi E, and Masland RH. 1998. The major cell populations of the mouse retina. J Neurosci 18:8936-46.

- Kamermans M, and Spekreijse H. 1999. The feedback pathway from horizontal cells to cones: A mini review with a look ahead. Vision Res. 39:2449-2468.

- Kamermans M, Fahrenfort I, Schultz K, Janssen-Bienhold U, Sjoerdsma T, and Weiler R.2001. Hemichannel-mediated inhibition in the outer retina. Science 292:1178-1180.

- Kamermans M, and Fahrenfort I. 2004. Ephaptic interactions within a chemical synapse:hemichannel-mediated ephaptic inhibition in the retina. Curr. Opin. Neurobiol. 14:531-541.

- Kamermans M. 2007. Retinal horizontal cell-specific promoter activity and protein expression of zebrafish connexin 52.6 and connexin 55.5. J. Comp. Neurol. 501:765-779.

- Kao Y-H, and Sterling P. 2003. Matching neural morphology to molecular expression: Single cell injection following immunostaining. J. Neurocytol. 32:245-51.

- Kao Y-H, and Sterling P. 2006. Displaced GAD65 amacrine cells of the guinea pig retina are morphologically diverse. Vis. Neurosci. 23:931-9.

- Kihara AH, de Castro LM, Moriscot AS, Hamassaki DE. 2006. Prolonged dark adaptation changes connexin expression in the mouse retina. J. Neurosci. Res. 83:1331-1341.

- Kim, IB., Lee MY, OH SJ, Kim KY, and Chun MH. 1998. Double-labeling techniques demonstrate that rod bipolar cells are under GABAergic control in the inner plexiform layer of the rat retina. Cell Tissue Res. 292: 17–25.

- Knabe W, Washausen S, Happel N, and Kuhn H-J. 2007. Development of starburst cholinergic amacrine cells in the retina of Tupaia belangeri. J. Comp. Neurol. 502:584-97.

- Kolb H. 1970. Organization of the outer plexiform layer of the primate retina: electron microscopy of golgi-impregnated cells. Phil. Trans. R. Soc. Lon. B. Biol. Sci. 258:58261-58283.

- Kolb H, and Famiglietti EV. 1974. Rod and cone pathways in the inner plexiform layer of cat retina. Science 186: 47-9.

- Kolb H. 1974. The connections between horizontal cells and photoreceptors in the retina of the cat: electron microscopy of Golgi preparations. J. Comp. Neurol. 155:1-14.

- Kolb H. 1977. The organization of the outer plexiform layer in the retina of the cat: electron microscopic observations. J. Neurocytol. 6:131-153.

- Kolb H, Nelson R, and Mariani A. 1981. Amacrine cells, bipolar cells and ganglion cells of the cat retina: A Golgi study. Vision Res. 21:1081-1114.

- Kolb H. 1982. The morphology of the bipolar cells, amacrine cells and ganglion cells in the retina of the turtle Pseudemys scripta elegans. Phil. Trans. R. Soc. Lond. Biol. Sci. 298:355-93.

- Kolb H, and Jones J. 1984. Synaptic organization of the outer plexiform layer of the turtle retina: an electron microscope study of serial sections. J. Neurocytol. 13:567-591.

- Kolb H. 2003. How the retina works. American Scientist, volume 91.

- Koontz MA, Hendrickson AE, and Ryan MK. 1989. GABA-immunoreactive synaptic plexus in the nerve fiber layer of primate retina. Vis. Neurosci. 2:19-25.

- Koontz MA. 1993. GABA-immunoreactive profiles provide synaptic input to the soma, axon hillock, and axon initial segment of ganglion cells in primate retina. Vis. Res. 33:2629-36.

- Kreuzberg, M.M., Söhl, G., Kim, JS., Verselis, VK., Willecke, K., and Bukauskas, F.F. 2005. Functional properties of mouse connexin30.2 expressed in the conduction system of the heart. Circ. Res., 96, 1169-77.

- Kreuzberg, M.M., Schrickel, J.W., Ghanem, A., Kim, J.S., Degen, J., Janssen-Bienhold, U., Lewalter, T., Tiemann, K., and Willecke, K. 2006. Connexin30.2 containing gap junction channels decelerate impulse propagation through the atrioventricular node. Proc. Natl. Acad. Sci. U S A., 103, 5959-64.

- Kreuzberg, M.M., Deuchars, J., Weiss, E., Schober, A., Sonntag, S., Wellershaus, K., Draguhn, A., and Willecke, K. 2008. Expression of connexin30.2 in interneurons of the central nervous system in the mouse. Mol. Cell. Neurosci., 37, 119-34.

- Kong, J.H., Fish, D.R., Rockhill, R.L., and Masland R.H. 2005. Diversity of ganglion cells in the mouse retina: unsupervised morphological classification and its limits. J. Comp. Neurol., 489, 293–310.

- Kwak, BR., Hermans, M.M., De Jonge, H.R., Lohmann, S.M., Jongsma, H.J., and Chanson, M. 1995. Differential regulation of distinct types of gap junction channels by similar phosphorylating conditions. Mol. Biol. Cell., 6, 1707-19.

- Laemmli UK. 1970. Cleavage of structural proteins during assembly of the head of bacteriophage T4. Nature 227:680-685.

- Laird, D. W. and Revel, J. P.1990. Biochemical and immunochemical analysis of the arrangement of connexin 43 in rat heart gap junction membranes. J. Cell Sci. 97: 109-117

- Laird DW. 2006. Life cycle of connexins in health and disease. Biochem. J. 394, 527–543.

- Lampe, P.D. 1994. Analyzing phorbol ester effects on gap junctional communication: a dramatic inhibition of assembly. J. Cell. Biol., 127, 1895-905.

- Lasansky A (1972) Cell junctions at the outer synaptic layer of the retina. IOVS 11:265-75.

- Lee, E.J., Han, J.W., Kim, H.J., Kim, I.B., Lee, M.Y., Oh, S.J., Chung, J.W., and Chun, M.H. 2003. The immunocytochemical localization of connexin 36 at rod and cone gap junctions in the guinea pig retina. Eur. J. Neurosci., 18, 2925-34.

- Lee EJ, Mann LB, Rickman DW, Lim EJ, Chun MH, and Grzywacz NM. 2006. AII amacrine cells in the distal inner nuclear layer of the mouse retina. J. Comp. Neurol. 494:651-62.

- Li W, Zhang J, and Massey SC. 2002. Coupling pattern of S1 and S2 amacrine cells in the rabbit retina. Vis. Neurosci. 19(2):119-31.

- Lima SM, Ahnelt PK, Carvahlo TO, Silveira JS, Rocha FA, Saito CA, and Silveira LC. 2005. Horizontal cells in the retina of a diurnal rodent, the agouti (Dasyprocta aguti). Vis. Neurosci. 22:707-720.

- Lin, B., Jakobs, T.C., and Masland, R.H. 2005. Different functional types of bipolar cells use different gap-junctional proteins. J. Neurosci., 25, 6696-701.

- Lin B, and Masland RH. 2006. Populations of wide-field amacrine cells in the mouse retina. J. Comp. Neurol. 499:797-809.

- Linberg KA, Suemune S, and Fisher SK. 1996. Retinal neurons of the California ground squirrel, Spermophilus beecheyi: a Golgi study. J. Comp. Neurol. 365:173-216

- Linden R, and Esbérard CE. 1987. Displaced amacrine cells in the ganglion cell layer of the hamster retina. Vision Res. 27:1071-6.

- Lu C, and McMahon DG. 1997. Modulation of hybrid bass retinal gap junctional channel gating by nitric oxide. J. Physiol. 499:689-699.

- Lyubarsky AL, Falsini B, Pennesi ME, Valentini P and Pugh Jr EN. 1999. UV- and midwave-sensitive cone-driven retinal responses of the mouse: a possible phenotype for coexpression of cone photopigments. J. Neurosci. 19:442-455.

- MacNeil MA, and Masland RH. 1998. Extreme diversity among amacrine cells: implications for function. Neuron 20:971-82.

- MacNeil MA, Heussy JK, Dacheux RF, Raviola E, and Masland RH. 1999. The shapes and numbers of amacrine cells: matching of photofilled with Golgi-stained cells in the rabbit retina and comparison with other mammalian species. J. Comp. Neurol. 413:305-26.

- Majumdar S, Heinze L, Haverkamp S, Ivanova E, and Wässle H. 2007. Glycine receptors of A-type ganglion cells of the mouse retina. Vis. Neurosci. 24:471-87.

- Mangel SC, and Dowling JE. 1985. Responsiveness and receptive field size of carp horizontal cells are reduced by prolonged darkness and dopamine. Science 229:1107-1109.

- Manthey D, Bukauskas F, Lee CG Kozak CA, Willecke K. 1999. Molecular cloning and functional expression of the mouse gap junction gene connexin-57 in human HeLa cells. J. Biol. Chem. 274:14716-14723.

- Marc RE, Murry RF, and Basinger SF. 1995. Pattern recognition of amino acid signatures in retinal neurons. J. Neurosci. 15:5106-29.

- Martin PR. 1986. The projection of different retinal ganglion cell classes to the dorsal lateral geniculate nucleus in the hooded rat. Experimental brain research 62: 77-88

- Masland RH, and Tauchi M. 1986. The cholinergic amacrine cell. TINS 9:218-223.

- Masland RH. 1988. Amacrine cells. TINS 11:405-410.

- Masland RH. 2001. The fundamental plan of the retina. Nature Neurosci. 4:877-86.

- Massey SC, and Redburn DA. 1987. Transmitter circuits in the vertebrate retina. Prog. Neurobiol. 28:55-96.

- Massey SC, Mills SL, and Marc RE. 1992. All indoleamine-accumulating cells in the rabbit retina contain GABA. J. Comp. Neurol. 322:275-91.

- Mastronarde DN. 1983a. Correlated firing of cat retinal ganglion cells. I. Spontaneously active inputs to X- and Y-cells. J. Neurophysiol. 49:303-24.

- Mastronarde DN. 1983b. Correlated firing of cat retinal ganglion cells. II. Responses of X- and Y-cells to single quantal events. J. Neurophysiol. 49:325-49.

- Mastronarde DN. 1983c. Interactions between ganglion cells in cat retina. J. Neurophysiol. 49:350-65.

- Masu M, Iwakabe H, Tagawa Y, Miyoshi T, Yamashita M, Fukuda Y, Sasaki H, Hiroi K, Nakamura Y, Shigemoto R, Takada M, Nakamura K, Nakao K, Katsuki M, and Nakanishi S. 1995. Specific deficit of the ON response in visual transmission by targeted disruption of the mGluR6 gene. Cell 80: 757-765.

- Matesic, D., Tillen, T., and Sitaramayya, A. 2003. Cx40 expression in bovine and rat retinae. Cell. Biol. Int., 27, 89-99.

- Maxeiner S, Dedek K, Janssen-Bienhold U, Ammermüller J, Brune H, Kirsch T, Pieper M, Degen J, Kruger O, Willecke K, and Weiler R. 2005. Deletion of connexin45 in mouse retinal neurons disrupts the rod/cone signaling pathway between AII amacrine and ON cone bipolar cells and leads to impaired visual transmission. J. Neurosci. 25:566-76.

- Menger N, Pow DV, and Wässle H. 1998. Glycinergic amacrine cells of the rat retina. J. Comp. Neurol. 401:34-46.

- Menger N, and Wässle H. 2000. Morphological and physiological properties of the A17 amacrine cell of the rat retina. Vis. Neurosci. 17:769-80.

- Milks, L. C., Kumar, N. M., Houghten, R., Unwin, N. and Gilula, N. B .1988. Topology of the 32-kd liver gap junction protein determined by site-directed antibody localizations. EMBO J. 7: 2967-2975

- Mills, S.L., O'Brien, J.J., Li, W., O'Brien, J., and Massey, S.C. 2001. Rod pathways in the mammalian retina use connexin 36. J. Comp. Neurol., 436, 336-50.

- Moreno, A.P., and Lau, A.F. 2007. Gap junction channel gating modulated through protein phosphorylation. Prog. Biophys. Mol. Biol., 94, 107-19

- Nelson R, Lützow AV, Kolb H, and Gouras P (1975) Horizontal cells in cat retina with independent dendritic systems. Science 189:137-139.

- Nelson R, and Kolb H. 1985. A17: a broad-field amacrine cell in the rod system of the cat retina. J. Neurophysiol. 54:592-614.

- Nielsen PA, Beahm DL, Giepmans BN, Baruch A, Hall JE, and Kumar NM. 2002. J. Biol. Chem. 277:38272-83.

- Nielsen PA, and Kumar NM. 2003. Differences in expression patterns between mouse connexin-30.2 (Cx30.2) and its putative human orthologue, connexin-31.9. FEBS Lett. 540: 151-6.

- Niemeyer G and Gouras P (1973) Rod and cone signals in S-potentials of the isolated perfused cat eye. Vision Res. 13:1603-1612.

- Nirenberg, S., and Cepko, C. 1993. Targeted ablation of diverse cell classes in the nervous system in vivo. J. Neurosci., 13, 3238-51.

- Nirenberg, S., & Meister, M. 1997. The light response of retinal ganglion cells is truncated by a displaced amacrine circuit. Neuron, 18, 637-50.

- O'Brien, J.J., Li, W., Pan, F., Keung, J., O'Brien, J., & Massey, S.C. (2006) Coupling between A-type horizontal cells is mediated by connexin 50 gap junctions in the rabbit retina. J. Neurosci., 26, 11624-36.

- Ölveczky BP, Baccus SA, and Meister M. 2003. Segregation of object and background motion in the retina. Nature 423:401-8.

- Panchin YV. 2005. Evolution of gap junction proteins--the pannexin alternative. J. Exp. Biol. 208:1415-9.

- Pang JJ, Gao F, and Wu SM. 2003. Light-evoked excitatory and inhibitory synaptic inputs to ON and OFF alpha ganglion cells in the mouse retina. J. Neurosci. 23:6063-73.

- Peichl L, and Wässle H. 1981. Morphological identification of on- and off-centre brisk transient (Y) cells in the cat retina. Proc. R. Soc. Lond. B. Biol. Sci. 212:139-53.

- Peichl L, Buhl EH, and Boycott BB. 1987. Alpha ganglion cells in the rabbit retina. J. Comp. Neurol. 263:25-41.

- Peichl L. 1989. Alpha and delta ganglion cells in the rat retina. J. Comp. Neurol. 286: 120-139.

- Peichl L, and Gonzalez-Soriano J. 1994. Morphological types of horizontal cell in rodent retinae: a comparison of rat, mouse, gerbil, and guinea pig. Vis. Neurosci. 11:501-517.

- Penuela S, Bhalla R, Gong XQ, Cowan KN, Celetti SJ, Cowan BJ, Bai D, Shao Q, and Laird DW. 2007. Pannexin 1 and pannexin 3 are glycoproteins that exhibit many distinct characteristics from the connexin family of gap junction proteins. J. Cell. Sci. 120:3772-83.

- Pérez de Sevilla Müller L, Shelley J, and Weiler R . 2007. Displaced amacrine cells of the mouse retina. J. Comp. Neurol. 505:177-189

- Perez MT, Larsson B, Alm P, Andersson KE, and Ehinger B. 1995. Localisation of neuronal nitric oxide synthase-immunoreactivity in rat and rabbit retinas. Exp. Brain Res. 104:207-17.

- Perry VH. 1979. The ganglion cell layer of the retina of the rat: A Golgi study. Proceedings of the royal society B. 204:363-375

- Perry VH, and Walker M. 1980. Amacrine cells, displaced amacrine cells and interplexiform cells in the retina of the rat. Proc R Soc Lond. Biol. Sci. 208: 415-31.

- Perlman I,and Ammermüller J. 1994. Receptive-field size of L1 horizontal cells in the turtle retina: effects of dopamine and background light. J. Neurophysiol. 72:2786-2795.

- Petit-Jacques J, Völgyi B, Rudy B, and Bloomfield S. 2005. Spontaneous oscillatory activity of starburst amacrine cells in the mouse retina. J. Neurophysiol. 94:1770-1780.

- Pinto LH, Invergo B, Shimomura K, Takahashi JS and Troy JB (2007) Interpretation of the mouse electroretinogram. Doc. Ophthalmol. ISSN: 1573-2622

- Pottek M, Schultz K, and Weiler R. 1997. Effects of nitric oxide on the horizontal cell network and dopamine release in the carp retina. Vision Res. 37:1091-1102.

- Pottek M, and Weiler R. 2000. Light-adaptive effects of retinoic acid on receptive field properties of retinal horizontal cells. Eur. J. Neurosci. 12:437-445.

- Pow DV, Wright LL and Vaney DI. 1995. The immunocytochemical detection of amino-acid neurotransmitters in paraformaldehyde-fixed tissues. J. Neurosci. Methods 56:115-23.

- Pow DV, and Hendrickson AE. 1999. Distribution of the glycine transporter glyt-1 in mammalian and nonmammalian retinae. Vis. Neurosci. 16:231-9.

- Pourcho RG, and Goebel DJ. 1985. A combined Golgi and autoradiographic study of (3H)glycine-accumulating amacrine cells in the cat retina. J. Comp. Neurol. 233:473-80.

- Pourcho RG, and Owczarzak MT. 1991. Connectivity of glycine immunoreactive amacrine cells in the cat retina. J. Comp. Neurol. 307: 549-61.

- Pourcho RG. 1996. Neurotransmitters in the retina. Curr. Eye Res. 15:797-803.
- Raven MA, Reese BE. 2002. Horizontal cell density and mosaic regularity in pigmented and albino mouse retina. J. Comp. Neurol. 454:168-176.

- Raviola and Gilula. 1973. Gap junctions between photoreceptor cells in the vertebrate retina. PNAS 70:1677-1681.

- Raviola and Gilula. 1975. Intramembrane organization of specialized contacts in the outer plexiform layer of the retina. J. Cell. Biol .65:192-222.

- Raviola E, and Dacheux RF. 1990. Axonless horizontal cells of the rabbit retina: synaptic connections and origin of the rod aftereffect. J. Neurocytol. 19:731-736.

- Ray A, Zoidl G, Weickert S, Wahle P, and Dermietzel R. 2005. Site-specific and developmental expression of pannexin1 in the mouse nervous system. Eur. J. Neurosci. 21:3277-90.

- Reese BE, Raven MA and Stagg SB. 2005. Afferents and homotypic neighbors regulate horizontal cell morphology, connectivity, and retinal coverage. J. Neurosci. 25:2167-2175.

- Revel JP and Karnovsky MJ. Hexagonal array of subunits in intercellular junctions of the mouse heart and liver. J Cell Biol 33: C7–C12, 1967.

- Robertson JD. 1963. The occurrence of a subunit pattern in the unit membranes of the club endings in Mauthner cell synapses in gold- fish brains. J. Cell. Biol. 19: 201–221.

- Rong P, Wang X, Niesman I, Wu Y, Benedetti LE, Dunia I, Levy E, Gong X. 2002. Disruption of Gja8 (W8 connexin) in mice leads to microphthalmia associated with retardation of lens growth and lens fibre maturation. Develop 129:167-174.

- Roska B, and Werblin F. 2003. Rapid global shifts in natural scenes block spiking in specific ganglion cell types. Nat. Neurosci. 6:600-8.

- Sandell JH, and Masland RH. 1986. A system of indoleamine-accumulating neurons in the rabbit retina. J. Neurosci. 6:3331-47.

- Sandell JH, Masland RH, Raviola E, and Dacheaux RF. 1989. Connections of indoleamine-accumulating cell in the rabbit retina. J. Comp. Neurol. 283:303-313.

- Sassoé-Pognetto M, Wässle H, Grünert U. 1994. Glycinergic synapses in the rod pathway of the rat retina: Cone bipolar cells express the _1 subunit of the glycine receptor. J. Neurosci. 14:5131-5146.

- Schubert, T., Degen, J., Willecke, K., Hormuzdi, S.G., Monyer, H., and Weiler, R. 2005a. Connexin36 mediates gap junctional coupling of alpha-ganglion cells in mouse retina. J. Comp. Neurol., 485, 191-201.

- Schubert, T, Maxeiner, S., Kruger, O., Willecke, K., and Weiler, R. 2005b. Connexin45 mediates gap junctional coupling of bistratified ganglion cells in the mouse retina. J. Comp. Neurol., 490, 29-39.

- Schultz K, Janssen-Bienhold U, Dirks P, Shelley J, Hilgen G, Hombach S, Willecke K, and Weiler R. 2007. Localization of Cx57 in dendro-dendritic and axo-axonal gap junctions of mouse horizontal cells. Poster presentation in Göttingen, Meeting of the Germany Neuroscience Society, 2007.

- Shelley, J., Dedek, K., Schubert, T., Feigenspan, A., Schultz, K., Hombach, S., Willecke, K., and Weiler, R. 2006. Horizontal cell receptive fields are reduced in connexin57-deficient mice. Eur. J. Neurosci., 23, 3176-3186.

- Shen W, and Jiang Z. 2007. Characterization of glycinergic synapses in vertebrate retinas. J. Biomed. Sci. 14: 5-13.

- Shestopalov VI, and Panchin Y. 2008. Pannexins and gap junction protein diversity. Cell. Mol. Life Sci. 65:376-94.

- Shields CR, Klooster J, Claassen Y, Ul-Hussain M, Zoidl G, Dermietzel R,Tornqvist K, Yang XL, and Dowling JE. 1988. Modulation of cone horizontal cell activity in the teleost fish retina. III. Effects of prolonged darkness and dopamine on electrical coupling between horizontal cells. J. Neurosci. 8:2279-2288.

- Silveira LC, Yamada ES, and Picanco-Diniz CW. 1989. Displaced horizontal cells and biplexiform horizontal cells in the mammalian retina. Vis. Neurosci. 3:483-488

- Singer JH, and Diamond JS. 2003. Sustained Ca^{2+} entry elicits transient postsynaptic currents at a retinal ribbon synapse. J. Neurosci. 23:10923-33.

- Simpson I, Rose B, and Loewenstein WR. 1977. Size limit of molecules permeating the junctional membrane channels. Science 195, 294-296.

- Smith RG, Freed MA, and Sterling P. 1986. Microcircuitry of the dark-adapted cat retina:functional architecture of the rod-cone network. J. Neurosci. 6:3505-3517.

- Söhl, G., Degen, J., Teubner, B., and Willecke, K. 1998. The murine gap junction gene connexin36 is highly expressed in mouse retina and regulated during brain development. FEBS Lett., 428, 27-31.

- Söhl G, and Willecke K. 2003. An update on connexin genes and their nomenclature in mouse and man. Cell Commun. Adhes. 10:173-80.

- Söhl, G., Maxeiner, S., and Willecke, K. 2005. Expression and functions of neuronal gap junctions. Nat. Rev. Neurosci., 6, 191-200.

- Steinberg RH. 1969a. Rod and cone contributions to s-potentials from the cat retina. ision Res 9:1319-1329.

- Steinberg RH. 1969b. Rod-cone interaction in s-potentials from the cat retina. Vision Res 9:1331-1344.

- Steinberg RH. 1969c. The rod after-effect in s-potentials from the cat retina. Vision Res. 9:1345-1355.

- Steinberg RH, Frishman LJ, and Sieving PA. 1991. Progress in retinal research. Oxford: Pergamon

- Stone J, Makarov F, and Hollander H. 1995. The glial ensheathment of the soma and axon hillock of retinal ganglion cells. Vis. Neurosci. 12:273-9.

- Strettoi E, Dacheux RF, and Raviola E. 1990. Synaptic connections of rod bipolar cells in the inner plexiform layer of the rabbit retina. J. Comp. Neurol. 295: 449–466, 1990.

- Strettoi E, Dacheux RF, Raviola E. 1992. Synaptic connections of rod bipolar cells in the inner plexiform layer of the rabbit retina. J. Comp. Neurol. 295: 449-66.

- Strettoi E, and Masland RH. 1995. The organization of the inner nuclear layer of the rabbit retina. J. Neurosci. 15:875-88.

- Strettoi E, and Masland RH. 1996. The number of unidentified amacrine cells in the mammalian retina. PNAS 93:14906-11.

- Strettoi E, Porciatti V, Falsini B, Pignatelli V and Rossi C. 2002. Morphological and functional abnormalities in the inner retina of the rd/rd mouse. J. Neurosci. 22:5492-5504.

- Sun, W., Li, N., & He, S. (2002a) Large-scale morphological survey of mouse retinal ganglion cells. J. Comp. Neurol., 451, 115–126.

- Sun, W., Li, N., & He, S. (2002b) Large-scale morphological survey of rat retinal ganglion cells. Vis. Neurosci., 19, 483-493.

- Suzuki H and Pinto LH. 1986. Response properties of horizontal cells in the isolated retina of wild-type and pearl mutant mice. J. Neurosci. 6:1122-1128.

- Tauchi M, Morigiwa K, and Fukuda Y.1992. Morphological comparisons between outer and inner ramifying alpha cells of the albino rat retina. Experimental brain research 88: 66-77.

- Taylor WR, and Vaney DI. 2003. New directions in retinal research. TINS 26:379-385.

- Tsukamoto Y, Morigiwa K, Ueda M and Sterling P. 2001. Microcircuits for night vision in mouse retina. J. Neurosci. 21:8616-8623.

- Urschel, S., Höher, T., Schubert, T., Alev, C., Söhl, G., Wörsdörfer, P., Asahara, T., Dermietzel, R., Weiler, R., and Willecke, K. 2006. Protein kinase A-mediated phosphorylation of connexin36 in mouse retina results in decreased gap junctional communication between AII amacrine cells. J. Biol. Chem., 281, 33163-71.

- Vaney DI. 1980. A quantitative comparison between the ganglion cell populations and axonal outflows of the visual streak and periphery of the rabbit retina. J. Comp. Neurol. 189:215-33.

- Vaney DI, Peichi L, and Boycott BB. 1981. Matching populations of amacrine cells in the inner nuclear and ganglion cell layers of the rabbit retina. J. Comp. Neurol. 199:373-91.

- Vaney, DI. 1986. Morphological identification of serotonin-accumulating neurons in the living retina. Science 233:444-6.

- Vaney DI. 1990. The mosaic of amacrine cells in the mammalian retina. Prog. Retinal Res. 9:49-100.

- Vaney, D.I. 1991. Many diverse types of retinal neurons show tracer coupling when injected with biocytin or Neurobiotin. Neurosci. Lett., 125, 187-90.

- Vaney DI. 1994. Pattern of neuronal coupling in the retina. Prog. Retin. Eye Res. 13:301–355.

- Vaney DI, Nelson JC, and Pow DV. 1998. Neurotransmitter coupling through gap junctions in the retina. J. Neurosci. 18: 10594-602.

- Vaney DI, and Pow DV. 2000. The dendritic architecture of the cholinergic plexus in the rabbit retina: selective labeling by glycine accumulation in the presence of sarcosine. J. Comp. Neurol. 421:1-13.

- Veruki ML, and Hartveit E. 2002. Electrical synapses mediate signal transmission in the rod pathway of the mammalian retina. J. Neurosci. 22:10558-66.-

- Verweij J, Dacey DM, Peterson BB and Buck SL .1999. Sensitivity and dynamics of rod signals in H1 horizontal cells of the macaque monkey retina. Vision Res. 39:3662-3672.

- Viney TJ, Balint K, Hillier D, Siegert S, Boldogkoi Z, Enquist LW, Meister M, Cepko CL and Roska B. 2007. Local retinal circuits of melanopsin-containing ganglion cells identified by transsynaptic viral tracing. Curr. Biol. 17:981-988.

- Völgyi B, Xin D, Amarillo Y, and Bloomfield SA. 2001. Morphology and physiology of the polyaxonal amacrine cells in the rabbit retina. J. Comp. Neurol. 440:109-25.

- Völgyi B, Xin D, and Bloomfield SA. 2002. Feedback inhibition in the inner plexiform layer underlies the surround-mediated responses of AII amacrine cells in the mammalian retina. J. Physiol., 539.2, pp. 603–614.

- Völgyi B, Deans MR, Paul DL and Bloomfield SA. 2004. Convergence and segregation of the multiple rod pathways in mammalian retina. J. Neurosci. 24:11182-11192.

- Völgyi, B., Abrams, J., Paul, D.L., and Bloomfield, S.A. 2005. Morphology and tracer coupling pattern of alpha ganglion cells in the mouse retina. J. Comp. Neurol., 492, 66-77.

- Wässle H, Chun MH, and Müller F. 1987a. Amacrine cells in the ganglion cell layer of the cat retina. J. Comp. Neurol. 265:391-408.

- Wässle H, Voigt T, and Patel B. 1987b. Morphological and immunocytochemical identification of indoleamine-accumulating neurons in the cat retina. J. Neurosci. 7:1574-85.

- Wässle H, and Boycott BB. 1991. Functional architecture of the mammalian retina. Physiol. Rev. 71: 447-80.

- Wässle H. 2004. Parallel processing in the mammalian retina. Nat. Rev. Neurosci. 5:747-57.

- Watt CB, Glazebrook PA, and Florack VJ. 1994. Localization of substance P and GABA in retinotectal ganglion cells of the larval tiger salamander. Vis. Neurosci. 11:355-362.

- Weiler R and Zettler F. 1978. The axon-bearing horizontal cells in the teleost retina are functional as well as structural units. Vision Res. 19:1261-1268.

- Weiler W, Schultz K, Pottek M, Tieding S, and Janssen-Bienhold U. 1998. Retinoic acid has light-adaptive effects on horizontal cells in the retina. Proc. Natl. Acad. Sci. USA 95:7139-7144.

- Weiler, R., Pottek, M., He, Su., and Vaney D.I. 2000. Modulation of coupling between retinal horizontal cells by retinoic acid and endogenous dopamine. Brain Res. Rev., 32, 121-9.

- Weng, S., Sun, W., and He, S. 2005. Identification of ON-OFF direction-selective ganglion cells in the mouse retina. J. Physiol., 562, 915-23.

- White TW, Bruzzone R, Goodenough DA, and Paul DL. 1992. Mouse Cx50, a functional member of the connexin family of gap junction proteins, is the lens fiber protein MP70. Mol. Biol. Cell. 3:711-720.

- Williams GA, Daigle KA and Jacobs GH. 2005. Rod and cone function in coneless mice. Vis. Neurosci. 22:807-816.

- Witkovsky P, Owen WG, and Woodworth M. 1983. Gap junctions among the perikarya,dendrites, and axon terminals of the luminosity-type horizontal cell of the turtle retina. J. Comp. Neurol. 216:359-368.

- Witkovsky P. 2004. Dopamine and retinal function. Doc. Ophthalmol. 108:17-40.

- Wolburg H, and Kurz-Isler G. 1985. Dynamics of gap junctions between horizontal cells in the goldfish retina. Exp. Brain. Res. 60:397-401.

- Wong RO, Wye-Dvorak J, and Henry GH. 1986. Morphology and distribution of neurons in the retinal ganglion cell layer of the adult tammar wallaby--Macropus eugenii. J. Comp. Neurol. 253:1-12.

- Wong RO, Hughes A. 1987. The morphology, number, and distribution of a large population of confirmed displaced amacrine cells in the adult cat retina. J. Comp. Neurol. 255:159-77.

- Wright, L.L., and Vaney, D.I. 2000. The fountain amacrine cells of the rabbit retina. Vis. Neurosci., 17, 1145-1156.

- Wright, L.L., and Vaney, D.I. 2004. The type 1 polyaxonal amacrine cells of the rabbit retina: a tracer-coupling study. Vis. Neurosci., 21, 145-55.

- Xia, X.B., and Mills, S.L. 2004. Gap junctional regulatory mechanisms in the AII amacrine cell of the rabbit retina. Vis. Neurosci., 21, 791-805.

- Xin, D., and Bloomfield, S.A. 1997. Tracer coupling pattern of amacrine and ganglion cells in the rabbit retina. J. Comp. Neurol., 383, 512-28.

- Xin D, and Bloomfield SA. 1999. Dark- and light-induced changes in coupling between horizontal cells in mammalian retina. J. Comp. Neurol. 405:75-87.

- Xin D, and Bloomfield SA. 2000. Effects of nitric oxide on horizontal cells in the rabbit retina. Vis. Neurosci. 17:799-811.

- Yagi T . 1986. Interaction between the soma and the axon terminal of retinal horizontal cells in cyprinus carpio. J. Physiol. 375:121-135.

- Yagi T and Kaneko A. 1988. The axon terminal of goldfish retinal horizontal cells: a low membrane conductance measured in solitary preparations and its implication to the signal conduction from the soma. J. Neurophysiol. 59: 482-494.

- Yancey, S. B., John, S. A, Lal, R., Austin, B. J., and Revel, J. P. 1989. The 43-kD polypeptide of heart gap junctions: immunolocalization, topology, and functional domains. J. Cell Biol. 108: 2241-2254.

- Zettler F and Weiler R. 1981. Propagation of non-spike signals in retinal neurons. Vision Res. 21:1589-1590.

- Zhang, J. and Nicholson , B. J. 1994. The topological structure of connexin 26 and its distribution compared to connexin 32 in hepatic gap junctions. J. Membr. Biol. 139: 15-29.

- Zhang J, Li W, Trexler EB, and Massey SC. 2002. Confocal Analysis of Reciprocal Feedback at Rod Bipolar Terminals in the Rabbit Retina. J. Neurosci. 22:10871–10882

- Zhang J, Yang Z, and Wu SM. 2004. Immunocytochemical analysis of spatial organization of photoreceptors and amacrine and ganglion cells in the tiger salamander retina. Vis. Neurosci. 21:157-166.

- Zhang J, Li W, Hoshi H, Mills SL, and Massey SC. 2005. Stratification of alpha ganglion cells and ON/OFF directionally selective ganglion cells in the rabbit retina. Vis. Neurosci. 22:535-549.

9. Contribution of Collaborators

Chapter 7.1.

Luis Pérez de Sevilla Müller, Jennifer Shelley, and Reto Weiler (2007). Displaced amacrine cells of the mouse retina. J Comp Neurol 505:177-189.

Tracer experiments and immunocytochemistry were carried out by Luis Pérez de Sevilla Müller. Classification of the cells was created by L. Pérez de Sevilla Müller and Reto Weiler and discussed by the three authors. Jennifer Shelley wrote the manuscript.

Chapter 7.2.

Jennifer Trümpler, Karin Dedek, Timm Schubert, Luis Pérez de Sevilla Müller, Mathias Seeliger, Peter Humphries, Martin Biel, and Reto Weiler (2007). Rod and cone contributions to horizontal cell light responses in the mouse retina (in press).

Electrophysiology experiments were performed by Jennifer Trümpler. Intracellular injections were done by Timm Schubert and Luis Pérez de Sevilla Müller. Transgenic mouse lines were created by Mathias Seeliger, Peter Humphries and Martin Biel. Karin Dedek and Reto Weiler supervised the project.

Chapter 7.3.

Luis Pérez de Sevilla Müller, Ulrike Janssen-Bienhold, Karin Dedek, Maria M. Kreuzberg, Susanne Lorenz, Klaus Willecke, and Reto Weiler. Expression and modulation of Connexin30.2, a novel gap junction protein in the mammalian retina. (Submitted in Eur. Neurosci.)

Transgenic mouse lines were generated by Maria M. Kreuzberg, and Klaus Willecke. Immunocytochemistry in slices was done by Susanne Lorenz and intracellular injections, immunocytochemistry in whole-mounts and confocal pictures were done by L. Pérez de Sevilla Müller. Reto Weiler, Ulrike Janssen-Bienhold and Karin Dedek supervised the project.

Chapter 7.4.

Ulrike Janssen-Bienhold , Jennifer Trümpler, Gerrit Hilgen, Konrad Schultz, Luis Pérez de Sevilla Müller, Stephan Sonntag, Karin Dedek, Petra Dirks, Klaus Willecke, and Reto Weiler. Connexin 57 is expressed in dendro-dendritic and axo-axonal gap junctions of mouse horizontal cells and its distribution is modulated by light. (submitted in J. Comp. Neurol.)

The concept of the work and writing of the manuscript were done by U. Janssen-Bienhold, Karin Dedek and Jennifer Trümpler. Gerrit Hilgen did the dark/light experiments and part of the immunohistochemistry. L. Pérez de Sevilla Müller carried out part of the immunohistochemistry and injections. Blots and part of the immunohistochemistry were done by U. Janssen-Bienhold. Konrad Schultz did the

work with the electron microscopy. Stephan Sonntag carried out the experiment with

Hela cells. Petra Dirks did the molecular biology and the Cx57 expression.

CURRICULUM VITAE

LUIS PÉREZ DE SEVILLA MÜLLER

PERSONAL INFORMATION

Name: Luis Pérez de Sevilla Müller
Date of birth: 14.07.1979
Place of birth: Madrid, Spain
Nationality: Spanish
Marital status: Single

EDUCATION

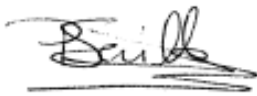|		
1985/1992	School "Joaquin Herrera"	Nerja, (Spain)
1992/1997	High School "Sierra de Almijara"	Nerja, (Spain)
1997–2003	University of Granada "Fuente Nueva" • Biology	Granada (Spain)
Sept 2004/Febr 2005	Practice in the Carl von Ossietzky University of Oldenburg Work: "Amacrine cells in the wild type mouse retina"	
Febr 2005/ June 2008	Doctoral dissertation in the university of Oldenburg Title: " Electrical synapsis: Cellular morphology and identification of connexins in the mouse retina" Thesis advisor: Prof. Dr. Reto Weiler	
August 2005-July 2008	Scholarship from the International Graduate School of Neuroscience of the Carl von Ossietzky University	

.

LANGUAGES

Spanish: mother language
German:
English: TOEFL
Russian: Beginner

Erklärung:

Hiermit erkläre ich, dass ich die vorliegende Dissertation selbstständig angefertigt, nur die angegebenen Hilfsmittel verwendet und in dieser oder ähnlicher Form noch nicht anderweitig eingereicht habe.

Oldenburg, den 18. September 2008

Luis Pérez de Sevilla Müller